

Targeting c-MYB in Acute Myeloid Leukaemia

Katherine Clesham

Developmental Biology and Cancer Section
Institute of Child Health
University College London

A thesis submitted for the Degree of Doctor of Philosophy

Declaration

'I, Katherine Clesham confirm that the work presented in this thesis is my own. Where information has been derived from other sources, I confirm that this has been indicated in the thesis.'

Signed

A solid black rectangular box used to redact the signature of Katherine Clesham.

Katherine Clesham

Abstract

Acute myeloid leukaemia (AML) is an aggressive haematological cancer affecting both children and adults. Clinical outcomes continue to improve from refinement of chemotherapy, risk stratification and stem cell transplantation. However, disease relapse remains problematic and contributes to the relatively poor overall survival. The transcription factor c-MYB is recognised to play a central role in AML. Irrespective of the upstream fusion oncogene, it maintains aberrant transcriptional networks ensuring self-renewal and a block in differentiation which are essential for the leukaemia cell. This makes it an attractive and rational target in all AML subtypes. Previous work in our laboratory generated a c-MYB gene expression signature and used it to probe the Connectivity Map database. A list of candidate drugs was generated predicted to inverse the c-MYB signature in AML. This thesis studies the steroidal lactone Withaferin A (WFA), derived from *Withania somnifera*, a candidate 'hit' predicted to inhibit c-MYB in AML. We provide evidence that WFA-induced gene expression changes are consistent with a block in the c-MYB transcriptional programme in AML. WFA interfered with c-MYB function by inducing loss of c-MYB protein. WFA-induced c-MYB loss occurred across a range of AML subtypes and resulted in loss of cell viability and differentiation of leukaemia cells. Using a degradation-resistant c-MYB, we demonstrate partial rescue of WFA-induced inhibition of colony formation, indicating that c-MYB is a critical target of WFA. WFA-treated gene expression changes demonstrate enrichment in gene sets implicated in protein translation, and WFA-induced c-MYB loss was accompanied by phosphorylation of eIF2 α . This implicates inhibition of protein translation as the likely cause of WFA-induced c-MYB loss. WFA led to inhibition of AML colony formation in AML cell lines and patient derived xenografts (PDX). In contrast, no significant reduction in colony formation was observed in normal haematopoietic progenitor cells. This study highlights WFA as a compound with anti-AML properties which are mediated through loss of c-MYB.

Impact Statement

The work contained in this thesis adds to the body of evidence that targeting the transcription factor c-MYB is an emerging therapeutic approach for all subtypes of AML, and in particular we highlight the steroidal lactone, WFA as a compound with anti-AML properties which are mediated through loss of c-MYB.

The impact that this work has achieved so far include:

- Presentation to academic staff and students within UCL and at international meetings.
- The findings have been shared with the funding charity, Children with Cancer and will then be shared with the wider patient and public community via their website or public engagements. This will facilitate public and patient involvement with scientific and clinical research.
- From a personal perspective, the expertise, knowledge and analytical skills I have learnt during this time will continue to improve my care for patients with acute leukaemia.

The future impact this data will have:

- Publication in a scientific journal. This will enable the wider scientific community to see our work targeting c-MYB as a therapeutic approach in AML. There is growing interest in different ways to modulate transcription factors as a therapeutic approach in leukaemia.
- The data and analysis contained offer other researchers the opportunity to study the effects of c-MYB perturbation on AML cells. The RNA-sequencing data will be available on open access platforms.
- Identifying the steroidal lactone, WFA, has anti-AML properties which are mediated through loss of c-MYB, may have future translational implications. This could be from a university or from the pharmaceutical industry.

Table of Contents

DECLARATION	1
ABSTRACT	2
IMPACT STATEMENT	3
TABLE OF CONTENTS	4
LIST OF FIGURES	7
LIST OF TABLES	10
ABBREVIATIONS	11
ACKNOWLEDGEMENTS	17
CHAPTER 1: INTRODUCTION	18
1.1 Haematopoiesis	18
1.2 Transcriptional regulation of haematopoeisis	25
1.3 Acute Myeloid Leukaemia (AML)	28
1.3.1 Management of AML in children and adults fit for intensive chemotherapy.	31
1.3.2 Management of AML in adults if intensive therapy is not appropriate.	32
1.4 Leukaemic stem cells (LSCs)	33
1.5 <i>KMT2A</i> (MLL) fusion proteins	36
1.6 c-MYB in haematopoiesis and leukaemogenesis	43
1.7 Targeting c-MYB in AML	49

PROJECT AIM	54
CHAPTER 2: MATERIALS AND METHODS	55
2.1 Molecular biology	55
2.1.1 Transformation of competent bacteria	55
2.1.2 Isolation of plasmid DNA	55
2.1.3 Restriction enzyme digests	56
2.1.4 DNA constructs	56
2.1.5 Western blot analysis	58
2.1.6 RNA isolation	60
2.1.7 cDNA preparation	60
2.1.8 Quantitative RT-PCR analysis	61
2.2 Animal work	62
2.3 Cell biology	62
2.3.1 Cell lines and tissue culture	62
2.3.2 Primary ALL and AML PDX samples	65
2.3.3 Co-culture experiments	66
2.3.4 Colony formation assays	67
2.3.5 Flow cytometric analysis	68
2.3.6 Lentiviral packaging cell line transfection	69
2.3.7 Retroviral transduction	70
2.4 RNA Sequencing	70
2.5 Gene set enrichment analysis (GSEA)	71
CHAPTER 3: IDENTIFYING COMPOUNDS TO INHIBIT C-MYB IN ACUTE LEUKAEMIA.	72
3.1 Introduction	72
3.2 Results	75
3.2.1 Effect of WFA on c-MYB protein and gene expression	75

3.3	Discussion	84
CHAPTER 4: CHARACTERISING THE ANTI-LEUKAEMIC EFFECTS OF WFA.		
		87
4.1	Introduction	87
4.2	Results	88
4.2.1	Effect of WFA on c-MYB in acute myeloid leukaemia	88
4.2.2	Studying consequences of WFA administration on cell viability.	91
4.2.3	Determining the role of c-MYB in the anti-leukaemic activity of WFA.	93
4.2.4	Exploring how WFA induces c-MYB loss.	97
4.2.5	The effect of WFA on protein translation.	103
4.3	Discussion	109
CHAPTER 5: INVESTIGATING THE EFFECT OF WFA IN AML <i>IN VITRO</i> AND <i>IN VIVO</i> .		
		115
5.1	Introduction	115
5.2	Identification of withaferin A	117
5.2.1	WFA induces differentiation of THP1 cells <i>in vitro</i>	117
5.2.2	Evaluating sensitivity of primary patient-derived B-ALL to WFA	119
5.2.3	Evaluating WFA in primary patient-derived AML	127
5.2.4	Withaferin A inhibits self-renewal capacity in human AML	133
5.2.5	Evaluating WFA activity <i>in vivo</i>	138
5.3	Discussion	142
CHAPTER 6: CONCLUSIONS		
		147

REFERENCES	152
------------	-----

APPENDICES	170
------------	-----

List of figures

Figure 1 Classical model of murine haematopoiesis	23
Figure 2 Alternative, composite and bypass models of haematopoiesis.	24
Figure 3 MLL and MLL fusion proteins.	42
Figure 4. Schematic diagram of c-MYB.	47
Figure 5. Schematic diagram of c-MYB targeting compounds.	53
Figure 6 Schematic diagram of lentiviral vectors	57
Figure 7 Identification of c-MYB targeting drugs in AML.	74
Figure 8. Changes in gene expression following treatment with WFA in THP1 cells.	79
Figure 9. Identification of WFA as a c-MYB targeting drug in AML	80
Figure 10. WFA interferes with c-MYB transcriptional program in AML.	81
Figure 11. WFA inhibits gene expression of <i>MYB</i> and its downstream targets	82
Figure 12. GSEA of WFA induced global gene expression changes	83
Figure 13. WFA induces degradation of c-MYB	89
Figure 14. WFA-induced c-MYB loss is not due to cell cycle inhibition.	90
Figure 15. WFA induces apoptosis in AML cell lines	92
Figure 16. Transient WFA treatment inhibits colony formation	95

Figure 17. Degradation resistant c-MYB partially rescues WFA induced c-MYB loss and colony formation	96
Figure 18 Time course of WFA treatment on protein and gene expression	100
Figure 19 WFA induces proteasomal degradation of c-MYB	101
Figure 20 Effect of HSP 70, HSP 90 and reactive oxygen species on WFA	102
Figure 21 WFA induces inhibition of translation	106
Figure 22 WFA inhibits translation associated genesets	107
Figure 23 WFA induces phosphorylation of eIF2S1 in THP1 cells.	108
Figure 24 WFA induced differentiation in AML cell lines.	118
Figure 25 Effects of RNA interference of c-MYB in B-ALL cell lines.	121
Figure 26 Effect of WFA on B-ALL cell lines	122
Figure 27 Co-culture of B-ALL PDX samples on MS5 cells.	123
Figure 28 Co-culture of 2 primary B-ALL samples on primary MSC cells.	124
Figure 29 MSC viability is not affected by WFA	125
Figure 30 Treatment of B-ALL PDX with WFA	126
Figure 31 Growth of AML PDX samples when co-cultured on human MSCs.	129
Figure 32 Treatment of AML PDX with WFA	130
Figure 33 WFA induced apoptosis in AML PDX	131
Figure 34 Quantification of WFA induced apoptosis in AML PDX	132
Figure 35 WFA inhibits leukaemic self-renewal in AML cells.	135

Figure 36 WFA inhibits colony formation by primary AML cells but not CD34+ CB cells.	136
Figure 37. Efficacy of WFA <i>in vivo</i>	140
Figure 38. Survival curve following pre-treatment with WFA <i>in vivo</i> .	141

List of tables

Table 1 Acute myeloid leukaemia and related precursor neoplasms according to the WHO classification (2017)	29
Table 2 2017 ELN risk stratification by genetics.	30
Table 3 Components of SDS-PAGE gels	59
Table 4 Primary antibodies used in western blot analysis	59
Table 5 Secondary antibodies used in western blot analysis	60
Table 6 Gene primers for Sybr-green	61
Table 7 Acute lymphoblastic leukaemia cell lines	63
Table 8 Acute myeloid leukaemia cell lines	64
Table 9 Characteristics of B-ALL PDX samples	65
Table 10 Characteristics of AML PDX samples	66
Table 11 Genesets used for GSEA	71

ABBREVIATIONS

ADH	Alcohol dehydrogenase
AF10	ALL1 fused gene from chromosome 10
AF4	ALL1 fused gene from chromosome 4
AF6	ALL1 fused gene from chromosome 6
AF9	ALL1 fused gene from chromosome 9
ALDH	Aldehyde dehydrogenase
ALL	Acute lymphoblastic leukaemia
AGM	Aorta-gonad-mesonephros
AML	Acute myeloid leukaemia
APML	Acute promyelocytic leukaemia
APS	Ammonium persulfate
BCR	Breakpoint cluster region
BD	Bromodomain
BFU	Burst-forming unit
CB	Cord blood
C/EBP	CCAAT/enhancer binding proteins
cDNA	Complementary deoxyribonucleic acid
CFU	Colony-forming unit
ChIP	Chromatin immunoprecipitation
ChIP-seq	Chromatin immunoprecipitation sequencing
CLP	Common lymphoid progenitor
c-MYB	Avian myeloblastosis viral oncogene homologue
CMP	Common myeloid progenitor

CMAP	Connectivity Map
CR	Complete remission
CREB	cAMP responsive element binding protein
CuCl ₂	Copper chloride
DDC	Diethyldithiocarbamate
DMEM	Dulbecco's modified eagle's Medium
DMSO	Dimethyl sulphoxide
DNMT1	DNA methyltransferase 1
DOT1L	Disruptor of telomeric silencing 1
DSB	Double strand breaks
EDTA	Ethylenediaminetetraacetic acid
EIF2	Eukaryotic initiation factor 2
ENL	Eleven-nineteen leukaemia
ELN	European Leukaemia Network
ER	Endoplasmic reticulum
ES	Embryonic stem cell
FAB	French-American-British
FACS	Fluorescence activated cell sorting
FcγRII/III	Fcγ receptor-II/III
FCS	Foetal calf serum
FDA	American food and drug administration
FDR	False discovery rate
FISH	Fluorescence in-situ hybridisation
FLT3	FMS-like tyrosine kinase 3

GATA-1	GATA binding factor 1
GES	Gene expression signature
GMP	Granulocyte/ Monocyte Progenitors
GM-CSF	Granulocyte macrophage colony stimulating factor
GFI1	Growth-factor independent 1
GO	Gemtuzumab orzoganamicin
GSEA	Gene set enrichment analysis
HSC	Haematopoietic stem cell
HSCT	Haematopoietic stem cell transplant
HDAC1	Histone deacetylase 1
HDAC2	Histone deacetylase 2
H3K4	Histone H3 lysine 4
H3K27ac	Acetylated Histone H3 lysine 27
HMA	Hypomethylating agents
HOX-A	Homeobox A cluster
HPC	Haematopoietic progenitor cells
HSC	Haematopoietic stem cells
HSP70/90	Heat shock protein 70/90
IDH1/2	Isocitrate dehydrogenase
IRF8	Interferon-regulatory factor 8
IMDM	Iscove's modified dulbecco's medium
IP	Intraperitoneal
KMT2A	Lysine (K)-specific MethylTransferase 2A
LEDGF	Lens epithelium derived growth factor

Lin	Lineage-associated surface markers
LMPP	Lymphoid-primed multipotent progenitors
LSC	Leukaemic stem cell
LT-HSC	Long term haematopoietic stem cells
LTR	Long terminal repeats
MBD	Menin binding domain
MeDDC	Methyl diethyldithiocarbamate
MEIS1	Myeloid ectropic viral integration site 1
MEP	Megakaryocytes/erythroid progenitors
MFI	Mean fluorescence intensity
MLL	Mixed lineage leukaemia
MII ^{-/-}	MII deficient mice
MLL ^C	C terminal fragment of MLL
MLL ^N	N terminal fragment of MLL
MLP	Multi lymphoid progenitors
MPP	Multipotent progenitors
MSC	Mesenchymal stromal cell
MSD	Matched sibling donor
MUD	Matched unrelated donor
MXT	Mitoxantrone
NaCl	Sodium chloride
NELF	Negative elongation factor
NES	Normalised enriched score
NGS	Next generation sequencing

NK cells	Natural killer cells
NOD	Non-obese diabetic
NSG	NOD.Cg-Prkdc ^{scid} Il2rg ^{tm1Wjl} / SzJ mice
ORR	Overall response rate
OS	Overall survival
PBS	Phosphate-buffered saline
PBS-T	PBS-Tween
PCR	Polymerase chain reaction
PDX	Patient derived xenograft
PHD finger	Plant homology domain
PI	Propidium Iodide
PMA	Phorbol myristate acetate
pTEFb	Positive transcription elongation factor
PU.1	Haematopoietic transcription factor PU.1
PVDF	Polivinyldene Fluoride
qRT-PCR	Quantitative real-time PCR
RAR α	Retinoic acid receptor alpha
RNA	Ribonucleic acid
RNA-seq	RNA sequencing
ROS	Reactive oxygen species
RPMI	Roswell Park Memorial Institute
Sca-1	Stem cell antigen 1
SCF	Stem cell factor

SCL/TAL1	Stem cell leukaemia/T-cell acute lymphoblastic leukaemia (T-ALL) 1
SCID	Severe combined immune-deficient
SFEM	Serum-free expansion medium
SL-IC	Leukaemia initiating stem cell
SNL1	Speckled nuclear localization signal 1
SNL2	Speckled nuclear localization signal 2
STAT	Signal transducer and activator of transcription
ST-HSC	Short term haematopoietic stem cells
TAD	Transcriptional activation domain
TEL	Translocation-ETS-leukaemia
TEMED	Tetramethylenediamine
TF	Transcription factor
TFIID	Transcription factor II D
TO-PRO3	Monomeric cyanine nucleic acid stain
WFA	Withaferin A
WHO	World Health Organisation

Acknowledgements

First and foremost, I would like to thank Professor Owen Williams. He has been a great supervisor. His knowledge, guidance and dedication to leukaemia research has been inspirational. I am very grateful for all the time he has given me.

The whole group has contributed to this work and I feel great fortune to have been a member these past years. I would like to thank my secondary supervisor, Dr Jasper de Boer for his astute critique and his optimistic and enthusiastic approach during laboratory work. Special thanks must go to Dr Luca Gasparoli, Dr Clemence Virely and Dr Sandra Cantilena. These fabulous scientists offered invaluable practical support and friendship. I would like to thank Dr. Mark Kristiansen, Tony Brooks and Dr. Paola Niola at UCL Genomics for running the RNA-sequencing experiments.

Thanks to my parents who continue to support and encourage me, their persistence and good humour are inspiring. And finally, thank you Jonathan, Julia and Isabelle for being wonderful and their daily questions about how the “speriments” were going.

Chapter 1: Introduction

1.1 Haematopoiesis

Haematopoiesis is the highly regulated process in which a haematopoietic stem cell (HSC) generates mature myeloid and lymphoid blood cells. After birth this occurs in the bone marrow, but during embryonic and foetal development there are sequential sites of haematopoiesis as the embryo develops *in utero*. The initial stage of blood production is termed 'primitive' haematopoiesis and is characterised by the production of red blood cells, containing foetal globins, which are able to deliver oxygen to the growing embryo. This process begins in the yolk sac, then moves to the aorta-gonad-mesonephros (AGM) and the placenta. The second phase is termed 'definitive' haematopoiesis and occurs when cells colonise the foetal liver (the predominant site of haematopoiesis *in utero*), spleen, thymus and finally the bone marrow (Orkin and Zon, 2008).

Haematopoiesis is a hierarchical process in which multipotent HSC's reside at the apex and undergo terminal differentiation as they mature. HSC's are critical for lifelong blood production and this is enabled by their ability to self-renew whilst giving rise to specific progenitor and precursors cells of the myeloid and lymphoid lineage. Myeloid precursors give rise to a number of distinct, fully differentiated, short-lived cell types including erythrocytes, megakaryocytes, granulocytes (neutrophils, eosinophils, and basophils), monocyte/macrophages and mast cells. Lymphoid cells include T, B and NK cells), which carry out adaptive and innate immune responses, respectively. Dendritic cells are a class of bone marrow derived cells that originate from lympho-myeloid haematopoiesis. They function as an essential interface between innate sensing of pathogens and the activation of the adaptive immunity.

To act as a stem cell, HSC's must demonstrate durable self-renewal and differentiation into all cell types of the haematopoietic system. The parallel and

overlapping study of murine and human haemopoietic cell models have been complementary to our understanding.

Formative studies in stem cell biology were undertaken in the mouse by transplanting purified cell populations into immunodeficient mice and detecting repopulation of the donor cell in the bone marrow. In murine haematopoiesis, HSC's are characterised by the lack of expression of lineage associated-surface-marker (Lin), but high expression of stem cell antigen-1 (Sca-1) and c-kit (LSK) and therefore have the phenotype Lin⁻ Sca⁺ c-Kit⁺. Within the LSK fraction, cells capable of durable repopulation over a prolonged time have been defined as long-term HSC's (LT-HSC), whereas those capable of generating all lineages, but only for a transient period are named as short-term HSC (ST-HSC) or multipotent progenitors (MPP). LT-HSCs reside in the CD34⁻, CD38⁻ or Thy1.1^{lo}, whereas ST-HSCs express the phenotype CD34⁺, CD38⁻ or Thy1.1⁻ (Iwasaki and Akashi, 2007).

Within the murine system there are differing models for myeloid and lymphoid differentiation. The classical model proposes myeloid and lymphoid development results from lineage-restricted multipotent progenitors: a common myeloid progenitor (CMP) and a common lymphoid progenitor (CLP). CLPs are characterised by expression of the interleukin-7 receptor α -chain (IL-7R α ⁺), and differentiate into B and T cell progenitors (Pro-B and Pro-T), and generate B and T lymphocytes and NK cells. In contrast, cells not expressing IL-7R α (IL-7R α ⁻) are CMPs and as they differentiate, this fraction can be further classified the basis of the Fc γ Receptor II/III (Fc γ RII/III) expression into three distinct myeloid progenitor subsets: Fc γ RII/III^{lo} CD34⁺ CMPs, Fc γ RII/III^{lo} CD34⁻ megakaryocyte-erythrocyte progenitors (MEPs) and Fc γ RII/III^{hi} CD34⁺ granulocyte-monocyte restricted progenitors (GMPs) (Akashi et al., 2000). The CMPs are able to generate all myeloid progeny, whilst GMPs and MEPs can only generate granulocyte/macrophage or megakaryocyte and erythroid progeny respectively (Figure 1).

An alternative model of murine haematopoiesis was proposed by Adolfsson and colleagues who identified a population of HSCs (lymphoid multipotent progenitors, LMPP) which were able to give rise to myeloid and lymphoid progenitors, but had lost their megakaryocytic-erythrocyte potential. These progenitors were distinguished by FMS-like tyrosine kinase 3 (Flt3) expression. Flt3 is a cytokine tyrosine kinase receptor selectively expressed in early stages of hematopoiesis and known to be a key and potent stimulator of murine and human HSC's (Lyman and Jacobsen, 1998). Experimentally, they identified short-term HSC's (Lin⁻ Sca⁺ c-Kit⁺ CD34⁺ cells) and purified by the expression of Flt3. Mice transplanted with LSK Flt3⁺ cells had bone marrow reconstitution with a combined myeloid (granulocyte-monocyte) and lymphoid (B and T) phenotype. Interestingly the myeloid component was found to decline, in contrast to the more robust lymphoid reconstitution (Adolfsson et al., 2001). The same group later identified that LMPP's lack megakaryocyte and erythroid developmental potential, contrary to what would be predicted from the classical model for hematopoietic lineage commitment (Adolfsson et al., 2005). A composite model proposed that ST-HSC could give rise separately to CMP and LMPP, which both had myeloid potential, but only the LMPP had lymphoid-restricted potential. Most recently, a myeloid bypass model has been described. This study identified lineage-committed HSC, which gave rise to one or a limited number of lineages, without passing through a multipotent progenitor (MPP) stage and were able to confer long-term reconstitution of these lineages (Yamamoto et al., 2013). These models are shown in Figure 2.

Human HSC development has been functionally evaluated through transplantation into immunodeficient mice since the 1980's with the discovery of severe combined immune-deficient (SCID) mice lacking B and T cells. (Bosma et al., 1983, Fulop and Phillips, 1990). Work by John Dick's group transplanted human bone marrow cells in to sub-lethally irradiated SCID mice infused with human IL-3, GM-CSF and SCF cytokines and identified myeloid

progenitors 4 months after initial transplantation (Kamel-Reid and Dick, 1988, Lapidot et al., 1992, Vormoor et al., 1994). These primitive cells engrafted, proliferated and differentiated in the mouse bone marrow, producing large numbers cells capable of initiating and maintaining progenitors using *in vitro* assays as well as immature CD34⁺Thy.1⁺, CD34⁺CD38⁻ cells and mature myeloid, erythroid and lymphoid cells. Functionally, these primitive cells were termed SCID repopulating cells (SRC). In order to combat the limitations of the SCID model, a new mouse strain was developed by backcrossing the SCID gene onto non-obese diabetic (NOD) mice (Shultz et al., 1995). This model was widely used to study human haematopoiesis *in vivo* but was complicated by the residual activity of NK cells which limited the engraftment of human HSC's. NOD/SCID/Gamma (NSG) mice were engineered by introducing an additional mutation in the IL2 receptor γ . These mice lack NK cells, live longer and support higher-level (5x) human HSC engraftment (Shultz et al., 2005).

The initial approach to purify SRC was based on the presence of CD34. Using NOD/SCID recipients, the SRC were exclusively found in a cell fraction that expressed high levels of CD34, but no CD38, a surface marker of more differentiated cells (Lin⁻, CD34⁺, CD38⁻) (Larochelle et al., 1996). Mice transplanted with CD34⁺, CD38⁺ did not engraft. The frequency of SRC was estimated to be one SRC in 600 CD34⁺, CD38⁻ cells and mice transplanted with one SRC (i.e. 600 CD34⁺, CD38⁻ cells) were able to produce at least 200000 progeny 6 weeks post transplantation (Bhatia et al., 1997). More recently CD34⁻ stem cells capable of long-term *in vivo* repopulation and multilineage differentiation have been identified (Anjos-Afonso et al., 2013, Bonnet, 2001).

Further insights into human haematopoiesis have been gained from global gene expression analysis of human haemopoietic stem and progenitor cells (HSPC's). Velten et al (Velten et al., 2017) found data incompatible with the classical model of haematopoiesis, which assumes a hierarchical tree-like structure of discrete progenitors downstream of HSC's. Human HSPC's (Lin⁻

CD34⁺), underwent flow cytometry and single cell RNA-seq analysis. The transcriptomic and immunophenotypic data was then integrated to identify the molecular and cellular events associated with the differentiation of human HSC's at the single cell level. The HSC, MPP and MLP's (Lin⁻ CD34⁺ CD38⁻) formed a single continuously connected entity, in contrast to more differentiated progenitors (Lin⁻ CD34⁺ CD38⁺), which could be separated into clusters corresponding to distinct progenitor types of all major types of haematopoiesis. They find that HSC's and their immediate progeny are initially part of a 'Continuum of Low-primed UnDifferentiated (CLOUD)-HSPC's and that discrete populations are only established when differentiation has progressed, typically associated with expression of CD38. HSC's found in the centre of the 'CLOUD' were found to gradually acquire lineage priming into either lympho/myeloid or megakaryocytic/erythroid populations and only later undergo single lineage separation.

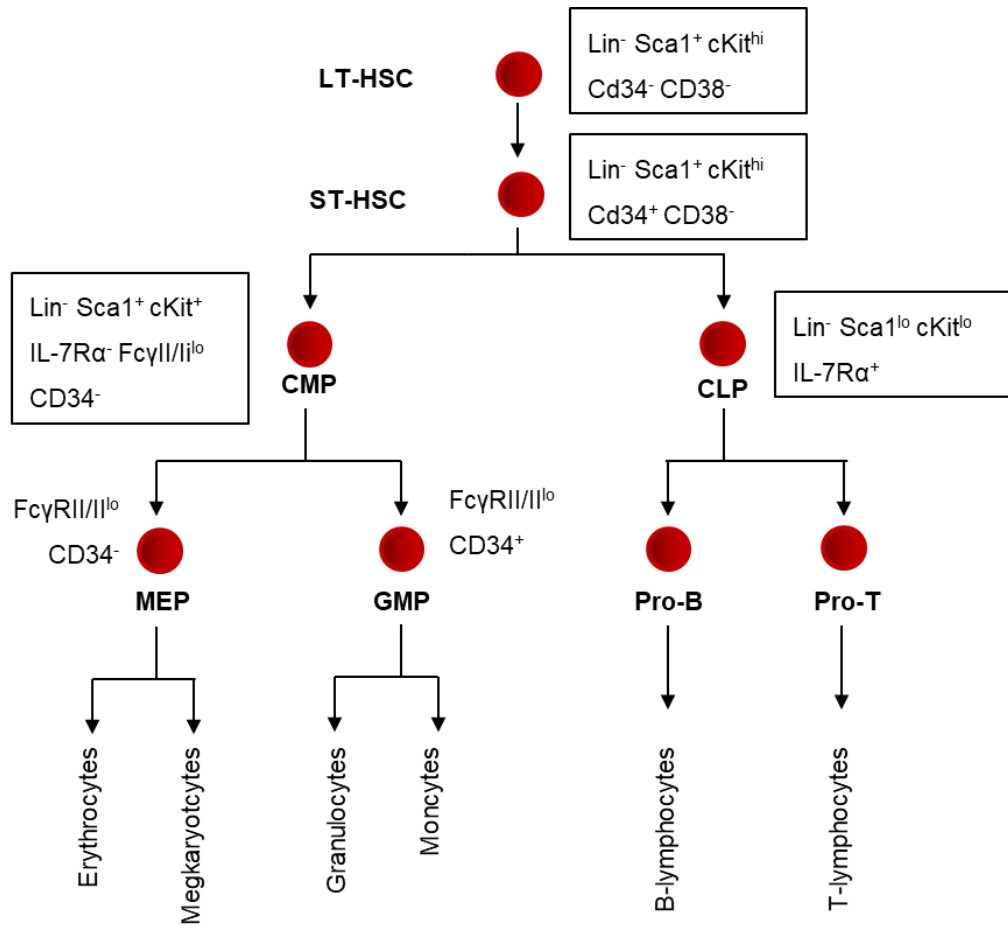


Figure 1 Classical model of murine haematopoiesis

Long term haematopoietic stem cells (LT-HSC) have the potential to self-renew and give rise to short-term haematopoietic stem cells (ST-HSC) with reduced self-renewal capacity. Subsequently, the ST-HSC can then differentiate into common myeloid progenitors (CMP) and common lymphoid progenitors (CLP). CMP generate megakaryocytes-erythrocyte progenitors (MEP) and granulocyte-macrophage progenitors (GMP) which will give rise to mature myeloid cells. CLP give rise to B-cell progenitors (ProB) and T-cell progenitors (Pro-T) which in turn give rise to cells of the mature lymphoid lineage (B, T lymphocytes and NK cells). Adapted from (Iwasaki and Akashi, 2007)

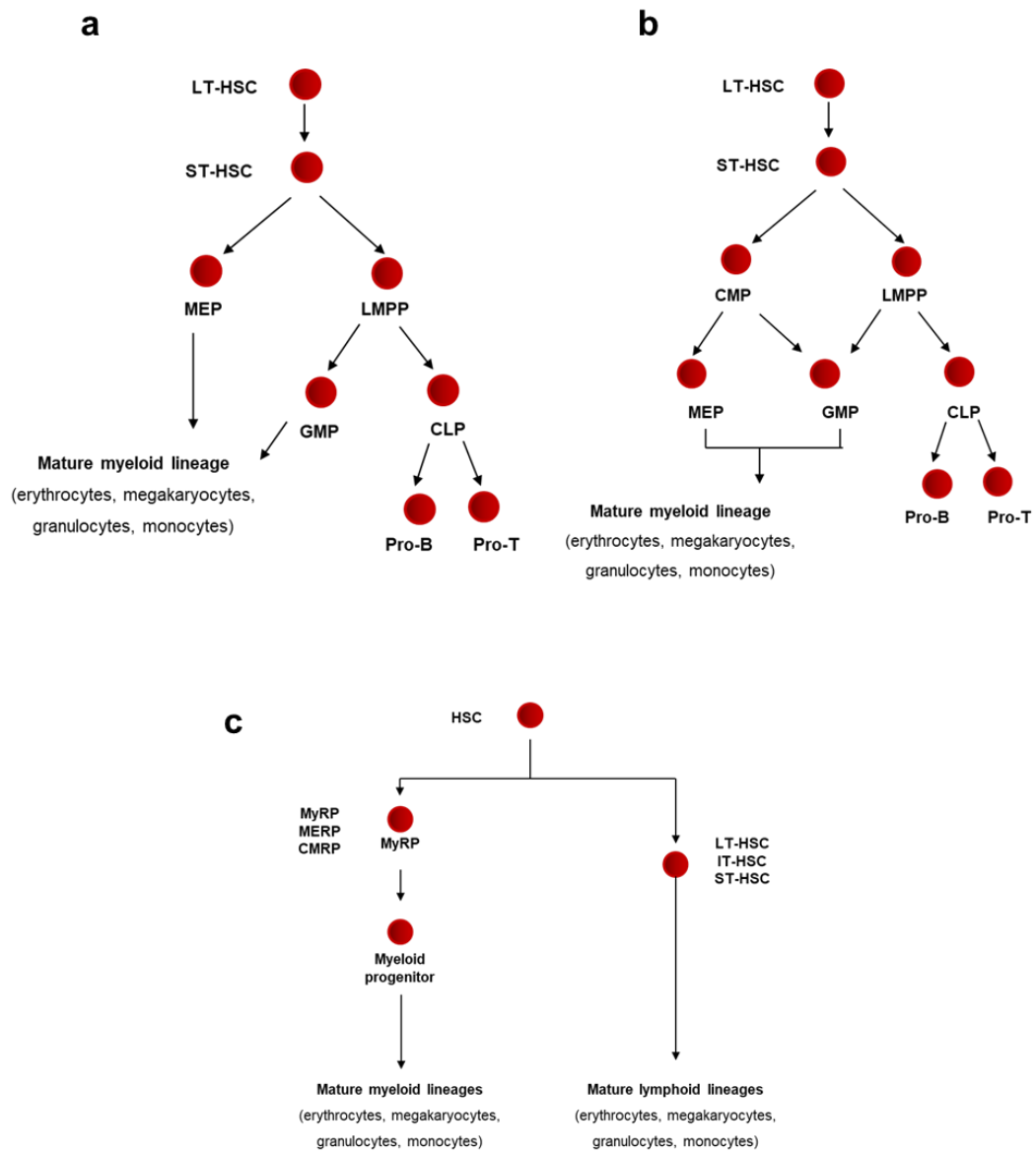


Figure 2 Alternative, composite and bypass models of haematopoiesis.

The alternate model (a) proposes the coexistence of a subset of lymphoid primed multipotent progenitors (LMPP) with lymphoid and myeloid potential. The composite model (b) combined the classical and the alternative model showing the coexistence of the CMP and LMPP. The myeloid bypass model (c) suggests the presence of a subset of myeloid restricted progenitor cells (MyRP). Adapted from (Adolfsson et al., 2001, Adolfsson et al., 2005, Yamamoto et al., 2013).

1.2 Transcriptional regulation of haematopoiesis

Transcription factors (TF) are essential effectors in the development and regulation of the HSC and the lineage-commitment and differentiation of the downstream progenitors. Those transcription factors involved exert either a positive or negative influence on gene expression which determines the survival, proliferation, commitment and differentiation of haematopoietic progenitors. Many of the transcription factors that control normal haematopoiesis are involved in chromosomal translocations or somatic mutations in haematological malignancies, which highlights their role as master regulatory molecules in the control of blood cell development.

Insights into the functions of TF have been acquired through conventional or conditional gene knockouts (KO) or from overexpression experiments in model systems (e.g mice, zebrafish, *Drosophila*). More recently, analysis of chromatin accessibility and transcriptional landscape have been defined (Corces et al., 2016, Velten et al., 2017). Conventional KO have demonstrated an essential requirement for some TF in the establishment of haematopoiesis. These include stem cell leukaemia/T-cell acute lymphoblastic leukaemia (T-ALL) 1 (SCL/TAL1) and its associated protein Lim-domain containing LM02, KMT2a (MLL), ETV6 (TEL), RUNX1 (AML1). Conditional KO studies suggest a more complicated picture for their function in adult haematopoiesis. This can be exemplified by SCL/TAL1.

SCL/TAL1 and LM02 are essential for the development of primitive and definitive haematopoiesis. Ablation of SCL/TAL1 activity in murine models led to the absence of yolk sac, primitive erythropoiesis and myelopoiesis and the mice died at embryonic day 9.5. This complete block in haematopoiesis indicated that SCL/TAL1 is one of the early-acting haematopoietic TF involved in haematopoietic development. SCL/TAL1 mRNA is expressed in the HSC compartment, myeloid progenitors and mature myeloid cells and is normally down-regulated during T-cell differentiation. In the adult HSC, SCL/TAL1 negatively regulates progression through the cell cycle and this quiescence

serves to preserve adult HSC integrity. In contrast, SCL/TAL1 activates cell cycle progression in progenitors (Porcher et al., 2017, Lacombe et al., 2010). Lineage commitment is decided by the balance between different TFs on progenitors downstream of HSC's. In B-cell development, the prominent factors are the E proteins, E2A, EBF1 and FOXO1, Ikaros and PAX5. E2A, EBF1 and FOXO1 act sequentially to activate a B-lineage-specific program of gene expression and PAX5 acts at multiple levels to commit cells to B-cell fate (Murre, 2018, Nechanitzky et al., 2013). The formation of myeloid cells is orchestrated by a relatively small number of transcription factors. Among them are PU.1, CCAAT/enhancer binding proteins (in particular, C/EBP α , C/EBP β and C/EBP ϵ), which are essential for establishing myeloid maturation and growth-factor independent 1 (GF11) and interferon-regulatory factor 8 (IRF8) which are necessary for neutrophil and macrophage maturation, respectively (Rosenbauer and Tenen, 2007). One of the most studied transcription factors in haematopoiesis is C/EBP α , which is mainly involved in cell fate decisions for myeloid differentiation (Avellino and Delwel, 2017). Conditional deletion of *Cebpa* in the bone marrow of adult mice failed to generate granulocyte/monocyte progenitors and resulted in a complete block of neutrophilic development at the common myeloid progenitor (CMP) stage (Zhang et al., 2004). During cell fate decisions, C/EBP α primes and activates the myeloid gene expression program in cooperation with other TF's, such as Pu.1 or Runx1 at very early stages of haematopoiesis. In addition, *Cebpa* is one of the primary targets to be shut down by other lineage-specific TFs in order to exclude myelopoiesis, emphasizing its important role as a granulocytic differentiation TF.

Analysis of gene expression in human HSC's as they differentiate to lineage commitment has demonstrated HSC's were characterised by expression of stem cell TF modules (including *HOXA3/PRDM16/HOXB6*) and associated with stem cell properties such as cell cycle quiescence, low expression of entire gene expression machinery, low RNA content and expression of CD38

(Velten et al., 2017). HSC's also expressed genes known to be associated with early lineage fate determination such as *FLT3/SATB1* for lymphoid/myeloid and *GATA2/NFE2* for megakaryocyte/erythroid indicating this first transcriptional priming occurs in the most primitive HSC's. During the continuous differentiation process, stem cell modules are turned off and lineage-specific gene modules upregulated, for example, *SPI1/GFI1* module for the neutrophil lineage. This corresponds with the observation that most progenitors at this stage display narrow restriction in their developmental potential. Finally, lineage-specific differentiation is accomplished by activation of gene modules such as *CEBPA/CEPBD* in neutrophils, *IRF8* module for the monocytic/dendritic lineage, *GPI1BB/PBX1* module for the megakaryocytic lineage and the *GATA1/KLF1* module for the erythroid lineage.

Corces *et al* used Assay for Transposase Accessible Chromatin using sequencing (ATAC-seq) to profile the chromatin accessibility landscape and transcriptome in 13 distinct cellular populations from nine healthy human donors (Corces et al., 2016). They found chromatin accessibility was able to classify cell-types accurately into very small populations. Analysis of the regulatory elements showed distal elements (>1000bp away from transcriptional start site (TSS)), were more accurate at classifying cell types than gene promoters. The transcription factor motifs found at each stage showed step-wise gains across developmental lineages and was exemplified by GATA and PAX motifs, which were strongly enriched in erythroid and lymphoid lineages, respectively. Using the same technique, analysis of AML revealed variation in DNA accessibility at different stages in HSC's, pre-leukaemia and overt disease. Normal haematopoiesis was co-opted by the leukaemic program and showed regulatory heterogeneity - single cells were found to have several normally distinct regulatory programs. Dysregulation of the regulatory networks in human haematopoiesis plays a critical role in the development of haematological malignancies. This may help to explain how otherwise differentiated cancer cells maintain self-renewal capability.

1.3 Acute Myeloid Leukaemia (AML)

Acute myeloid leukaemia (AML) is an aggressive haematological cancer which is characterised by a blockade in differentiation of haemopoietic stem cells and a clonal expansion of myeloid blasts in the bone marrow and peripheral blood.

From 2014-2016, there were on average 3102 new cases of AML diagnosed each year and incidence rates were highest in patients aged 85-89, reflecting it being predominantly a disease of the elderly. In contrast, there are approximately 80 cases of paediatric AML in the UK each year (www.cancerresearchuk.org).

AML has been well characterised primarily because of the ease of acquiring primary cancerous cells. Disease classification has changed over recent years from solely morphological assessment (French-American-British FAB) (Bennett et al., 1976) to the current situation which involves immunophenotypic, cytogenetic and molecular assessment. Since its introduction in 2001, the World Health Organisation (WHO) classification has unified well-established (cytomorphology, immunophenotyping, chromosome analysis) and molecular-orientated diagnostic disciplines (FISH, molecular genetics) for a comprehensive classification of AML. The WHO classification of myeloid disorders is summarised in Table 1.

Table 1 Acute myeloid leukaemia and related precursor neoplasms according to the WHO classification (2017)

Subclassification	Subtypes
AML with recurrent genetic abnormalities	<ul style="list-style-type: none"> • AML with t(8;21)(q22;q22.1); <i>RUNX1-RUNX1T1</i> • AML with inv(16)(p13.1q22) or t(16;16)(p13.1;q22); <i>CBFB-MYH11</i> • Acute promyelocytic leukemia with <i>PML-RARA</i> • AML with t(9;11)(p21.3;q23.3); <i>MLLT3-KMT2A</i> • AML with t(6;9)(p23;q34.1); <i>DEK-NUP214</i> • AML with inv(3)(q21.3q26.2) or t(3;3)(q21.3;q26.2); <i>GATA2,MECOM(EVI1)</i> • AML (megakaryoblastic) with t(1;22)(p13.3;q13.3); <i>RBM15-MKL1</i> • Provisional entity: AML with <i>BCR-ABL1</i>
AML with myelodysplasia-related changes	
Therapy-related myeloid neoplasms	
AML, not otherwise specified (AML NOS)	<ul style="list-style-type: none"> • AML with minimal differentiation • AML without maturation • AML with maturation • Acute myelomonocytic leukaemia • Acute monoblastic/monocytic leukaemia • Pure erythroid leukaemia • Acute megakaryoblastic leukaemia • Acute panmyelosis with myelofibrosis
Myeloid sarcoma	
Myeloid proliferations related to Down syndrome	<ul style="list-style-type: none"> • Transient abnormal myelopoiesis • Myeloid leukaemia associated with Down syndrome

Table 2 2017 ELN risk stratification by genetics.

Risk category	Genetic abnormality
Favourable	<ul style="list-style-type: none"> • t(8;21)(q22;q22.1); <i>RUNX1-RUNX1T1</i> • inv(16)(p13.1q22) or t(16;16)(p13.1;q22); <i>CBFB-MYH11</i> • Mutated <i>NPM1</i> without <i>FLT3-ITD</i> or with <i>FLT3-ITD^{low}</i> • Biallelic mutated <i>CEBPA</i>
Intermediate	<ul style="list-style-type: none"> • Mutated <i>NPM1</i> and <i>FLT3-ITD^{high}</i> • Wild-type <i>NPM1</i> without <i>FLT3-ITD</i> or with <i>FLT3-ITD^{low}</i> (without adverse-risk genetic lesions) • t(9;11)(p21.3;q23.3); <i>MLLT3-KMT2A</i> • Cytogenetic abnormalities not classified as favourable or adverse
Adverse	<ul style="list-style-type: none"> • t(6;9)(p23;q34.1); <i>DEK-NUP214</i> • t(v;11q23.3); <i>KMT2A</i> rearranged • t(9;22)(q34.1;q11.2); <i>BCR-ABL1</i> • inv(3)(q21.3q26.2) or t(3;3)(q21.3;q26.2); <i>GATA2,MECOM(EVI1)</i> • -5 or del(5q); -7; -17/abn(17p) • Complex karyotype, monosomal karyotype • Wild-type <i>NPM1</i> and <i>FLT3-ITD^{high}</i> • Mutated <i>RUNX1</i> • Mutated <i>ASXL1</i> • Mutated <i>TP53</i>

1.3.1 Management of AML in children and adults fit for intensive chemotherapy.

The management of all patients who are considered fit for intensive chemotherapy falls into several distinct areas.

Remission induction is the first cycle of chemotherapy following diagnosis and includes 7-10 days treatment with cytarabine and 3 doses of an anthracycline (daunorubicin in adults, mitoxantrone in children). This is often referred to as a '7+3' regimen, and has been the cornerstone of remission induction for many years. In addition to daunorubicin/cytarabine induction, additional therapies can be offered following initial cytogenetic and molecular assessment. Gemtuzumab ozogamicin (GO), the CD33-directed antibody-drug conjugate is now routinely used in parallel with induction chemotherapy. Survival benefit appears to be limited to patients with favourable, and to some extent, intermediate risk disease (Burnett et al., 2011, Hills et al., 2014, Juliette et al., 2019). The FLT3 inhibitor, midostaurin was shown to improve survival benefit and has subsequently been approved for patients with newly presenting AML with FLT3 mutations and should be administered alongside daunorubicin/cytarabine (Stone et al., 2017).

Initial treatment of children and young adults up to the age of 18 with AML is broadly the same. Patients are offered treatment in the multicentre-randomised phase III trial MyeChild (ISRCTN12389567). Standard chemotherapy with cytarabine and the anthracycline, mitoxantrone are offered, alongside a dose finding study to establish the optimal number of doses of GO that can be safely delivered to younger patients.

Following blood count recovery after remission induction therapy, a disease re-assessment is made. This incorporates results of morphological assessment from a bone marrow aspirates, with presenting cytogenetic and molecular markers, and a risk assessment made according to the European Leukaemia Network (ELN) risk stratification guidelines (Dohner et al., 2017) (Table 2). For patients deemed to have a favourable risk assessment after the

first cycle of chemotherapy, consolidation therapy is then offered which typically includes a second course of cytarabine and anthracycline, followed by 1-2 further cycles of cytarabine alone.

The role of allogeneic transplantation (HSCT) in AML is continuing to evolve. In the paediatric setting, only patients with an adverse risk assessment should be considered for allogeneic stem cell transplantation (HSCT) in 1st complete remission (CR1). Those patients with favourable or intermediate cytogenetics are managed currently on the Myechild protocol with chemotherapy alone, with HSCT reserved for CR2. The number of adults allografted for AML has risen sharply over the last decade. This is due to the combination of the limitation of intensive chemotherapy in offering long-term remission coupled with reduced transplant toxicity and increased donor availability. The decision whether to recommend HSCT in CR1 is dependent on the reduction in relapse risk from HSCT and whether it outweighs the associated non-relapse mortality (NRM). Studies have shown that, on average, HSCT halves the relapse risk for CR1 patients in comparison with chemotherapy, a finding across all cytogenetic risk groups. The NRM of fit adults transplanted using a matched sibling donor (MSD) or matched unrelated donor (MUD) is predicted to be around 15%, patients with a relapse risk of >50%, are likely to benefit for receiving an HSCT. This approach means adult patients with intermediate or adverse risk assessment should undergo HSCT in CR1, and a chemotherapy alone strategy reserved for those with favourable risk disease.

1.3.2 Management of AML in adults if intensive therapy is not appropriate.

Elderly patients considered to be not suitable for intensive chemotherapy have historically been difficult to treat due to both patient-related and disease-related risk factors. There is an increased likelihood of adverse-risk cytogenetics, co-morbidities and poor performance score. Utilising hypomethylating agents (HMA) such as azacytidine in combination with novel agents such as the BCL2 inhibitor, venetoclax are promising combinations.

The combination of azacytidine with venetoclax resulted in an overall response rate (ORR) of 67% (CR:37%, CRi: 30%) and median OS of 17.5 months. They observed low early mortality rates of 3% within 30 days and 8% at 60 days in a study group with a median age of 74 years, and whom nearly 50% had poor-risk cytogenetics (DiNardo et al., 2019).

For patients with targetable mutations in isocitrate dehydrogenase (*IDH1* or 2) or *FLT3*, targeted agents are available or under investigation in clinical trials. Both the *IDH1* inhibitor, ivosidenib and the *IDH2* inhibitor, enasidenib, demonstrate single agent activity with overall response rates (OR) of 59% and 38%, respectively (Roboz et al., 2019, Pollyea et al., 2019). Their role in combination therapy with HMA's are being evaluated in clinical trials. The role of FLT3 inhibitors in this population is also being studied, for example, gilteritinib, a potent and selective FLT3 inhibitor, gained FDA approval after it was shown to improve OS in relapsed/refractory AML compared to salvage chemotherapy (Perl et al., 2019). It is now being evaluated in combination with azacytidine in elderly patients.

1.4 Leukaemic stem cells (LSCs)

Like haematopoiesis, leukemogenesis is organised as a hierarchical process with the LSC positioned at the apex and capable of self-renewal and the ability to proliferate and undergo limited differentiation into leukaemic blasts.

Identification of an AML-initiating cell came about when human AMLs samples were transplanted into severe combined immunodeficient (SCID) mice. The disease that arose in the mice was initiated by a primitive cell, termed leukaemia initiating stem cell (SL-IC), a term used interchangeably with LSC (Lapidot et al., 1994). In these initial experiments, secondary transplants were not performed and transplantation of small cell doses or purified cells from myelomonocytic subtypes of AML using SCID recipients was not possible, meaning SL-IC were not shown to have the potential for self-renewal. The same group later demonstrated that transplantation of human

AML samples into non-obese diabetic (NOD)/SCID mice was preferable to the SCID model as fewer cells (10-20 fold) led to the same degree of engraftment. Using this model, it was also possible for peripheral blood leucocytes to engraft in the donor mice. This enhanced engraftment allowed estimates of SL-IC frequency and determined them to be between 0.2-100 SL-ICs per 10^6 mononuclear cells (Bonnet and Dick, 1997).

Characterisation of the cell-surface phenotype of the SL-IC revealed interesting findings. Using expression of CD34, expression of CD34⁺ cells initiated the proliferation of leukaemic cells in recipient mice, whereas CD34⁻ cells did not (even at 100x the number of cells). CD34⁺ cells were then sorted by expression of CD38. Cells expressing the phenotype CD34⁺/CD38⁻ were able to engraft recipient mice with as few as 5×10^3 transplanted cells. The greater proportion of the CD34⁺ cells (CD34⁺/CD38⁺) failed to engraft in recipient mice. This proved to be consistent in 7 human AML samples, both for an undifferentiated AML sample as well as those expressing extensive myelomonocytic differentiation markers. The phenotype of SL-ICs was similar to that of normal stem cells, thereby suggesting that primitive normal stem cells, rather than committed progenitors, are the target of leukemic transformation. SL-ICs were transplanted into secondary recipients with engrafted with equivalent levels of human cells, and unchanged morphology and cell-surface phenotype of the leukaemic blasts, thereby demonstrating SL-IC's can proliferate, differentiate and renew themselves (Bonnet and Dick, 1997).

However, LSCs bearing immunophenotypes other than CD34⁺CD38⁻ have since been identified and demonstrate that LSCs can arise from more committed progenitors that have acquired self-renewal capacity. Krivtsov et al showed that leukaemic transformation can occur in a committed granulocyte macrophage progenitor (GMP) through introduction of MLL–AF9 fusion protein, encoded by the t(9;11)(p22;q23) chromosomal translocation. They transduced GMP and observed AML similar to other MLL fusion leukaemia

models. They found that leukaemic-GMP's (L-GMP's) possessed an immunophenotype similar to normal GMP's. They were also highly enriched for LSCs that could initiate leukaemia in secondary recipient mice, demonstrating acquisition of self-renewal properties. Gene expression analysis demonstrated the GMP-derived LSC shared a programme most similar to the progenitor from which they arose, but had reactivated a self-renewal-associated programme normally expressed in HSC (Krivtsov et al., 2006).

A different MLL fusion, *MLL-ENL*, was also shown to transform committed progenitors by the Weissman group. Here HSC, CMP, GMP, MEP and CLP compartments were isolated from a murine model and transduced with a vector encoding the fusion gene *MLL-ENL*. These cells were transplanted into congenic recipients and transduced cells from all compartments, with the exception of MEP and CLP, were able to initiate *MLL*-associated AML over a similar timescale (Cozzio et al., 2003).

Not all leukaemia-associated oncogenes have the capacity to confer self-renewal properties of leukemic stem cells to hematopoietic progenitors that inherently lack the ability to self-renew. Huntly et al identified *MOZ-TIF2* and *BCR-ABL* as representative members of the transcription factor/cofactor or tyrosine kinase fusion oncogene families. CMP and GMP transduced with *MOZ-TIF2*, but not *BCR-ABL* led to properties of self-renewal in *in vitro* serial replating assays. The leukaemia induced *in vivo* following retroviral transduction of *MOZ-TIF2*, led to acute monocytic leukaemia which was indistinguishable to human AML bearing the same mutation. The leukaemic cells bearing *MOZ-TIF2* could be serially transferred into secondary recipients (Huntly et al., 2004). These experiments demonstrate that committed progenitors can acquire self-renewal ability, although because they normally persist for a short time, the opportunity to acquire such mutations is reduced compared to HSCs. It is interesting that other oncogenes, including *BCR-ABL*

and FLT3-ITD were not able to alter the self-renewal properties of progenitors (Horton and Huntly, 2012).

Relapse of AML is a frequent clinical problem. Minor clones present at diagnosis re-emerge with new sub-clonal changes. In the rare cases of late-relapse, it is usually residual LSC's from founder clones that are responsible for the disease (Yilmaz et al., 2019). LSCs are associated with chemotherapy resistance and AML relapse, and AML with higher LSC frequency and activity are associated with poorer clinical outcome in AML (van Rhenen et al., 2005). Whilst it is not feasible to assess individual patient LSC functional activity, gene expression signatures (GES) have been characterised in LSC-enriched populations. This has led Ng *et al* to develop a 17-gene signature, which is formulated into a clinical score, where higher scores are associated with worse clinical outcomes. The association between LSC-GES and known molecular alternations have become integrated into the recommended risk assessment in AML (Ng et al., 2016) (Dohner et al., 2017). The response of LSC's during chemotherapy, their metabolism and propensity to lie quiescent, together with their interaction with the bone marrow niche are key factors to understand and exploit to eradicate LSCs (Vetrie et al., 2020)

1.5 *KMT2A* (MLL) fusion proteins

The *MLL* gene is the mammalian homologue of the *Drosophila Trithorax* (Trx) gene. MLL and Trx are an evolutionary conserved family of proteins, the trithorax group (Trx-G), transcription factors which positively regulate gene expression during development and antagonise the function of Polycomb (PcG) group proteins (Hess, 2004). Wild-type MLL encodes a histone lysine methyltransferase which has led to the gene being officially renamed Lysine (K)-specific MethylTransferase 2A (KMT2A). Here, we will continue to refer to the older, more popular name MLL (mixed lineage leukaemia). Figure 3 demonstrates the structure of MLL and MLL fusion proteins.

The *MLL* gene is located at chromosome 11, band q23. The size of the gene is approximately 90Kb and it encodes a protein containing 3969 amino acids with a molecular weight of 430 kDA, which, in the cytoplasm undergoes post-translational cleavage. The threonine protease taspase1 cleaves MLL into two fragments: an N-terminal 320kDA (MLL^N) and a C-terminal 180 kDA (MLL^C). After cleavage, both MLL^N and MLL^C peptides remain noncovalently associated through the FYRN and FYRC domains. Both fragments are components of a large macromolecular complex with other partner proteins essential for efficient gene transcription. The two MLL fragments (MLL^N and MLL^C) display opposite transcriptional properties. The MLL^N is involved in chromatin targeting and regulation of MLL activity and represses transcription of target genes. When MLL^C dimerises with MLL^C, the complex activates transcription.

The first domain at the N-terminus of the MLL^N is the menin-binding domain (MBD). Following binding to menin (multiple endocrine neoplasia 1, a protein lost in familial cancer syndromes), the menin/MLL interface then binds to LEDGF (lens epithelium-derived growth factor). LEDGF recognises di and tri-methylated H3K36 a mark of active transcription and is important in recruiting MLL to active chromatin. This tethering of the MLL complex to chromatin is an interaction found to persist in leukaemia.

The MBD is followed by three AT hooks, and their function is to recognise and bind to the minor groove of AT-rich DNA regions. These AT hooks stabilise protein-DNA interactions or mediate protein-protein interactions. Two highly conserved sub-nuclear localisation domains, SNL1 and SNL2, mediate the nuclear localisation of MLL proteins. The region following this has transcriptional repressive activity and recruits histone deacetylases HDAC1, HDAC2, co-repressor proteins CTBP and the polycomb proteins HPC2 and BMI-1. Within the repression domain is contained a domain showing homology with two proteins: DNA methyltransferase1 (DNMT1) and with methyl binding domain protein 1 (MBD1), both regulating transcription through methylation.

This region is a cysteine-rich zinc finger CXXC domain, responsible for MLL binding to unmethylated CpG DNA sequences which are frequently found in CpG islands marking active promoters (Daser and Rabbitts, 2005, Ayton and Cleary, 2003, Birke et al., 2002).

Next to the CXXC domain there are 4 plant homeodomain fingers (PHD), important for protein-protein interactions, and a bromodomain, which mediates binding to acetylated histones (Winters and Bernt, 2017) .

Within the MLL^C fragment there is a transcriptional activation domain (TAD), which promotes transcription by interacting directly with the histone acetyltransferases p300/CBP, MOZ and MOF transferring acetyl groups to H3K27, H3K9 and H4K16. The next histone modification activity is characterized by a C-terminal SET (Suppressor of variegation, Enhancer of zeste and Tritorax) domain that works as histone methyltransferase. SET domains catalyse the transfer of a methyl group from S-adenosylmethionine to a protein substrate and in the case of MLL, this is lysine 4 on histone H3, which can be monomethylated, dimethylated or trimethylated (H3K4me_{1,2,3}). H3K4me is a hallmark of actively transcribed chromatin, with monomethylation marking enhancers while dimethylation and trimethylation are found around the transcription start sites of active genes. It is this function that has led to MLL being renamed KMT2A, where lysine=K methyltransferase. In total six, enzymes with this catalytic activity have been identified in mammalian cells KMT2A (MLL1), 2B (MLL4), 2C (MLL3), 2D (MLL2), 2 F (SET1A) and 2G (SET1B). Optimal MLL SET domain activity is dramatically enhanced with the addition of three other proteins. The WD-repeat protein 5 (WDR5) presents the H3K4 tail for its methylation and together with retinoblastoma binding protein 5 (RbBP5) interacts directly with the SET domain of MLL. ASH2L does not bind directly MLL^C but interacts with RbBP5 and together they stabilise the MLL complex (Cao et al., 2014).

The MLL complex is recruited at the promoter of genes with poised transcriptional machinery, to methylate H3K4 and to activate transcription of

target genes. One of the most well described MLL targets are *homeobox* (*HOX*) genes. They are transcription factors involved in the control of development and haematopoietic differentiation. MLL is expressed in myeloid and lymphoid tissues and positively regulates expression of the clustered *HOX* genes through H3K4 methylation. The expression of these genes is later downregulated when terminal differentiation is induced in normal haematopoiesis. In *MLL*-rearranged leukaemia, the fusion also regulates the expression of the *HOXA* genes, but transcriptional repression does not occur. The aberrant expression of these genes, coupled with others, induces leukogenesis (Hess, 2004) .

In *MLL*-rearranged leukaemia, the balanced chromosomal translocations result in the deletion of the region encoding the MLL C-terminal moiety and the consequent in frame fusion of the region encoding the N-terminal MLL region with the 3' region of the translocation partner gene. The translocation results in the generation of chimeric proteins which alter the epigenetic landscape (Eguchi et al., 2003). The LMI, AT hooks and the CXXC domain are present in every known MLL fusion protein and have been determined to be necessary and sufficient to create a transforming protein if joined to an MLL fusion partner. The SET domain, the only defined area of wild type MLL to have catalytic methyltransferase activity, is not present in any MLL fusion oncoproteins. A loss of H3K4 methylation is likely to be complemented by other H3K4 methyltransferases or by remaining wild-type MLL encoded by the non-rearranged allele (Milne et al., 2002).

The chromosomal rearrangements of the *MLL* gene are associated with infant, paediatric, adult and therapy-induced acute leukaemia. To date, a total of 135 different *MLL* fusion partners have been identified, but a small number make up the majority of cases; AF9 (MLLT3), t(11:9); AF10 (MLLT10), t(11:10); AF6, (MLLT4), t(11.6); ELL (MLLT1) t(11:19); ENL (MLLT1) t(11:19) occur in 39%, 19%, 8%, 7% and 6% of MLL rearranged paediatric AML, respectively (Meyer et al., 2018). Here we have focussed predominantly on the chromosomal

translocations identified in paediatric AML, but detailed characterisation of the MLL fusion proteins found in infant ALL, paediatric ALL, adult ALL and therapy-induced leukaemia is available from the latest publication of the MLL Recombinome of acute leukaemia (Meyer et al., 2018).

The most frequent fusions partners are nuclear proteins: AF4, AF9, AF10, ENL and ELL. These are reviewed by (Dou and Hess, 2008). These fusion partners were found to participate in the super elongation complex (SEC), which suggests their function in the MLL fusions is to confer aberrant transcriptional elongation, leading to constitutive activation of MLL target genes (Lin et al., 2010) (Smith et al., 2011). The expression of MLL fusion proteins induces an abnormal epigenetic state with mis-targeting of transcriptional activity. *HOXA* genes are actively transcribed in MLL transformed cells and exhibit chromatin marks consistent with actively transcribed loci, included in H3 and H4 acetylation. MLL fusion proteins induce leukaemic transformation by maintaining upregulated expression of the A-cluster *HOX* genes, particularly *HOXA7*, *HOXA9* and the *HOX* co-factor *MEIS1*. It is frequently not overexpression of these genes, but rather that *Hox* expression is frozen at a level present in normal early haematopoietic stem and progenitor cells. The *HOX* genes in combination with *MEIS1* determine the self-renewal potential in this stem and progenitor population. The importance of dysregulated *Hox* gene expression in leukaemia has been demonstrated in several models. *HoxA7* and *HoxA9* were shown to mediate the myeloid transforming properties of the MLL fusion protein MLL-ENL. *HoxA9* was found to be required to induce MLL-leukaemogenesis *in vivo*, as *HoxA9* deficient murine bone marrow cells transduced with MLL-ENL did not induce leukaemia in recipient mice (Aytton and Cleary, 2003). The *Hox* code was studied by work from our laboratory using an inducible model of MLL-ENL leukaemia in murine progenitor cells and demonstrated that loss of the MLL-ENL fusion protein led to decreased expression of *Hox* cluster genes (Horton et al., 2005). Despite the importance and evidence that MLL fusions lead to aberrant *HOXA* expression, there are examples where the *HOXA* signature is

unaffected. Trentin et al studied patients with t(4;11) infant leukaemia with MLL AF4. The cases fell into 2 distinct groups, one of which did not show the characteristic *HOXA* signature (Trentin et al., 2009). The absence of the typical *HOXA* signature was associated with a 3–4 times higher risk of relapse (Stam et al., 2010). Work from the Slany lab demonstrated that MLL-ENL leukaemogenic activity could be substituted by *HOXA9* and *MEIS1* overexpression (Zeisig et al., 2004). Further studies showed that the transcription factor c-MYB was a transcriptional target of *HOXA9/MEIS1*, necessary but not sufficient for their leukaemogenic activity (Hess et al., 2006).

Having shown the essential role of c-MYB in MLL-ENL transformation, Jin et al demonstrated that c-MYB is recruited to the MLL histone methyltransferase complex by menin, a protein recruited to the LMI region on the MLL N-terminus and that it substantially contributes to MLL-mediated H3K4me. Silencing c-MYB led to a global decrease in H3K4 methylation, an unexpected decrease in *HOXA9* and *MEIS1* gene expression, and decreased MLL and menin occupancy in the *HOXA9* gene locus. They proposed that c-MYB, and *HOXA9* and *MEIS1* are linked in an autoregulatory loop in MLL-associated leukemogenesis (Jin et al., 2010).

The role of c-MYB has been highlighted with other *MLL* fusion genes. Zuber et al demonstrated that MLL-AF9 contributes to leukaemia maintenance by enforcing a genetic signature similar to that regulated by c-MYB. Here, MLL-AF9 was found to directly regulate *c-Myb* transcription by binding to its promoter (Zuber et al., 2011). In this study, other genes directly regulated by MLL-AF9 included *Meis1*, *Irx5*, *FoxP1* and *c-Myc*. A different study identified that *c-Myb*, *Hmgb3* and *Cbx5* were sufficient to immortalised myeloid progenitors in the absence of *HoxA* gene upregulation (Somerville et al., 2009). Taken together, these studies indicate that c-MYB functions to mediate the oncogenic activity of MLL-fusions in MLL rearranged AML.

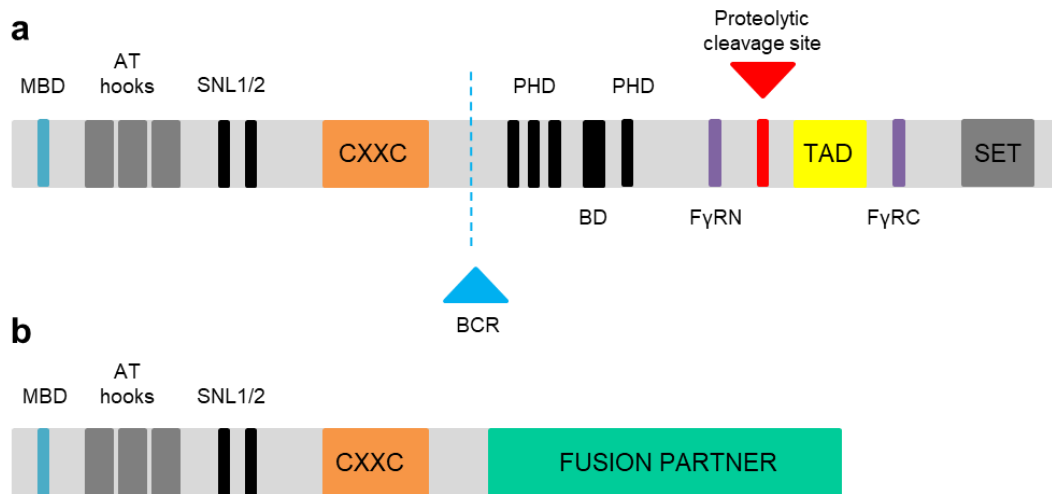


Figure 3 MLL and MLL fusion proteins.

Schematic diagram illustrated (a) Wild-type MLL and (b) MLL fusion proteins. In the upper diagram (a), MBD, Menin-binding domain; AT hooks: SNL, speckled nuclear localisation domains; CXXC domain; BCR, breakpoint cluster region; PHD, PHD fingers; BD, bromodomain; FyRN and FyRC are the domains whereby MLL-N and MLL-C interact after cleavage; TAD, transactivation domain; SET, H3K4 histone methyltransferase domain. The lower diagram (b) in which MLL fusion proteins are caused by chromosomal rearrangements between N-terminal MLL (to the BCR) and a fusion partner. PHD, transactivation domains and the SET domain are lost. Figure adapted from (Winters and Bernt, 2017).

1.6 c-MYB in haematopoiesis and leukaemogenesis

The transcription factor c-MYB has a central role in the regulation of normal haematopoiesis and leukaemogenesis. It is the cellular counterpart of *v-myb*, first identified as an oncogene capable of forming leukaemia in chickens. It is part of a family of transcription factors with A-MYB (Mybl1) and B-Myb (Mybl2) which have different roles in various tissues.

The *MYB* gene locus is located at chromosome band 6q23.3. The encoded protein c-MYB is a 75 kDA transcription factor that acts as a transcriptional activator that recognises and binds to the sequence t/cAAcT/gG, known as the MYB binding site (MBS) (Biedenkapp et al., 1988). The c-MYB protein has three distinct functional domains; a C-terminal negative regulatory domain (NRD); a central transactivation domain (TAD) and a highly conserved N-terminal DNA-binding domain (DBD) through which gene expression is regulated. A schematic diagram of c-MYB is seen in Figure 4

The TAD of MYB has been shown to bind to multiple coactivators, including the KIX domain of the lysine acetyltransferases CBP/p300. The c-MYB:CBP/p300 complex enhances transcription modifying chromatin at promoters, acetylating c-MYB and bridging the gap between c-MYB and the basal transcription machinery. Negative regulation of transcription can occur when c-MYB interacts with the histone acetyltransferase, TIP60 (Zhao et al., 2012). The negative regulatory function of the NRD was demonstrated when its deletion was shown to increase DNA binding and transactivation, and it was shown to be important for post-translational modification of c-MYB including ubiquitination which can negatively regulate its activity and stability (Corradini et al., 2005).

In normal haematopoiesis, regulation of c-MYB is tightly co-ordinated at different stages of differentiation and maturation. Both *c-myb* mRNA and protein are highly expressed in immature haematopoietic precursors and levels decrease as the cells mature and differentiate (Gonda and Metcalf, 1984) (Duprey and Boettiger, 1985). These studies review a key function of

MYB is to maintain the proliferative progenitor-cell phenotype and that downregulation is necessary for differentiation. MYB has a short half-life (~30 minutes) and undergoes post-translational modifications such as ubiquitylation, phosphorylation, acetylation and sumoylation, which affects activity by altering protein level, DNA binding or transactivation capacity (Ramsay and Gonda, 2008). To examine the function of c-MYB in human bone marrow mononuclear cells, *c-myb* antisense oligodeoxynucleotides were used to reduce expression, which led to decreased *in vitro* colony forming activity (Gewirtz and Calabretta, 1988). To better define its biological function, Mucenski *et al*, inactivated the *c-myb* gene by homologous recombination in embryonic stem cells (ES). Heterozygous mice carrying this *c-myb* mutant (*c-myb*^{+/-}) allele appeared phenotypically normal, but their *c-myb*^{-/-} progeny died by embryonic day 15 because of a failure to establish definitive haematopoiesis. (Mucenski *et al.*, 1991). Additional work using ES *c-myb*^{-/-} chimeras, suggested that haematopoiesis can be initiated in the absence of *c-myb*, but subsequent development is prevented (Sumner *et al.*, 2000). Emambokus *et al*, described the effects of a knockdown allele of *c-myb*, which expresses 5-10% of the wild-type level of c-MYB and show this reduced level is sufficient to allow progenitor development and expansion (Emambokus *et al.*, 2003). However, there was a differential effect on their stage- and lineage-commitment with reduced erythroid (BFU-E), and granulocytic (CFU-G or CFU-GM) colonies, and an increase in monocyte/macrophage (CFU-M) and megakaryocytic colonies. Lymphoid differentiation was also impaired. Finer control of c-MYB at different stages of cellular maturation has been examined using a tetracycline-inducible *c-myb* transgene. It is interesting that activation of expression of c-MYB, as well as down-regulation is important for c-MYB to regulate differentiation in haemopoietic cells. For instance, activation of the *c-myb* transgene in *c-myb*^{-/-} mice was able to rescue *in vitro* haematopoiesis, however, forced expression of c-MYB appeared to inhibit terminal maturation of megakaryocytes and erythrocytes (Sakamoto *et al.*, 2006). A conditional *c-myb* knockout was used

to interrogate the role of *c-myb* in adult haematopoietic stem cells. Disruption of *c-myb* resulted in reduced HSC numbers, impairment of their self-renewal capability and aberrant differentiation. This data suggest a critical role of *c-myb* in the maintenance of adult HSC and haematopoiesis (Lieu and Reddy, 2009).

MYB target genes are numerous, mostly positively regulated and can be separated into three broad functional groups. The first are those that act as 'housekeeping genes' (*MAT2A* and *GSTM1*). Secondly, genes that confer a specific function of a differentiated cell type, for example *ELA2* (neutrophil elastase) to a neutrophil. The third group can be categorised into those leading to proliferation (*MYC*, *CCNA1*), cellular survival (*BCL2*, *HSP70*) and differentiation (*GATA3*).

Expression of c-Myb also plays a key role in stem cells from other tissues, including epithelial cells in colonic crypts and neural stem cells in adult brain. The relative activity of the *MYB* promoter is constant from one cell type to another, but mature *MYB* mRNAs are closely restricted to tissues with high cellular turnover where it plays a role in proliferation and differentiation (haematopoietic system and intestinal tissues). Within the gastrointestinal tract, MYB has been found to be a key regulator of the adult colonic crypt: *MYB* hypomorphic mutant mice were found to have a reduction in crypt size and proliferation and cellular differentiation was disordered when compared to normal (Ramsay and Gonda, 2008). In the adult brain, MYB has been shown to have effects on ependymal cells which support the neurogenic stem cell niche and in particular, neural progenitor cells (NPC's). Reduction of *MYB* in mouse models led to structural brain and cranial abnormalities, and morphological abnormalities of the supporting ependymal cells and loss of expression of the key neurogenesis genes *Pax6* and *Sox2* (Malaterre et al., 2008).

In contrast to its expression normal haematopoiesis, when c-MYB is not tightly regulated at different stages of differentiation and maturation, it can promote

neoplastic transformation (Zuber et al., 2011). Overall *c-MYB* is rarely mutated in acute leukaemia. Recurrent chromosomal translocations involving the *c-MYB* locus have been reported in patients with T-cell acute lymphoblastic leukaemia (T-ALL) (Clappier et al., 2007) and in rare cases of AML (Murati et al., 2009). In a subset of T-ALL, MYB has also been shown to play an important role. Mansour et al observed that around 25% of T-ALL expressed high levels of the *TAL1* oncogene, encoding a DNA-binding transcription factor, but did not contain the previously identified large rearrangements near *TAL1* that could explain the high expression level. Sequencing of cell lines and primary T-ALL samples revealed small insertions of 2 to 18 base pairs located upstream of the *TAL1* transcription start site. All the insertions introduced novel binding sites for c-MYB. c-MYB binding also recruited other transcription factors that regulate haematopoiesis (GATA3, TCF12, RUNX1, and TAL1), as well as the transcriptional coactivator CBP, to the affected region. This small insertion led to super-enhancer formation driving expression of the *TAL1* oncogene. The identification of c-MYB, which functions as a master transcription factor, and the subsequent recruitment of other components of the transcription machinery such as CDK7 and BRD4, offers new promising targets in future therapeutic approaches, as these are now specifically targetable with drugs (Mansour et al., 2014).

Much of the data characterising the role of c-MYB in the maintenance of AML uses AML models with an MLL fusion oncoprotein (MLL-AF9 or MLL-ENL). Zuber *et al* (Zuber et al., 2011) used inducible MLL-AF9 knockdown in a mouse model and identified *c-myb* as the most differentially expressed direct target. They demonstrate binding of the *c-myb* promoter by the MLL fusion, and differential effects between normal haemopoietic and leukaemia cells of *c-myb* silencing. Knockdown of *c-myb* in MLL-AF9 cells led to eradication of leukaemia and increased survival of transplanted mice, underpinning its therapeutic potential. They and others (Somervaille et al., 2009) have demonstrated that c-MYB regulates a leukaemic stem cell transcriptional programme. The role of c-MYB in maintaining an aberrant transcriptional

network is not restricted to MLL fusion induced leukaemogenesis. A number of recurrent chromosomal translocations giving rise to fusion genes such as *AML-ETO*, *E2A-HLF* and *BCR-ABL* have been shown to increase c-MYB expression or require c-MYB expression to induce transformation (Pattabiraman and Gonda, 2013) (Waldron et al., 2012).

The evidence that predominantly unmutated *MYB* is located functionally downstream of genomic alterations such as *MLL*-fusions and other fusion oncogenes, and yet is necessary and sufficient for leukaemia maintenance, indicates that it functions as a master regulator in leukaemia (Califano and Alvarez, 2017). If we hypothesize that irrespective of the upstream genetic fusion or epigenetic modification, c-MYB maintains aberrant transcriptional pathways essential for the cancer cell, this makes targeting c-MYB a rational approach for treatment for many different subtypes of acute leukaemia.

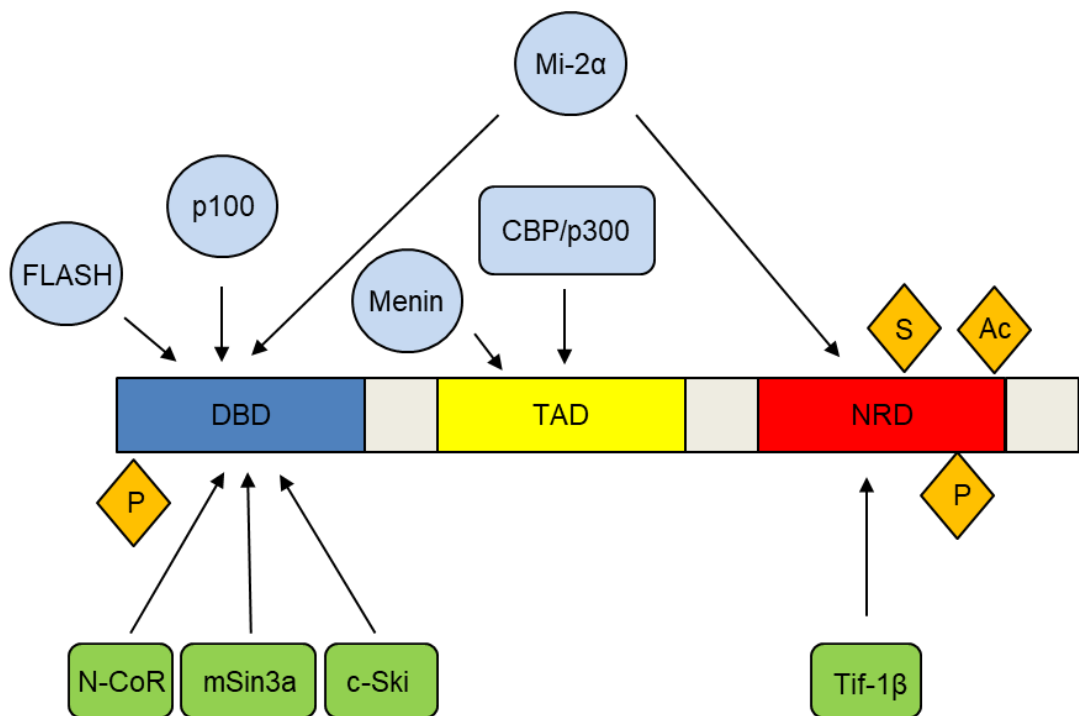


Figure 4. Schematic diagram of c-MYB.

Schematic diagram showing the tree main functional domains of c-MYB: DBD, DNA-binding domain; TAD, transactivation domain and an NRD, negative regulatory domain. The major regulators of c-MYB activity and function (pale blue: co-activators, green: co-repressors, orange; post-translational modifications). Adapted from (Pattabiraman and Gonda, 2013).

1.7 Targeting c-MYB in AML

Targeting c-MYB offers the potential to specifically disrupt leukaemia specific transcriptional programs that are used by the majority of AML subtypes. Much like other transcription factors, MYB is difficult to target due to the lack of a clear functional pocket or structure which is amenable to small molecule drug inhibition. Different strategies have been developed to overcome or circumvent these problems and may offer a solution to targeting c-MYB in AML. A schematic diagram of the sites of action described below can be seen in Figure 5.

The first approach is to disrupt the association of MYB from its coactivators or epigenetic regulators. The best described is the KIX domain of the lysine acetyltransferases CBP/p300. MYB and p300 interact via a LXXLL motif located in the TAD of c-MYB and the KIX-domain of p300. Mutations within the LXXLL motif disrupt the interaction and lead to an almost complete loss of MYB activity. Celastrol, a small molecule inhibitor derived from a plant was identified as an inhibitor of this interaction. Molecular docking studies suggested that Celastrol binds to the same hydrophobic groove of the KIX domain, thereby competing with MYB (Uttarkar et al., 2016). The same group also identified another compound, Naphthol AS-E phosphate, which inhibits MYB by a similar manner demonstrating this interaction is amenable to pharmacological inhibition (Uttarkar et al., 2015). Treatment with these agents led to anti-leukaemic activity *in vitro* and *in vivo*. More recently, Ramaswamy *et al*, developed a stabilized, cell-penetrant peptidomimetic inhibitor of MYB:CBP/P300 binding, termed MYBMIM. Treatment with this inhibitor led to disassembly of the MYB:CBP/P300 complex. MYB was eliminated from enhancers and promoters of target genes and led to down-regulation of MYB-dependant gene expression in AML cells. Functionally, this led to induction of apoptosis in AML cell lines and reduction of leukaemia progression in mouse xenografts of AML (Ramaswamy et al., 2018). Inhibition of the interaction between MYB and a different transcriptional coactivator, TFIID (transcription

factor II D) has also been reported. TFIID comprises a TATA-box binding protein (TBP) and 13 TBP-associated factors (TAF's) and whilst the whole complex is needed for transcriptional activation, individual TAF subunits perform specialised functions for different TF. Xu *et al*, identified that TAF12 is a coactivator of MYB and protects it from degradation. The heterodimer of TAF12 and 4 interacts with the TAD of MYB. Expression of a peptide capable of repressing this interaction impaired MYB function and led to regression of AML in mouse models (Xu et al., 2018).

BRD4 inhibition is a novel therapeutic approach currently in clinical trials. BRD4 is a prominent example of a chromatin reader protein and belongs to the bromodomain and extra terminal (BET) family of proteins. As a reader of the histone code, BRD4 accumulates on hyper-acetylated chromatin regions where it recruits a large platform of transcription regulating proteins, which forms a bridge between enhancers and promoters, favouring and stabilising the binding of RNA-POLII. Inhibition by the recently developed BET-inhibitors (BETi) competes with acetylated residues at the BRD4 bromodomains, releasing BRD4 from chromatin and reducing RNA-POLII throughput and transcription of key genes (Donati et al., 2018). Originally thought to be specific for MLL fusion leukaemia (Dawson et al., 2011), it has since been shown several haematopoietic TF (PU.1, FLI1, ERG, C/EBP α and MYB) use BRD4 and p300/CBP as linked cofactors to maintain the leukaemia state, and BET inhibition leads to the blockade of TF-dependant transcriptional activation (Roe et al., 2015). Despite promising pre-clinical studies, this efficacy has not yet been translated clinically. A phase 1 trial of the Bet inhibitor MK-8628 (formally known as OTX015) in refractory adult patients with only 3/36 cases achieving complete remission (CR) or complete remission with incomplete count recovery (CRi) (Berthon et al., 2016). Other BET inhibitors, such as CPI-0610 are being assessed in phase 1 and 2 trials in adults with AML (NCT02698189).

A different approach is to interrupt TF binding to DNA. Whilst not reported in c-MYB, it has been used for the critical transcription factor in AML, PU.1. Here a small molecule inhibitor that specifically prevents PU.1-chromatin binding by interaction with the DNA minor groove that flanks its binding motifs. This physical interruption led to downregulation of PU.1 transcriptional targets, and in mouse AML models, treatment resulted in prolonged survival (Antony-Debre et al., 2017).

An alternative strategy is to promote degradation of oncogenic transcription factors. Small molecules or peptides are designed to bind the protein of interest. These molecules can then be fused to a linker that brings them into proximity of an E3 ubiquitin ligase. These ubiquitinated proteins would then be susceptible to proteasomal degradation. This has been demonstrated in Burkitt's lymphoma (BL), when a Proteolysis Targeting Chimera (PROTAC) (ARV 825) was used to recruit BRD4 to the E3 ubiquitin ligase cereblon, leading to fast, efficient and prolonged degradation of BRD4 in all BL cell lines tested (Lu et al., 2015). Recently, the same construct led to BRD4 degradation in AML and simultaneously targeted LSCs and the leukaemia microenvironment and led to prolonged survival in a mouse model of human leukaemia which included AML patient-derived xenografts (AML PDX) (Piya et al., 2019).

Our group recently reported that mebendazole, the widely used anti-worm medication led to proteasomal degradation of c-MYB and *in vitro* and *in vivo* antileukemic activity across different AML subtypes (Walf-Vorderwulbecke et al., 2018). The approach used was to identify a c-MYB gene expression signature from *MLL*-rearranged AML to probe the connectivity Map database, hosted by the Broad institute. Mebendazole was identified as the top hit, predicated to inverse the c-MYB signature in AML. Treatment led to inhibition of colony formation across a panel of AML cell lines, with different oncogenic mutations, demonstrating its use was not restricted to *MLL*-rearranged AML. Reassuringly, there was no impact of transient exposure to mebendazole on

colony formation by normal CD34⁺ cells. The heat shock protein 70 (HSP70) chaperone system was implicated as targeting c-MYB for enhanced degradation. Further pre-clinical validation is required before mebendazole can be taken forward into clinical trials in AML. This work will be further discussed in the results chapters.

In summary, there is a renewed interest in targeting of c-MYB as a therapeutic approach in AML. The examples discussed above have modulated transcriptional activation via different mechanisms and generated encouraging pre-clinical data that c-MYB is a valid and attractive target in the care of patients with AML.

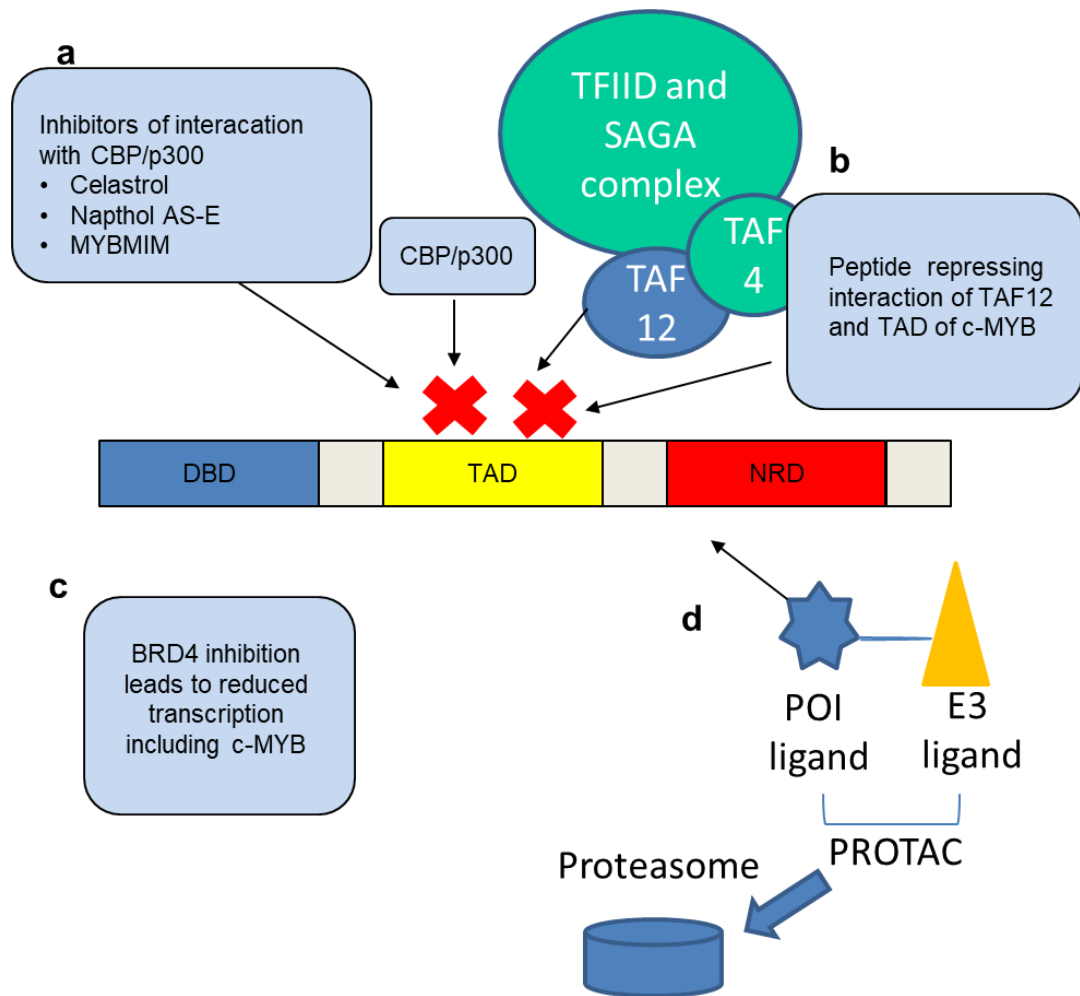


Figure 5. Schematic diagram of c-MYB targeting compounds.

Schematic diagram showing the tree main functional domains of c-MYB: DBD, DNA-binding domain; TAD, transactivation domain and a NRD, negative regulatory domain. Sites where c-MYB-targeting drugs have been identified to function. (a) Inhibitors of the interaction between the TAD of c-MYB and its coactivator CBP/p300. (b) Inhibition of a different coactivator of c-MYB, TFIID. (c) BRD4 inhibition reduces transcription. (d) Promotion of degradation of c-MYB by proteolysis targeting chimera (PROTAC). Here, the Protein of Interest (POI) is brought into contact with ubiquitin by the PROTAC and then targeted for proteasomal degradation.

Project Aim

The transcription factor c-MYB is recognised to play a central role in the development and maintenance of AML. Recent studies have demonstrated pre-clinical evidence that c-MYB can be deregulated to impair leukaemia progression in AML models. A strategy developed by my host laboratory has identified compounds predicted to inhibit c-MYB in AML. The aim of this PhD project was to investigate the steroidal lactone, withaferin A (WFA), a candidate hit predicted to inhibit c-MYB in AML.

Therefore, my objectives were:

- To determine if WFA inhibits c-MYB by interfering through c-MYB transcriptional pathways in AML
- To characterise WFA activity *in vitro* using AML cell lines and determine the mechanism by which WFA deregulates c-MYB protein levels.
- To determine whether AML and ALL PDX cells are susceptible to WFA and whether WFA treatment could limit leukaemia progression *in vivo*, using pre-clinical leukaemia models?

Chapter 2: Materials and Methods

2.1 Molecular biology

2.1.1 Transformation of competent bacteria

One Shot™ Stbl3™ Chemically Competent *E. coli* (Invitrogen) or Sub-cloning Efficiency DH5α™ Competent cells (Invitrogen) were used. According to manufacturer's instructions, bacteria were thawed on ice, mixed with 10-100ng plasmid DNA and left for 30 minutes on ice. The cells were heat-shocked for 20-40 seconds at 42°C, then returned to ice for 2 minutes. 250 µl of pre-warmed SOC medium was added to the cells and incubated in a shaker at 37°C for 1 hour. The total volume (or dilution of it) was spread onto agar plates containing LB (for 100 ml LB, 15g bacto Agar) and 100 µg/ml ampicillin (Sigma Aldrich) and incubated overnight at 37°C.

2.1.2 Isolation of plasmid DNA

Individual bacterial colonies were inoculated in 5 ml LB broth (1% w/v Bacto Tryptone (BD Bioscience). 0.5% w/v Bacto Yeast Extract (CD Bioscience), 1% w/v Sodium Chloride [pH7.0]), containing 100 µg/ml ampicillin for selection and incubated in the shaker (225 rpm) overnight at 37°C. Plasmid DNA was then isolated from the bacterial culture using Zyppy™ Plasmid Miniprep Kit (Zymo Research) according to manufacturer's instructions. For larger amounts of DNA, individual bacterial colonies were inoculated in 3 ml LB broth with 100 µg/ml ampicillin and incubated in the shaker (225 rpm) at 37°C for 6 hours. 400 µl of this culture was added to 400 ml of LB with 100 µg/ml ampicillin and incubated overnight in a shaker at 37°C. The plasmid DNA was extracted using the Genopure Plasmid Maxi or Midi Kit (Roche) according to manufacturer's instructions. Following either extraction method, the DNA concentration was measured using a NanoDrop N-1000 (Labtech International). The spectrophotometer measures the absorbance at 260 nm and 280 nm, a ratio of 1.8 or higher is acceptable for DNA.

2.1.3 Restriction enzyme digests

Restriction enzymes (Thermo Scientific) were used to cleave double stranded DNA. The digests were set up according to the manufacturer's instructions. Briefly, up to 1 µg of plasmid DNA was digested with 1 µl of fast digest enzyme in the presence of 2 µl of 10x restriction buffer. The total volume was made up to 20 µl with water. The digested product was incubated as per the enzymes specification. The product was subjected to electrophoresis on 1% w/v Agarose gels (Agarose (Invitrogen), 1 x TAE buffer, National diagnostics), 1x GelGreen® (Biotium)).

2.1.4 DNA constructs

- Lentiviral gene overexpression

The Δ MYB cDNA (Corradini et al., 2005) was cloned into pCSGW-IRES-eGFP vector (Demaison et al., 2002). This cloning had been performed by Dr Jasper de Boer (Figure 6).

- Constitutive gene downregulation.

Previous work in the group had validated one shMYB (shMYB 17; TRCN0000295917), but we required an additional construct, to control for possible off-target effects. The following short-hairpin sequences (TRCN0000009853; TRCN0000040062; CN0000010388, dharmacon) were in a MISSION® pLKO.1-puro vector (Figure 6).

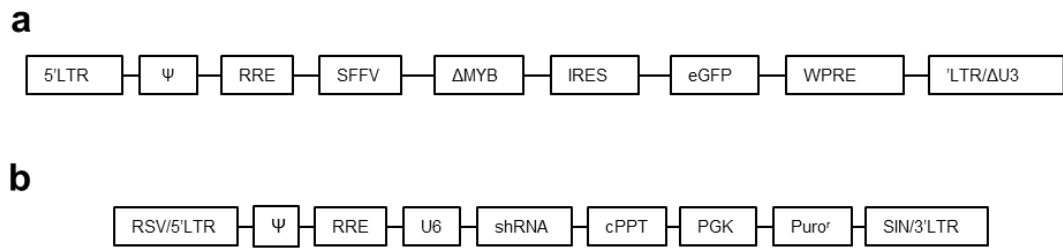


Figure 6 Schematic diagram of lentiviral vectors

(a) CSGW-IRES-eGFP vector, (b) MISSION® pLKO.1-puro vector. LTR, long terminal repeat; Ψ , viral packaging signal; RRE, Rev-Response Element; SFFV, Spleen focus-forming virus promoter; IRES, Internal ribosome entry site; GFP, Green Fluorescent protein; WPRE, Woodchuck response element; RSV, respiratory syncytial virus; cPPT, Central Polypurine tract; Puro^r, Puromycin resistance gene.

2.1.5 Western blot analysis

1×10^6 cells were centrifuged at 525 xg for 5 minutes and supernatant discarded. Cell pellets were lysed in 110 μ l of Reducing Sample Buffer (200 mM Dithiothreitol (DTT), 2% w/v Sodium dodecyl sulphate (SDS), 10% w/v Glycerol, 125 mM TRISHCL (ph 6.8)). Samples were incubated at 100°C, for 5 minutes, vortexed for 10 seconds and centrifuged at 11688 xg for 10 minutes at 4°C. The total cell lysate supernatants were collected and stored at -80°C or used immediately. In order to denature proteins before loading, samples were incubated at 100°C for 5 minutes and kept on ice until loading.

Protein samples were resolved on 10% polyacrylamide gels (Table 3) in a 1x running buffer diluted from 20x MOPS (1M TRIS, 1M MOPS, 20mM EDTA, 20% w/v SDS) supplemented with 5 mM Sodium bisulphate (NaHSO₄). Gels were transferred onto nitrocellulose (LI-COR Biosciences, Cambridge, UK) membranes for 3 hours at 400 mA, at 4°C in 1x transfer buffer diluted from 10x TRIS/Glycine (0.27 M TRIS, 1.92M Glycine) with 20% v/v Methanol. Membranes were blocked in either PBS/0.1% v/v Tween 20 (PBST) with 5% w/v non-fat milk or TBS/0.1% v/v Tween 20 (TBST) with 5% w/v bovine serum albumin (BSA) for 1 hour at room temperature and then stained overnight in primary antibody at 4°C (Table 4). The membranes were washed with PBST/TBST 3 times over 20 minutes and the incubated for 1 hour with secondary antibody diluted in PBST/5% w/v non-fat milk or TBST with 5% w/v bovine serum albumin at room temperature (Table 5). The membranes were then washed with PBST 3 times over 20 minutes. Membranes were visualised and quantified using the Odyssey® CLx and Image studio software (LI-COR Biosciences). This system provides accurate quantification of protein band intensity. Primary and secondary antibodies used are listed below. In some experiments membranes were stripped using NewBlot™ IR Stripping Buffer, 5X (LI-COR Biosciences) for 20 minutes and room temperature and then re-probed with different primary and secondary antibodies.

Table 3 Components of SDS-PAGE gels

	10% resolving gel		10% Stacking gel	
	1 gel	2 gels	1 gel	2 gels
H ₂ O	3.4 ml	6.8ml	2.1 ml	4.2 ml
1.25M Bis-Tris(ph6.8)	2.6ml	5.3ml	0.7ml	1.4ml
30% w/v acrylamide	3ml	6ml	0.7ml	2.2 ml
10% w/v APS	50µl	100µl	50 µl	100 µl
Temed	6µl	12µl	6 µl	12 µl

Table 4 Primary antibodies used in western blot analysis

Name	Dilution	Supplier
c-MYB EPR 718	1:1000	Abcam, Cambridge, UK
β-Actin mouse (sc-47778)	1:1000	Santa Cruz Biotechnology
Phospho-eIF2α (ab131505)	1:1000	Cell Signaling Technology
eIF2α (ab137626)	1:1000	Cell Signaling Technology

Table 5 Secondary antibodies used in western blot analysis

Name	Dilution	Supplier
Donkey anti-Rabbit IRDYe R 800CW	1:10000	LICOR Biosciences
Donkey anti-Mouse IRDye R 680RD	1:10000	LICOR Biosciences

2.1.6 RNA isolation

Total RNA was isolated using the RNeasy Mini Kit (Qiagen) according to manufacturer's instructions. Cells were disrupted by adding lysis buffer RLT, containing β -mercaptoethanol. To ensure complete homogenization, samples were vortexed for 30 seconds at the highest settings. One volume of 70% ethanol was added to the samples and the mixture transferred into an RNeasy spin column. Columns were centrifuged for 15 seconds at 10,000 xg and the flow-through was discarded. 700 μ l of wash buffer RW1 were added to the column followed by centrifugation. Samples were then washed twice with 500 μ l of wash buffer RPE. The RNA was eluted with 30 μ l of nuclease free water and the concentration determined using a spectrophotometer (NanoDrop ND-1000, Lebtch International). The ratio of absorbance at 260 nm to 280 nm was used to assess the purity of RNA. A ratio of \sim 2.0 is accepted as pure for RNA (NanoDrop user's manual)

2.1.7 cDNA preparation

RNA was converted into cDNA using the High Capacity RNA-to-cDNA kit (Applied Biosystems) according to the manufacturer's instructions. 1 μ g of RNA was converted using 1 μ l of 20x enzyme mix, 10 μ l of 2x RT Buffer Mix in a total volume of 10 μ l, made up with water.

2.1.8 Quantitative RT-PCR analysis

Quantitative Reverse Transcription (qRT-PCR) was performed on isolated cDNA. Quantitative RT-PCR was also performed on mRNA using Sybr-green technology, SensiFAST™ SYBR Hi-Rox mastermix (BIOLINE) (Table 6). In all measurements *UBC* was used as the housekeeping gene. All reactions were performed on a Step One Plus (Applied Biosystems). Melting curves analysis was performed to verify the assay.

Table 6 Gene primers for Sybr-green

Gene	Forward	Reverse
<i>MYB</i>	AGCAGGTGCTACCAACACAG	GCAGAGATGGAGTGGAGTGG
<i>IRF8</i>	TGACGGGGTACACCACCTAC	GCCCCATAGTAGAAGCTGA
<i>IRX3</i>	CTCTCCCTGCTGGGCTCT	CCAAGGCACTACAGCGATCT
<i>GFI-1</i>	AACGGAGCTCGGAGTTTGA	ATGGGCACATTGACTTCTCC
<i>MYC</i>	CAGCGACTCTGAGGAGGAAC	GCTGCGTAGTTGTGCTGATG
<i>UBC</i>	TTATATAAGGACGCGCCGGG	CACGAAGATCTGCATTGTCAAGT

2.2 Animal work

All mice were maintained in the UCL Great Ormond Street Institute of Child Health animal facilities. Experiments were performed according to and approved by the United Kingdom Home Office regulations and followed UCL Great Ormond Street Institute of Child Health institutional guidelines. Dr. Owen Williams and Dr. Luca Gasparoli performed xenotransplantations on 5-12-week-old NOD.Cg-Prkdc^{scid}Il2rg^{tm1Wjl}/SzJ (NSG) mice. NSG mice lack mature T cells, B cells and natural killer (NK) cells and are deficient in multiple cytokine signalling pathways, they have multiple defects in innate immunity.

2.3 Cell biology

2.3.1 Cell lines and tissue culture

Human leukaemic cell lines (Table 7 and Table 8) were obtained from DSMZ or ATCC. The identity of the cell lines was confirmed by STR profiling by the Great Ormond Street Hospital haematology department. With the exception of SHI-1, the other ALL and AML cell lines were cultured in Roswell Park Memorial Institute medium (RPMI, Sigma), supplemented with 10%-20% v/v heat-inactivated FCS, 100U/ml Penicillin, 100ug/ml Streptomycin and 2mM L-glutamine (RPMI 10%). SHI-1 (AML) cells were cultured in Iscove's Modified Dulbecco's Medium (IMDM, Sigma) supplemented with 20% v/v heat-inactivated FCS, 100U/ml Penicillin, 100ug/ml Streptomycin and 2mM L-glutamine (complete IMDM). Each cell line was sub-cultured every 3-4 days and plated according to the supplier's guidelines. These cell lines were selected as they are derived from predominantly paediatric B-ALL and AML, and harbour common cytogenetic changes frequently found in these diseases. Cell lines were regularly tested for Mycoplasma pneumoniae.

Table 7 Acute lymphoblastic leukaemia cell lines

Cell lines	Translocation	Fusion gene	Clinical origin of cell line (year developed)
REH	t(12;21)	ETV6-RUNX1	15-year-old girl at 1 st relapse of B-ALL (1973)
697	t(1;19)	TCF3-PBX	12-year-old boy with B-ALL (1979)
SUPB15	t(9;22)	BCR-ABL	9-year-old boy with 2 nd relapse of B-ALL (1984)
SEMK2	t(4;11)	MLL-AF4	5-year-old girl at 1 st relapse of B-ALL (1990)
BEL-1	t(4;11)	MLL-AF4	41-year-old female with B-ALL (2004)

Table 8 Acute myeloid leukaemia cell lines

Cell lines	Translocation	Fusion gene	Clinical origin of cell line (year developed)
THP-1	t(9;11)	MLL-AF9	1-year-old boy relapsed AML, monocytic morphology (1978)
SHI-1	t(6;11)	MLL- AF6	37-year-old man with relapsed AML, monocytic morphology (2002)
MV4-11	t(4;11)	MLL-AF4	10-year-old boy with biphenotypic B-myelomonocytic leukemia.
OCIAML3	Normal cytogenetics	NPM1 mutation	57-year-old man with AML, monocytic morphology. (1987)
U937	N.A Histiocytic Sarcoma)	N.A	37-year-old man with diffuse histiocytic lymphoma (1974)

2.3.2 Primary ALL and AML PDX samples

Primary ALL/AML PDX models were generated from excess diagnostic material from patients diagnosed with leukaemia at Great Ormond Street Hospital for Children (REC ref# 14/EM/0134), or from collaborating institutions. Diagnostic samples were injected into NOD-SCID- $\gamma^{-/-}$ (NSG; The Jackson Laboratory, Bar Harbour, ME, USA) sub-lethally irradiated (2Gy) 24 hours prior to transplant by Dr Owen Williams and Dr Luca Gasparoli. Their characteristics are listed in Table 9 and Table 10.

The mice were monitored and when they showed signs of distress or disease they were sacrificed. Leukaemia cells were recovered from bone marrow and spleen and cryopreserved. For experiments in this thesis, cells were thawed, and human cells enriched by mouse cell depletion using magnetic separation (Miltenyi biotec) and stored in liquid nitrogen.

Table 9 Characteristics of B-ALL PDX samples

ID	Sex	Immunophenotype	Age	Fusion gene/Cytogenetics
#1	M	Pre-B ALL	2.3	46 XY, gain of chromosomes X, 9, 21. Gain DXZ1, D9Z3, ABL1, RUNX1 and relative loss of one CDKN2A.
#2	F	Pro-B ALL	1.8	MLL-AF9

Table 10 Characteristics of AML PDX samples

ID	Sex	Age	Cytogenetics
#1	M	1.8	Complex karyotype
#2	F	3.3	MLL AF9
#3	N/A	N/A	MLL-AF9
#4	N/A	N/A	MLL-AF9
#5	F	6.4	Normal karyotype, AML FISH panel negative
#6	F	2.2	MLL-AF9
#6(r)	F	3	MLL-AF9 (same mutation)
#7	F	8.8	MLL-AF9
#8	M	0.5	Monosomy 7

N/A; not available.

2.3.3 Co-culture experiments

Mouse stromal cells (MS5) were cultured in Minimal Essential Medium (MEM, Sigma), supplemented with 10% v/v heat-inactivated FCS, 100 U/ml Penicillin, 100 µg/ml Streptomycin and 2 mM L-glutamine (complete MEM). $1.25 \times 10^5/\text{cm}^2$ MS5 cells were plated in 100 µl of complete MEM, in 96 well plates.

Human MSCs (MSC) were cultured in low glucose Dulbecco's Modified Eagle's Medium (DMEM, Sigma, supplemented with 20% v/v heat-inactivated FCS, 100 U/ml Penicillin, 100 µg/ml Streptomycin and 2 mM L-glutamine. Recombinant Human Protein (FGF-Basic, Gibco), was added 8 ng/ml just prior to use. $8 \times 10^4/\text{cm}^2$ MSCs were plated were plated in 100 µl of media, in 96 well plates.

For co-culture of B-ALL PDX cells, medium was removed from the stromal cells (MS5s and MSCs) cells 48-72 hours after plating when they had become confluent. Primary patient-derived ALL samples were thawed, counted and suspended in StemSpan™ Serum-Free Expansion Medium II (SFEM II, STEMCELL™ Technologies), supplemented with 50 ng/ml of IL7, IL3 and FLT3L. 2×10^5 cells per well were plated in 200 μ l of medium onto the MS5/MSC feeder layer. Cells were examined by microscopy, harvested, counted and re-plated at the same initial density in fresh medium every 3-4 days onto fresh feeder cells.

The same process was undertaken for AML PDX samples. After thawing, they were counted and suspended in StemSpan™ Serum-Free Expansion Medium II (SFEM II, STEMCELL™ Technologies), supplemented with StemSpan™ Myeloid expansion supplement (1x), 50 ng/ml of IL3 and FLT3L 50ng/ml. Leukaemia cells were plated at a density of 0.25×10^6 /ml in a 200 μ l of medium on to the MSC feeder layer.

In both cases, cells were examined by microscopy, harvested, counted and re-plated at the same initial density in fresh medium every 3-4 days onto fresh feeder cells.

All primary cells were harvested from underlying stromal layer by gentle pipetting. Examination by microscopy revealed the feeder layer was intact and minimal leukaemic cells remained *in situ*.

2.3.4 Colony formation assays

AML cell lines were plated at 150-500 cells/well in methylcellulose medium (HSC002, R&D system) in 24 well plates. Plates were incubated for 7-14 days and colonies visualised by staining with 1mg/ml p-iodonitrotetrazolium (INT). Transduced THP1 and B-ALL cells were plated at 500-1000 cells per well and visualised after 14-21 days. For pre-stimulation, THP1 cells were cultured in DMSO or 1.1 μ M WFA for 16 hours in complete RPMI. Cells were washed, counted and equal numbers of viable cells plated into HSC002. INT-stained

plates were scanned with a calibrated densitometer (GS-800, BioRad) and colonies quantified with the software package, OpenCFU. Colony numbers were averaged and then normalised against vehicle and/or vector only controls or plotted as colony forming frequency (number of colonies/number of cells plated).

Cord blood and AML PDX cells were plated at 1000 cells/well in 35 mm plates in HSC005 methylcellulose medium (R&D system) containing 50 ng/ml human SCF, 20 ng/ml IL3, IL6, G-CSFD, GM-CSF and 3 IU/ml EPO.

CD34⁺ human cord-blood derived cells were plated in HSC005 with DMSO or 1.0 μ M WFA, further supplemented with 100ng/ml human SCF, TPO and FLT3L (all growth factors from Peprotech). AML PDX cells were plated in HSC005 with DMSO or 1.0 μ M WFA, further supplemented with 50 ng/ml TPO and FLT3L. Plates were incubated for 10-14 days, after which colony morphology was assessed and scored.

2.3.5 Flow cytometric analysis

Cells were washed twice with FACS buffer (PBS supplemented with 1% w/v Bovine Serum Albumin (BSA) and 0.1% w/v Sodium Azide). Following staining, the cells were washed and re-suspended in 200 μ l FACS buffer.

Apoptosis was measured using Annexin V stain (BD biosciences) and Propidium Iodide (PI) and analysed on CyAn ADP (Beckman Coulter). Cells were washed with 1ml of 1x Annexin V binding buffer from a 10x stock solution (0.1 M Hepes[pH 7.4], 1.4M NaCl, 25 mM CaCl₂ solution) and incubated with fluorochrome-conjugated Annexin V (5 μ l per condition with 95 μ l binding buffer) for 15 minutes at room temperature in the dark. Cells were then washed with binding buffer and stained with 5 μ l PI with 95 μ l binding buffer on ice. 100 μ l of binding buffer was added prior to analysis.

Cell cycle analysis was performed using the Click-iT EdU Alexa Fluor 647 Flow Cytometry Assay Kit (Invitrogen, Life Technologies). Briefly, 10 μ M EdU was added to the cell culture 45 minutes prior to cell collection. Cells were

washed with FACS buffer, then fixed in 4% paraformaldehyde for 15 minutes. Cells were then washed again with FACS buffer and then 100 µL of 1X Click-iT® saponin-based permeabilisation and wash reagent. The Click-iT® Reaction components were prepared by mixing TBS pH8.5, CuSO₄, Alexa Fluor 647 fluorescent dye, 100 mM Ascorbic acid and water (reagents must be mixed in this order) and added to the cell pellet and incubated for 30 minutes in the dark. Cells were finally washed and re-suspended in Click-iT® saponin-based permeabilisation and wash reagent supplemented with Ribonuclease A and 50 µg/ml PI.

Flow cytometry was performed on an LSRII analyser (BD Bioscience) or CyAN ADP (Beckman Coulter), and the data analysed FlowJo®.

2.3.6 Lentiviral packaging cell line transfection

The packaging cell line 293FT (Invitrogen) were cultured in Dulbecco's Modified Eagle's medium (DMEM, Sigma) supplemented with 10% v/v heat-inactivated FCS, 100 U/ml Penicillin, 100 µg/ml Streptomycin and 2 mM L-glutamine (complete DMEM). To re-plate them, cells were washed with 5 ml PBS (Gibco) followed by trypsinisation using 1 ml of 1 x Trypsin/EDTA (Gibco) for 5 minutes at 37°C. Cells were then diluted in complete DMEM and centrifuged at 300 xg for 5 minutes at room temperature. Stock plates were plated at 0.35x10⁶/ml, and re-plated every 3-4 days.

The 293FT cells were plated 24 hours before transfection at a density of 4.8x10⁶ cells in 8 mls on a 10cm dish. On the day of transfection 5 µg lentiviral expression vector DNA, 3.75 µg pCMV-PAX2 construct and 1.5 µg pVSV-G envelope construct were added to 1 ml Opti-MEM™ (ThermoFisher Scientific). 30 µl of Polyethylenimine (PEI, Polyscience Inc) was added and the mixture quickly vortexed for 10 seconds. After incubating the DNA/PEI mixture at room temperature for 10 minutes, the mixture was added dropwise to the HEK293FT plate. 24 hours after transfection, the medium was replaced with 7-8 ml of warm complete DMEM. At 48 hours, the viral supernatant was

harvested, filtered using through a 0.45 µm filter (Sartorius stedim UK Ltd.) and then either frozen in aliquots at -80°C or used immediately.

2.3.7 Retroviral transduction

Human leukaemia cells were plated in a 24 well plated at a density of 0.5×10^6 in 500 µl of complete RPMI, supplemented with 10 µg/ml Hexadimethrine Bromide (Polybrene), and 0.5 ml viral supernatant and were transduced by spinoculation at 507 xg for 45 minutes at room temperature. 24 hours after transduction 1 ml of complete RPMI was added to each well. In some experiments, the transduced cells were selected with 2 µg/ml puromycin for 72 hours.

2.4 RNA Sequencing

Total RNA was extracted using the RNeasy Plus Mini Kit (Qiagen) according to manufacturer's instructions. For each sample, RNA integrity was assessed was verified using the Agilent's 2200 TapeStation (Agilent Technologies, Santa Clara, CA) prior to proceeding with amplification. The RIN was between 9.5 and 10.0. All samples were submitted to UCL Genomics for RNA-seq and processed using an Illumina TruSeq RNA sample prep kit Version2 (p/n RS-122-2001) according to manufacturer's instructions (Illumina, Cambridge, UK). mRNA was first selected using paramagnetic dT beads and fragmented by metal hydrolysis to approximately 150bp lengths. Random primed cDNA was generated and ligated to adapters compatible with Illumina sequencing and then amplified by 12 cycles of PCR. Libraries generated were quantified, normalised and then pooled prior to sequencing on the Illumina NextSeq 500 (Illumina). For each sample were generated 20 million reads. RNA-seq data were visualised using the RNA express workflow on the Illumina BaseSpace (Illumina) website. The STAR aligner allowed first the alignment of the sequencing reads to the human genome (GRCh38) and then the mapping to genes. Then DESeq2 evaluated the differentially expressed genes between our treated and untreated samples. Genes were ordered by base mean

expression levels. Those genes with very low expression levels were excluded and those remaining ranked by significance and fold change in expression.

2.5 Gene set enrichment analysis (GSEA)

GSEA was undertaken using the Broad institute platform (<http://software.broadinstitute.org/gsea/index.jsp>), and used to examine enrichment the following genesets (Table 11).

Table 11 Genesets used for GSEA

Authors	Genesets	Ref
Zhao	MYB activated/repressed	(Zhao et al., 2011)
Zuber	shMYB Up/Down (top 500)	(Zuber et al., 2011)
Xu	sgMYB Up/Down (top 500)	(Xu et al., 2018)
Ramaswamy	MYBMIM Up/Down	(Ramaswamy et al., 2018)
Sommerville	LSC	(Somerville et al., 2009)
Fantom	CEBP β	(Suzuki et al., 2009)
Fantom	PMA induced/repressed	(Suzuki et al., 2009)

Chapter 3: Identifying compounds to inhibit c-Myb in acute leukaemia.

3.1 Introduction

In order to identify candidate drugs and compounds that would be able to inhibit c-MYB in acute leukaemia, past and present members of the group elected to use the Connectivity Map (CMAP) database (Lamb, 2007). The connectivity map is an open access platform which allows interrogation of drug-induced gene expression changes, from 1309 compounds tested in 4 cancer cell lines (from the Broad Institute), with gene expression signature of interest.

A c-MYB signature was generated from the genes bound by c-MYB in mouse ERMV cells (Zhao et al., 2011), and deregulated in THP1 cells following siRNA-mediated c-MYB silencing (Suzuki et al., 2009). These genes were then integrated with gene expression changes (Affymetrix arrays) following MLL fusion silencing in an MLL-ENL and MLL-AF9 conditional mouse model. This list was converted to human gene names and used to interrogate the connectivity map (CMAP) using the SPIEDw web tool (<http://www.spied.org.uk/>) (Williams, 2013). An output list of candidate drugs and compounds is generated which are predicted to inverse the c-MYB signature in AML.

The top hit was the drug Mebendazole, an anti-helminth agent used worldwide for the treatment of parasitic worm infections. Further work confirmed its administration led to c-MYB degradation in leukaemia cells. The anti-leukaemic activity of this drug both *in-vitro* and *in-vivo* has recently been published by our laboratory (Walf-Vorderwulbecke et al., 2018). A schematic diagram of the approach is shown in Figure 7.

In this chapter we will introduce one of the other candidate 'hits' that was predicted to target c-MYB in AML. We will discuss the initial validation and

effects on gene expression. In order to evaluate the effect of WFA on gene expression we analysed RNA-seq results using Gene Set Enrichment Software Analysis (GSEA) (<http://software.broadinstitute.org/gsea/index.jsp>). GSEA is an analytical tool for interpreting gene expression data and evaluates changes at the level of gene sets instead of individual genes. The gene sets are based on prior biological knowledge. It has advantages over single-gene methods by identifying pathways and processes that are likely to be involved in addition to being more reproducible and interpretable (Subramanian et al., 2005).

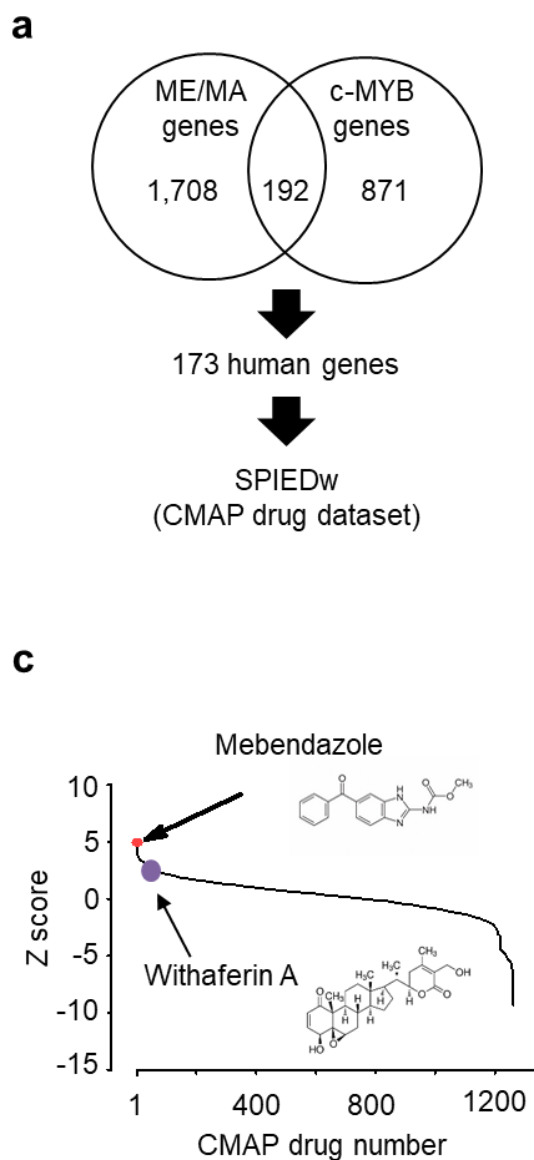


Figure 7 Identification of c-MYB targeting drugs in AML.

(a) Diagram summarising the generation of a c-MYB signature used to interrogate the CMAP database using SPIEDw. (b) The 1309 CMAP drugs are ranked based on the significance of regression scores between their transcriptional profiles and that of the query. The z-score corresponds to the number of standard deviations of the score away from the mean. Inset are Mebendazole (rank 1) and WFA (rank 14). Both figures are adapted from (Walf-Vorderwulbecke et al., 2018)

3.2 Results

3.2.1 Effect of WFA on c-MYB protein and gene expression

Withaferin A was placed at position 14 in the list of drugs identified by CMAP. Other compounds identified from the CMAP analysis are shown in Appendix 1. Previous work in the group had excluded those in positions 2-13, because they either failed to consistently reduce c-MYB protein and RNA following 6 hour incubation or were unsuitable for cell culture experiments.

As all drugs on the list were predicted to have an effect on c-MYB, the first step was to validate its effects *in vitro*. We treated the human AML cell line, THP1, with 1 μ M WFA for 6 hours and showed that treatment led to 90% reduction of c-MYB protein, when compared to DMSO-treated cells. This reduction was encouraging that the predictive nature of the CMAP analysis would have biological effect (Figure 9 a, b).

In order to explore whether WFA was interfering with c-MYB transcriptional pathways in leukaemia, we undertook RNA-sequencing (RNA-seq) on WFA treated cells. THP1 cells were treated with DMSO or 1 μ M WFA for 6 hours. In order to ensure optimal and representative samples for sequencing, the experiment was performed in triplicate, with parallel protein samples being taken and analysed by western blot to ensure c-MYB loss. After incubation with the drug/control, total RNA was extracted. RNA integrity number (RIN) was assessed by a tape station report and a high score identified samples suitable for downstream analysis. Samples were then submitted to UCL genomics (ich.genomics@ucl.ac.uk) for sequencing.

Gene expression changes were ordered by base mean expression levels and plotted in a volcano plot in Figure 8. These represent fold gene expression changes in THP1 cells following treatment with WFA. Labelled are some of the known downstream c-MYB target genes (*GFI1*, *MYC*, *IRF8* and *IRX3*) which are confirmed to be down-regulated following treatment with WFA.

Appendix 2 and Appendix 3 contain detail the top 500 most down-regulated and up-regulated genes, respectively.

A number of c-MYB related gene sets were examined with the RNA-Seq data. Zhao *et al*, integrated global gene expression changes following modulation of c-MYB in a mouse model, with genome-wide chromatin immunoprecipitation followed by sequencing (ChIP-Seq) to map MYB occupancy. This generated a MYB specific leukaemic signature (Zhao et al., 2011). Using this, we can demonstrate negative enrichment for genes activated by c-MYB. Negative enrichment indicates an anti-correlation, genes upregulated by c-MYB were downregulated following treatment with WFA. The reverse was also true, genes repressed by c-MYB were activated following WFA (Figure 9 c, d).

Gene expression changes following MYB perturbation with the peptidomimetic MYBMIM (Ramaswamy et al., 2018), short hairpin interference of MYB (Zuber et al., 2011) and CRISPR based targeting of MYB (Xu et al., 2018), in AML cells generated MYB specific gene signatures that all demonstrated enrichment following WFA treatment (Figure 10).

To validate our RNA-seq data, we measured the expression of *c-MYB*, and some known downstream *MYB* target genes (*IRF8*, *IRX3*, *GFI1* and *MYC*) in the presence or absence of WFA. We treated THP1 cells for 6 hours with DMSO or 1 μ M WFA and measured the expression levels using qRT-PCR. In THP1 cells we observed marked reduction *c-MYB* and the target genes *IRF8*, *IRX3*, *GFI1* and *MYC* following treatment (Figure 11 **Error! Reference source not found.**).

One of the functional consequences of reduced MYB is myeloid cell differentiation. To examine this aspect of whether WFA was exerting its action through MYB, we utilised data from the FANTOM Consortium (Suzuki et al., 2009). This study provides comprehensive analysis of the transcriptional network involved in growth arrest and differentiation in THP1 cells. THP1 cells were treated with the differentiating agent phorbol myristate acetate (PMA). A

subclone was analysed in which the majority of cells become adherent, consistent with differentiation in this myelomonocytic cell line. The resultant RNA was sequenced using the novel deepCAGE method. Cap analysis of gene expression (CAGE) allows high-throughput identification of sequencing tags corresponding to the 5' ends of mRNA at the cap site. These tags are extracted, reverse-transcribed to cDNA and PCR-amplified. Following deepCAGE sequencing (>10-fold previous CAGE studies) these CAGE tags were mapped to the human genome and used for identification of active transcription start sites (TSS) and measure time-dependant expression analysis. Following exposure to PMA, deepCAGE was used to identify core transcription factor motifs in a dynamic pattern (related to how long they had been exposed to PMA). Within this core transcriptional network, one of the down-regulated motifs included MYB. To explore the relationship between different transcription factors (TF) on these core motifs, siRNA of 52 TF was undertaken. They found that MYB had by far (69%) the biggest differentiative overlap, and not only affected the MYB motif, but also most motifs in the core network. This was in the same direction as PMA time course. The MYB signature following KD, induced 35%, and repressed 19%, of the genes upregulated and downregulated by PMA, respectively.

We used the signatures from this study to look for enrichment in our data. The PMA induced gene set indicates cells undergoing differentiation, here we demonstrate positive enrichment in WFA-treated cells. The reverse is true, there was negative enrichment of genes repressed by PMA, which is analogous to cells remaining undifferentiated (Figure 12 a, b). Assuming MYB is the key transcription factor in the above model and has significant overlap with the PMA induced differentiation, then enrichment in the appropriate direction of PMA induced gene sets following WFA is correlative the WFA is exerting its effects through MYB.

Since c-MYB has been shown to be critical for maintaining the self-renewal of leukaemia stem cells, we hypothesized that WFA would inhibit this function in

AML cells. Using GSEA, we compared the signature from WFA-treated THP1 cells with a published AML leukaemic stem cell signature (Somerville et al., 2009). The analysis shows negative enrichment of the LSC signature, indicating expression of genes positively associated with LSCs are downregulated following treatment with WFA (Figure 12 c).

During the course of our experiments, Falkenberg *et al*, sought to identify small-molecule inhibitors using the Myb reporter cell line HD11–C3-GFP1 (Falkenberg et al., 2017). This myeloid chicken cell line carries an eGFP reporter gene, driven by promoter and enhancer of the Myb-inducible chicken *mim-1* gene. In addition, the cells express Myb in a doxycycline-inducible manner, and fluorescence acted as a read-out for Myb. This system was used to screen drugs and WFA was identified as inhibiting Myb activity. Despite its identification in a Myb reporter line, WFA-induced inhibition is then attributed to C/EBP β due to cooperative action via the *mim-1* gene. Mechanistically, WFA was found to modify cysteine residues of C/EBP β and disrupt the interaction with its cofactor p300. In order to see if C/EBP β was enriched in our RNA-seq, we interrogated the C/EBP β signature from the FANTOM database. We demonstrated positive enrichment of C/EBP β activated genes against our RNA-seq data (Figure 12 d). This indicates that the effect of WFA is enhancing this activation and not inhibiting it. There was no enrichment in the reverse direction when considering C/EBP β repressed genes. Our data does not support WFA acting through C/EBP β . This increase in C/EBP β is consistent with cellular differentiation, since C/EBP β activity has been shown to increase during differentiation. (Rosenbauer and Tenen, 2007).

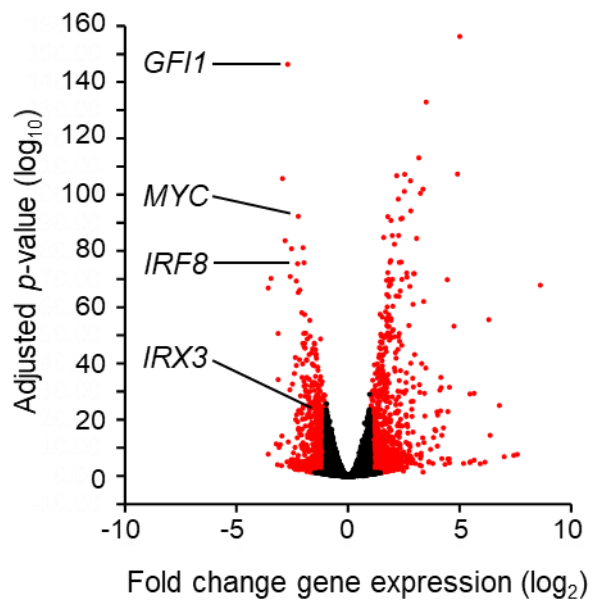


Figure 8. Changes in gene expression following treatment with WFA in THP1 cells.

Volcano plots of fold gene expression changes in THP1 cells following treatment with 1 μ M WFA for 6 hours. Genes coloured red are those with more than 2-fold change and significant ($p_{adj} < 0.05$). Identified are some known c-MYB target genes (*GF11*, *MYC*, *IRF8* and *IRX3*) which are confirmed to be down-regulated.

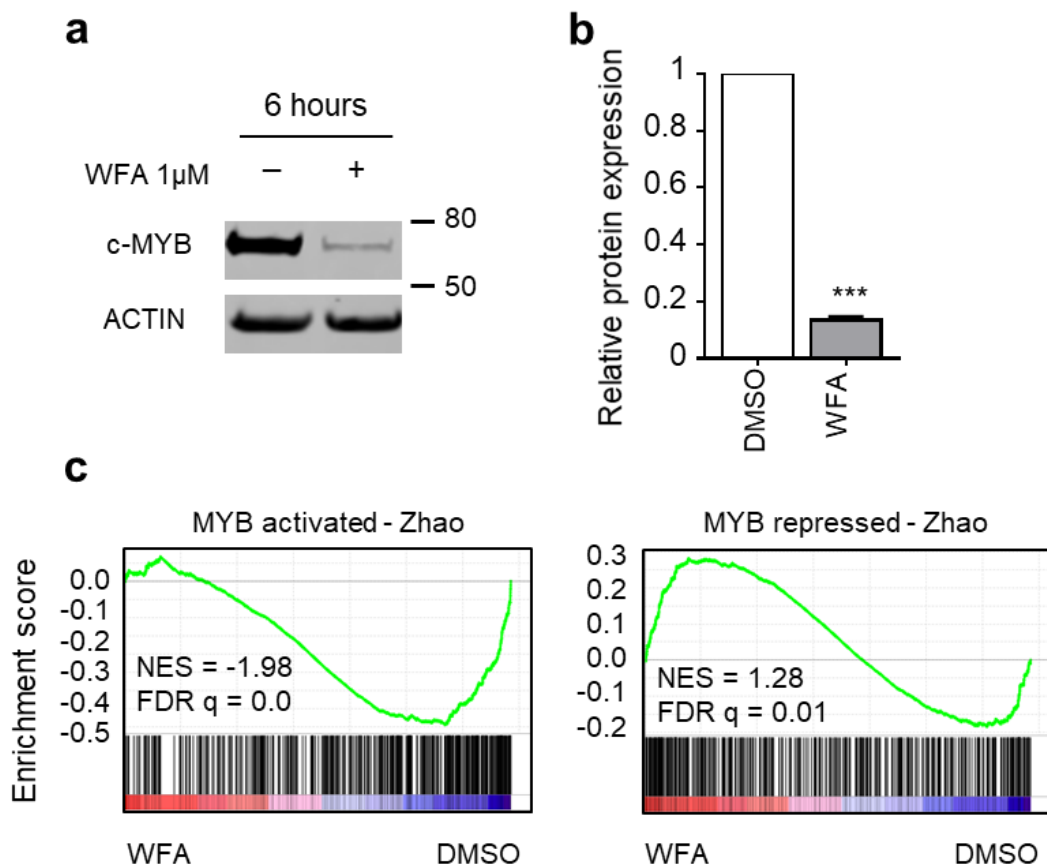


Figure 9. Identification of WFA as a c-MYB targeting drug in AML

a) 6 hour treatment of THP1 cells with 1 μ M WFA showed reduction of c-MYB protein compared to control. (b) Quantification of c-MYB protein following 6 hour incubation with DMSO or 1 μ M WFA, Bars and error bars are means and s.d of n=3. ***P<0.001, one sample t-test (two sided). (c) GSEA of c-MYB activated and repressed gene sets in global gene expression changes in THP1 cells following 6 hour exposure to DMSO or 1 μ M WFA. NES: normalised enriched score, FDR: false discovery rate.

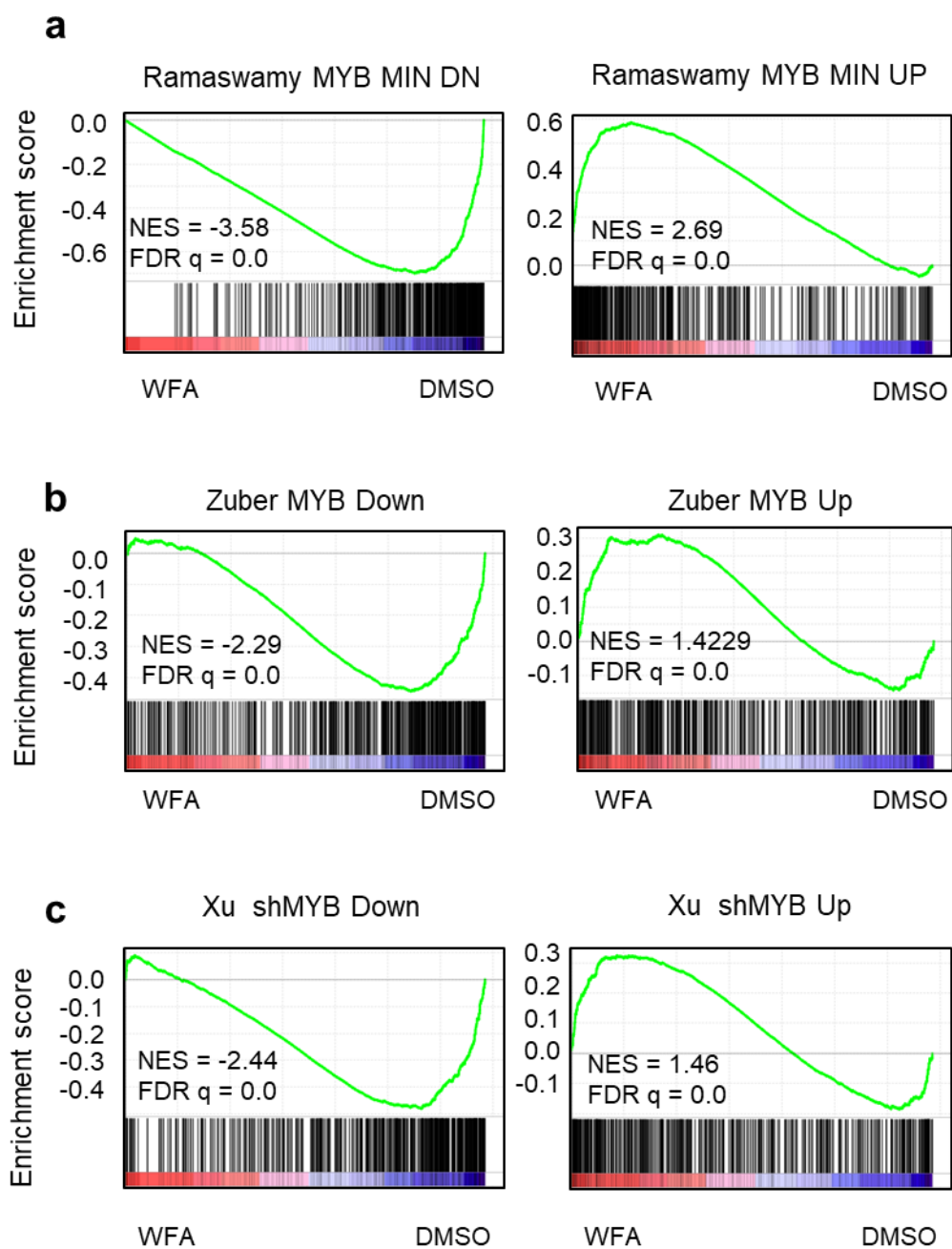


Figure 10. WFA interferes with c-MYB transcriptional program in AML.

GSEA of (a) peptidomimetic (b) shRNA, (c) CRISPr-mediated c-MYB targeting in AML cells in global gene expression changes from THP1 cells treated for 6 hours with DMSO or 1 μ M WFA. NES: normalised enriched score, FDR: false discovery rate.

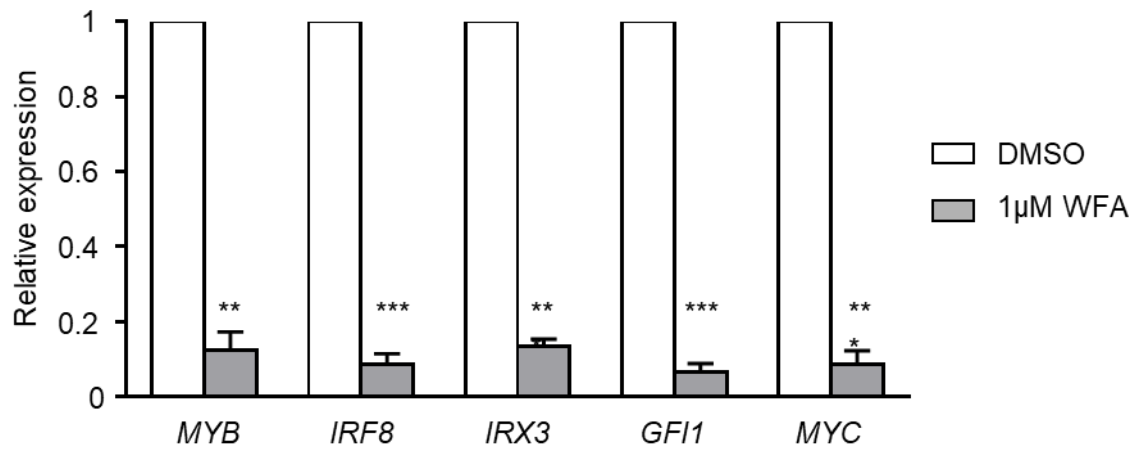


Figure 11. WFA inhibits gene expression of *MYB* and its downstream targets
 Relative mRNA expression of genes in THP1 cells after 6 hours treatment with DMSO or 1µM WFA. Bars and error bars are means and s.d of three independent experiments. *** $P < 0.001$, ** $P < 0.01$, (relative to DMSO controls), one sample *t*-test.

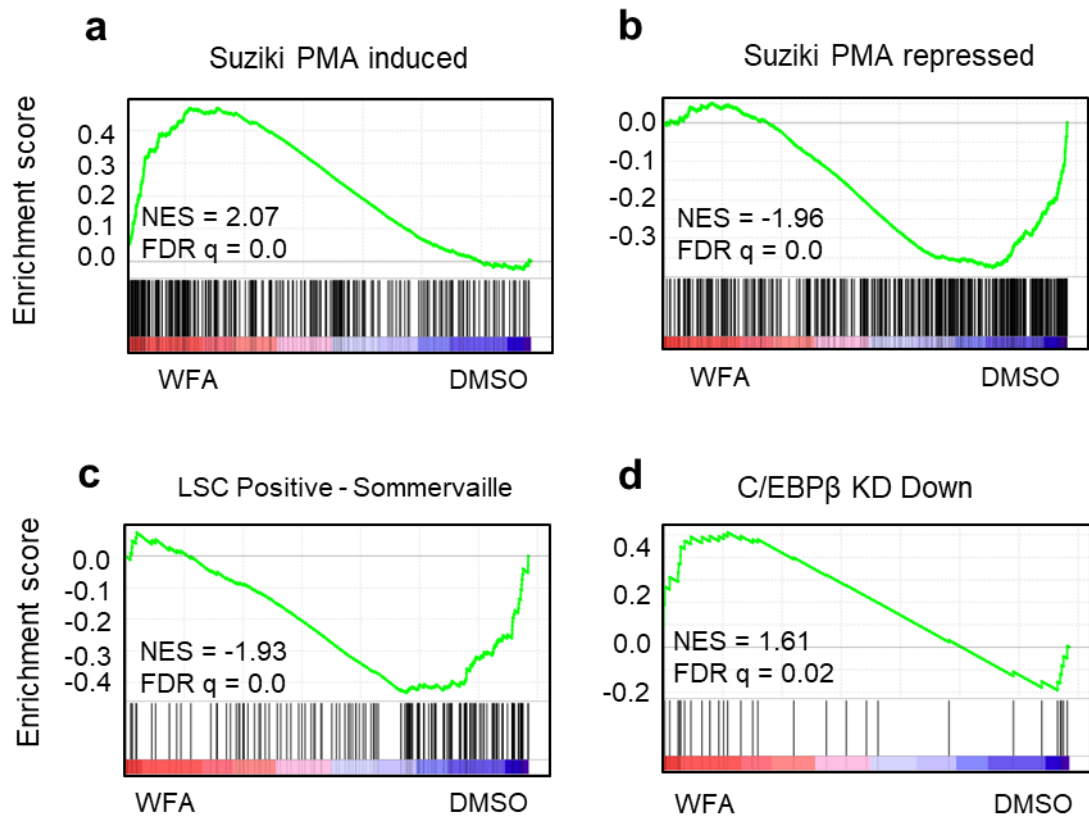


Figure 12. GSEA of WFA induced global gene expression changes

GSEA of (a) PMA induced and (b) PMA repressed. (c) Gene sets positively correlating with leukaemia stem cell frequency. (d) shRNA interference of C/EBP β in global gene expression changes in THP1 cells following 6 hour exposure to DMSO or 1 μ M WFA. NES: normalised enriched score, FDR: false discovery rate.

3.3 Discussion

From the list of drugs predicted by CMAP analysis, WFA was found in position 14. Previous members of the group had excluded those in positions 2-13, because they either failed to consistently reduce c-MYB protein and RNA following 6 hour incubation or were not suitable candidates for drug repositioning (personal communication and unpublished work, Dr Williams).

In order to validate the identification of WFA from the CMAP database, RNA-seq was undertaken in WFA treated cells. We used this gene expression signature to see if WFA was interfering in the known c-MYB transcriptional networks in AML. Different signatures were compared, each had perturbed c-MYB in a different way (siRNA, drug interference). In each, genes activated by c-MYB were negatively enriched following treatment with WFA. This indicates that WFA led to decreased expression of genes normally activated by c-MYB. In addition, positive enrichment was seen for genes normally repressed by c-MYB. This bi-directional enrichment increases our confidence that WFA is interfering with the c-MYB-regulated transcriptional pathways in AML. To confirm that WFA resulted in functional impairment of c-MYB activity, we used a gene set which had induced differentiation using PMA and had shown involvement of c-MYB. Doing this, we observed enrichment in the direction with known c-MYB function. The enrichment seen in c-MYB and PMA induced signatures in WFA-treated cells is very similar to those identified in the FANTOM database, where siRNA-interference of c-MYB reconstituted a large proportion of the changes caused by PMA treatment. Our findings would be consistent with the finding that WFA is exerting both of these effects through MYB. In contrast we showed no evidence of enrichment against C/EBP β , a transcription factor previously shown to be important in the activity of WFA. This previous study identified WFA through Myb-based screening, but conclude the predominant effects are exerted through C/EBP β . Our results do not show WFA is exerting its effects through C/EBP β . Our RNA-seq results

do not show WFA exerting its effects through C/EBP β , instead, they indicate WFA enhancing C/EBP β activation and not inhibiting it.

Taken together, these results indicate that a major part of WFA activity is through interference of the c-MYB leukaemic transcriptional programme.

WFA is a steroidal lactone, first isolated from the medicinal plant, *Withania somnifera* (Ashwagandha). Different parts of the plant have long been used in Ayurvedic medicine. WFA has been shown to display multiple pharmacological effects including anti-cancer, anti-inflammatory, pro-apoptotic and antidiabetic (Vanden Berghe et al., 2012). Preclinical studies focussed on testing its antitumour and pro-apoptotic properties have been published and show effects in breast, lung, cervical, prostate, b-cell lymphoma and colon cancer cell models (Lee and Choi, 2016). However, to date, the mechanisms of its antitumour effects are varied and appear to be cell specific. The majority of the literature reports the production of downstream apoptotic pathways in tumour cells. The proposed mechanisms are divided between those known to directly affect apoptosis, inhibition of NF-kappaB (NFK β) signalling, proteasomal function or inhibition of the heat shock protein 90 (HSP90) chaperone complex.

Increased apoptosis was noted in WFA-treated human AML and myelodysplastic cell lines as a result of activating c-Jun N-terminal kinase (JNK) (Oben et al., 2017) and reactive oxygen species (ROS) (Malik et al., 2007) or inactivation of the protein kinase B (AKT) pathway (Oh et al., 2008), all of which resulted in caspase-mediated apoptosis. Several reports describe the NFK β inhibiting effects of WFA (Ichikawa et al., 2006) (Malara et al., 2008). This has been attributed to hyperphosphorylation of a member kinase, IKK β , leading to inhibition of the pathway (Kaileh et al., 2007). A different group found that by mutating a cysteine residue in IKK β , they were able to demonstrate loss of interaction with WFA and localise its mode of action (Heyninck et al., 2014). In addition to WFA leading to direct inhibition of the proteasome (Yang et al., 2012), there is evidence that it binds to HSP90 and

leads to degradation of the HSP90 client protein, and in turn apoptosis in pancreatic cancer cells(Yu et al., 2010).

The data presented in this chapter validates WFA and its identification from the CMAP database as a compound able to inhibit c-MYB an AML cell line. Gene expression analysis from treated cells demonstrate WFA is interfering with the c-MYB transcriptional program in AML and may represent a novel approach to targeting c-MYB in AML. Given these data, we continued to study the effect of WFA on c-MYB in AML.

Chapter 4: Characterising the anti-leukaemic effects of WFA.

4.1 Introduction

In the previous chapter of this thesis we outlined the identification of WFA as a c-MYB targeting agent. Short-term treatment led to reduction of protein and inhibition of c-MYB regulated transcriptional pathways in AML

The data described in this chapter explores whether this effect can be extended across a broader range of AML subtypes and the functional significance of this. We hypothesise this will be the case as *MYB* expression is critical in different subtypes of AML.

Initial data presented in Chapter 3, showed that a major part of WFA activity is through inhibition of oncogenic activation of c-MYB target genes. In this chapter, we will utilise a mutant c-MYB, express it in our cell line model and determine if we can rescue a c-MYB specific function in the mutant following exposure to WFA.

The final focus in this chapter will elucidate how WFA leads to c-MYB loss. The mechanisms proposed for WFA activity in the literature are cell type specific and incompletely understood, but here we describe a systematic approach of how this critical protein is reduced following exposure to WFA.

4.2 Results

4.2.1 Effect of WFA on c-MYB in acute myeloid leukaemia

The concentration of WFA used by the CMAP database was 1 μ M, and in the previous chapter we demonstrated that this concentration over 6 hours caused c-MYB loss in THP1 cells. We extended this analysis by conducting dose-response studies to determine the minimum concentration of WFA that would lead to c-MYB loss in a panel of AML cell lines. Using this panel, we observe a concentration of 1 μ M over a treatment of 6 hours is sufficient to reduce c-MYB by 80-90% in four of the cell lines (THP1, OCI-AML3, SH11 and U937), although c-MYB loss in MV4;11 cells was less marked at this concentration (Figure 13).

Myb expression is known to change at different points in the cell cycle (Gewirtz et al., 1989) (Oh and Reddy, 1999), peak levels found in mid to late G1 or S phase. More recently c-MYB has also been shown to directly regulate cyclin B1 expression in haemopoietic cells and thus play a role in the G2/M transition (Nakata et al., 2007). The half-life of c-MYB protein and m-RNA is short: around 30 minutes *in vivo* (Feiková et al., 2000), and WFA *in vivo* (from limited data, as discussed later, around 4 hours (Dai et al., 2019). We initially wanted to see whether the WFA-mediated c-MYB protein loss was due to alteration in the cell cycle and accumulation at a particular point. Analysis of cell cycle after 6 hour incubation showed no change between the relative proportions of cells in each stage of the cell cycle, (G1/G ~70%, S-phase ~20% and G2M ~10%). This would indicate that the loss of c-MYB is not due to acute changes in the cell cycle. However c-MYB loss would eventually be expected to lead to a block in cell cycle. In order to determine whether this was the case we analysed cells after 24 hours drug treatment. At this point, there was a significant increase in cells at the G2M stage in WFA-treated vs control, and a concomitant reduction in cells in S-phase (**Error! Reference source not found.**).

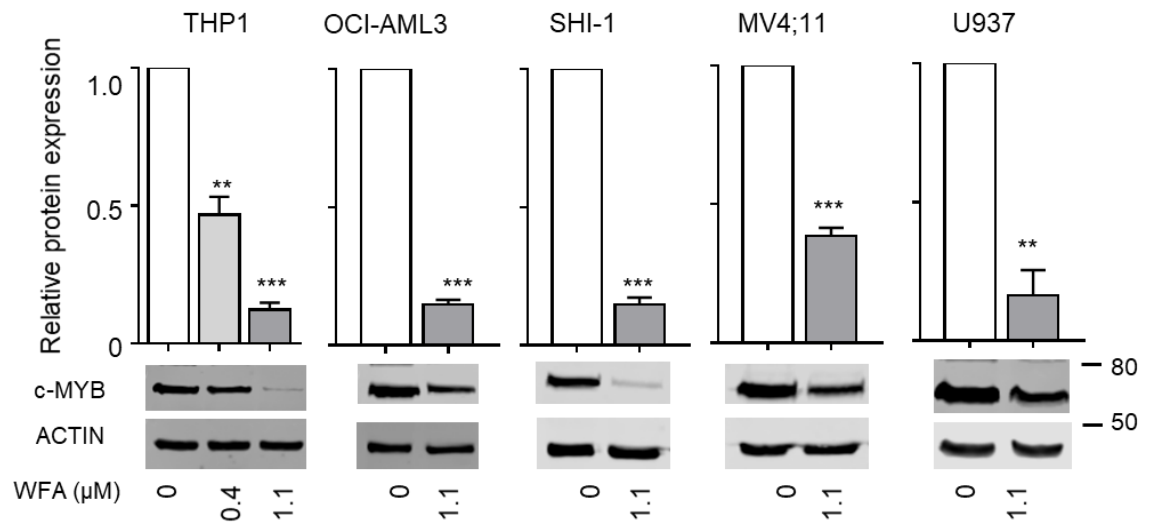


Figure 13. WFA induces degradation of c-MYB

c-MYB protein expression in AML cells after 6 hour treatment with DMSO (0) or indicated WFA concentrations, relative to ACTIN. Graphs represent quantification of c-MYB protein levels normalised to DMSO controls (0). Examples are shown in the lower panel. Bars and error bars are mean and s.d. of three independent experiments. *** $P < 0.001$, ** $P < 0.01$ (relative to DMSO controls), one sample t-test.

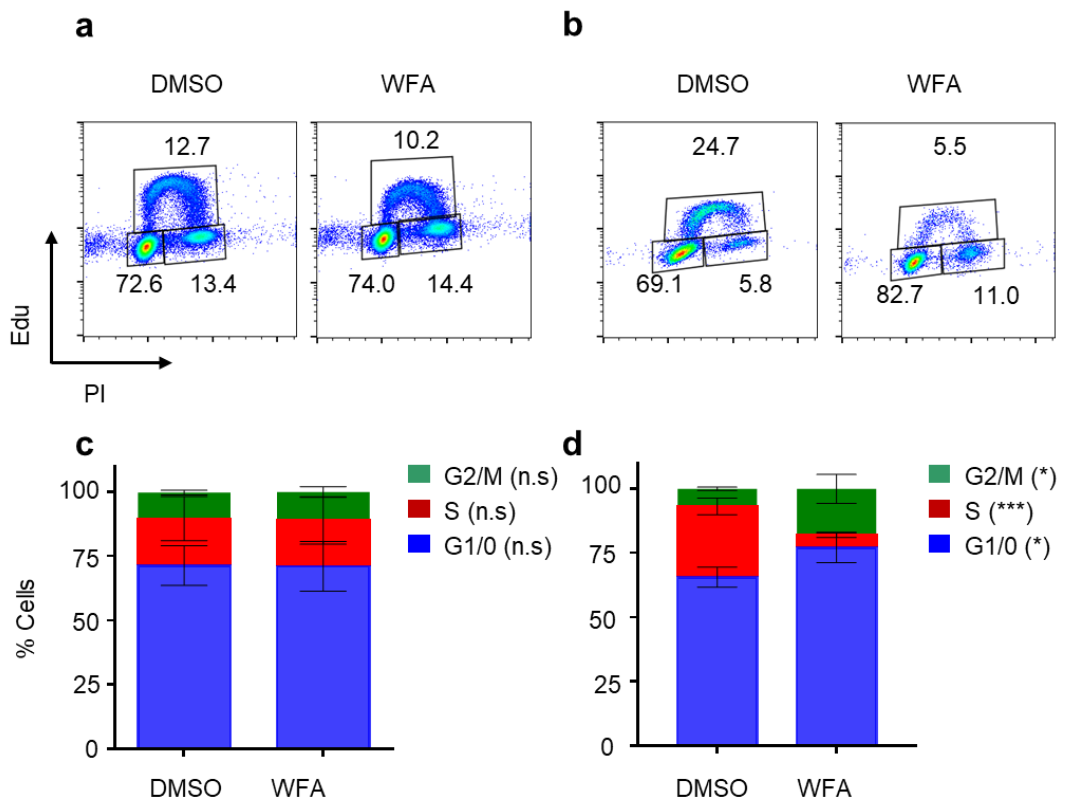


Figure 14. WFA-induced c-MYB loss is not due to cell cycle inhibition.

(a) Examples of flow cell cycle cytometry plots of THP1 cells treated for 6 hours (a) or 24 hours (b) with DMSO or 1 μ M WFA. Numbers inside plots are percentages of cells in G0/G1 (bottom left), S (top) and G2/M (bottom right) phases of the cell cycle. (c,d) Bars and error bars are means and s.d. of percentages of THP1 cells in different phases of the cell cycle after 6 (c) and 24 (d) hours of treatment with DMSO or WFA from three independent experiments. ***P<0.05, *P<0.05, n.s., not significant, unpaired student's t-test between DMSO and WFA in each stage in the cell cycle.

4.2.2 Studying consequences of WFA administration on cell viability.

As AML cells require MYB gene expression for growth and survival, we reasoned that WFA should exhibit growth suppressive effects on AML cells. A time course experiment was undertaken in THP1 cells at 24, 48 or 72 hours after treatment with DMSO or 1 μ M WFA (Figure 15). WFA treatment induced apoptosis, in a time-dependant manner as assessed by cell surface annexin V staining. This was followed by dose-response titration across an AML cell line panel. When the concentrations were plotted on a logarithmic scale against total apoptotic cells, non-linear regression curves were fitted to determine the IC₅₀. Remarkably the range of IC₅₀'s across the cell line panel was very small (0.7- 1.4 μ M). These results are concordant with our findings that 1 μ M treatment leads to reduced c-MYB protein and gene expression.

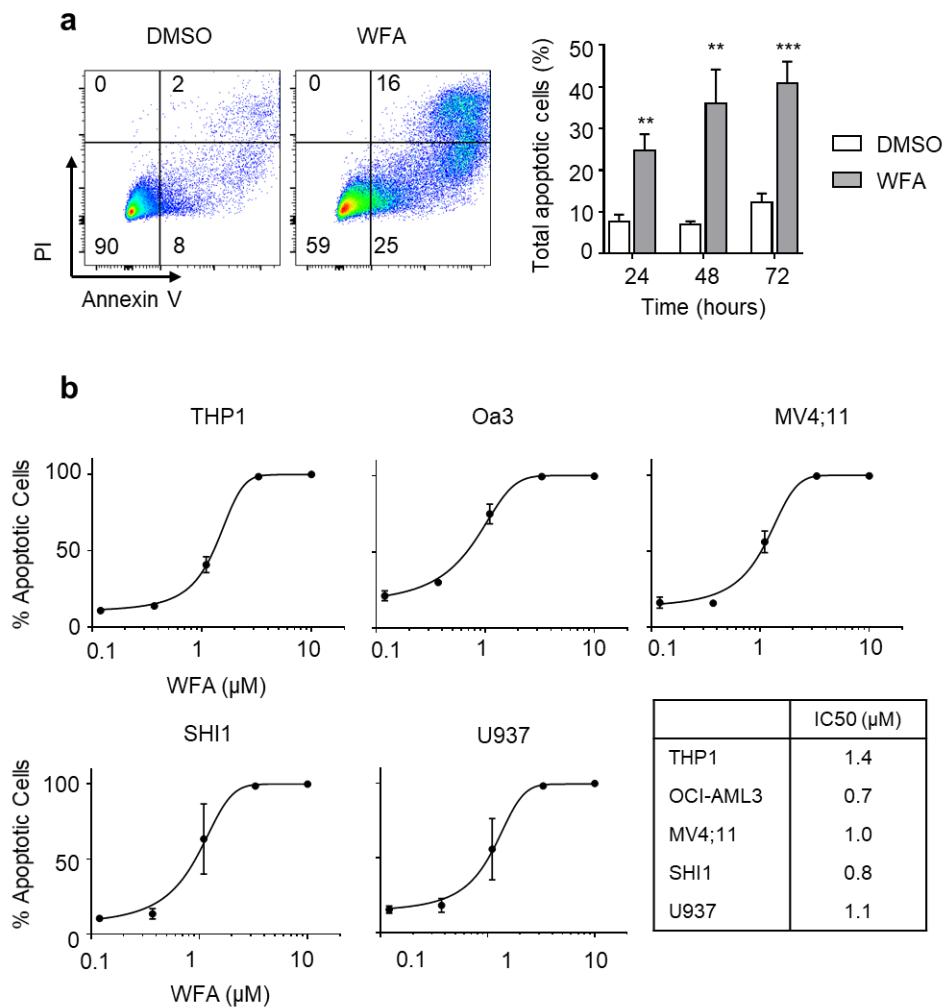


Figure 15. WFA induces apoptosis in AML cell lines

(a) Examples of Annexin V/PI staining of THP1 cells treated for 72 hours with DMSO or 1μM WFA. The chart on the right shows the quantification of total apoptotic cells (AV⁺/PI⁻ and AV⁺/PI⁺) of THP1 cells treated with DMSO or 1μM WFA at different time points. Bars and error bars are means and s.d. of three independent experiments. ***P <0.001, ** P<0.01, unpaired student's t-test between DMSO and WFA treated cells. (b) AML cell lines (THP1, OCI-AML3, MV4;11, SHI-1 and U937) were treated with DMSO or increasing concentrations of WFA for 72 hours, from three independent experiments. Total annexin V positive cells were plotted and the IC50 was calculated from non-linear regression.

4.2.3 Determining the role of c-MYB in the anti-leukaemic activity of WFA.

In chapter 3, we provide initial validation that WFA is exerting its effects through c-MYB. The enrichment from c-MYB specific gene sets in leukaemia is supportive that WFA is interfering with the transcriptional pathways in AML.

The premise in the next set of experiments is that c-MYB has been shown to be critical for maintaining the self-renewal of leukaemic progenitors and the colony formation assay is an *in vitro* measure of this. Additionally, shRNA interference of c-MYB in AML cell lines leads to inhibition of colony formation (Walf-Vorderwulbecke et al., 2018).

We began by utilising an existing model developed in our laboratory. Here we transiently expose THP1 cells to drug X, and then measure inhibition of colony formation compared to control. This assay estimates the degree of self-renewal inhibition achieved through such transient drug exposure. I began by transiently exposing THP1 cells to DMSO or 1 μ M WFA for 16 hours overnight. Following treatment, cells were collected and washed. Viability of WFA treated cells was 80% (+/- 10%), of control-treated cells over the course of three independent experiments. Equal numbers of viable cells were plated in methylcellulose. Analysis of the resulting colonies demonstrated a significant reduction in the WFA group, when compared to control (Figure 16).

If c-MYB loss was a critical component of WFA anti-leukaemia activity, we could reason that stabilised c-MYB would have the potential to rescue this WFA induced loss of self-renewal. Like many proteins Myb is degraded by the ubiquitin/proteasome system; one of the proteins that target Myb for ubiquitylation is Fbw7, the binding of which appears to be regulated by Myb phosphorylation. (Kitagawa et al., 2009). We utilised a degradation resistant c-MYB mutant which has a deletion in the inhibitory C-terminal domain (Δ MYB) (Corradini et al., 2005). It retains the DNA-binding domain which is required for transcriptional activity but has enhanced stability, due to reduced targeting for proteasomal degradation by ubiquitination. The Δ MYB cDNA was

cloned into the pCSGW vector (Demaison et al., 2002), which was made by replacing the GFP cDNA from pCSGW with an IRES-GFP cassette. Viral supernatant was generated, pooled and aliquoted and then titrated using test cells to ensure equivalent GFP expression between Δ MYB, or empty control. THP1 cells were transduced with the vector expressing Δ MYB, or empty control. Transduced cells were then treated with DMSO or 1 μ M WFA for 8 hours, cells collected, washed and equal numbers of viable cells plated in methylcellulose. The cells expressing the degradation-resistant mutant were able to partially rescue the WFA-induced inhibition of colony formation (Figure 17). It was found that Δ MYB increased the colony forming efficiency, but the number of colonies is normalised to account for this. Protein lysates were also taken after 8 hours treatment, and demonstrate that Δ MYB protein was more resistant to WFA-induced protein loss than endogenous c-MYB. Taken together, these results indicate that c-MYB is a critical target of WFA in AML cells.

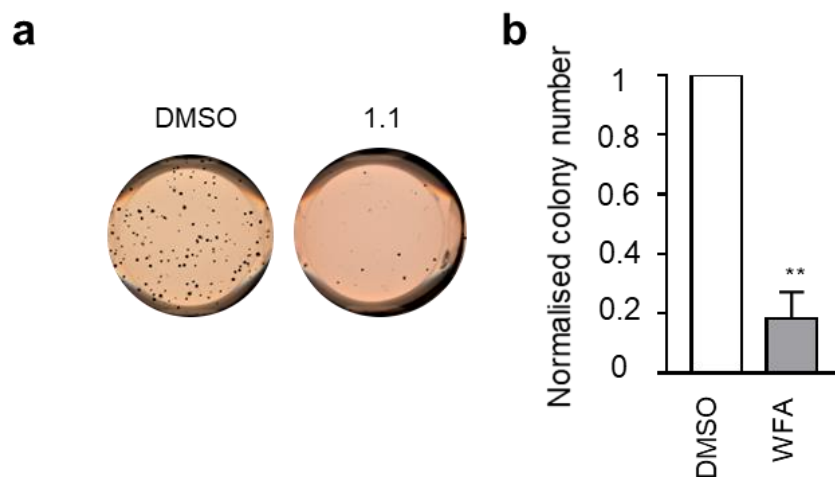


Figure 16. Transient WFA treatment inhibits colony formation

(a) Example of THP1 colony formation after pre-treatment with DMSO or 1.1 μ M WFA. Cells were treated for 16 hours with DMSO or WFA for 16 hours, washed, counted and equal numbers of viable cells were plated into methylcellulose. (b) The graph represents quantification of colonies, bars and error bars are means and s.d. of three independent experiments, normalised to DMSO controls. **P<0.01, one sample t-test.

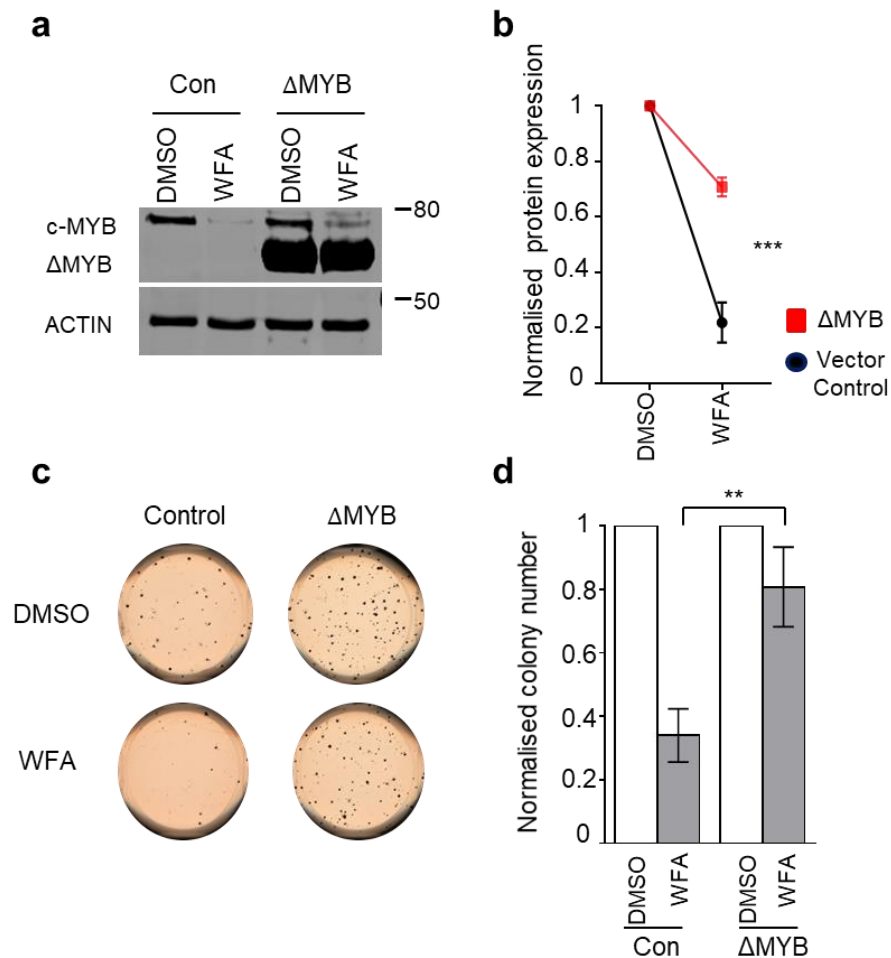


Figure 17. Degradation resistant c-MYB partially rescues WFA induced c-MYB loss and colony formation

(a) c-MYB protein expression in empty vector (Con) or Δ MYB transduced THP1 cells following 8 hour pre-treatment with DMSO or $1\mu\text{M}$ WFA. (b) Line graph represents quantification of c-MYB or Δ MYB protein relative to ACTIN and normalised to Con or Δ MYB DMSO controls. Bars and error bars are means and s.d. of three independent experiments. *** $P < 0.001$, unpaired Student t-test. (c) Examples of colony formation in THP1 cells transduced with empty vector (con) or c-MYB deletion mutant (Δ MYB) following 8 hour pre-treatment with DMSO or $1\mu\text{M}$ WFA. (d) Bars represent means and s.d. of colony numbers, from three independent experiments, normalised to Con or Δ MYB DMSO controls. ** $P < 0.01$, unpaired Student's t-test.

4.2.4 Exploring how WFA induces c-MYB loss.

To determine whether the reduction in c-MYB was a result of changes in expression at the transcriptional and/or post-transcriptional level we examined protein and RNA expression over a time course. Three AML cell lines were treated with DMSO or 1.1 μ M WFA and samples were collected at 1, 2, 4 and 6 hour time-points to assess c-MYB protein and RNA expression. Withaferin A led to reduced protein and RNA expression in each cell line at broadly similar time-points. This reduction occurred slightly earlier in THP1 cells (1-2 hours) than in SHI-1 and OCI-AML3 cells (2-4 hours) (Figure 18). This approach failed to separate effects at the protein level from transcriptional control and might be understood by considering that expression of c-myb in haematopoietic cells is modulated by an autoregulatory loop in which the DNA-binding domain region of c-MYB plays a role in enhancing its own regulation (Nicolaidis et al., 1991).

We proceeded to examine the effects separately. If c-MYB loss was occurring primarily because of increased degradation via the proteasome, then this would be rescued by proteasomal inhibition. We used the known proteasome inhibitor MG132 at a concentration of 10 μ M in combination with WFA/Control to see if this was the case. In THP1 cells, the loss of c-MYB induced by WFA could be rescued by addition of proteasome inhibitor, indicating part of its loss was mediated by the proteasome (Figure 19 a). However, c-MYB protein was only rescued to the level of the DMSO treated controls and not to the MG132 treated cells, implying other mechanisms may be involved. This effect was consistent in the AML cell panel, except OCI-AML3 cells, in which MG132 rescued c-MYB to DMSO treated controls, but MG132 alone was not significant different to DMSO or WFA and MG132 treated cells (Figure 19 b).

In order to address the question of how WFA induces c-MYB degradation, we took a stepwise approach. There were some similarities with mebendazole induced c-MYB degradation and it was plausible that the same mechanism might be involved. In this paper, the Heat shock protein (HSP) HSP70/HSC70

was found to associate with c-MYB in THP1 cells, but this effect was lost upon treatment with MBZ (Walf-Vorderwulbecke et al., 2018). They concluded that this chaperone complex protects c-MYB from degradation. This finding has also been demonstrated in a prostate cancer model, where c-MYB was also shown to be an HSC70 client protein in prostate cancer cells (Li et al., 2013) (Liu et al., 2015). Molecular chaperones are essential for guarding proteins that are essential for normal cellular functions. As an additional example, HSP90 is a different molecular chaperone which plays a role in stabilizing and activating target proteins, so called “clients”. Cancer cells use Hsp90 to chaperone an array of mutated and overexpressed oncoproteins to protect them from misfolding and degradation, and are an attractive target for cancer therapy.

We aimed to see if WFA was interfering with this chaperone complex in AML. THP1 cells were treated for 6 hours with WFA and/ or the HSP70 inhibitors KNK or VER (Figure 20 a). No rescue of c-MYB was observed with either inhibitor, indicating this pathway was unlikely to be involved.

We then attempted to see if WFA was interrupting the activity of HSP90. HSP90 is another member of the HSP family involved in protein folding and chaperone function. Additionally, WFA has been shown to inhibit HSP90 and lead to HSP90 client protein degradation in pancreatic cancer cells (Gu et al., 2014). We treated THP1 cells with the HSP 90 inhibitor, ganetespib alone or in combination with WFA (Figure 20 b). There was no rescue to c-MYB following this treatment, suggesting in this cell line, HSP90 is not involved

Reactive oxygen species (ROS) have been implicated in the anti-cancer effects of WFA in a different AML cell line (HL-60) (Malik et al., 2007) and a myelodysplasia model (Oben et al., 2017). In both of these studies, WFA was reported to induce oxidant stress in the malignant cells, leading to apoptosis. Reduction in WFA-induced apoptosis was seen in the HL-60 AML cell line when the ROS inhibitor N-acetyl cysteine (NAC) was co-administered. In the myelodysplasia cell line, MDS-L, addition of NAC to WFA led to inhibition of

WFA induced ROS. To explore whether mechanism was contributory here, THP1 cells were treated for 6 hours in the presence of DMSO, 1 μ M WFA and/or NAC. Co-administration of WFA and NAC appear equivocal, and may show slight rescue of c-MYB. It should be noted, this was only one experiment and would need repeating to draw firmer conclusions (Figure 20 c).

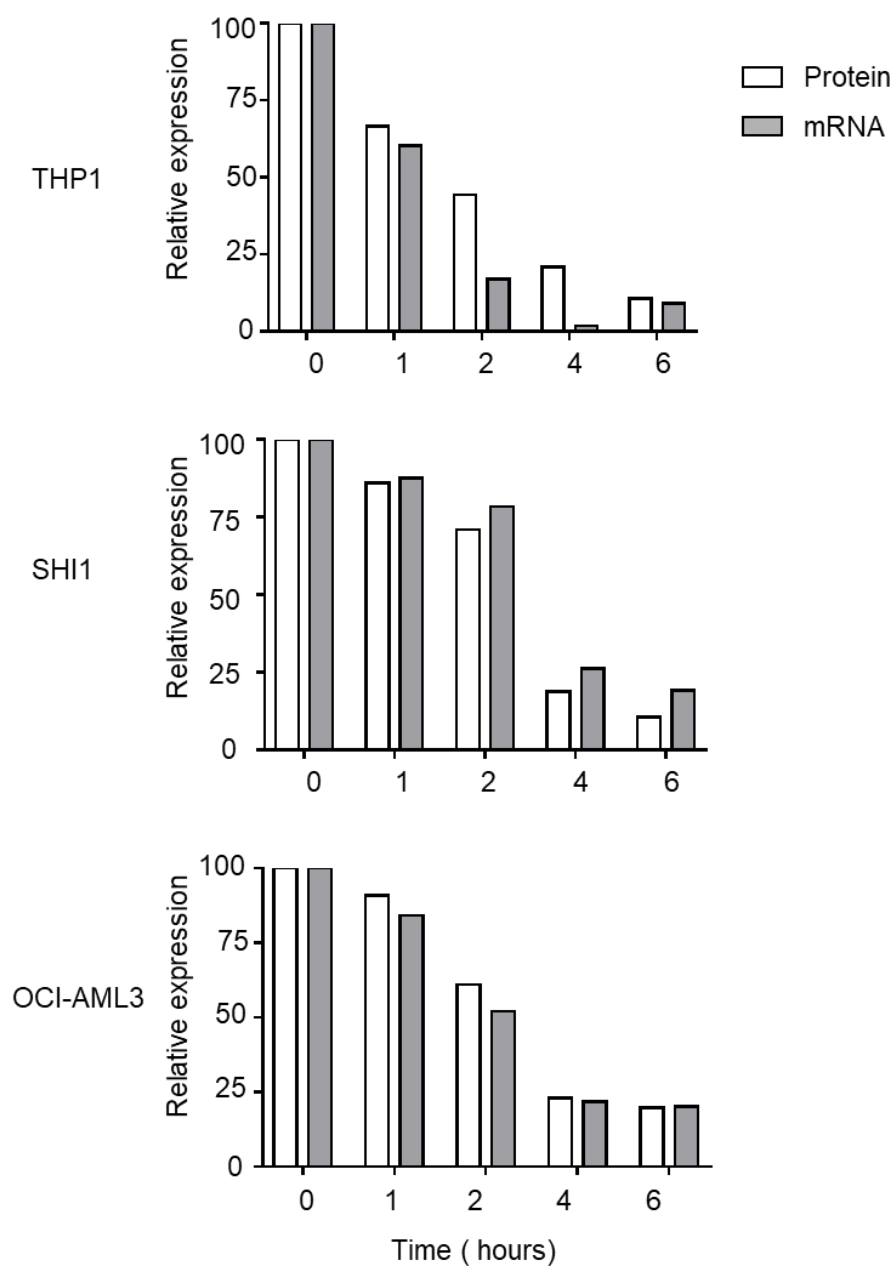


Figure 18 Time course of WFA treatment on protein and gene expression

c-MYB Protein and RNA expression in AML cell lines (THP1, SHI-1 and OCI-AML3) following treatment for 6 hours with 1 μ M WFA, normalised to DMSO control at 1, 2, 4 and 6 hour time points. c-MYB protein was normalised to ACTIN, and c-MYB gene expression used HRPT1 as a housekeeping gene. N=1 in each cell lines.

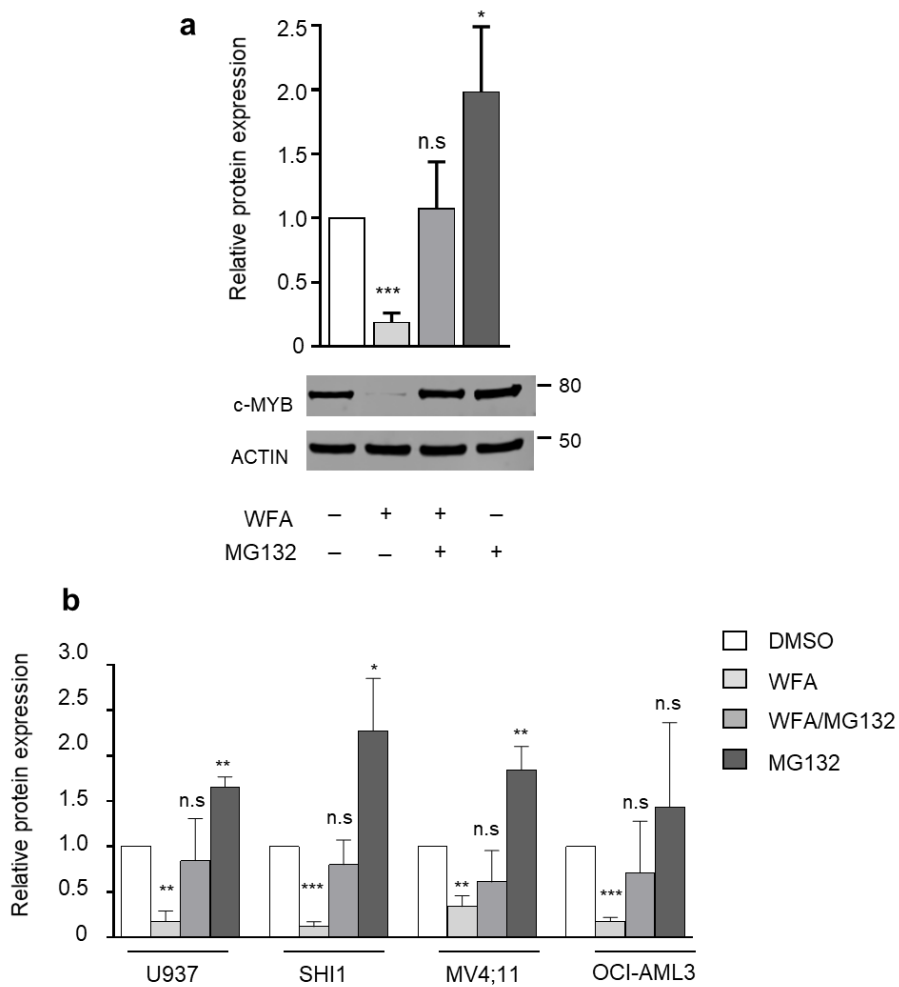


Figure 19 WFA induces proteasomal degradation of c-MYB

a) Top panel, quantification of c-MYB protein in THP1 cells, relative to ACTIN and normalised to DMSO following 6 hour treatment with DMSO, 1µM WFA and/or 10µM MG132. Bars and error bars are means and s.d. of four independent experiments. *** $P < 0.001$, ** $P < 0.01$, * $P < 0.05$, n.s., not significant (relative to DMSO controls), one sample t -test. On the lower panel are representative images. (b) c-MYB protein expression in AML cell lines cells treated for 6 hours with DMSO, 1µM WFA and/or 10µM MG132, relative to ACTIN and normalised to DMSO controls. Bars and error bars are means and s.d. of four independent experiments. *** $P < 0.001$, ** $P < 0.01$, * $P < 0.05$, n.s., not significant (relative to DMSO controls), one sample t -test.

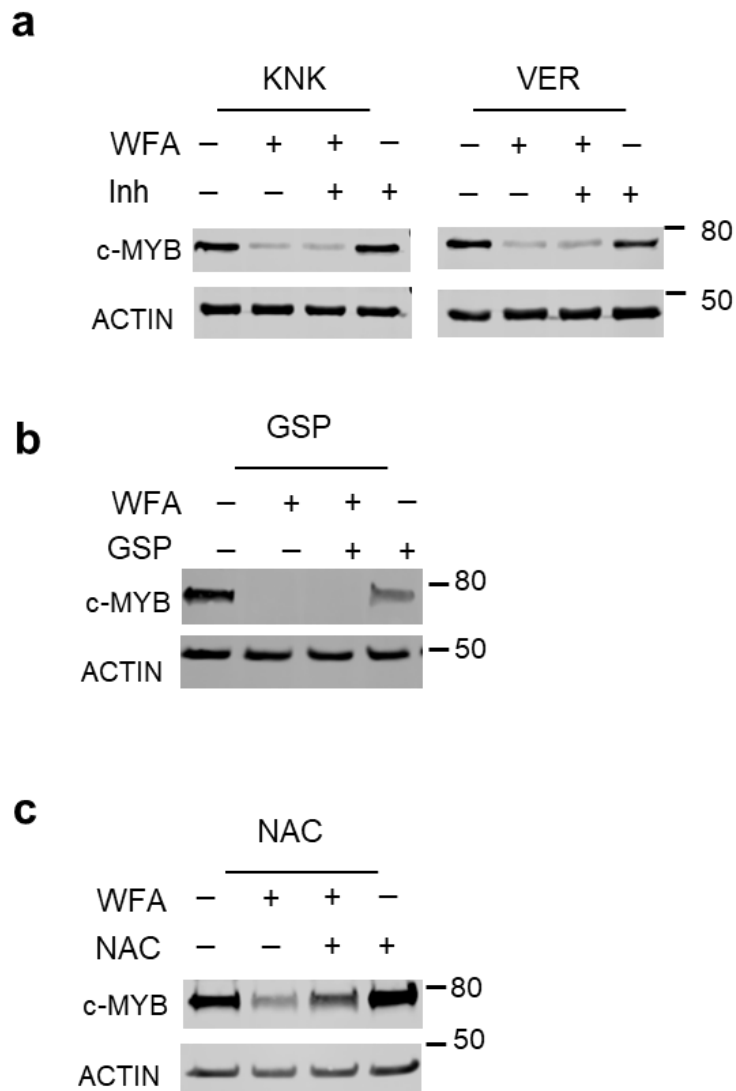


Figure 20 Effect of HSP 70, HSP 90 and reactive oxygen species on WFA

(a) THP1 cells treated for 6 hours with DMSO, 1 μ M WFA and/or the HSP70 inhibitors KNK437 or VER155008 at 20 μ M. (b) THP1 cells treated for 6 hours with DMSO, 1 μ M WFA or the HSP90 inhibitor Ganetespib (GSP). (c) THP1 cells treated for 6 hours with DMSO, 1 μ M WFA or 50 μ M N-acetyl-L-Cysteine (NAC). N=1 in each experiment.

4.2.5 The effect of WFA on protein translation.

In the previous section, we demonstrated that addition of a proteasome inhibitor was able to partially rescue c-MYB, indicating that a proportion of the WFA-induced c-MYB loss is mediated by the proteasome. The finding that it was not rescued to the MG132 alone treated cells, led us to question whether there could be inhibition of protein production. If this were the case, less c-MYB would be available and might explain the partial rescue of c-MYB with MG132. To assess this, we treated THP1 cells with WFA +/- MG132 and compared this to cyclohexamide (an inhibitor of protein translation) +/- MG132. Treatment of THP1 cells with cyclohexamide +/- MG132 mimicked WFA +/- MG132, with c-MYB being rescued to DMSO-treated controls. This is consistent with our hypothesis that a major component of c-MYB loss is due to inhibition of protein production (Figure 21)

Inhibition of protein translation has been identified as a mechanism of WFA anti-leukaemic activity in T-cell acute lymphoblastic lymphoma (T-ALL) (Sanchez-Martin et al., 2017). This study utilised the CMAP database to identify target drugs that would enhance the effects of NOTCH1 (an oncogenic driver in T-ALL) inhibition. The most efficacious of the candidates identified was WFA, where it was found to have potent *in vitro* and *in vivo* efficacy in combination with a NOTCH1 inhibitor. When considering the mechanism of WFA, this group also hit upon the obstacle facing us that multiple pathways have been implicated in its mode of action. They analysed GSEA of gene expression changes following WFA treatment in T-ALL cell lines and found negative enrichment in genes and pathways involved in protein translation. We decided to examine whether the decrease in c-MYB production could be due to inhibition of protein translation. Using these same gene sets, we undertook GSEA of the WFA-induced gene expression changes. We demonstrated negative enrichment in translational elongation (GO:0006414) and ribosomal function (GO:0005840) gene sets, indicating genes activated

in these cellular mechanisms are down regulated following treatment with WFA (Figure 22).

They additionally analysed these gene expression changes using a regulatory network algorithm for the identification of potential drug mechanisms as deregulated nodes (DeMAND). Translation machinery was again identified in the top 50 nodes, and notably included two subunits of the eukaryotic initiation factor 2 (eIF2 α), eIF2S1 and eIF2S2. The eIF2 α kinases are a family of serine-threonine kinases involved with regulation of translation. Translational initiation is a complex process that begins with the interaction of the cap-binding protein complex, eukaryotic initiation factor-4F, with the mRNA 5'-end cap structure. The 40S ribosomal subunit is recruited and is thought to scan the 5' untranslated region (UTR) until it recognises the initiation codon AUG. The 40S subunit, is further bound by the ternary complex – consisting of eIF2, methionyl-initiation tRNA (Met-tRNA^{iMet}), and GTP. Phosphorylation of eIF2 α prevents the formation of eIF2 α Met-tRNA^{iMet} complexes and leads to inhibition of protein synthesis (Holcik and Sonenberg, 2005). This occurs under conditions of cellular stress and biases translational initiation machinery towards translation of mRNAs of genes with roles in stress responses. Causes of endoplasmic reticular stress (ER) include accumulation of misfolded proteins, oxidative stress, and inhibition of glycosylation or alternation in Ca²⁺ homeostasis. These cellular conditions lead to accumulation of eIF2 β , which can affect ternary complex availability and thus translation. Data in renal carcinoma and prostate cell lines have documented ER stress after treatment with WFA (Choi et al., 2011) (Nishikawa et al., 2015), which led to increased p-eIF2 α .

To ascertain if WFA was inhibiting translation by the same mechanism as in T-ALL, we exposed THP1 cells to WFA for 6 hours and observed a dose-dependent increase in p-eIF2 α , alongside a concomitant reduction in c-MYB. There was no change in the total eIF2S α (Figure 23 a). We did not validate their findings using a T-ALL model. We then aimed to stimulate conditions of

ER stress as these are known to lead to such translational inhibition and would be expected to lead to reduction in c-MYB if this hypothesis is correct. For this we used thapsigargin, a compound known to cause ER stress and subsequent phosphorylation of eIF2 α (Kaufman, 1999). Following 6-hour treatment in THP1 cell line, we observed the same pattern, an increase in p-eIF2 α , alongside a reduction in c-MYB and no change in overall eIF2 α (Figure 23 b). These data are consistent with the hypothesis that WFA leads to translational inhibition, and contributes to the reduction in c-MYB.

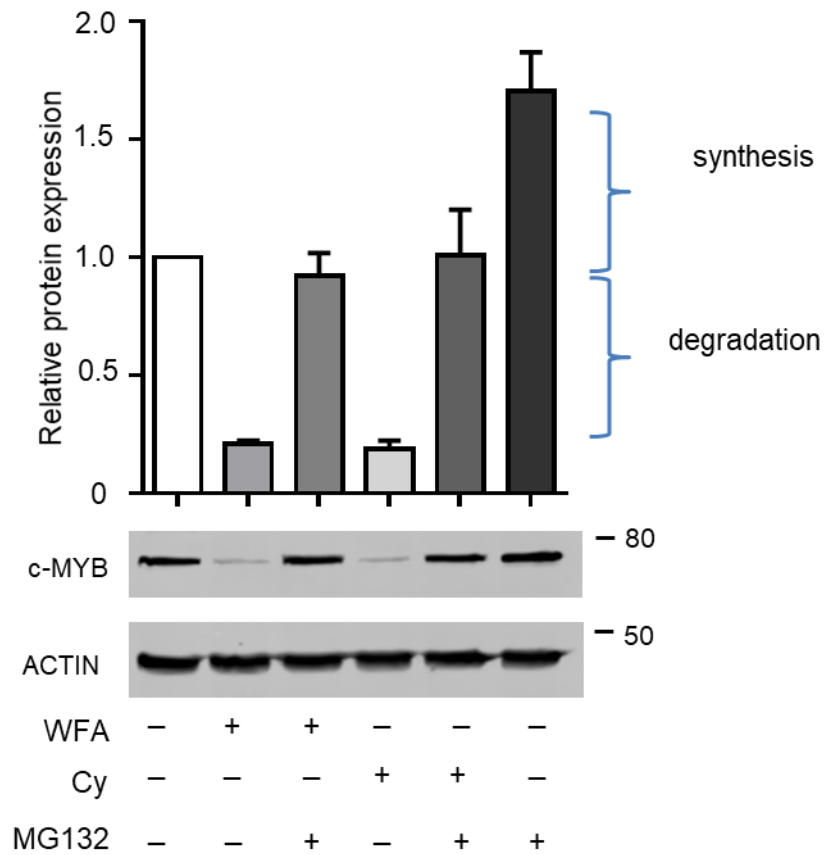


Figure 21 WFA induces inhibition of translation

(a) Protein expression in THP1 cells treated for 6 hours with DMSO, WFA (1 μ M), MG132 (10 μ M), Cyclohexamide (Cy) (25 μ g/ml) normalised to DMSO controls. Bars and error bars are means and s.d. of three independent experiments. *** $P < 0.001$, ** $P < 0.01$, * $P < 0.05$, n.s., not significant (relative to DMSO controls), one sample t -test.

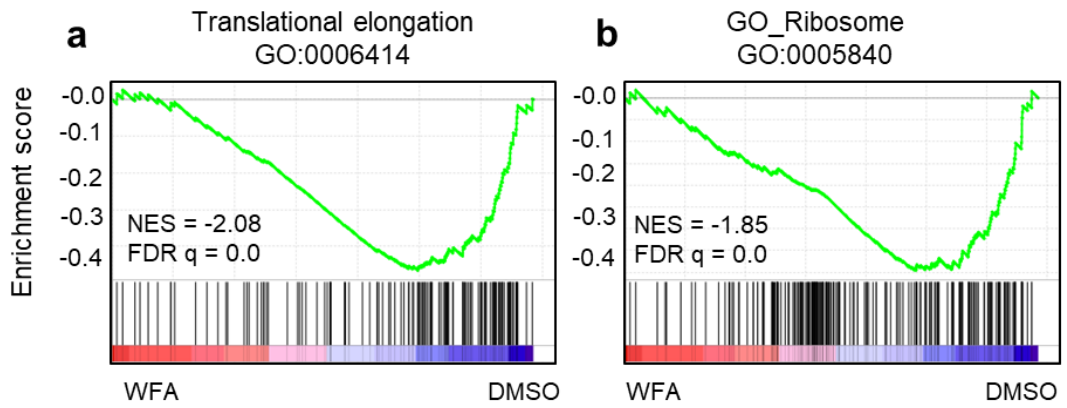


Figure 22 WFA inhibits translation associated genesets

GSEA of the gene expression changes following 6 hour exposure in THP1 cells to DMSO or 1 μ M WFA in (a) Translational elongation and (b) Ribosomal gene sets. NES: normalised enriched score, FDR: false discovery rate.

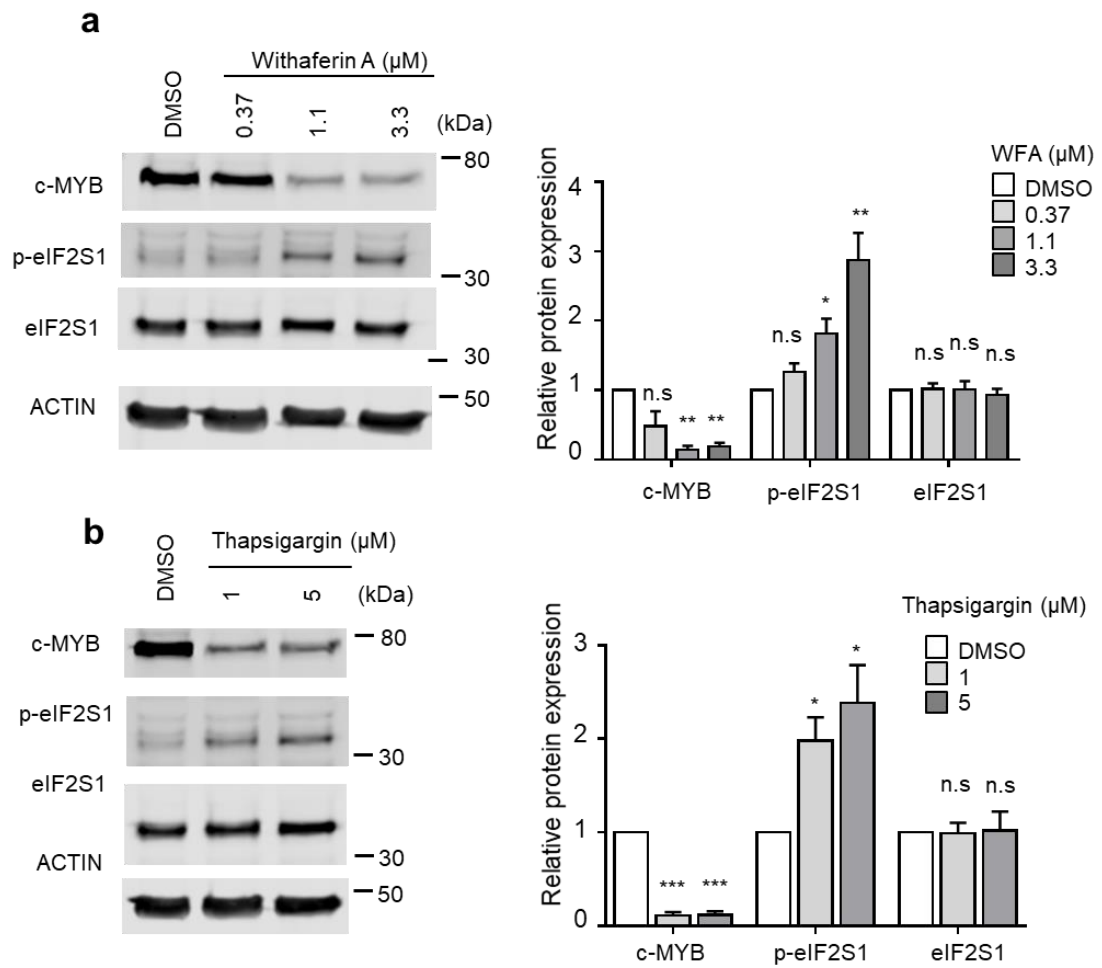


Figure 23 WFA induces phosphorylation of eIF2S1 in THP1 cells.

(a) Left panel, examples, right panel, quantification of protein expression in THP1 cells treated for 6 hours with DMSO and increasing concentrations of WFA, normalised to DMSO controls. (b) Left panel, examples, right panel, quantification of protein expression in THP1 treated for 6 hours with DMSO and Thapsigargin (1 and 5 μM). Blots stained with c-MYB, p-eIF2S1, eIF2S1 and Actin. Bars and error bars are means and s.d. of three independent experiments. *** $P < 0.001$, ** $P < 0.01$, * $P < 0.05$, n.s., not significant (relative to DMSO controls), one sample t -test.

4.3 Discussion

In this chapter we have presented characterisation of the antileukaemic effect of WFA in AML cell lines. Our data demonstrate that 1µM WFA is optimal and sufficient to lead to 90% reduction in c-MYB protein in THP1 cells. This data is reproducible not only in THP1 but in a panel of AML cell lines with different cytogenetics. As with the identification of mebendazole to target c-MYB in AML, even though an *MLL* rearranged model of leukaemia was used to generate the signature, WFA is able to cause c-MYB loss in a range of AML subtypes. c-MYB acts downstream of *MLL* where it leads to transcriptional dysregulation, but it is also recognised as an oncogenic mediator in non-*MLL* rearranged AML. These findings are consistent and encouraging that targeting c-MYB is a rational target for all AML subtypes, irrespective of the upstream oncogenic fusion or epigenetic modification.

We demonstrated that the reduction of c-MYB protein is not due to drug-induced block at a stage of the cell cycle associated with low c-MYB expression (Oh and Reddy, 1999) over a six hour period. In contrast, the WFA induced block at the G2/M phase at 24 hours is consistent with c-MYB regulating the cell cycle (Nakata et al., 2007).

WFA treatment leads to cellular death via an apoptotic pathway in AML cell lines as assessed via annexin V/PI staining. This is consistent with data from previous studies showing therapeutic targeting of c-MYB by small molecule inhibitors, peptidomimetic agents and mebendazole leads to cellular death by apoptosis in AML cell lines (Coulibaly et al., 2018) (Ramaswamy et al., 2018) (Walf-Vorderwulbecke et al., 2018). The narrow range of IC₅₀ (0.7-1.4 µM) found across AML subtypes corresponds to the concentration at which c-MYB protein loss is induced. The narrow IC₅₀ range is striking and is in contrast to the range of mebendazole concentrations necessary to target c-MYB in AML, in which there was up to a 3 fold change between some cell lines (Walf-Vorderwulbecke et al., 2018).

In contrast to novel drug development, where a target is identified and a compound developed to inhibit its function, drug repurposing takes a different approach. Normally it involves extending the scope of a drug beyond its original indication. WFA is obviously in a different category of agent, as it is not an FDA approved drug. Nevertheless, it is the active component isolated from Ashwagandha, which has been taken safely for hundreds of years and is currently widely available and taken as a health supplement. Recently there has been increasing scientific focus on its possible use in several repurposing situations. In chapter 3, we observed WFA-induced inhibition of c-MYB regulated transcriptional pathways in AML. Our next focus was to demonstrate experimentally that c-MYB was a critical target of WFA in AML. Earlier work by our group and others utilised a degradation-resistant c-MYB which retains the DNA binding function of c-MYB, but is less susceptible to proteasomal degradation (Δ MYB). Using this mutant, we expressed Δ MYB in THP1 cells and were able to show partial rescue of WFA-induced inhibition of colony formation compared to control. This data indicates WFA inhibits colony formation by disrupting the c-MYB regulated LSC self-renewal program and is consistent with the GSEA findings.

Having established that c-MYB is a major target in the antileukaemic activity of WFA, we then questioned whether the reduction in protein was primarily due to increased degradation or transcriptional repression. We observed reduced expression in both protein and RNA after treatment, but performing a time course experiment at a fixed concentration, we were unable to elicit an effect on protein without RNA reduction. Expression of c-myb in haematopoietic cells is modulated by an autoregulatory loop (Nicolaidis et al., 1991), in which the DNA-binding domain region of c-MYB plays a role in enhancing its own regulation. Physiologically, this aids maintaining high levels of c-MYB in cells undergoing proliferation or differentiation. This positive autoregulation was also identified in a subtype of T-ALL, in which MYB was found to bind to its own enhancer (Mansour et al., 2014). More recently, when mebendazole was shown to lead to c-MYB degradation in AML, reduction in

RNA was also seen in some cell lines alongside reduction in protein (Walf-Vorderwulbecke et al., 2018). However, protein loss was shown to occur at a lower concentration than required for inhibition of RNA expression. This suggests that the latter is a consequence of c-MYB protein loss. Taken together, these findings would be consistent with a secondary reduction in RNA as a consequence of c-MYB protein loss. It is possible that measuring c-MYB protein and RNA at a fixed time with varying concentrations of WFA might have separated the effects more clearly.

Our initial finding that proteasomal inhibition with MG132 partially rescued c-MYB loss, suggested drug-induced proteasomal degradation was at play. However, the failure of WFA+MG132 to rescue c-MYB protein to MG132-alone treated levels, implied its effects were not solely dependent upon proteasomal-mediated loss. By treating with both a translational and proteasomal inhibitor, we observed the same degree of protein loss and rescue as WFA alone and in combination with MG132. This allowed us to separate WFA-induced c-MYB loss into synthesis and degradation components.

The recent publication that WFA exerts translational inhibition in T-ALL was informative to our studies (Sanchez-Martin et al., 2017). Our data showed negative enrichment of ribosomal and translational elongation signatures against WFA-induced gene expression signatures. In THP1 cells, WFA treatment led to upregulation of p-eIF2 α in THP1 cells, and a concomitant reduction in c-MYB. This effect was mirrored by treatment with the known ER stressor thapsigargin, suggesting WFA plays a similar role. ER stress leads to the integrated stress response within cells and This finding may also relate to the equivocal rescue of c-MYB protein when treated with WFA and NAC. These results are consistent with data in T-ALL and in a renal carcinoma model where WFA has a direct role of eIF2 α phosphorylation and inhibition of eIF2 α -dependent translation as a mediator of their anti-cancer effects (Choi et al., 2011). It is also interesting to consider that ER stress leads to the oxidative

stress in cells and may explain the equivocal of c-MYB protein when treated with WFA and NAC. It would be valuable to confirm this finding on repeated experiments and also observe whether upregulation of p-eIF2 α in THP1 cells following WFA treatment could be reversed with co administration with NAC. Future work could further explore specific genesets looking at the integrated stress response and whether we could demonstrate negative enrichment with our RNA-seq data.

The effect of WFA on translation may be global, i.e. reduces total protein synthesis in an unselective manner or may be specific to c-MYB translation. When considering if these effects could be specific to c-MYB, we examined the 5' untranslated regions (5'UTR) of *MYB* mRNA transcripts. Importantly, whereas eIF2 α phosphorylation may be associated with a reduction in global translational levels, the translation of some transcripts is upregulated. The mechanism underlying this is the presence of multiple upstream open reading frames (uORFs) within such transcripts. Such additional uORFs can overlap the coding region, and prevent translation. The 5'UTRs were conserved in *MYB* transcripts, meaning there is no structural cause for translation of c-MYB to be selectively or preferentially inhibited. Alternatively, to determine if the effect on total protein synthesis was unselective, it is possible to measure global nascent protein synthesis in DMSO and WFA-treated cells. This can be done using a flow cytometric assay that detects an analogue of methionine that can be linked to a fluorescent azide. We would hypothesise that the nascent synthesis would be reduced in the WFA-treated cells, and whilst this effect wouldn't be specific to c-MYB, c-MYB and other cellular proteins with short half-lives and rapid cellular turnover would be preferentially affected by this.

Translational control is a crucial component of cancer development and progression (Silvera et al., 2010). There have been efforts to target specific components of translational machinery as a therapeutic approach in cancer. Firstly, protein translational inhibition has been studied in AML. In the UK

NRCI AML17 study, the addition of everolimus, a rapamycin analogue, was a randomised therapy for patients undergoing post-induction chemotherapy for patients without core-binding-factor leukaemia, high-risk disease (defined by a multifactorial score) and who were not eligible for FLT3 randomisation. Everolimus inhibits mTORC1, which among other cellular processes regulates cap-dependant translation through the eukaryotic initiation factor, eIF4E, and translational elongation through its effects on eIF4B. Unfortunately, addition of everolimus did not improve relapse-free survival, cumulative incidence of relapse or overall survival for these patients and was associated with significant gastrointestinal side effects (Burnett et al., 2018).

Other regulatory aspects of protein translation have been targeted in haematological malignancy, for example, the chronic myelocytic leukaemia (CML) driver oncogene BCR-ABL is highly susceptible to translational inhibition by omacetaxine mepesuccinate (Homoharringtonine). It prevents the elongation step of protein synthesis by interacting with the A-site of the ribosome and disrupts the positioning of aminoacyl-tRNAs and has been FDA approved since 2012 for use in patients with CML resistant to tyrosine kinase inhibitors (Meir and David, 2011). This same inhibitor was identified by an *in vitro* drug screen as an adjunct for patients with relapsed/refractory AML. This group identified its synergistic potential with FLT3 inhibitors to suppress FLT3-ITD. Mechanistically they showed the effect was mediated by protein synthesis inhibition and reduction of short-lived proteins, including total and phosphorylated forms of FLT3 and downstream signalling proteins. A phase 2 clinical trial of this therapy in combination with the FLT inhibitor resulted in complete remission of 20/24 patients (83%), reduction of allelic ITD burden and prolonged leukaemia-free survival. It allowed 'bridge to transplant' for 5 patients and was well tolerated in patients unfit for conventional chemotherapy (Lam et al., 2016).

Inhibition of proteins with short half-life that are essential to the cancer cell was the emphasis by the work of Chen *et al*, a group focussed on targeting

Mcl-1 in Chronic lymphocytic leukaemia (CLL). Interestingly they identified a natural compound, Pateamine A (PatA), which inhibits translation by binding to the initiation factor eIF4A. Mcl-1 is a major component of the anti-apoptotic response, is short-lived and must be continually resynthesised. Treatment with a synthetic derivative of PatA blocked mRNA translation, preferentially reduced Mcl-1 protein and initiated apoptosis in CLL cells. Normal cells did not have this addiction to the anti-apoptotic protein and were less sensitive to Mcl-1 reduction (Chen et al., 2019).

This is the first report of WFA-induced translational inhibition in AML. Translational inhibition, even if not specific to c-MYB would have a disproportionate effect on short-lived transcription factors. We hypothesise that the impact of this inhibition is striking due to the requirement of c-MYB for leukaemia transformation and maintenance (Zuber et al., 2011). This, coupled with its short half-life (Bies and Wolff, 1997) and rapid cellular turnover mean that loss has a functional impact on leukaemia cells.

In summary, we have demonstrated treatment with 1 μ M WFA over 6 hours leads to reduction of c-MYB across a panel of AML cell lines, with different underlying cytogenetics, and administration led to cell death by apoptosis. We have shown experimentally that c-MYB is a critical target of WFA as overexpression of a stable c-MYB protein was able to rescue self-renewal. Finally, WFA-treated gene expression changes demonstrate enrichment in gene sets implicated in protein translation, and WFA-induced c-MYB loss was accompanied by phosphorylation of eIF2S α . This implicates inhibition of protein translation as the likely cause of WFA-induced c-MYB loss. Taking this data forward, we will now examine the effect of WFA functionally in AML cell lines, using primary patient-derived AML and *in vivo* AML models.

Chapter 5: Investigating the effect of WFA in AML *in vitro* and *in vivo*.

5.1 Introduction

Acute myeloid leukaemia is an aggressive haematological cancer that is characterised by malignant self-renewal and a block in myeloid differentiation. Accumulation of immature leukaemic cells frequently leads to bone marrow failure and suppression of normal haematopoiesis. It is widely accepted that only a small fraction of these leukaemic cells have the ability to initiate and maintain its growth, so-called Leukaemia Stem Cells (LSC). In chapter 3, we highlighted that c-MYB has been implicated in the leukaemic transcriptional regulation of the LSC and myeloid differentiation. GSEA analysis of gene expression changes following treatment of THP1 cells with WFA demonstrated negative enrichment of the LSC self-renewal signature and differentiation gene sets. In the following chapter, we will explore whether WFA treatment influences differentiation in leukaemic cell lines and additionally, if WFA inhibits self-renewal in cell lines and in AML patient-derived xenografts. The impact of WFA treatment on normal haematopoietic progenitor cells will also be assessed in the following chapter.

Our primary aim is to identify therapies suitable for repurposing that can be translated into clinical care for the treatment of patients with acute leukaemia, and so it is sensible to evaluate their use in material that represents their disease. One method of acquiring such cells is from AML patient-derived xenografts (PDX). Here, excess diagnostic blood or bone marrow from patients is transplanted into immunodeficient mice, and once engrafted, cells from the bone marrow are harvested. These PDX specimens offer an advantage over cell lines because they have not adapted to long-term liquid culture, and more accurately represent the molecular complexity of patient disease. However, liquid culture of AML PDX cells commonly leads to cell cycle arrest and any subsequent drug treatment only exacerbates cell death.

Culturing PDX cells on human mesenchymal stem cells recapitulates some of the complex interactions occurring in the bone marrow and allows expansion of a range of primary ALL cells (Pal et al., 2016). We collaborated with the authors Professor Heidenreich and Dr Pal, from Newcastle University, to set up human MSC co-cultures for primary AML and ALL samples. In this chapter we will characterise the growth and viability of patient derived ALL and AML samples when cultured with human MSCs, and assess the response of WFA treatment.

The final part of this chapter aims to see if WFA treatment in leukaemia models are efficacious *in vivo*.

5.2 Identification of withaferin A

5.2.1 WFA induces differentiation of THP1 cells *in vitro*

We have previously demonstrated enrichment with a phorbol myristate acetate (PMA) induced differentiation signature in WFA-induced gene expression changes (Figure 12 a). This geneset was shown to have significant overlap with the c-MYB signature (Suzuki et al., 2009), and so we hypothesised that WFA-induced c-MYB loss would lead to differentiation in cell lines. THP-1 is a human monocytic leukemia cell line. After treatment with PMA, THP-1 cells differentiate into macrophage-like cells and are known to upregulate CD11b, an integrin which forms a dimer with CD18 to form complement receptor 3 or MAC1. This complex is responsible for some of the phagocytic functions of the cell and upregulation of its expression reflects a stage of maturation from immature precursors. CD14 is a mature monocyte marker which is absent from immature precursors. We treated AML cell lines with DMSO or 1 μ M WFA for 72 hours and then measured the expression of these markers by flow cytometry (Figure 24). In THP1 cells, treatment led to significant upregulation of CD11b, and to a lesser extent CD14. This pattern was repeated, albeit to a lesser extent in SHI-1 and U937. The MV4;11 cell line failed to upregulate these cell markers in these conditions. Overall, these results are consistent with the GSEA data that WFA-induced c-MYB loss contributes to cellular differentiation.

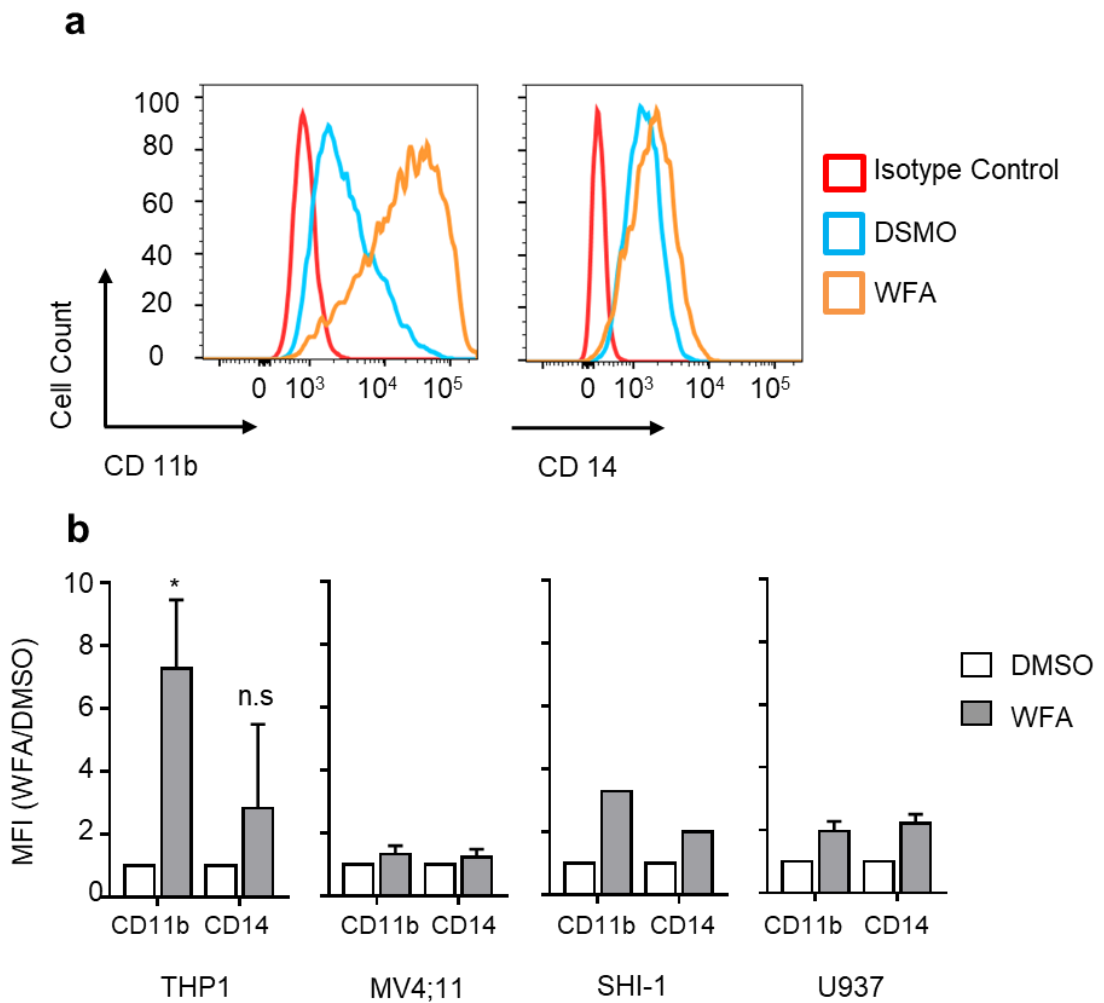


Figure 24 WFA induced differentiation in AML cell lines.

(a) Examples of flow cytometry plots showing increased expression of myeloid differentiation markers after 72 hour treatment with DMSO or 1 μ M WFA in THP1 cells. (b) The bar charts show the quantification across AML cell lines when treated for 72 hours with DMSO or 1 μ M WFA. The ratio of mean fluorescence index (MFI) of treated/untreated was plotted. Bars and error bars are mean and s.d. of three independent experiments in THP1, (data from 2 independent experiments in MV4;11, U937 and 1 in SHI1). * $P < 0.01$, One sample t-test.

5.2.2 Evaluating sensitivity of primary patient-derived B-ALL to WFA

Our collaborators in Newcastle identified a number of primary human MSC samples that were capable of supporting B-ALL cell growth. A previous project had focussed on whether the efficacy of mebendazole-induced c-MYB loss in AML could be extended to B-ALL. In advance of testing c-MYB targeting agents in B-ALL, we aimed to investigate if there was an effect of c-MYB knockdown in B-ALL cell lines. Previous studies have shown short hairpin (sh) interference of c-MYB in the B-ALL cell line 697 leads to arrest of the cell cycle, reduction in viability and induction of apoptosis. (Sarvaiya et al., 2012), We hypothesised SEMK2, and BEL-1 cell lines would show sensitivity to c-MYB reduction as the oncogenic fusion protein is MLL AF4 in both, and c-MYB is known to be a downstream target. However, there was no evidence in the literature if REH cells (fusion protein ETV6/RUNX1) were sensitive to c-MYB silencing. Transduction of a panel of B-ALL cell lines with two shMYB constructs (17 and 53) demonstrated reduction in c-MYB protein and had the functional consequence of impairing self-renewal, indicating that c-MYB is a critical target in all the B-ALL cell lines examined (Figure 25). Having shown the effect of c-MYB silencing in both *MLL*-rearranged and non-*MLL*-rearranged B-ALL cell lines, we then proceeded to treat these cell lines with WFA. WFA treatment led to reduction of c-MYB protein after six-hour treatment and reduced the colony-forming ability in a panel of B-ALL cell lines (Figure 26).

Using this data and the experience of our collaborators in culturing B-ALL, we decided to undertake preliminary experiments using PDX B-ALL cells. We initially tested whether a mouse stromal cell (MS5) could support expansion of primary patient-derived ALL samples, initially selecting two primary patient-derived samples. Counting viable cells demonstrated that co-culture on MS5 cells did not support expansion of these ALL PDX samples (Figure 27). The leukaemia cells failed to expand, and gradually lost viability indicating this stromal support is unlikely to assist with our project aim.

We then proceeded to co-culture the same primary patient-derived ALL samples with and without the human MSC feeder layer, and in the presence or absence of cytokines. Growth curves over 11 days showed that cell expansion was improved when cells were cultured with human MSCs (Figure 28 a). The presence of cytokines only had marginal effect in this small experiment. We analysed one of the cultures (B-ALL#2) by flow cytometry to assess cell viability and expression of the common leucocyte antigen, CD45 and the B-cell marker CD19. Cell viability was markedly reduced in the –MSC/-cytokines condition, compared to the others. The best viability (83% DAPI negative cells) was seen in the +MSC/+cytokine condition (Figure 28 b).

As we proposed treating the B-ALL cells with WFA whilst in co culture with MSCs, we ascertained that WFA did not affect MSC viability using an MTS assay (Figure 29).

Following this, we decided to treat the ALL samples with DMSO or 1 μ M WFA for 96 hours. At this point, the leukaemia cells were removed (leaving the MSC layer intact when viewed microscopically), stained and assayed by flow cytometry (Figure 30). B-ALL#1 had similar proportions of DAPI negative cells in treated and control cells, and of those DAPI negative cells, nearly 100% retained CD45 and CD19 expression. In B-ALL#2, the proportion of DAPI negative cells was lower than when the cells had been assayed with no treatment. There was a difference in the proportion of DAPI negative cells in WFA vs control treated. Of those DAPI negative cells, there was also a change in the appearance of the CD45/CD19 positive gate. The population was slightly smaller in comparison the control, and the population on the FSC vs SSC was less compact, consistent with early stage cell death. It is impossible to say from one sample whether this would represent a consistent finding following WFA treatment.

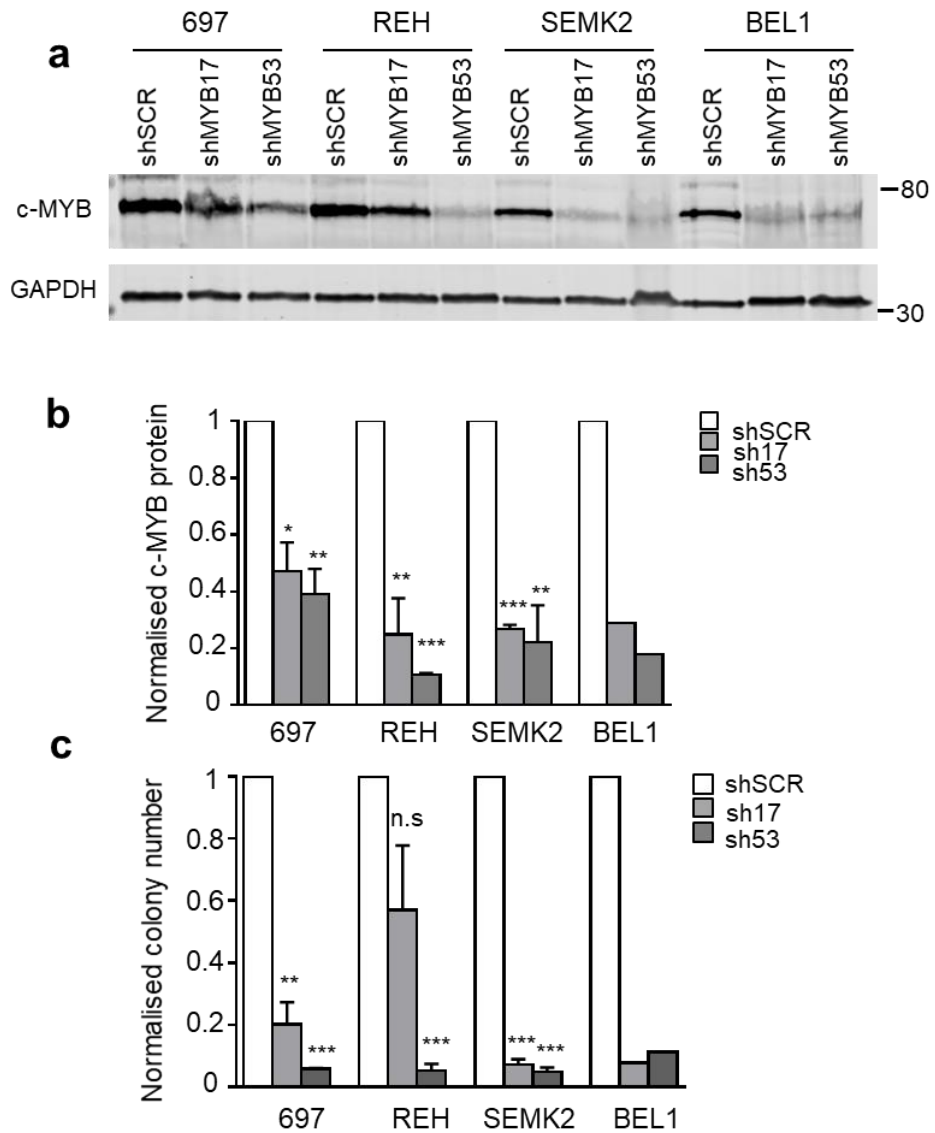


Figure 25 Effects of RNA interference of c-MYB in B-ALL cell lines.

(a) B-ALL cell lines (697, REH, SEMK2 and BEL-1) were transduced with a control non-targeting shRNA (scr) or shMYB constructs 17 and 53. Following puromycin selection cell lysates were isolated. Example images show loss of c-MYB protein after silencing with shMYB17 and shMYB53 in THP1 cells. (b) Bars and error bars are means and s.d. of c-MYB relative to GAPDH and normalised to scr from three independent experiments (data with BEL1 is from one experiment). * $P < 0.05$, ** $P < 0.01$, *** $P < 0.001$, one sample t-test.

(c) Transduced B-ALL cells were counted and an equal number plated in methylcellulose. 14 days later, cultures were INT stained and colonies counted. Bars and error bars are means and s.d. of colonies normalised to scr controls from three independent experiments (data with BEL-1 is from one experiment). ** $P < 0.01$, *** $P < 0.001$, n.s. > 0.05 , one sample t-test.

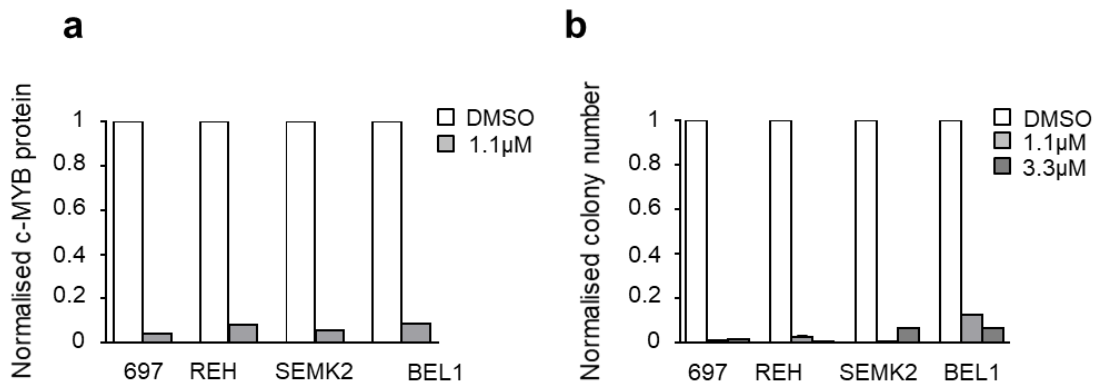


Figure 26 Effect of WFA on B-ALL cell lines

(a) B-ALL cell lines treated for 6 hours with DMSO or 1.1 μM WFA. Bars are quantification of c-MYB protein, relative to Actin and normalised to DMSO controls from one independent experiment. (b) B-ALL cell lines were plated in methylcellulose with DMSO or indicated concentrations of WFA. After 7-14 days the cultures were stained with INT and colonies counted. Bars represent colony number relative to DMSO control from one experiment.

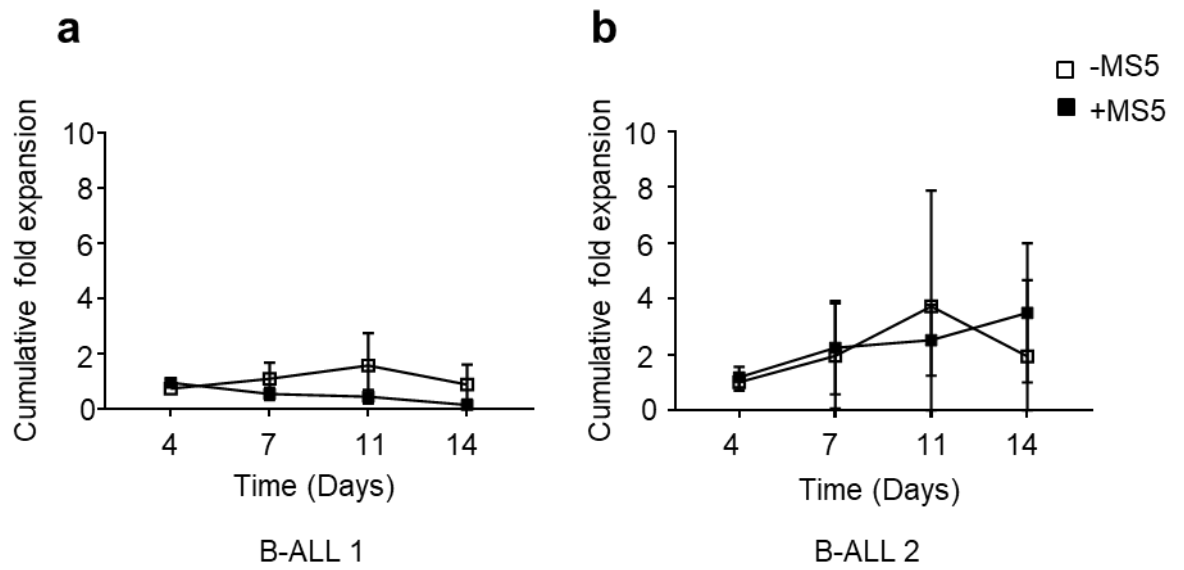


Figure 27 Co-culture of B-ALL PDX samples on MS5 cells.

(a) and (b) Two B-ALL PDX samples (characteristics detailed in table 1) were cultured in SFEM supplemented with 50 ng/ml IL7, IL3 and FLT3L, with or without a feeder layer of MS5 cells. At each time point the cells were harvested, examined, counted and re-plated at the initial density. Line graphs represent cumulative means and s.d. from three independent experiments.

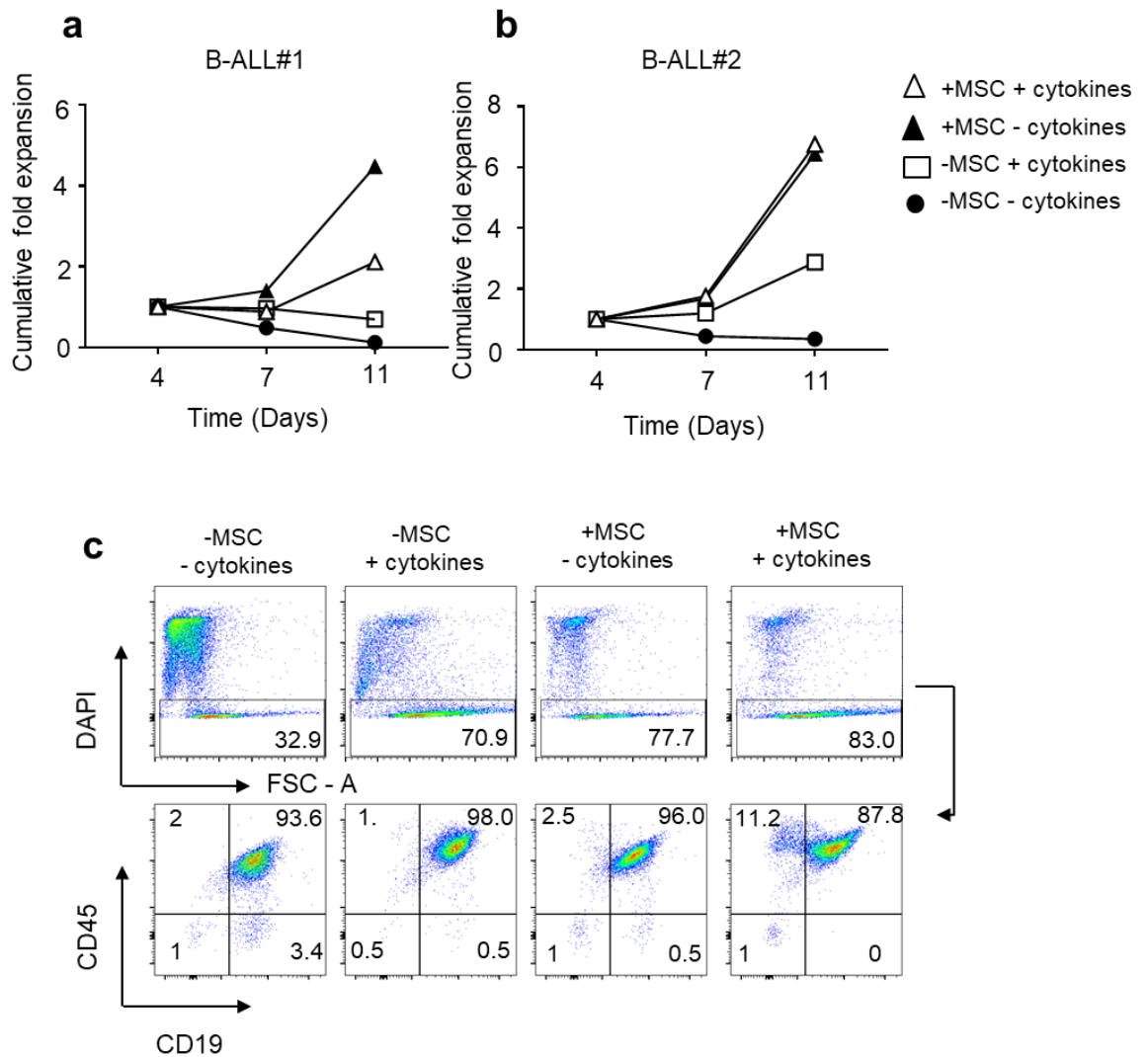


Figure 28 Co-culture of 2 primary B-ALL samples on primary MSC cells.

Two patient-derived primary ALL samples (characteristics detailed in table 1) were cultured SFEM supplemented with 50 ng/ml IL7, IL3 and FLT3L, with or without a feeder layer of primary MSC. At each time point the cells were harvested, examined, counted and re-plated at the initial density. Line graphs represent cumulative means are from one experiment. (a) B-ALL#1, (b) B-ALL#2. (c) Examples of flow cytometry plots of B-ALL 2 cultured on MSC for 72 hours and stained with DAPI, CD45 and CD19.

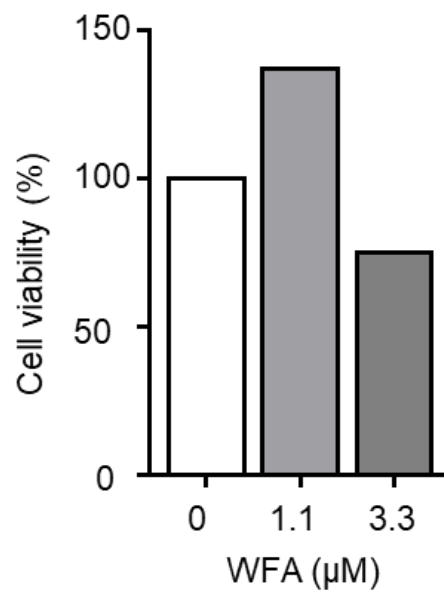


Figure 29 MSC viability is not affected by WFA

Human MSC were plated and treated with DMSO (0) or indicated WFA concentrations for 24 hours. Cell viability was assessed using an MTS colourimetric assay, absorbance was measured at 490nm. Bars represent values normalised to DMSO controls from one experiment.

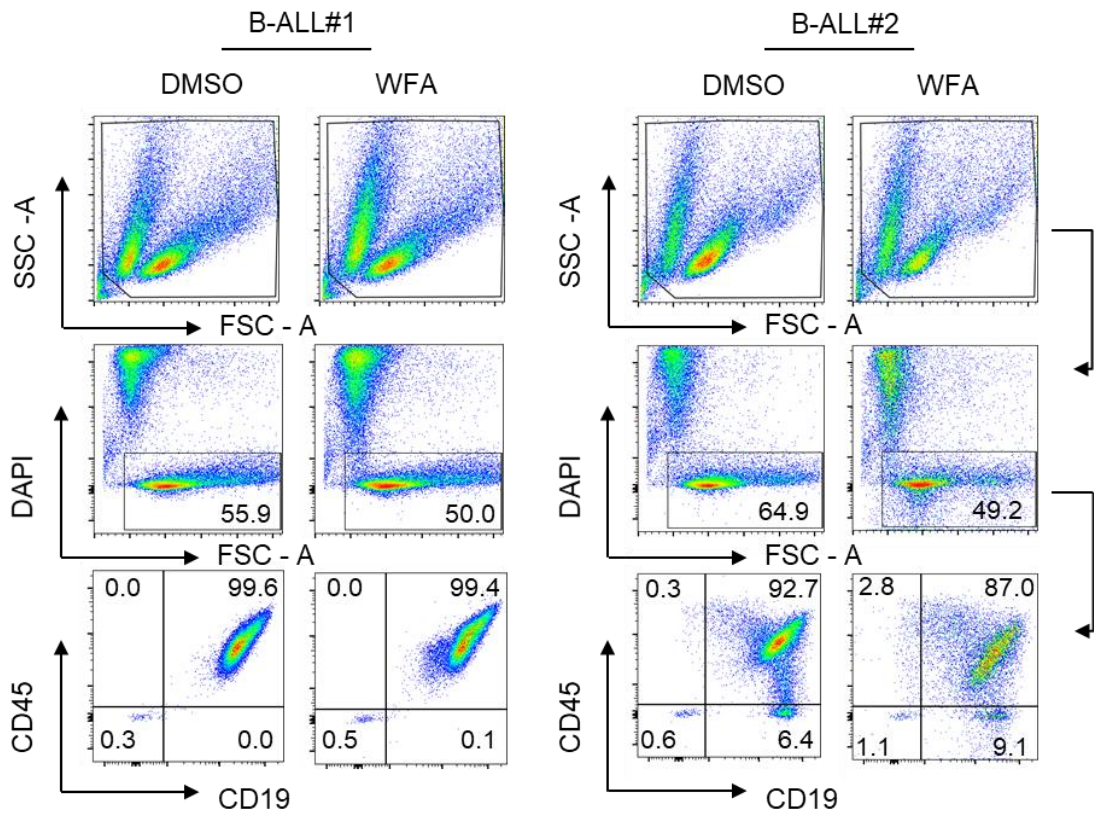


Figure 30 Treatment of B-ALL PDX with WFA

Two B-ALL PDX samples (characteristics detailed in table 1) were cultured in SFEM (no cytokines) with a feeder layer of primary human MSC. Cultures were treated with DMSO or 1 μ M WFA for 96 hours. Examples of flow cytometry plots when cells were harvested and stained with DAPI, CD45 and CD19. Data from one experiment.

5.2.3 Evaluating WFA in primary patient-derived AML

Our focus then turned to primary patient-derived AML cells. Using the same primary MSC feeder layer, we identified and cultured a number of primary patient-derived AML samples that represented a range of cytogenetic subtypes of AML. The primary samples were plated on the feeder layer and viable cells counted by typhan blue staining to estimate cell proliferation. Of the six initially cultured, 3 samples (#1, 2 and 6), demonstrated a greater than 2 fold increase in cell number, 2 had modest increases (#4 and 5), and 1 sample failed to proliferate at all (#3) (Figure 31).

AML samples #1 and #2 were then treated with DMSO or 1 μ M WFA for 96 hours. In this case, because of the variable expression of myeloid markers on the primary AML samples, we decided initially to stain with PI and the common leucocyte antigen CD45 (Figure 32). In AML#1, both control and WFA-treated cells had a high percentage of cell death, when assessed on FSC vs SSC and PI staining. Only 19 and 16% of the cells fell in the PI negative gate in control and WFA-treated cells, respectively. Of this population, CD45 expression was equivalent between control and WFA-treated conditions. Viability of AML #2 cells in the co-culture was greater, 78% and 75% of cells were PI negative, in control and WFA-treated, respectively. Within the PI negative population, 92% of control-treated cells retain CD45 expression. WFA treatment led to a reduction in CD45 expression in a proportion (48.6%) of these cells, possibly due to early stage cell death.

We then attempted to see if these effects were due to drug induced apoptosis. In order to do so, the primary AML cells were co-cultured on primary MSCs. As before, they were treated *in situ* for 72 hours with DMSO or 1 μ M WFA and then harvested and stained with Annexin V and PI (Figure 33 and Figure 34). Of the 4 samples treated, sample #1 had a high level of cell death (70%) in the control-treated sample. There was no appreciable change in WFA-treated cells. AML samples #2 and #5 showed an increase in the AV⁺/PI⁺ compartment from 14.2 to 22.5% and 47 to 57% in control and WFA-treated,

respectively. These changes were associated with a corresponding decrease in the AV⁻/PI⁻ve cells. AML #6 was the strongest responder in which AV⁺/PI⁺ cells increased from 26% to 89% and had a corresponding loss of viable (AV⁻/PI⁻) following WFA treatment.

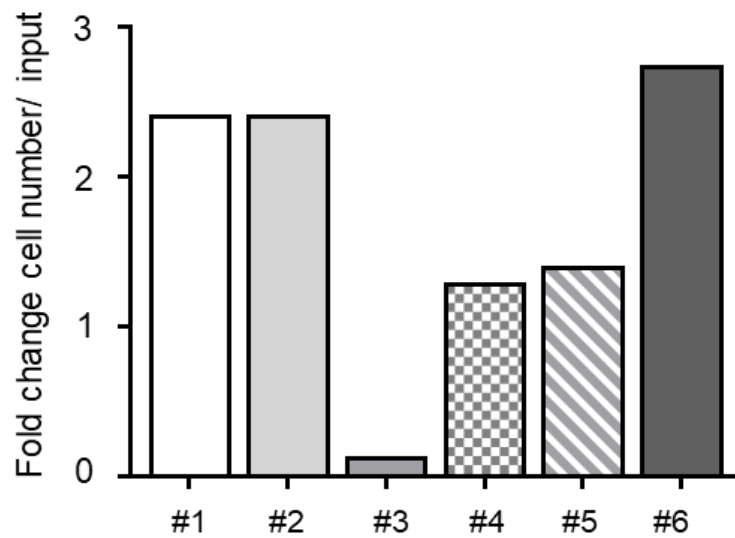


Figure 31 Growth of AML PDX samples when co-cultured on human MSCs.

AML PDX samples (characteristics detailed in table 2) were cultured in SFEM supplemented with StemSpan™ Myeloid expansion supplement (1x), 50ng/ml IL3 and FLT3L with a feeder layer of primary human MSC. Viable cells were counted at day 8 (day 6 for #6) and plotted as fold change/input. Initial cell density was 0.25×10^6 /ml. Data from one experiment.

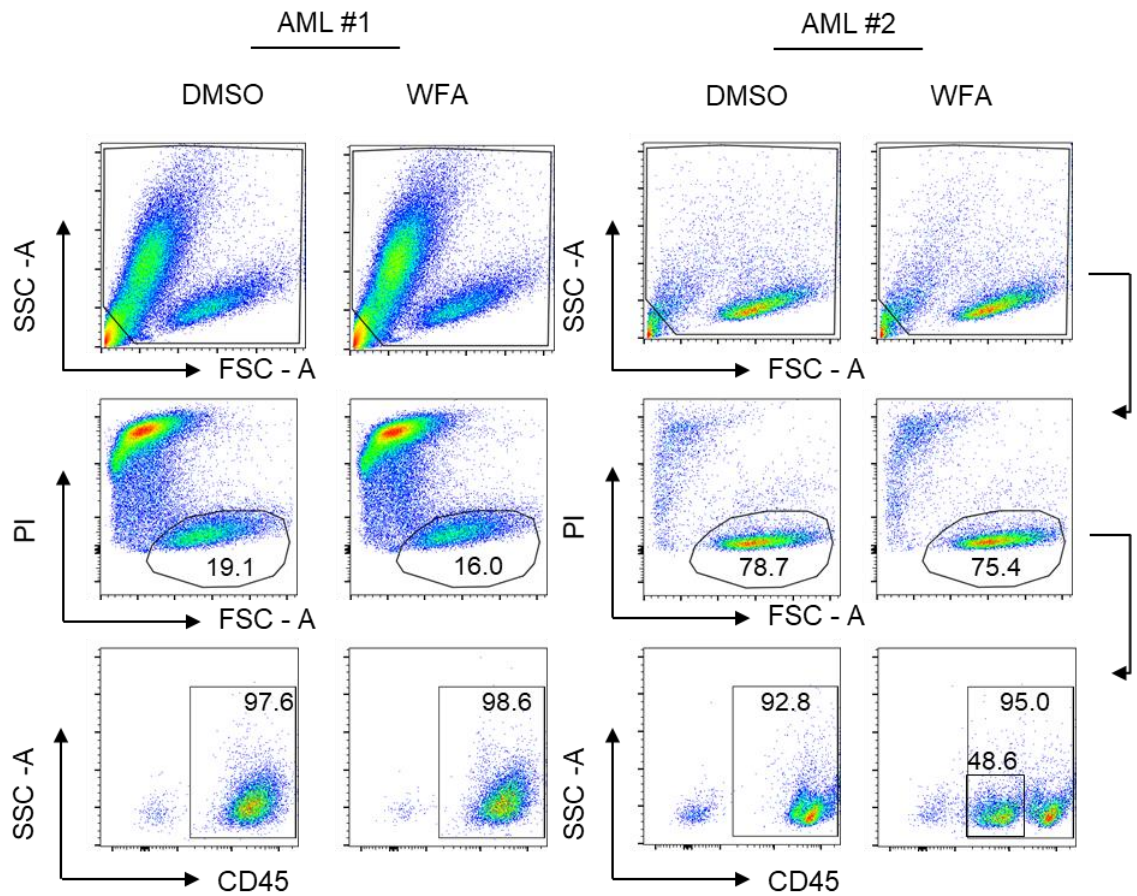


Figure 32 Treatment of AML PDX with WFA

Two AML PDX samples (characteristics detailed in table 1) were cultured in SFEM supplemented with StemSpan™ Myeloid expansion supplement (1x), IL3 50ng/ml and FLT3L 50ng/ml with a feeder layer of primary human MSC. Cultures were treated with DMSO or 1µM WFA for 96 hours. Images of flow cytometry plots when cells were harvested and stained with PI and CD45 . Data from one experiment.

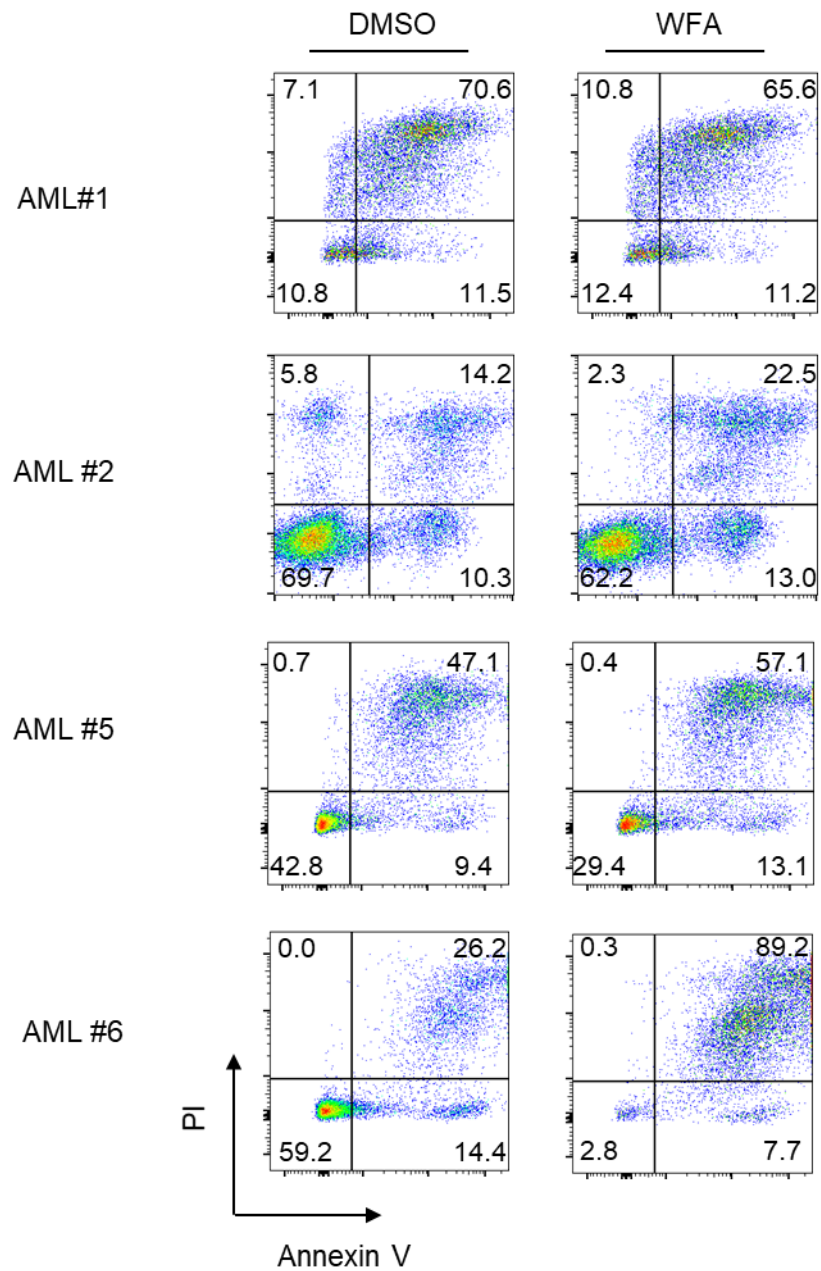


Figure 33 WFA induced apoptosis in AML PDX

AML PDX samples (characteristics in table) were cultured on human MSC in SFEM supplemented with StemSpan™ Myeloid expansion supplement (1x), 50ng/ml IL3 and FLT3L 50ng/ml, and treated with DMSO or 1µM WFA for 72 hours (AML #2 treated for 96 hours). Images of flow cytometry plots when cells were harvested and stained with PI and Annexin V. Data from one experiment.

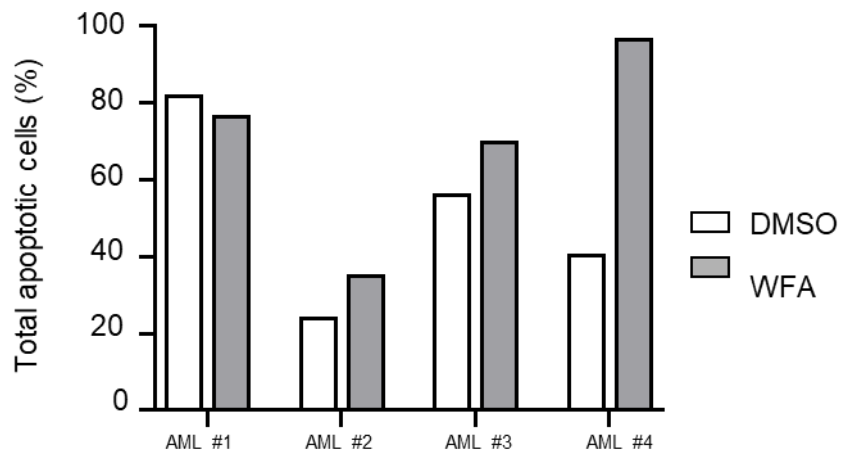


Figure 34 Quantification of WFA induced apoptosis in AML PDX

The chart shows the quantification of total apoptotic cells (AV⁺/PI⁻ and AV⁺/PI⁺) for different AML PDX (from Figure 32) cells treated with DMSO or 1 μ M WFA for 72 hours (AML#2 treated for 96 hours). Data from one experiment.

5.2.4 Withaferin A inhibits self-renewal capacity in human AML

Many cases of AML relapse are due to failure of treatment to target and eradicate the LSC. These cells, which are able to initiate and maintain leukaemia, possess or have acquired the capacity to self-renew. Since c-MYB has been shown to be critical in maintaining the self-renewal capability of the LSC, we examined whether c-MYB loss inhibit this function. Data presented in Chapter 3 showed negative enrichment of genes positively associated with a LSC in WFA gene expression changes. That is, WFA led to down-regulation of a gene set upregulated in LSCs. To examine the functional consequences of this effect, we utilised the colony forming assay. This is an *in-vitro* assay which tests the ability of isolated haematopoietic progenitors and AML cells to clonally proliferate and differentiate and form colonies in a semi-solid media. A panel of AML cell lines were plated in methylcellulose in the presence of DMSO or WFA (Figure 35). THP1 and OCI-AML3 cells were sensitive, with complete colony inhibition at 1.1µM WFA. SH11 and U937, showed a lesser, but significant colony reduction at 1.1µM, with complete inhibition at 3.3µM. MV4;11 demonstrated non-significant reduction at 1.1µM, but significant reduction at 3.3 µM. As these cell lines demonstrate a range of cytogenetic subtypes of AML, it appears this WFA effect is not restricted to *MLL* rearranged subtypes, consistent with data from other c-MYB targeting drugs (Walf-Vorderwulbecke et al., 2018) .

We then proceeded to see if the same effect was observed in primary patient-derived AML samples. We plated primary AML cells in enriched methylcellulose, in the presence of DMSO or WFA. Morphologically, colonies appeared heterogeneous between different AML samples, but colonies were homogeneous within each tumour type. The colony forming capacity varied between primary samples, but in all samples, treatment with WFA led to inhibition of colonies, when compared to control-treated cells (Figure 36). To evaluate the possibility of a therapeutic window, we plated human CD34⁺ cord blood with DMSO or WFA and assessed colonies when plated in

methylcellulose. In contrast to the leukaemia samples, there was no reduction in colonies in the WFA-treated cells. When individual colonies were morphologically scored in the cord blood cultures, there was a reduction in CFU-GEMM, with all other progenitor types remaining unchanged. These data suggest that the self-renewal capacity of LSC in AML might be selectively targeted by WFA-induced c-MYB loss.

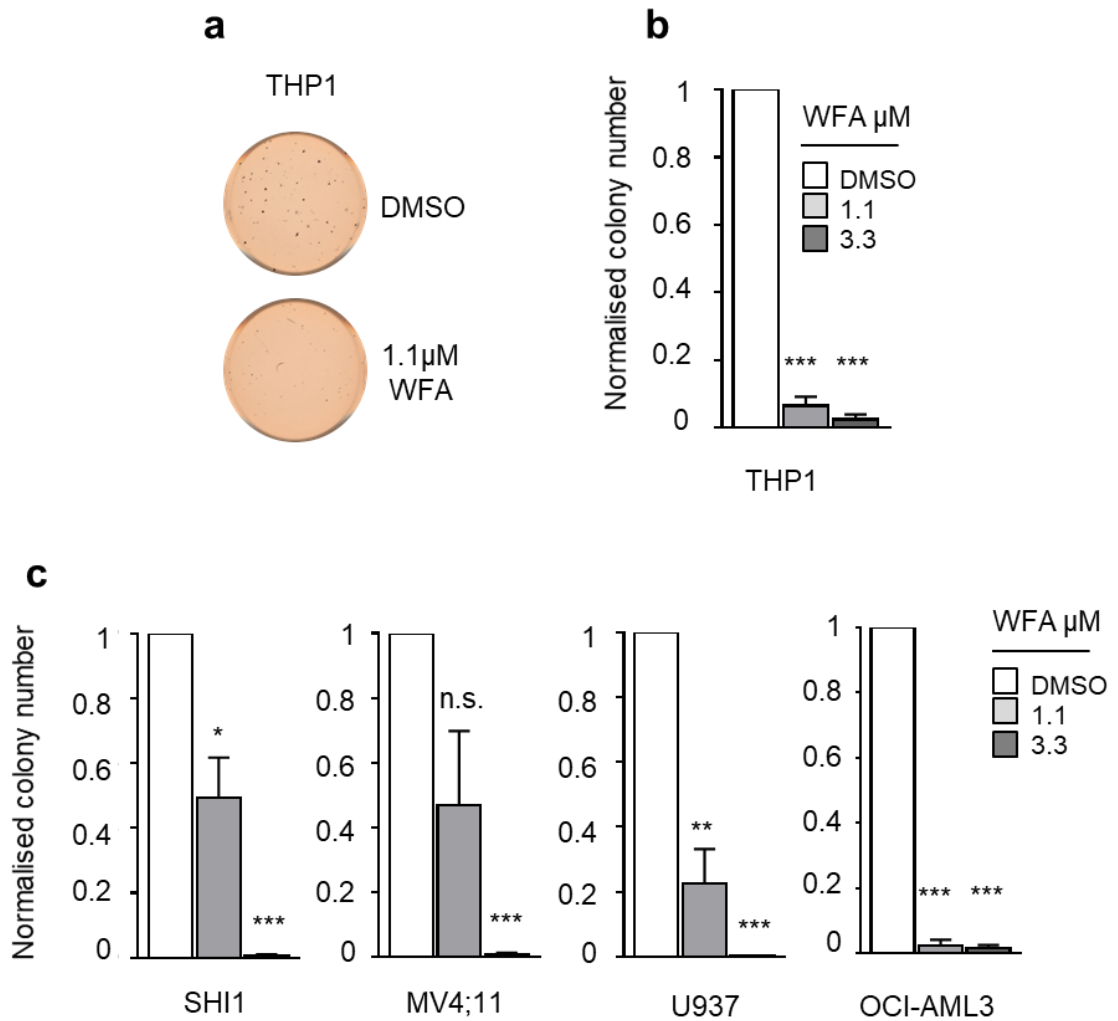


Figure 35 WFA inhibits leukaemic self-renewal in AML cells.

(a) Example images and (b) Quantification of colonies of THP1 cells plated in methylcellulose with DMSO or indicated concentrations of WFA. After 7-14 days the cultures were stained with INT and counted. Bars and error bars represent means and s.d. of colonies normalised to DMSO controls from three independent experiments. *** $P < 0.001$ (c) Colony number, normalised to DMSO from SHI-1, MV4;11, U937 and OCI-AML3 cells. Bars and error bars represent means and s.d. of colonies normalised to DMSO controls from three independent experiments. * $P < 0.05$, ** $P < 0.01$, *** $P < 0.001$ n.s. > 0.05 , one sample t-test.

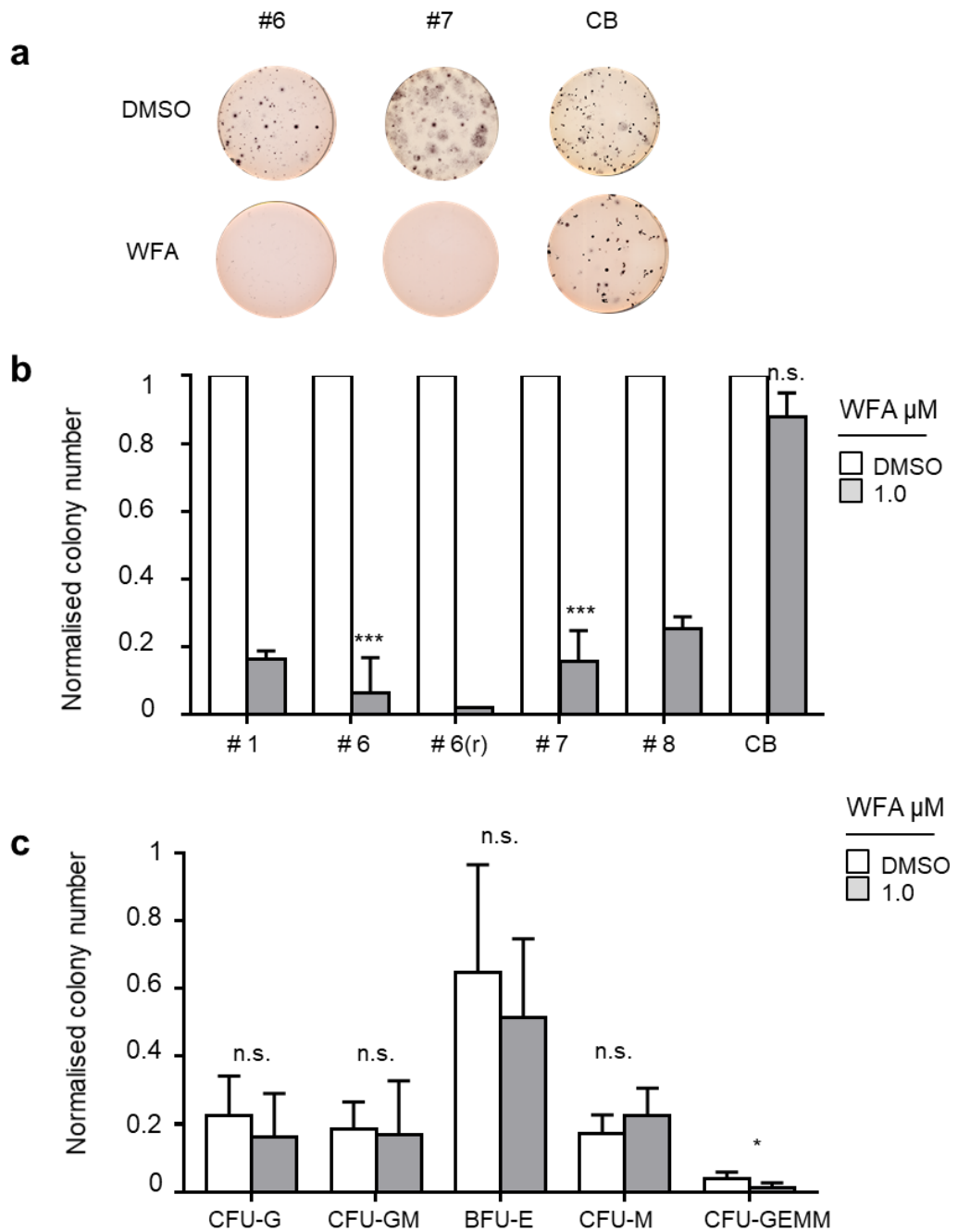


Figure 36 WFA inhibits colony formation by primary AML cells but not CD34+ CB cells.

(a) Examples of primary AML samples and normal CD34⁺ cord blood sample treated with DMSO or 1µM WFA in enriched methylcellulose supplemented with 50ng/ml TPO and FLT3. (b) Bars and error bars represent means and

s.d. of colonies normalised to DMSO controls from three independent experiments (Data from 2 independent experiments in #1, #6(r) and #8). *** $P < 0.001$ n.s. > 0.05 , one sample t-test. Mean colony forming frequency in DMSO treated controls was #1, 0.05, #6 0.2, #6(r) 0.02, #7 0.1, #8 0.03, CB 0.14 (c) Morphological assessment of colony subtypes from three CD34⁺ cord blood experiments (a) and (b), colonies scored as CFU-G, CFU-GM, CFU-E, CFU-M and CFU-GEMM. * $P < 0.05$, n.s. not significant, unpaired student's t-test.

5.2.5 Evaluating WFA activity *in vivo*

Having shown an antileukaemic effect of WFA *in vitro* using cell lines and primary patient-derived AML samples, we then progressed to test the response of treatment *in vivo*. Luciferase expressing THP1 cells were transplanted into non-irradiated NOD-SCID- $\gamma^{-/-}$ (NSG) mice. All transplantations were performed by Dr Owen Williams or Dr Luca Gasparoli. Recipient mice underwent bioluminescent imaging at day 11 to ensure leukaemia engraftment. Mice were randomly allocated to control or WFA-containing diet by flipping a coin (N=4 in each group). Group sizes were chosen based on previous estimates of disease latency in transplanted mice and experiments in the literature performing similar studies. No samples or animals were excluded from analysis. No blinding was used. It was not possible to control for cage-effects because the WFA was administered in the food. Imaging after 17 days of treatment demonstrated a significant reduction in luminescence in the treated group. However, this reduction in leukaemia progression did not translate into prolonged survival in the WFA-treated group (Figure 37). Repeat experiments were performed with smaller numbers of mice, but unfortunately imaging was performed on different days and therefore non-comparable.

Data presented in chapter 4 demonstrated that transient exposure of leukaemia cells to WFA inhibited colony formation, we reasoned that pre-treatment would inhibit leukaemia engraftment *in vivo*. We selected one primary patient-derived AML sample, #1, and transiently exposed the cells to DMSO or 1 μ M WFA for 24 hours. Following treatment, cells were washed and equivalent numbers of viable cells (0.5×10^6) were transplanted into NOD-SCID- $\gamma^{-/-}$ (NSG) mice that had been irradiated 24 hours before. Mice were randomly assigned to receive DMSO-treated or WFA-treated cells by flipping a coin. Because these cells do not express a bioluminescent marker, we observed the mice for signs of disease progression and the mice were culled at this point. In this experiment, mice were fed normal diet and the control and

treated mice were not kept separate to control for cage-effects. This approach also failed to lead to a difference in survival for the WFA-treated group, with both groups developing disease at similar times (Figure 38). Ongoing work by the group is using different formulations of WFA to demonstrate if WFA has and effect *in vivo*.

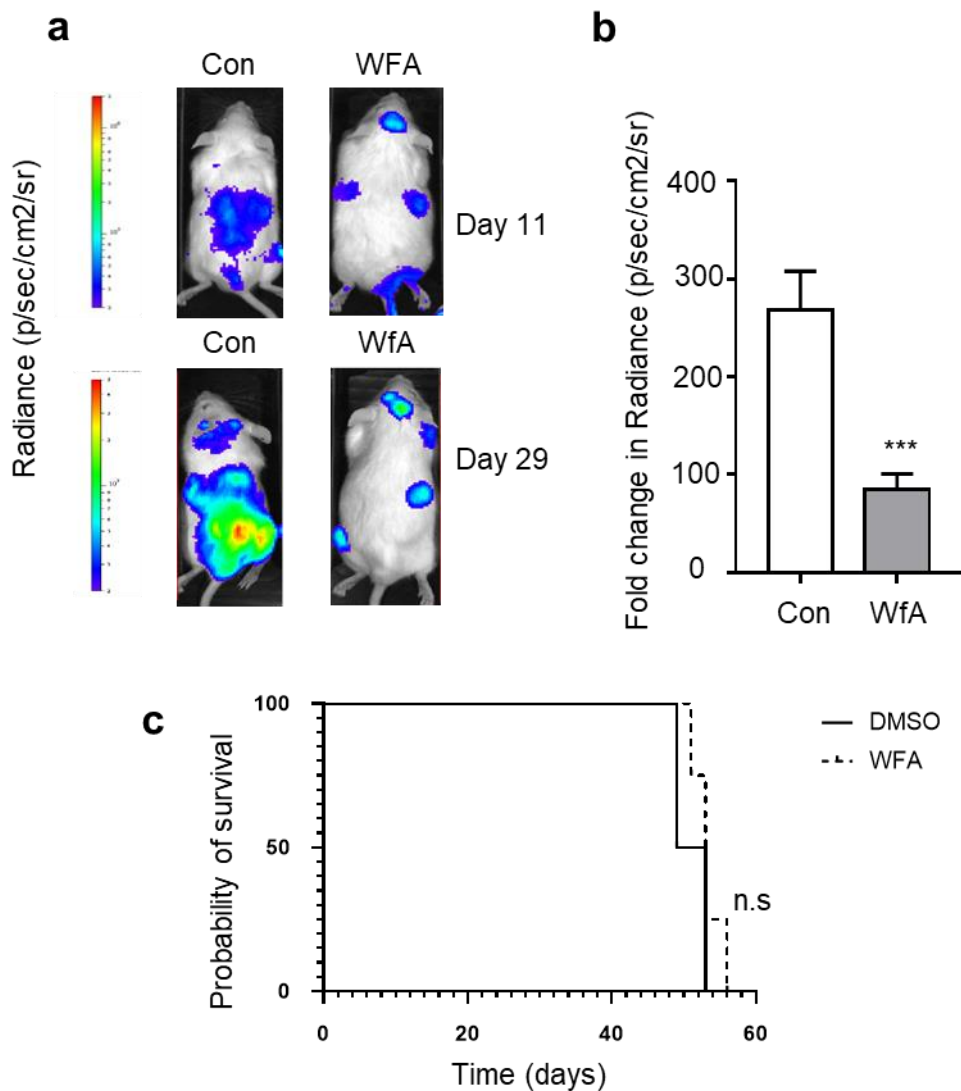


Figure 37. Efficacy of WFA *in vivo*

(a) Bioluminescence imaging of NSG recipient mice 11 days after injection in THP1-LUC2 cells and before drug treatment (day 11, top), and at day 29 after treatment with normal or WFA-containing diet (bottom). Bars for luminescence signal represent photons/s/cm² steradian. (b) luminescence signal in treatment groups from imaging at day 29 (17 days) after treatment with normal or WFA-containing diet. Bars and error bars are means and s.d. of values from control and WFA-treated groups (both n=4). ***, P<0.001, unpaired students *t*-test. (c) Survival curve for NSG recipient mice following treatment

with normal or drug-containing diet, these were not significantly different ($P=.25$), Log-rank (Mantel-Cox) test.

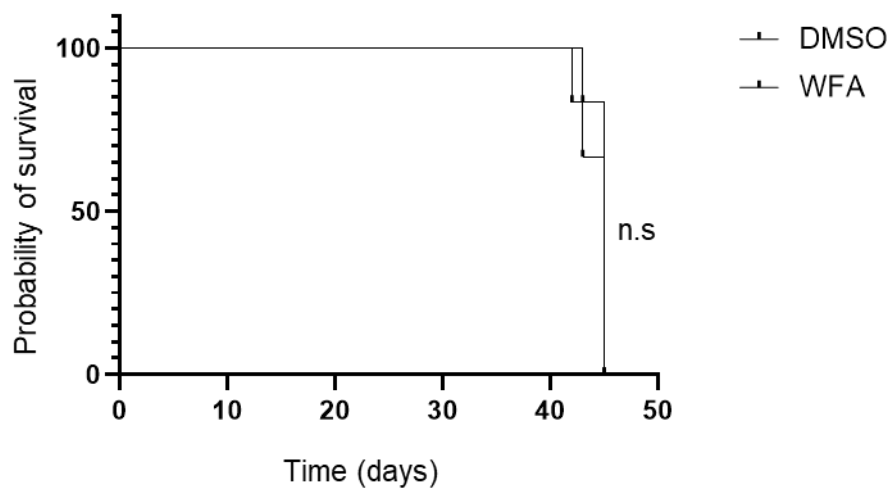


Figure 38. Survival curve following pre-treatment with WFA *in vivo*.

Survival curve for NSG recipient mice following treatment following injection with a primary patient-derived AML sample #1. This AML PDX had been treated in liquid culture for 24 hours with DMSO or 1 μ M WFA for 24 hours. After incubation, the cells were washed, counted and equal numbers of viable cells re-injected into recipient mice. Survival curves were not statistically different between the two groups ($P= 0.47$), Log-rank (Mantel-Cox) test.

5.3 Discussion

In this chapter we demonstrate that WFA exhibits anti-leukaemic activity against both the blast and self-renewal components of AML cells. Immature myeloid blasts account for the majority of the disease, they do not possess the ability to self-renew, but accumulate and lead to failure of normal haematopoiesis. Blast cells are 'stuck' in an immature phenotype, which is known as a differentiation block and is one of the defining features in AML. Our data show that WFA leads to human AML cells acquiring changes in cell surface antigen expression consistent with differentiation. This maturation of the blast cells following treatment could again be attributed to loss of *c-MYB* which is a key player in the differentiation process. Whilst the upregulation of these markers was evident in most of the cell lines, it may be that a different experimental approach might have been preferable. As differentiation markers are measured on live cells, treatment of cells with a lower concentration of WFA over a longer period of time might have led to less cell death and revealed pro-differentiation activity of WFA in these cell lines.

These findings are consistent with work showing that reversal of expression of the fusion oncoprotein MLL-AF9 or its downstream target *c-MYB* initiates terminal AML differentiation (Zuber et al., 2011) (Suzuki et al., 2009). Differentiation therapy in a particular subtype of AML, APML has led to outstanding clinical response rates. The majority of APML are characterised by a specific t(15;17) chromosomal translocation that encodes the promyelocytic leukaemia protein (PML) – retinoic acid receptor- α (RAR α) fusion protein. Expression of this fusion results in transcriptional repression of differentiation genes, and retinoic acid (RA) therapy leads to dissociation of these repressors, thereby resuming differentiation (de The, 2018). The wider use of differentiating agents has no current role in the treatment of AML. Some of the new epigenetic modifiers, BRD4 and IDH1/2 inhibitors, have been shown to promote differentiation, however, the overall message from these

studies is that induction of differentiation alone will have a debulking effect but will be insufficient for full leukaemia clearance (de The, 2018).

The second component are the leukaemic stem cells with the ability to self-renew and therefore have the capacity to initiate, sustain and expand the disease. Sommerville *et al*, showed in an *MLL* rearranged AML, *c-MYB* is an essential transcription factor required for maintaining the transcriptional program of the LSC (Somerville et al., 2009). Our data show treatment with WFA led to inhibition of colony formation in cell lines and primary AML samples. This *in vitro* assay estimates the inhibition of self-renewal of the LSC. The finding that WFA inhibits colony formation in primary cells are particularly interesting as it suggests that *c-MYB* directed therapy would preferentially target the leukaemia stem cell which might have advantageous outcomes for patients. Lack of reduction of colonies in WFA-treated cord blood samples indicates there may be a therapeutic window for targeting *c-MYB* in AML, whereby there is a preferential selection for leukaemia cells and the normal haemopoietic cells are relatively unaffected. It is interesting to consider why the cord blood is not affected given how important *c-MYB* is to establishing erythropoiesis. We would propose this selectivity between leukaemia and normal HSCs reflects the evidence that low levels of *c-MYB* are sufficient to allow normal haematopoiesis and colony formation in the HSCs, whereas leukaemic cells have an increased functional reliance for *c-MYB* and so this reduction leads to inhibition of colony formation. It has been previously shown mebendazole induced *c-MYB* loss in CB is less acute than AML cells (Walf-Vorderwulbecke et al., 2018). This suggests another possibility for the lack of effect of WFA on CB cells is that it may induce smaller changes in the *c-MYB* expression levels. This could be tested in future experiments.

Our next approach was to see if we could extend our pre-clinical modelling and use AML PDX cells as they are more representative of AML in patients. Our aim was to culture primary samples in an *ex-vivo* setting and then this platform could be used for other novel drug testing. Our collaborators at

Newcastle University had shown that culturing primary leukaemia cells on human mesenchymal stem cells, as a feeder layer, allowed long term expansion of a range of primary ALL cells retaining their clonal composition and self-renewal capacity (Pal et al., 2016). Our results show that two primary B-ALL samples were able to proliferate on an MSC feeder layer. The effects were more varied for AML samples; three proliferated well, two modestly and one, not at all.

There were mixed responses to WFA treatment in these primary samples, AML #6, showed a strong apoptotic response to WFA treatment, and two other samples exhibited lesser responses. When we consider the reasons for this, the high cell death of controls suggests sub-optimal culture conditions and this background apoptosis made any effect of the drug difficult to observe. We must also consider whether MSCs are providing protection to leukaemia cells. It is well recognised that drug responses on stromal support are different to liquid culture, in which the MSCs can protect the tumour from drug responses (Ede et al., 2018). The impact of WFA on MSC viability was measured, no gross changes were identified which might have negatively contributed to leukaemic cell viability. It is possible that the culture system would have performed better in a hypoxic environment. Griessinger *et al* used the mouse stromal line, MS-5 with IL3+ G-CSF+TPO in 3%O₂ culture as an efficient niche-like culture system for maintaining a range of human AML samples *in vitro*. This system was able to maintain the leukaemia initiating cells, which the authors propose could serve as a read out for multiple perturbations (Griessinger et al., 2014).

Several groups have developed platforms for *ex vivo* drug sensitivity testing to inform doctors about actionable targets for patients with ALL or AML (Pemovska et al., 2013). Frismantas *et al* used a serum-free ALL coculture system on hTERT immortalized human bone marrow-derived mesenchymal stromal cells (MSCs) (Frismantas et al., 2017). This was linked to an automated microscopic image readout for drug testing. This platform is now

used clinically in patients with relapsed ALL to inform clinicians about actionable targets. Such stromal-based drug profiling platforms are likely to better reflect true drug sensitivity as they capture the response of the interaction between the leukaemic cell and the bone marrow niche.

Overall, the concept of culturing primary patient samples in a more representative environment to the bone marrow niche is clearly desirable. It appears that a simple 2-dimensional co-culture system where primary AML samples are supported by human MSC does not provide this. More sophisticated techniques are being developed by different groups, however, the relative infrequency of the LIC and the difficulty culturing *ex vivo* remains challenging. To date, the NOD/SCID- $\gamma^{-/-}$ model has so far been the most promising model to study the AML stem cell compartment (Pearce et al., 2006).

Having demonstrated anti-leukaemic activity of WFA *in vitro* using cell lines and primary patient-derived AML samples, it was important to evaluate its activity in an *in vivo* model of AML. Our initial experiment using the THP1 AML cell line transduced with a bioluminescent marker was advantageous for disease monitoring and assessing treatment response. Our finding that WFA treatment led to a significant reduction of luciferase signal was encouraging of anti-leukaemic effect *in vivo*. It was also in-keeping with the data published by Sanchez-Martin *et al*, in which WFA was identified as a synergistic therapy in NOTCH1-induced T-ALL. Using a murine *Notch1*-positive, *Pten*-positive murine leukaemia, monotherapy with WFA led to less than 10- fold reduction in luciferase signal. This was following intraperitoneal administration of WFA (10mg/kg). Consistent with our findings, WFA did not translate into a survival benefit, it was only when WFA was combined with the other study medication that a difference in latency was observed. We did not demonstrate any improvement in survival using WFA *in vivo*, either by including WFA in the diet or when primary AML cells were pre-treated with WFA,

Although several preclinical studies have identified WFA for various indications, few, if any have studied its pharmacokinetics or potential difficulties with administration. The two most cited repurposing papers are concerning its use as a synergistic therapy in T-ALL (mentioned above), and as a potent leptin sensitiser, where it demonstrated antidiabetic properties in mice (Lee et al., 2016). Data concerning the pharmacokinetics of WFA are limited and there is no robust data in humans. Mouse data exists and Dai et al recently studied the pharmacokinetics of WFA in rats (Dai et al., 2019). This study determined the oral bioavailability of WFA in male rats was affected by intestinal permeability, metabolism and degradation by bacterial microflora. Six hours after 5mg/kg IV or 10mg/kg oral administration, the plasma concentrations were 100ng/ml, and these had fallen to 50ng/ml by 24 hours. The curves for PO/IV administration were closely aligned. Bioavailability was estimated to be 30%. Bioavailability of more soluble derivatives was limited by first-pass metabolism. We propose the reason we failed to demonstrate efficacy *in vivo* is because of these pharmacological reasons. Despite the potential administration difficulties, should pre-clinical data using WFA continue to be promising, then collaboration with medicinal chemists would be essential in developing WFA into a drug and acquiring pharmacokinetic data in humans.

In summary, in this chapter we have studied the effects on WFA *in vitro* and *in vivo* using functional assays. Our efforts to culture primary AML samples in an *ex-vivo* setting and use them to test anti-c-MYB drugs using a co-culture system with MSCs did not prove to be an optimal system. The culture conditions failed to deliver high levels of viability to assess drug response. We have shown that treatment with WFA led to induction of differentiation in AML cell lines, inhibition of colony formation in AML cell lines and in primary patient-derived AML samples without inhibition of colony formation in cord blood samples. We have demonstrated initial evidence of anti-leukaemic efficacy *in vivo*, with experiments ongoing.

Chapter 6: Conclusions

The management of AML continues to progress from improvements in understanding its pathophysiology to novel diagnostic and therapeutic advances. Despite these developments, treatment options remain challenging for many patients and novel therapies are needed. A hallmark of AML is aberrant gene expression that leads to leukaemia self-renewal and a block in differentiation. Subtype-specific leukaemia oncogenes converge on a number of mediators that drive this transcriptional dysregulation. The transcription factor c-MYB acts as one such mediator. Previous work in our laboratory aimed to identify drugs and compounds capable of inhibiting c-MYB that might be used clinically. To do so they generated a c-MYB gene expression signature and used it to probe the Connectivity Map database. A list of candidate drugs was generated predicted to inverse the c-MYB signature in AML. This approach was successful in identifying and validating mebendazole, the anti-helminth drug, as a c-MYB targeting drug. In this thesis we aimed to study the steroidal lactone Withaferin A (WFA), derived from *Withania somnifera*, an additional candidate 'hit' predicted to inhibit c-MYB in AML.

Our initial experiments confirmed WFA inhibited c-MYB function in an AML cell line leading to loss of c-MYB. We undertook RNAseq of WFA-treated THP1 cells to examine the global gene expression changes following treatment. A number of c-MYB related gene signatures were examined with the RNA-Seq data and all demonstrated enrichment following WFA treatment. c-MYB has been implicated in the leukaemic transcriptional regulation of the LSC and myeloid differentiation. GSEA analysis of gene expression changes following treatment of THP1 cells with WFA demonstrated negative enrichment of the LSC self-renewal signature and differentiation gene sets. Importantly, we did not observe enrichment against a C/EBP β signature, a pathway in which WFA was reported to act. Taken together, these results

indicate that that a major part of WFA activity is through interference of the c-MYB leukaemic transcriptional programme.

We then progressed to establish that inhibition of c-MYB function could be extended across a panel of AML cell lines, with different underlying cytogenetics. This was observed as loss of c-MYB and induction of apoptosis following exposure. By using a degradation-resistant mutant (Δ MYB), we demonstrated THP1 cells expressing Δ MYB were less susceptible to WFA-induced protein loss. We then studied the critical function of c-MYB in maintaining self-renewal of leukaemia progenitors and showed transient WFA treatment was able to inhibit colony formation. Δ MYB expressing THP1 cells partially rescued WFA-induced inhibition of colony function. Together, these experiments highlight the significance of c-MYB in the anti-AML effects of WFA.

When considering how WFA led to c-MYB loss in AML cells, we identified that WFA-treated gene expression changes demonstrated enrichment in pathways implicated in protein translation. We then showed WFA-induced c-MYB loss was accompanied by phosphorylation of $\text{elf}2\alpha$, implicating protein translation as the likely cause of WFA-induced c-MYB loss. It is likely this inhibition is not c-MYB specific, but rather has a disproportionate effect on short-lived transcription factors such as c-MYB because of their short half-life and rapid cellular turnover.

Finally, we demonstrated that WFA exhibits anti-leukaemic activity against both the blast and self-renewal components of AML cells. Upregulation of differentiation markers was observed in THP1 cells following drug treatment. The cells possessing self-renewal capability are those that have the potential to initiate, sustain and expand the disease. We were able to demonstrate in both cell lines and AML PDX, that WFA treatment impaired the ability to self-renew when assessed by colony formation assays. In contrast, WFA treatment had minimal impact on colony formation when cord-blood derived progenitor cells were used, highlighting the possibility of a therapeutic window. We

present preliminary data that this translated into impaired leukaemia progression *in vivo*.

This work adds to the growing body of evidence that targeting transcription factors is an attractive and rational therapeutic approach in AML. c-MYB is required for definitive haematopoiesis and plays a key role in the differentiation of different lineages. In AML, c-MYB has been shown to be a critical mediator of MLL-rearranged AML and more recently, c-MYB silencing was shown to inhibit self-renewal across a range of AML subtypes. This demonstrates that c-MYB acts as an effector of the oncogenic programmes imposed by upstream drivers. It is their role downstream of different oncogenic drivers where they maintain aberrant transcriptional pathways required by the leukaemia cell that makes them particularly exciting as therapeutic targets, as it offers the possibility of new therapies applicable to a wide range of AML subtypes.

It has historically been considered difficult to develop molecules targeting transcription factors, including c-MYB, as they do not have an easily identifiable druggable domain. However, recently strategies have been developed to circumvent this. These include identification and development of small molecules (Uttarkar et al., 2016) and peptidomimetics (Ramaswamy et al., 2018) that inhibit the interaction between c-MYB and the CBP/p300 transcriptional co-activator complex, and identification of drugs that target c-MYB for proteasomal degradation (Walf-Vorderwulbecke et al., 2018). The data presented in this thesis demonstrates consistent findings that loss of c-MYB (irrespective of the mode of targeting c-MYB) leads to apoptosis of leukaemia cells, loss of regulation of c-MYB regulated genes, inhibition of leukaemia cell self-renewal and anti-AML effect *in vivo*. In addition, all studies, including ours, highlight the potential of a therapeutic window, whereby normal haematopoietic progenitors are relatively unaffected by c-MYB loss, and leukaemia cells are adversely affected.

Withaferin A is a steroidal lactone derived from the medical plant *Withania somnifera*. It has been used in ayurvedic medicine for centuries. Whilst not an

FDA approved drug, there has been increased scientific focus recently with two highly cited repurposing papers. Most relevant to our work is that WFA exerts protein translation inhibition in T-ALL (Sanchez-Martin et al., 2017). Our findings are the first report of WFA leading to translation inhibition in AML, and in which the critical target has been identified. Data concerning the pharmacokinetics of WFA are limited and there is no robust data in humans. Future work would need collaboration with medicinal chemists to explore the feasibility of developing WFA into a drug and acquiring pharmacokinetic data in humans. To date, inhibition of protein translation has not been a significant therapeutic approach in cancer, but this may represent a novel compound with the potential to modulate c-MYB through a different approach.

Being able to offer c-MYB directed therapy to all patients with AML, irrespective of their cytogenetic or molecular subtype would be a shift away from subtype-specific therapy. The emphasis on precision medicine in leukaemia has moved treatment from a 'one-size fits all' to a more individualised approach with the development and availability of targeted therapy. This approach has been a success for APL, where the fusion protein is degraded by all-trans retinoic acid (ATRA) and Arsenic trioxide and leads to overall survival rates of over 90% (Burnett et al., 2015). Targeted therapies such as FLT3 and IDH1/2 inhibitors are still being evaluated in order to optimise their use, frequently in combination therapy. The majority of these trials are being conducted in adults in whom stem cell transplantation may not be possible. In paediatric AML, there are frequently no cytogenetic or molecular abnormalities to target. Hill *et al* recognises there are challenges in trial design in the face of precision medicine, "Greater delineation gives rise to a wider variety of treatments, and treatment combinations, targeted at ever smaller groups of patients". An excellent example of non-subtype specific therapy is CAR-T therapy and the bispecific T-cell engager, blinatumomab. Both target CD19, a cell surface marker found on B-ALL cells, irrespective of subtype. In both therapies, efficacy has been proven and they are recognised treatments in first high-risk relapse of B-ALL (Maude et al., 2018, Topp et al.,

2015, Stackelberg et al., 2016). Whilst CAR-T is a cellular therapy, its undoubted success in targeting multiple subtypes of B-ALL serve as a promising model for c-MYB directed therapy.

In summary, this thesis adds to the body of evidence that targeting c-MYB is an emerging therapeutic approach for all subtypes of AML, and in particular we highlight the steroidal lactone, WFA as a compound with anti-AML properties which are mediated through loss of c-MYB.

References

- ADOLFSSON, J., BORGE, O. J., BRYDER, D., THEILGAARD-MONCH, K., ASTRAND-GRUNDSTROM, I., SITNICKA, E., SASAKI, Y. & JACOBSEN, S. E. 2001. Upregulation of Flt3 expression within the bone marrow Lin(-)Sca1(+)c-kit(+) stem cell compartment is accompanied by loss of self-renewal capacity. *Immunity*, 15, 659-69.
- ADOLFSSON, J., MANSSON, R., BUZA-VIDAS, N., HULTQUIST, A., LIUBA, K., JENSEN, C. T., BRYDER, D., YANG, L., BORGE, O. J., THOREN, L. A., ANDERSON, K., SITNICKA, E., SASAKI, Y., SIGVARDSSON, M. & JACOBSEN, S. E. 2005. Identification of Flt3+ lympho-myeloid stem cells lacking erythro-megakaryocytic potential a revised road map for adult blood lineage commitment. *Cell*, 121, 295-306.
- AKASHI, K., TRAVER, D., MIYAMOTO, T. & WEISSMAN, I. L. 2000. A clonogenic common myeloid progenitor that gives rise to all myeloid lineages. *Nature*, 404, 193-197.
- ANJOS-AFONSO, F., CURRIE, E., PALMER, H. G., FOSTER, K. E., TAUSSIG, D. C. & BONNET, D. 2013. CD34(-) cells at the apex of the human hematopoietic stem cell hierarchy have distinctive cellular and molecular signatures. *Cell Stem Cell*, 13, 161-74.
- ANTONY-DEBRE, I., PAUL, A., LEITE, J., MITCHELL, K., KIM, H. M., CARVAJAL, L. A., TODOROVA, T. I., HUANG, K., KUMAR, A., FARAHAT, A. A., BARTHOLDY, B., NARAYANAGARI, S. R., CHEN, J., AMBESI-IMPIOMBATO, A., FERRANDO, A. A., MANTZARIS, I., GAVATHIOTIS, E., VERMA, A., WILL, B., BOYKIN, D. W., WILSON, W. D., POON, G. M. & STEIDL, U. 2017. Pharmacological inhibition of the transcription factor PU.1 in leukemia. *J Clin Invest*, 127, 4297-4313.
- AVELLINO, R. & DELWEL, R. 2017. Expression and regulation of C/EBP α in normal myelopoiesis and in malignant transformation. *Blood*, 129, 2083-2091.
- AYTON, P. M. & CLEARY, M. L. 2003. Transformation of myeloid progenitors by MLL oncoproteins is dependent on Hoxa7 and Hoxa9. *Genes Dev*, 17, 2298-307.
- BENNETT, J. M., CATOVSKY, D., DANIEL, M. T., FLANDRIN, G., GALTON, D. A., GRALNICK, H. R. & SULTAN, C. 1976. Proposals for the classification of the acute leukaemias. French-American-British (FAB) co-operative group. *Br J Haematol*, 33, 451-8.
- BERTHON, C., RAFFOUX, E., THOMAS, X., VEY, N., GOMEZ-ROCA, C., YEE, K., TAUSSIG, D. C., REZAI, K., ROUMIER, C., HERAIT, P., KAHATT, C., QUESNEL, B., MICHALLET, M., RECHER, C., LOKIEC, F., PREUDHOMME, C. & DOMBRET, H. 2016. Bromodomain inhibitor

- OTX015 in patients with acute leukaemia: a dose-escalation, phase 1 study. *Lancet Haematol*, 3, e186-95.
- BHATIA, M., WANG, J. C. Y., KAPP, U., BONNET, D. & DICK, J. E. 1997. Purification of primitive human hematopoietic cells capable of repopulating immune-deficient mice. *Proceedings of the National Academy of Sciences*, 94, 5320-5325.
- BIEDENKAPP, H., BORGMEYER, U., SIPPEL, A. E. & KLEMPNAUER, K. H. 1988. Viral myb oncogene encodes a sequence-specific DNA-binding activity. *Nature*, 335, 835-7.
- BIES, J. & WOLFF, L. 1997. Oncogenic activation of c-Myb by carboxyl-terminal truncation leads to decreased proteolysis by the ubiquitin-26S proteasome pathway. *Oncogene*, 14, 203-212.
- BIRKE, M., SCHREINER, S., GARCÍA-CUÉLLAR, M. P., MAHR, K., TITGEMEYER, F. & SLANY, R. K. 2002. The MT domain of the proto-oncoprotein MLL binds to CpG-containing DNA and discriminates against methylation. *Nucleic Acids Res*, 30, 958-65.
- BONNET, D. 2001. Normal and leukemic CD34-negative human hematopoietic stem cells. *Rev Clin Exp Hematol*, 5, 42-61.
- BONNET, D. & DICK, J. E. 1997. Human acute myeloid leukemia is organized as a hierarchy that originates from a primitive hematopoietic cell. *Nature Medicine*, 3, 730-737.
- BOSMA, G. C., CUSTER, R. P. & BOSMA, M. J. 1983. A severe combined immunodeficiency mutation in the mouse. *Nature*, 301, 527-30.
- BURNETT, A., WETZLER, M. & LOWENBERG, B. 2011. Therapeutic advances in acute myeloid leukemia. *J Clin Oncol*, 29, 487-94.
- BURNETT, A. K., DAS GUPTA, E., KNAPPER, S., KHWAJA, A., SWEENEY, M., KJELDSSEN, L., HAWKINS, T., BETTERIDGE, S. E., CAHALIN, P., CLARK, R. E., HILLS, R. K., RUSSELL, N. H. & GROUP, U. N. A. S. 2018. Addition of the mammalian target of rapamycin inhibitor, everolimus, to consolidation therapy in acute myeloid leukemia: experience from the UK NCRI AML17 trial. *Haematologica*, 103, 1654-1661.
- BURNETT, A. K., RUSSELL, N. H., HILLS, R. K., BOWEN, D., KELL, J., KNAPPER, S., MORGAN, Y. G., LOK, J., GRECH, A., JONES, G., KHWAJA, A., FRIIS, L., MCMULLIN, M. F., HUNTER, A., CLARK, R. E. & GRIMWADE, D. 2015. Arsenic trioxide and all-trans retinoic acid treatment for acute promyelocytic leukaemia in all risk groups (AML17): results of a randomised, controlled, phase 3 trial. *Lancet Oncol*, 16, 1295-305.

- CALIFANO, A. & ALVAREZ, M. J. 2017. The recurrent architecture of tumour initiation, progression and drug sensitivity. *Nat Rev Cancer*, 17, 116-130.
- CAO, F., TOWNSEND, E. C., KARATAS, H., XU, J., LI, L., LEE, S., LIU, L., CHEN, Y., OUILLETTE, P., ZHU, J., HESS, J. L., ATADJA, P., LEI, M., QIN, Z. S., MALEK, S., WANG, S. & DOU, Y. 2014. Targeting MLL1 H3K4 methyltransferase activity in mixed-lineage leukemia. *Molecular cell*, 53, 247-261.
- CHEN, R., ZHU, M., CHAUDHARI, R. R., ROBLES, O., CHEN, Y., SKILLERN, W., QIN, Q., WIERDA, W. G., ZHANG, S., HULL, K. G., ROMO, D. & PLUNKETT, W. 2019. Creating novel translation inhibitors to target pro-survival proteins in chronic lymphocytic leukemia. *Leukemia*, 33, 1663-1674.
- CHOI, M. J., PARK, E. J., MIN, K. J., PARK, J. W. & KWON, T. K. 2011. Endoplasmic reticulum stress mediates withaferin A-induced apoptosis in human renal carcinoma cells. *Toxicol In Vitro*, 25, 692-8.
- CLAPPIER, E., CUCCUINI, W., KALOTA, A., CRINQUETTE, A., CAYUELA, J. M., DIK, W. A., LANGERAK, A. W., MONTPELLIER, B., NADEL, B., WALRAFEN, P., DELATTRE, O., AURIAS, A., LEBLANC, T., DOMBRET, H., GEWIRTZ, A. M., BARUCHEL, A., SIGAUX, F. & SOULIER, J. 2007. The C-MYB locus is involved in chromosomal translocation and genomic duplications in human T-cell acute leukemia (T-ALL), the translocation defining a new T-ALL subtype in very young children. *Blood*, 110, 1251-61.
- CORCES, M. R., BUENROSTRO, J. D., WU, B., GREENSIDE, P. G., CHAN, S. M., KOENIG, J. L., SNYDER, M. P., PRITCHARD, J. K., KUNDAJE, A., GREENLEAF, W. J., MAJETI, R. & CHANG, H. Y. 2016. Lineage-specific and single-cell chromatin accessibility charts human hematopoiesis and leukemia evolution. *Nat Genet*, 48, 1193-203.
- CORRADINI, F., CESI, V., BARTELLA, V., PANI, E., BUSSOLARI, R., CANDINI, O. & CALABRETTA, B. 2005. Enhanced proliferative potential of hematopoietic cells expressing degradation-resistant c-Myb mutants. *J Biol Chem*, 280, 30254-62.
- COULIBALY, A., HAAS, A., STEINMANN, S., JAKOBS, A., SCHMIDT, T. J. & KLEMPNAUER, K.-H. 2018. The natural anti-tumor compound Celastrol targets a Myb-C/EBP β -p300 transcriptional module implicated in myeloid gene expression. *PloS one*, 13, e0190934-e0190934.
- COZZIO, A., PASSEGUE, E., AYTON, P. M., KARSUNKY, H., CLEARY, M. L. & WEISSMAN, I. L. 2003. Similar MLL-associated leukemias arising from self-renewing stem cells and short-lived myeloid progenitors. *Genes Dev*, 17, 3029-35.

- DAI, T., JIANG, W., GUO, Z., WANG, Z., HUANG, M., ZHONG, G., LIANG, C., PEI, X. & DAI, R. 2019. Studies on oral bioavailability and first-pass metabolism of withaferin A in rats using LC-MS/MS and Q-TRAP. *Biomed Chromatogr*, 33, e4573.
- DASER, A. & RABBITTS, T. H. 2005. The versatile mixed lineage leukaemia gene MLL and its many associations in leukaemogenesis. *Semin Cancer Biol*, 15, 175-88.
- DAWSON, M. A., PRINJHA, R. K., DITTMANN, A., GIOTOPOULOS, G., BANTSCHOFF, M., CHAN, W. I., ROBSON, S. C., CHUNG, C. W., HOPF, C., SAVITSKI, M. M., HUTHMACHER, C., GUDGIN, E., LUGO, D., BEINKE, S., CHAPMAN, T. D., ROBERTS, E. J., SODEN, P. E., AUGER, K. R., MIRGUET, O., DOEHNER, K., DELWEL, R., BURNETT, A. K., JEFFREY, P., DREWES, G., LEE, K., HUNTLY, B. J. & KOUZARIDES, T. 2011. Inhibition of BET recruitment to chromatin as an effective treatment for MLL-fusion leukaemia. *Nature*, 478, 529-33.
- DE THE, H. 2018. Differentiation therapy revisited. *Nat Rev Cancer*, 18, 117-127.
- DEMAISON, C., PARSLEY, K., BROUNS, G., SCHERR, M., BATTMER, K., KINNON, C., GREZ, M. & THRASHER, A. J. 2002. High-level transduction and gene expression in hematopoietic repopulating cells using a human immunodeficiency [correction of immunodeficiency] virus type 1-based lentiviral vector containing an internal spleen focus forming virus promoter. *Hum Gene Ther*, 13, 803-13.
- DINARDO, C. D., PRATZ, K., PULLARKAT, V., JONAS, B. A., ARELLANO, M., BECKER, P. S., FRANKFURT, O., KONOPLEVA, M., WEI, A. H., KANTARJIAN, H. M., XU, T., HONG, W. J., CHYLA, B., POTLURI, J., POLLYEA, D. A. & LETAI, A. 2019. Venetoclax combined with decitabine or azacitidine in treatment-naive, elderly patients with acute myeloid leukemia. *Blood*, 133, 7-17.
- DOHNER, H., ESTEY, E., GRIMWADE, D., AMADORI, S., APPELBAUM, F. R., BUCHNER, T., DOMBRET, H., EBERT, B. L., FENAUX, P., LARSON, R. A., LEVINE, R. L., LO-COCO, F., NAOE, T., NIEDERWIESER, D., OSSENKOPPELE, G. J., SANZ, M., SIERRA, J., TALLMAN, M. S., TIEN, H. F., WEI, A. H., LOWENBERG, B. & BLOOMFIELD, C. D. 2017. Diagnosis and management of AML in adults: 2017 ELN recommendations from an international expert panel. *Blood*, 129, 424-447.
- DONATI, B., LORENZINI, E. & CIARROCCHI, A. 2018. BRD4 and Cancer: going beyond transcriptional regulation. *Molecular Cancer*, 17, 164.
- DOU, Y. & HESS, J. L. 2008. Mechanisms of transcriptional regulation by MLL and its disruption in acute leukemia. *International Journal of Hematology*, 87, 10-18.

- DUPREY, S. P. & BOETTIGER, D. 1985. Developmental regulation of c-myc in normal myeloid progenitor cells. *Proc Natl Acad Sci U S A*, 82, 6937-41.
- EDE, B. C., ASMARO, R. R., MOPPETT, J. P., DIAMANTI, P. & BLAIR, A. 2018. Investigating chemoresistance to improve sensitivity of childhood T-cell acute lymphoblastic leukemia to parthenolide. *Haematologica*, 103, 1493-1501.
- EGUCHI, M., EGUCHI-ISHIMAE, M. & GREAVES, M. 2003. The role of the MLL gene in infant leukemia. *Int J Hematol*, 78, 390-401.
- EMAMBOKUS, N., VEGIOPOULOS, A., HARMAN, B., JENKINSON, E., ANDERSON, G. & FRAMPTON, J. 2003. Progression through key stages of haemopoiesis is dependent on distinct threshold levels of c-Myb. *Embo j*, 22, 4478-88.
- FALKENBERG, K. D., JAKOBS, A., MATERN, J. C., DORNER, W., UTTARKAR, S., TRENTMANN, A., STEINMANN, S., COULIBALY, A., SCHOMBURG, C., MOOTZ, H. D., SCHMIDT, T. J. & KLEMPNAUER, K. H. 2017. Withaferin A, a natural compound with anti-tumor activity, is a potent inhibitor of transcription factor C/EBPbeta. *Biochim Biophys Acta*, 1864, 1349-1358.
- FEIKOVÁ, S., WOLFF, L. & BIES, J. 2000. Constitutive ubiquitination and degradation of c-myc by the 26S proteasome during proliferation and differentiation of myeloid cells. *Neoplasia*, 47, 212-8.
- FRISMANTAS, V., DOBAY, M. P., RINALDI, A., TCHINDA, J., DUNN, S. H., KUNZ, J., RICHTER-PECHANSKA, P., MAROVCA, B., PAIL, O., JENNI, S., DIAZ-FLORES, E., CHANG, B. H., BROWN, T. J., COLLINS, R. H., UHRIG, S., BALASUBRAMANIAN, G. P., BANDAPALLI, O. R., HIGI, S., EUGSTER, S., VOEGELI, P., DELORENZI, M., CARIO, G., LOH, M. L., SCHRAPPE, M., STANULLA, M., KULOZIK, A. E., MUCKENTHALER, M. U., SAHA, V., IRVING, J. A., MEISEL, R., RADIMERSKI, T., VON STACKELBERG, A., ECKERT, C., TYNER, J. W., HORVATH, P., BORNHAUSER, B. C. & BOURQUIN, J. P. 2017. Ex vivo drug response profiling detects recurrent sensitivity patterns in drug-resistant acute lymphoblastic leukemia. *Blood*, 129, e26-e37.
- FULOP, G. M. & PHILLIPS, R. A. 1990. The scid mutation in mice causes a general defect in DNA repair. *Nature*, 347, 479-482.
- GEWIRTZ, A., ANFOSSI, G., VENTURELLI, D., VALPREDA, S., SIMS, R. & CALABRETTA, B. 1989. G1/S transition in normal human T-lymphocytes requires the nuclear protein encoded by c-myc. *Science*, 245, 180-183.

- GEWIRTZ, A. M. & CALABRETTA, B. 1988. A c-myb antisense oligodeoxynucleotide inhibits normal human hematopoiesis in vitro. *Science*, 242, 1303-6.
- GONDA, T. J. & METCALF, D. 1984. Expression of myb, myc and fos proto-oncogenes during the differentiation of a murine myeloid leukaemia. *Nature*, 310, 249.
- GRIESSINGER, E., ANJOS-AFONSO, F., PIZZITOLA, I., ROUAULT-PIERRE, K., VARGAFTIG, J., TAUSSIG, D., GRIBBEN, J., LASSAILLY, F. & BONNET, D. 2014. A Niche-Like Culture System Allowing the Maintenance of Primary Human Acute Myeloid Leukemia-Initiating Cells: A New Tool to Decipher Their Chemoresistance and Self-Renewal Mechanisms. *STEM CELLS Translational Medicine*, 3, 520-529.
- GU, M., YU, Y., GUNAHERATH, G. M., GUNATILAKA, A. A., LI, D. & SUN, D. 2014. Structure-activity relationship (SAR) of withanolides to inhibit Hsp90 for its activity in pancreatic cancer cells. *Invest New Drugs*, 32, 68-74.
- HESS, J. L. 2004. MLL: a histone methyltransferase disrupted in leukemia. *Trends Mol Med*, 10, 500-7.
- HESS, J. L., BITTNER, C. B., ZEISIG, D. T., BACH, C., FUCHS, U., BORKHARDT, A., FRAMPTON, J. & SLANY, R. K. 2006. c-Myb is an essential downstream target for homeobox-mediated transformation of hematopoietic cells. *Blood*, 108, 297-304.
- HEYNINCK, K., LAHTELA-KAKKONEN, M., VAN DER VEKEN, P., HAEGEMAN, G. & VANDEN BERGHE, W. 2014. Withaferin A inhibits NF-kappaB activation by targeting cysteine 179 in IKKbeta. *Biochem Pharmacol*, 91, 501-9.
- HILLS, R. K., CASTAIGNE, S., APPELBAUM, F. R., DELAUNAY, J., PETERSDORF, S., OTHUS, M., ESTEY, E. H., DOMBRET, H., CHEVRET, S., IFRAH, N., CAHN, J. Y., RECHER, C., CHILTON, L., MOORMAN, A. V. & BURNETT, A. K. 2014. Addition of gemtuzumab ozogamicin to induction chemotherapy in adult patients with acute myeloid leukaemia: a meta-analysis of individual patient data from randomised controlled trials. *Lancet Oncol*, 15, 986-96.
- HOLCIK, M. & SONENBERG, N. 2005. Translational control in stress and apoptosis. *Nat Rev Mol Cell Biol*, 6, 318-27.
- HORTON, S. J., GRIER, D. G., MCGONIGLE, G. J., THOMPSON, A., MORROW, M., DE SILVA, I., MOULDING, D. A., KIOUSSIS, D., LAPPIN, T. R., BRADY, H. J. & WILLIAMS, O. 2005. Continuous MLL-ENL expression is necessary to establish a "Hox Code" and maintain immortalization of hematopoietic progenitor cells. *Cancer Res*, 65, 9245-52.

- HORTON, S. J. & HUNTLY, B. J. 2012. Recent advances in acute myeloid leukemia stem cell biology. *Haematologica*, 97, 966-74.
- HUNTLY, B. J., SHIGEMATSU, H., DEGUCHI, K., LEE, B. H., MIZUNO, S., DUCLOS, N., ROWAN, R., AMARAL, S., CURLEY, D., WILLIAMS, I. R., AKASHI, K. & GILLILAND, D. G. 2004. MOZ-TIF2, but not BCR-ABL, confers properties of leukemic stem cells to committed murine hematopoietic progenitors. *Cancer Cell*, 6, 587-96.
- ICHIKAWA, H., TAKADA, Y., SHISHODIA, S., JAYAPRAKASAM, B., NAIR, M. G. & AGGARWAL, B. B. 2006. Withanolides potentiate apoptosis, inhibit invasion, and abolish osteoclastogenesis through suppression of nuclear factor-kappaB (NF-kappaB) activation and NF-kappaB-regulated gene expression. *Mol Cancer Ther*, 5, 1434-45.
- IWASAKI, H. & AKASHI, K. 2007. Myeloid Lineage Commitment from the Hematopoietic Stem Cell. *Immunity*, 26, 726-740.
- JIN, S., ZHAO, H., YI, Y., NAKATA, Y., KALOTA, A. & GEWIRTZ, A. M. 2010. c-Myb binds MLL through menin in human leukemia cells and is an important driver of MLL-associated leukemogenesis. *J Clin Invest*, 120, 593-606.
- JULIETTE, L., CÉCILE, P., CHRISTINE, T., EMMANUEL, R., PASCAL, T., DENIS, C., OLLIVIER, L., XAVIER, T., CLAUDE, G., KARÏN, G.-M., STEPHEN, D. R., REBECCA, J. B., PIERRE, B., CLAUDE, P., SYLVIE, C., HERVE, D. & SYLVIE, C. 2019. Gemtuzumab ozogamicin for de novo acute myeloid leukemia: final efficacy and safety updates from the open-label, phase III ALFA-0701 trial. *Haematologica*, 104, 113-119.
- KAILEH, M., VANDEN BERGHE, W., HEYERICK, A., HORION, J., PIETTE, J., LIBERT, C., DE KEUKELEIRE, D., ESSAWI, T. & HAEGEMAN, G. 2007. Withaferin a strongly elicits I kappa B kinase beta hyperphosphorylation concomitant with potent inhibition of its kinase activity. *J Biol Chem*, 282, 4253-64.
- KAMEL-REID, S. & DICK, J. 1988. Engraftment of immune-deficient mice with human hematopoietic stem cells. *Science*, 242, 1706-1709.
- KAUFMAN, R. J. 1999. Stress signaling from the lumen of the endoplasmic reticulum: coordination of gene transcriptional and translational controls. *Genes Dev*, 13, 1211-33.
- KITAGAWA, K., HIRAMATSU, Y., UCHIDA, C., ISOBE, T., HATTORI, T., ODA, T., SHIBATA, K., NAKAMURA, S., KIKUCHI, A. & KITAGAWA, M. 2009. Fbw7 promotes ubiquitin-dependent degradation of c-Myb: involvement of GSK3-mediated phosphorylation of Thr-572 in mouse c-Myb. *Oncogene*, 28, 2393-405.
- KRIVTSOV, A. V., TWOMEY, D., FENG, Z., STUBBS, M. C., WANG, Y., FABER, J., LEVINE, J. E., WANG, J., HAHN, W. C., GILLILAND, D. G., GOLUB, T. R. & ARMSTRONG, S. A. 2006. Transformation from

committed progenitor to leukaemia stem cell initiated by MLL-AF9. *Nature*, 442, 818-22.

- LACOMBE, J., HERBLOT, S., ROJAS-SUTTERLIN, S., HAMAN, A., BARAKAT, S., ISCOVE, N. N., SAUVAGEAU, G. & HOANG, T. 2010. Scl regulates the quiescence and the long-term competence of hematopoietic stem cells. *Blood*, 115, 792-803.
- LAM, S. S. Y., HO, E. S. K., HE, B.-L., WONG, W.-W., CHER, C.-Y., NG, N. K. L., MAN, C.-H., GILL, H., CHEUNG, A. M. S., IP, H.-W., SO, C.-C., TAMBURINI, J., SO, C. W. E., HO, D. N., AU, C.-H., CHAN, T.-L., MA, E. S. K., LIANG, R., KWONG, Y.-L. & LEUNG, A. Y. H. 2016. Homoharringtonine (omacetaxine mepesuccinate) as an adjunct for FLT3-ITD acute myeloid leukemia. *Science Translational Medicine*, 8, 359ra129-359ra129.
- LAMB, J. 2007. The Connectivity Map: a new tool for biomedical research. *Nat Rev Cancer*, 7, 54-60.
- LAPIDOT, T., PFLUMIO, F., DOEDENS, M., MURDOCH, B., WILLIAMS, D. E. & DICK, J. E. 1992. Cytokine stimulation of multilineage hematopoiesis from immature human cells engrafted in SCID mice. *Science*, 255, 1137-41.
- LAPIDOT, T., SIRARD, C., VORMOOR, J., MURDOCH, B., HOANG, T., CACERES-CORTES, J., MINDEN, M., PATERSON, B., CALIGIURI, M. A. & DICK, J. E. 1994. A cell initiating human acute myeloid leukaemia after transplantation into SCID mice. *Nature*, 367, 645-648.
- LAROCHELLE, A., VORMOOR, J., HANENBERG, H., WANG, J. C., BHATIA, M., LAPIDOT, T., MORITZ, T., MURDOCH, B., XIAO, X. L., KATO, I., WILLIAMS, D. A. & DICK, J. E. 1996. Identification of primitive human hematopoietic cells capable of repopulating NOD/SCID mouse bone marrow: implications for gene therapy. *Nat Med*, 2, 1329-37.
- LEE, I. C. & CHOI, B. Y. 2016. Withaferin-A--A Natural Anticancer Agent with Pleiotropic Mechanisms of Action. *Int J Mol Sci*, 17, 290.
- LEE, J., LIU, J., FENG, X., SALAZAR HERNANDEZ, M. A., MUCKA, P., IBI, D., CHOI, J. W. & OZCAN, U. 2016. Withaferin A is a leptin sensitizer with strong antidiabetic properties in mice. *Nat Med*, 22, 1023-32.
- LI, L., YANG, G., REN, C., TANIMOTO, R., HIRAYAMA, T., WANG, J., HAWKE, D., KIM, S. M., LEE, J. S., GOLTSOV, A. A., PARK, S., ITTMANN, M. M., TRONCOSO, P. & THOMPSON, T. C. 2013. Glioma pathogenesis-related protein 1 induces prostate cancer cell death through Hsc70-mediated suppression of AURKA and TPX2. *Mol Oncol*, 7, 484-96.
- LIEU, Y. K. & REDDY, E. P. 2009. Conditional c-myb knockout in adult hematopoietic stem cells leads to loss of self-renewal due to impaired

- proliferation and accelerated differentiation. *Proc Natl Acad Sci U S A*, 106, 21689-94.
- LIN, C., SMITH, E. R., TAKAHASHI, H., LAI, K. C., MARTIN-BROWN, S., FLORENS, L., WASHBURN, M. P., CONAWAY, J. W., CONAWAY, R. C. & SHILATIFARD, A. 2010. AFF4, a component of the ELL/P-TEFb elongation complex and a shared subunit of MLL chimeras, can link transcription elongation to leukemia. *Mol Cell*, 37, 429-37.
- LIU, W., VIELHAUER, G. A., HOLZBEIERLEIN, J. M., ZHAO, H., GHOSH, S., BROWN, D., LEE, E. & BLAGG, B. S. 2015. KU675, a Concomitant Heat-Shock Protein Inhibitor of Hsp90 and Hsc70 that Manifests Isoform Selectivity for Hsp90alpha in Prostate Cancer Cells. *Mol Pharmacol*, 88, 121-30.
- LU, J., QIAN, Y., ALTIERI, M., DONG, H., WANG, J., RAINA, K., HINES, J., WINKLER, J. D., CREW, A. P., COLEMAN, K. & CREWS, C. M. 2015. Hijacking the E3 Ubiquitin Ligase Cereblon to Efficiently Target BRD4. *Chem Biol*, 22, 755-63.
- LYMAN, S. D. & JACOBSEN, S. E. 1998. c-kit ligand and Flt3 ligand: stem/progenitor cell factors with overlapping yet distinct activities. *Blood*, 91, 1101-34.
- MALARA, N., FOCA, D., CASADONTE, F., SESTO, M. F., MACRINA, L., SANTORO, L., SCARAMUZZINO, M., TERRACCIANO, R. & SAVINO, R. 2008. Simultaneous inhibition of the constitutively activated nuclear factor kappaB and of the interleukin-6 pathways is necessary and sufficient to completely overcome apoptosis resistance of human U266 myeloma cells. *Cell Cycle*, 7, 3235-45.
- MALATERRE, J., MANTAMADIOTIS, T., DWORKIN, S., LIGHTOWLER, S., YANG, Q., RANSOME, M. I., TURNLEY, A. M., NICHOLS, N. R., EMAMBOKUS, N. R., FRAMPTON, J. & RAMSAY, R. G. 2008. c-Myb is required for neural progenitor cell proliferation and maintenance of the neural stem cell niche in adult brain. *Stem Cells*, 26, 173-81.
- MALIK, F., KUMAR, A., BHUSHAN, S., KHAN, S., BHATIA, A., SURI, K. A., QAZI, G. N. & SINGH, J. 2007. Reactive oxygen species generation and mitochondrial dysfunction in the apoptotic cell death of human myeloid leukemia HL-60 cells by a dietary compound withaferin A with concomitant protection by N-acetyl cysteine. *Apoptosis*, 12, 2115-33.
- MANSOUR, M. R., ABRAHAM, B. J., ANDERS, L., BEREZOVSKAYA, A., GUTIERREZ, A., DURBIN, A. D., ETCHIN, J., LAWTON, L., SALLAN, S. E., SILVERMAN, L. B., LOH, M. L., HUNGER, S. P., SANDA, T., YOUNG, R. A. & LOOK, A. T. 2014. Oncogene regulation. An oncogenic super-enhancer formed through somatic mutation of a noncoding intergenic element. *Science*, 346, 1373-7.

- MAUDE, S. L., LAETSCH, T. W., BUECHNER, J., RIVES, S., BOYER, M., BITTENCOURT, H., BADER, P., VERNERIS, M. R., STEFANSKI, H. E., MYERS, G. D., QAYED, M., DE MOERLOOSE, B., HIRAMATSU, H., SCHLIS, K., DAVIS, K. L., MARTIN, P. L., NEMECEK, E. R., YANIK, G. A., PETERS, C., BARUCHEL, A., BOISSEL, N., MECHINAUD, F., BALDUZZI, A., KRUEGER, J., JUNE, C. H., LEVINE, B. L., WOOD, P., TARAN, T., LEUNG, M., MUELLER, K. T., ZHANG, Y., SEN, K., LEBWOHL, D., PULSIPHER, M. A. & GRUPP, S. A. 2018. Tisagenlecleucel in Children and Young Adults with B-Cell Lymphoblastic Leukemia. *N Engl J Med*, 378, 439-448.
- MEIR, W. & DAVID, S. 2011. Omacetaxine as an Anticancer Therapeutic: What is Old is New Again. *Current Pharmaceutical Design*, 17, 59-64.
- MEYER, C., BURMEISTER, T., GRÖGER, D., TSAUR, G., FECHINA, L., RENNEVILLE, A., SUTTON, R., VENN, N. C., EMERENCIANO, M., POMBO-DE-OLIVEIRA, M. S., BARBIERI BLUNCK, C., ALMEIDA LOPES, B., ZUNA, J., TRKA, J., BALLERINI, P., LAPILLONNE, H., DE BRAEKELEER, M., CAZZANIGA, G., CORRAL ABASCAL, L., VAN DER VELDEN, V. H. J., DELABESSE, E., PARK, T. S., OH, S. H., SILVA, M. L. M., LUND-AHO, T., JUVONEN, V., MOORE, A. S., HEIDENREICH, O., VORMOOR, J., ZERKALENKOVA, E., OLSHANSKAYA, Y., BUENO, C., MENENDEZ, P., TEIGLER-SCHLEGEL, A., ZUR STADT, U., LENTES, J., GÖHRING, G., KUSTANOVICH, A., ALENIKOVA, O., SCHÄFER, B. W., KUBETZKO, S., MADSEN, H. O., GRUHN, B., DUARTE, X., GAMEIRO, P., LIPPERT, E., BIDET, A., CAYUELA, J. M., CLAPPIER, E., ALONSO, C. N., ZWAAN, C. M., VAN DEN HEUVEL-EIBRINK, M. M., IZRAELI, S., TRAKHTENBROT, L., ARCHER, P., HANCOCK, J., MÖRICKE, A., ALTEN, J., SCHRAPPE, M., STANULLA, M., STREHL, S., ATTARBASCHI, A., DWORZAK, M., HAAS, O. A., PANZER-GRÜMAYER, R., SEDÉK, L., SZCZEPAŃSKI, T., CAYE, A., SUAREZ, L., CAVÉ, H. & MARSCHALEK, R. 2018. The MLL recombinome of acute leukemias in 2017. *Leukemia*, 32, 273-284.
- MILNE, T. A., BRIGGS, S. D., BROCK, H. W., MARTIN, M. E., GIBBS, D., ALLIS, C. D. & HESS, J. L. 2002. MLL targets SET domain methyltransferase activity to Hox gene promoters. *Mol Cell*, 10, 1107-17.
- MUCENSKI, M. L., MCLAIN, K., KIER, A. B., SWERDLOW, S. H., SCHREINER, C. M., MILLER, T. A., PIETRYGA, D. W., SCOTT, W. J., JR. & POTTER, S. S. 1991. A functional c-myb gene is required for normal murine fetal hepatic hematopoiesis. *Cell*, 65, 677-89.
- MURATI, A., GERVAIS, C., CARBUCCIA, N., FINETTI, P., CERVERA, N., ADELAIDE, J., STRUSKI, S., LIPPERT, E., MUGNERET, F., TIGAUD, I., PENTHER, D., BASTARD, C., POPPE, B., SPELEMAN, F., BARANGER, L., LUQUET, I., CORNILLET-LEFEBVRE, P., NADAL,

- N., NGUYEN-KHAC, F., PEROT, C., OLSCHWANG, S., BERTUCCI, F., CHAFFANET, M., LESSARD, M., MOZZICONACCI, M. J. & BIRNBAUM, D. 2009. Genome profiling of acute myelomonocytic leukemia: alteration of the MYB locus in MYST3-linked cases. *Leukemia*, 23, 85-94.
- MURRE, C. 2018. 'Big bang' of B-cell development revealed. *Genes & Development*, 32, 93-95.
- NAKATA, Y., SHETZLINE, S., SAKASHITA, C., KALOTA, A., RALLAPALLI, R., RUDNICK, S. I., ZHANG, Y., EMERSON, S. G. & GEWIRTZ, A. M. 2007. c-Myb contributes to G2/M cell cycle transition in human hematopoietic cells by direct regulation of cyclin B1 expression. *Molecular and cellular biology*, 27, 2048-2058.
- NECHANITZKY, R., AKBAS, D., SCHERER, S., GYÖRY, I., HOYLER, T., RAMAMOORTHY, S., DIEFENBACH, A. & GROSSCHEDL, R. 2013. Transcription factor EBF1 is essential for the maintenance of B cell identity and prevention of alternative fates in committed cells. *Nature Immunology*, 14, 867-875.
- NG, S. W., MITCHELL, A., KENNEDY, J. A., CHEN, W. C., MCLEOD, J., IBRAHIMOVA, N., ARRUDA, A., POPESCU, A., GUPTA, V., SCHIMMER, A. D., SCHUH, A. C., YEE, K. W., BULLINGER, L., HEROLD, T., GORLICH, D., BUCHNER, T., HIDDEMANN, W., BERDEL, W. E., WORMANN, B., CHEOK, M., PREUDHOMME, C., DOMBRET, H., METZELER, K., BUSKE, C., LOWENBERG, B., VALK, P. J., ZANDSTRA, P. W., MINDEN, M. D., DICK, J. E. & WANG, J. C. 2016. A 17-gene stemness score for rapid determination of risk in acute leukaemia. *Nature*, 540, 433-437.
- NICOLAIDES, N. C., GUALDI, R., CASADEVALL, C., MANZELLA, L. & CALABRETTA, B. 1991. Positive autoregulation of c-myb expression via Myb binding sites in the 5' flanking region of the human c-myb gene. *Molecular and Cellular Biology*, 11, 6166-6176.
- NISHIKAWA, Y., OKUZAKI, D., FUKUSHIMA, K., MUKAI, S., OHNO, S., OZAKI, Y., YABUTA, N. & NOJIMA, H. 2015. Withaferin A Induces Cell Death Selectively in Androgen-Independent Prostate Cancer Cells but Not in Normal Fibroblast Cells. *PLoS One*, 10, e0134137.
- OBEN, K. Z., ALHAKEEM, S. S., MCKENNA, M. K., BRANDON, J. A., MANI, R., NOOTHI, S. K., JINPENG, L., AKUNURU, S., DHAR, S. K., SINGH, I. P., LIANG, Y., WANG, C., ABDEL-LATIF, A., STILLS, H. F., JR., ST CLAIR, D. K., GEIGER, H., MUTHUSAMY, N., TOHYAMA, K., GUPTA, R. C. & BONDADA, S. 2017. Oxidative stress-induced JNK/AP-1 signaling is a major pathway involved in selective apoptosis of myelodysplastic syndrome cells by Withaferin-A. *Oncotarget*, 8, 77436-77452.

- OH, I.-H. & REDDY, E. P. 1999. The myb gene family in cell growth, differentiation and apoptosis. *Oncogene*, 18, 3017-3033.
- OH, J. H., LEE, T. J., KIM, S. H., CHOI, Y. H., LEE, S. H., LEE, J. M., KIM, Y. H., PARK, J. W. & KWON, T. K. 2008. Induction of apoptosis by withaferin A in human leukemia U937 cells through down-regulation of Akt phosphorylation. *Apoptosis*, 13, 1494-504.
- ORKIN, S. H. & ZON, L. I. 2008. Hematopoiesis: an evolving paradigm for stem cell biology. *Cell*, 132, 631-44.
- PAL, D., BLAIR, H. J., ELDER, A., DORMON, K., RENNIE, K. J., COLEMAN, D. J., WEILAND, J., RANKIN, K. S., FILBY, A., HEIDENREICH, O. & VORMOOR, J. 2016. Long-term in vitro maintenance of clonal abundance and leukaemia-initiating potential in acute lymphoblastic leukaemia. *Leukemia*, 30, 1691-700.
- PATTABIRAMAN, D. R. & GONDA, T. J. 2013. Role and potential for therapeutic targeting of MYB in leukemia. *Leukemia*, 27, 269-77.
- PEARCE, D. J., TAUSSIG, D., ZIBARA, K., SMITH, L. L., RIDLER, C. M., PREUDHOMME, C., YOUNG, B. D., ROHATINER, A. Z., LISTER, T. A. & BONNET, D. 2006. AML engraftment in the NOD/SCID assay reflects the outcome of AML: implications for our understanding of the heterogeneity of AML. *Blood*, 107, 1166-73.
- PEMOVSKA, T., KONTRO, M., YADAV, B., EDGREN, H., ELDFORS, S., SZWAJDA, A., ALMUSA, H., BESPALOV, M. M., ELLONEN, P., ELONEN, E., GJERTSEN, B. T., KARJALAINEN, R., KULESSKIY, E., LAGSTROM, S., LEHTO, A., LEPISTO, M., LUNDAN, T., MAJUMDER, M. M., MARTI, J. M., MATTILA, P., MURUMAGI, A., MUSTJOKI, S., PALVA, A., PARSONS, A., PIRTTINEN, T., RAMET, M. E., SUVELA, M., TURUNEN, L., VASTRIK, I., WOLF, M., KNOWLES, J., AITTOKALLIO, T., HECKMAN, C. A., PORKKA, K., KALLIONIEMI, O. & WENNERBERG, K. 2013. Individualized systems medicine strategy to tailor treatments for patients with chemorefractory acute myeloid leukemia. *Cancer Discov*, 3, 1416-29.
- PERL, A. E., MARTINELLI, G., CORTES, J. E., NEUBAUER, A., BERMAN, E., PAOLINI, S., MONTESINOS, P., BAER, M. R., LARSON, R. A., USTUN, C., FABBIANO, F., ERBA, H. P., DI STASI, A., STUART, R., OLIN, R., KASNER, M., CICERI, F., CHOU, W.-C., PODOLTSEV, N., RECHER, C., YOKOYAMA, H., HOSONO, N., YOON, S.-S., LEE, J.-H., PARDEE, T., FATHI, A. T., LIU, C., HASABOU, N., LIU, X., BAHCECI, E. & LEVIS, M. J. 2019. Gilteritinib or Chemotherapy for Relapsed or Refractory FLT3-Mutated AML. *New England Journal of Medicine*, 381, 1728-1740.
- PIYA, S., MU, H., BHATTACHARYA, S., LORENZI, P. L., DAVIS, R. E., MCQUEEN, T., RUVOLO, V., BARAN, N., WANG, Z., QIAN, Y., CREWS, C. M., KONOPLEVA, M., ISHIZAWA, J., YOU, M. J.,

- KANTARJIAN, H., ANDREEFF, M. & BORTHAKUR, G. 2019. BETP degradation simultaneously targets acute myelogenous leukemia stem cells and the microenvironment. *J Clin Invest*, 129, 1878-1894.
- POLLYEA, D. A., TALLMAN, M. S., DE BOTTON, S., KANTARJIAN, H. M., COLLINS, R., STEIN, A. S., FRATTINI, M. G., XU, Q., TOSOLINI, A., SEE, W. L., MACBETH, K. J., AGRESTA, S. V., ATTAR, E. C., DINARDO, C. D. & STEIN, E. M. 2019. Enasidenib, an inhibitor of mutant IDH2 proteins, induces durable remissions in older patients with newly diagnosed acute myeloid leukemia. *Leukemia*, 33, 2575-2584.
- PORCHER, C., CHAGRAOUI, H. & KRISTIANSEN, M. S. 2017. SCL/TAL1: a multifaceted regulator from blood development to disease. *Blood*, 129, 2051-2060.
- RAMASWAMY, K., FORBES, L., MINUESA, G., GINDIN, T., BROWN, F., KHARAS, M. G., KRIVTSOV, A. V., ARMSTRONG, S. A., STILL, E., DE STANCHINA, E., KNOEHEL, B., KOCHER, R. & KENTSIS, A. 2018. Peptidomimetic blockade of MYB in acute myeloid leukemia. *Nature Communications*, 9, 110.
- RAMSAY, R. G. & GONDA, T. J. 2008. MYB function in normal and cancer cells. *Nat Rev Cancer*, 8, 523-34.
- ROBOZ, G. J., DINARDO, C. D., STEIN, E. M., DE BOTTON, S., MIMS, A. S., PRINCE, G. T., ALTMAN, J. K., ARELLANO, M. L., DONNELLAN, W., ERBA, H. P., MANNIS, G. N., POLLYEA, D. A., STEIN, A. S., UY, G. L., WATTS, J. M., FATHI, A. T., KANTARJIAN, H. M., TALLMAN, M. S., CHOE, S., DAI, D., FAN, B., WANG, H., ZHANG, V., YEN, K. E., KAPSALIS, S. M., HICKMAN, D., LIU, H., AGRESTA, S. V., WU, B., ATTAR, E. C. & STONE, R. M. 2019. Ivosidenib induces deep durable remissions in patients with newly diagnosed IDH1-mutant acute myeloid leukemia. *Blood*.
- ROE, J. S., MERCAN, F., RIVERA, K., PAPPIN, D. J. & VAKOC, C. R. 2015. BET Bromodomain Inhibition Suppresses the Function of Hematopoietic Transcription Factors in Acute Myeloid Leukemia. *Mol Cell*, 58, 1028-39.
- ROSENBAUER, F. & TENEN, D. G. 2007. Transcription factors in myeloid development: balancing differentiation with transformation. *Nat Rev Immunol*, 7, 105-17.
- SAKAMOTO, H., DAI, G., TSUJINO, K., HASHIMOTO, K., HUANG, X., FUJIMOTO, T., MUCENSKI, M., FRAMPTON, J. & OGAWA, M. 2006. Proper levels of c-Myb are discretely defined at distinct steps of hematopoietic cell development. *Blood*, 108, 896-903.
- SANCHEZ-MARTIN, M., AMBESI-IMPIOMBATO, A., QIN, Y., HERRANZ, D., BANSAL, M., GIRARDI, T., PAIETTA, E., TALLMAN, M. S., ROWE, J. M., DE KEERSMAECKER, K., CALIFANO, A. & FERRANDO, A. A.

2017. Synergistic antileukemic therapies in NOTCH1-induced T-ALL. *Proc Natl Acad Sci U S A*, 114, 2006-2011.
- SARVAIYA, P. J., SCHWARTZ, J. R., HERNANDEZ, C. P., RODRIGUEZ, P. C. & VEDECKIS, W. V. 2012. Role of c-Myb in the survival of pre B-cell acute lymphoblastic leukemia and leukemogenesis. *Am J Hematol*, 87, 969-76.
- SHULTZ, L. D., LYONS, B. L., BURZENSKI, L. M., GOTT, B., CHEN, X., CHALEFF, S., KOTB, M., GILLIES, S. D., KING, M., MANGADA, J., GREINER, D. L. & HANDGRETINGER, R. 2005. Human lymphoid and myeloid cell development in NOD/LtSz-scid IL2R gamma null mice engrafted with mobilized human hemopoietic stem cells. *J Immunol*, 174, 6477-89.
- SHULTZ, L. D., SCHWEITZER, P. A., CHRISTIANSON, S. W., GOTT, B., SCHWEITZER, I. B., TENNENT, B., MCKENNA, S., MOBRAATEN, L., RAJAN, T. V., GREINER, D. L. & ET AL. 1995. Multiple defects in innate and adaptive immunologic function in NOD/LtSz-scid mice. *J Immunol*, 154, 180-91.
- SILVERA, D., FORMENTI, S. C. & SCHNEIDER, R. J. 2010. Translational control in cancer. *Nat Rev Cancer*, 10, 254-66.
- SMITH, E., LIN, C. & SHILATIFARD, A. 2011. The super elongation complex (SEC) and MLL in development and disease. *Genes Dev*, 25, 661-72.
- SOMERVILLE, T. C., MATHENY, C. J., SPENCER, G. J., IWASAKI, M., RINN, J. L., WITTEN, D. M., CHANG, H. Y., SHURTLEFF, S. A., DOWNING, J. R. & CLEARY, M. L. 2009. Hierarchical maintenance of MLL myeloid leukemia stem cells employs a transcriptional program shared with embryonic rather than adult stem cells. *Cell Stem Cell*, 4, 129-40.
- STACKELBERG, A. V., LOCATELLI, F., ZUGMAIER, G., HANDGRETINGER, R., TRIPPETT, T. M., RIZZARI, C., BADER, P., O'BRIEN, M. M., BRETHON, B., BHOJWANI, D., SCHLEGEL, P. G., BORKHARDT, A., RHEINGOLD, S. R., COOPER, T. M., ZWAAN, C. M., BARNETTE, P., MESSINA, C., MICHEL, G., DUBOIS, S. G., HU, K., ZHU, M., WHITLOCK, J. A. & GORE, L. 2016. Phase I/Phase II Study of Blinatumomab in Pediatric Patients With Relapsed/Refractory Acute Lymphoblastic Leukemia. *Journal of Clinical Oncology*, 34, 4381-4389.
- STAM, R. W., SCHNEIDER, P., HAGELSTEIN, J. A., VAN DER LINDEN, M. H., STUMPEL, D. J., DE MENEZES, R. X., DE LORENZO, P., VALSECCHI, M. G. & PIETERS, R. 2010. Gene expression profiling-based dissection of MLL translocated and MLL germline acute lymphoblastic leukemia in infants. *Blood*, 115, 2835-44.

- STONE, R. M., MANDREKAR, S. J., SANFORD, B. L., LAUMANN, K., GEYER, S., BLOOMFIELD, C. D., THIEDE, C., PRIOR, T. W., DÖHNER, K., MARCUCCI, G., LO-COCO, F., KLISOVIC, R. B., WEI, A., SIERRA, J., SANZ, M. A., BRANDWEIN, J. M., DE WITTE, T., NIEDERWIESER, D., APPELBAUM, F. R., MEDEIROS, B. C., TALLMAN, M. S., KRAUTER, J., SCHLENK, R. F., GANSER, A., SERVE, H., EHNINGER, G., AMADORI, S., LARSON, R. A. & DÖHNER, H. 2017. Midostaurin plus Chemotherapy for Acute Myeloid Leukemia with a FLT3 Mutation. *New England Journal of Medicine*, 377, 454-464.
- SUBRAMANIAN, A., TAMAYO, P., MOOTHA, V. K., MUKHERJEE, S., EBERT, B. L., GILLETTE, M. A., PAULOVICH, A., POMEROY, S. L., GOLUB, T. R., LANDER, E. S. & MESIROV, J. P. 2005. Gene set enrichment analysis: a knowledge-based approach for interpreting genome-wide expression profiles. *Proc Natl Acad Sci U S A*, 102, 15545-50.
- SUMNER, R., CRAWFORD, A., MUCENSKI, M. & FRAMPTON, J. 2000. Initiation of adult myelopoiesis can occur in the absence of c-Myb whereas subsequent development is strictly dependent on the transcription factor. *Oncogene*, 19, 3335-3342.
- SUZUKI, H., FORREST, A. R., VAN NIMWEGEN, E., DAUB, C. O., BALWIERZ, P. J., IRVINE, K. M., LASSMANN, T., RAVASI, T., HASEGAWA, Y., DE HOON, M. J., KATAYAMA, S., SCHRODER, K., CARNINCI, P., TOMARU, Y., KANAMORI-KATAYAMA, M., KUBOSAKI, A., AKALIN, A., ANDO, Y., ARNER, E., ASADA, M., ASAHARA, H., BAILEY, T., BAJIC, V. B., BAUER, D., BECKHOUSE, A. G., BERTIN, N., BJORKEGREN, J., BROMBACHER, F., BULGER, E., CHALK, A. M., CHIBA, J., CLOONAN, N., DAWE, A., DOSTIE, J., ENGSTROM, P. G., ESSACK, M., FAULKNER, G. J., FINK, J. L., FREDMAN, D., FUJIMORI, K., FURUNO, M., GOJOBORI, T., GOUGH, J., GRIMMOND, S. M., GUSTAFSSON, M., HASHIMOTO, M., HASHIMOTO, T., HATAKEYAMA, M., HEINZEL, S., HIDE, W., HOFMANN, O., HORNQUIST, M., HUMINIECKI, L., IKEO, K., IMAMOTO, N., INOUE, S., INOUE, Y., ISHIHARA, R., IWAYANAGI, T., JACOBSEN, A., KAUR, M., KAWAJI, H., KERR, M. C., KIMURA, R., KIMURA, S., KIMURA, Y., KITANO, H., KOGA, H., KOJIMA, T., KONDO, S., KONNO, T., KROGH, A., KRUGER, A., KUMAR, A., LENHARD, B., LENNARTSSON, A., LINDOW, M., LIZIO, M., MACPHERSON, C., MAEDA, N., MAHER, C. A., MAQUNGO, M., MAR, J., MATIGIAN, N. A., MATSUDA, H., MATTICK, J. S., MEIER, S., MIYAMOTO, S., MIYAMOTO-SATO, E., NAKABAYASHI, K., NAKACHI, Y., NAKANO, M., NYGAARD, S., OKAYAMA, T., OKAZAKI, Y., OKUDA-YABUKAMI, H., ORLANDO, V., OTOMO, J., PACHKOV, M., PETROVSKY, N., et al. 2009. The transcriptional network that

- controls growth arrest and differentiation in a human myeloid leukemia cell line. *Nat Genet*, 41, 553-62.
- TOPP, M. S., GÖKBUGET, N., STEIN, A. S., ZUGMAIER, G., O'BRIEN, S., BARGOU, R. C., DOMBRET, H., FIELDING, A. K., HEFFNER, L., LARSON, R. A., NEUMANN, S., FOÀ, R., LITZOW, M., RIBERA, J. M., RAMBALDI, A., SCHILLER, G., BRÜGGEMANN, M., HORST, H. A., HOLLAND, C., JIA, C., MANIAR, T., HUBER, B., NAGORSEN, D., FORMAN, S. J. & KANTARJIAN, H. M. 2015. Safety and activity of blinatumomab for adult patients with relapsed or refractory B-precursor acute lymphoblastic leukaemia: a multicentre, single-arm, phase 2 study. *Lancet Oncol*, 16, 57-66.
- TRENTIN, L., GIORDAN, M., DINGERMANN, T., BASSO, G., TE KRONNIE, G. & MARSCHALEK, R. 2009. Two independent gene signatures in pediatric t(4;11) acute lymphoblastic leukemia patients. *Eur J Haematol*, 83, 406-19.
- UTTARKAR, S., DASSE, E., COULIBALY, A., STEINMANN, S., JAKOBS, A., SCHOMBURG, C., TRENTMANN, A., JOSE, J., SCHLENKE, P., BERDEL, W. E., SCHMIDT, T. J., MULLER-TIDOW, C., FRAMPTON, J. & KLEMPNAUER, K. H. 2016. Targeting acute myeloid leukemia with a small molecule inhibitor of the Myb/p300 interaction. *Blood*, 127, 1173-82.
- UTTARKAR, S., DUKARE, S., BOPP, B., GOBLIRSCH, M., JOSE, J. & KLEMPNAUER, K. H. 2015. Naphthol AS-E Phosphate Inhibits the Activity of the Transcription Factor Myb by Blocking the Interaction with the KIX Domain of the Coactivator p300. *Mol Cancer Ther*, 14, 1276-85.
- VAN RHENEN, A., FELLER, N., KELDER, A., WESTRA, A. H., ROMBOUTS, E., ZWEEGMAN, S., VAN DER POL, M. A., WAISFISZ, Q., OSSENKOPPELE, G. J. & SCHUURHUIS, G. J. 2005. High stem cell frequency in acute myeloid leukemia at diagnosis predicts high minimal residual disease and poor survival. *Clin Cancer Res*, 11, 6520-7.
- VANDEN BERGHE, W., SABBE, L., KAILEH, M., HAEGEMAN, G. & HEYNINCK, K. 2012. Molecular insight in the multifunctional activities of Withaferin A. *Biochem Pharmacol*, 84, 1282-91.
- VELTEN, L., HAAS, S. F., RAFFEL, S., BLASZKIEWICZ, S., ISLAM, S., HENNIG, B. P., HIRCHE, C., LUTZ, C., BUSS, E. C., NOWAK, D., BOCH, T., HOFMANN, W.-K., HO, A. D., HUBER, W., TRUMPP, A., ESSERS, M. A. G. & STEINMETZ, L. M. 2017. Human haematopoietic stem cell lineage commitment is a continuous process. *Nature cell biology*, 19, 271-281.
- VETRIE, D., HELGASON, G. V. & COPLAND, M. 2020. The leukaemia stem cell: similarities, differences and clinical prospects in CML and AML. *Nature Reviews Cancer*, 20, 158-173.

- VORMOOR, J., LAPIDOT, T., PFLUMIO, F., RISDON, G., PATTERSON, B., BROXMEYER, H. E. & DICK, J. E. 1994. Immature human cord blood progenitors engraft and proliferate to high levels in severe combined immunodeficient mice. *Blood*, 83, 2489-97.
- WALDRON, T., DE DOMINICI, M., SOLIERA, A. R., AUDIA, A., IACOBUCCI, I., LONETTI, A., MARTINELLI, G., ZHANG, Y., MARTINEZ, R., HYSLOP, T., BENDER, T. P. & CALABRETTA, B. 2012. c-Myb and its target Bmi1 are required for p190BCR/ABL leukemogenesis in mouse and human cells. *Leukemia*, 26, 644-53.
- WALF-VORDERWULBECKE, V., PEARCE, K., BROOKS, T., HUBANK, M., VAN DEN HEUVEL-EIBRINK, M. M., ZWAAN, C. M., ADAMS, S., EDWARDS, D., BARTRAM, J., SAMARASINGHE, S., ANCLIFF, P., KHWAJA, A., GOULDEN, N., WILLIAMS, G., DE BOER, J. & WILLIAMS, O. 2018. Targeting acute myeloid leukemia by drug-induced c-MYB degradation. *Leukemia*, 32, 882-889.
- WILLIAMS, G. 2013. SPIEDw: a searchable platform-independent expression database web tool. *BMC Genomics*, 14, 765.
- WINTERS, A. C. & BERNT, K. M. 2017. MLL-Rearranged Leukemias-An Update on Science and Clinical Approaches. *Front Pediatr*, 5, 4.
- XU, Y., MILAZZO, J. P., SOMERVILLE, T. D. D., TARUMOTO, Y., HUANG, Y. H., OSTRANDER, E. L., WILKINSON, J. E., CHALLEN, G. A. & VAKOC, C. R. 2018. A TFIID-SAGA Perturbation that Targets MYB and Suppresses Acute Myeloid Leukemia. *Cancer Cell*, 33, 13-28.e8.
- YAMAMOTO, R., MORITA, Y., OOEHARA, J., HAMANAKA, S., ONODERA, M., RUDOLPH, K. L., EMA, H. & NAKAUCHI, H. 2013. Clonal analysis unveils self-renewing lineage-restricted progenitors generated directly from hematopoietic stem cells. *Cell*, 154, 1112-1126.
- YANG, H., WANG, Y., CHERYAN, V. T., WU, W., CUI, C. Q., POLIN, L. A., PASS, H. I., DOU, Q. P., RISHI, A. K. & WALI, A. 2012. Withaferin A inhibits the proteasome activity in mesothelioma in vitro and in vivo. *PLoS One*, 7, e41214.
- YILMAZ, M., WANG, F., LOGHAVI, S., BUESO-RAMOS, C., GUMBS, C., LITTLE, L., SONG, X., ZHANG, J., KADIA, T., BORTHAKUR, G., JABBOUR, E., PEMMARAJU, N., SHORT, N., GARCIA-MANERO, G., ESTROV, Z., KANTARJIAN, H., FUTREAL, A., TAKAHASHI, K. & RAVANDI, F. 2019. Late relapse in acute myeloid leukemia (AML): clonal evolution or therapy-related leukemia? *Blood Cancer J*, 9, 7.
- YU, Y., HAMZA, A., ZHANG, T., GU, M., ZOU, P., NEWMAN, B., LI, Y., GUNATILAKA, A. A., ZHAN, C. G. & SUN, D. 2010. Withaferin A targets heat shock protein 90 in pancreatic cancer cells. *Biochem Pharmacol*, 79, 542-51.

- ZEISIG, B. B., MILNE, T., GARCÍA-CUÉLLAR, M. P., SCHREINER, S., MARTIN, M. E., FUCHS, U., BORKHARDT, A., CHANDA, S. K., WALKER, J., SODEN, R., HESS, J. L. & SLANY, R. K. 2004. Hoxa9 and Meis1 are key targets for MLL-ENL-mediated cellular immortalization. *Mol Cell Biol*, 24, 617-28.
- ZHANG, P., IWASAKI-ARAI, J., IWASAKI, H., FENYUS, M. L., DAYARAM, T., OWENS, B. M., SHIGEMATSU, H., LEVANTINI, E., HUETTNER, C. S., LEKSTROM-HIMES, J. A., AKASHI, K. & TENEN, D. G. 2004. Enhancement of hematopoietic stem cell repopulating capacity and self-renewal in the absence of the transcription factor C/EBP alpha. *Immunity*, 21, 853-63.
- ZHAO, H., JIN, S. & GEWIRTZ, A. M. 2012. The Histone Acetyltransferase TIP60 Interacts with c-Myb and Inactivates Its Transcriptional Activity in Human Leukemia. *Journal of Biological Chemistry*, 287, 925-934.
- ZHAO, L., GLAZOV, E. A., PATTABIRAMAN, D. R., AL-OWAIDI, F., ZHANG, P., BROWN, M. A., LEO, P. J. & GONDA, T. J. 2011. Integrated genome-wide chromatin occupancy and expression analyses identify key myeloid pro-differentiation transcription factors repressed by Myb. *Nucleic Acids Res*, 39, 4664-79.
- ZUBER, J., RAPPAPORT, A. R., LUO, W., WANG, E., CHEN, C., VASEVA, A. V., SHI, J., WEISSMUELLER, S., FELLMANN, C., TAYLOR, M. J., WEISSENBOECK, M., GRAEBER, T. G., KOGAN, S. C., VAKOC, C. R. & LOWE, S. W. 2011. An integrated approach to dissecting oncogene addiction implicates a Myb-coordinated self-renewal program as essential for leukemia maintenance. *Genes Dev*, 25, 1628-40.

Appendices

Rank	Compound
1	Mebendazole
2	Terfenadine
3	Medrysone
4	Oxybutynin
5	Methylergometrine
6	Mefloquine
7	Prochlorperazine
8	Thioridazine
9	Alexidine
10	Cefixime
11	Loperamide
12	Phthalylsulfathiazole
13	Colchicine
14	Withaferin A

Appendix 1. Compounds identified by CMAP

Gene	Base Mean	Mean DMSO	Mean WFA	Fold Change	log2 Fold Change	pvalue	padj
GFI1	1258.01	2181	335	0.153	-2.704	2.84E-150	3.75E-147
THBD	1357.98	2404	311	0.13	-2.946	1.97E-109	1.68E-106
MYC	1258.47	2076	441	0.213	-2.234	7.90E-96	4.78E-93
ALDH1B1	777.83	1363	192	0.142	-2.821	4.83E-87	2.13E-84
FRY	1733.11	2784	683	0.245	-2.029	1.44E-84	5.99E-82
RRS1	733.4	1252	215	0.172	-2.538	3.06E-84	1.23E-81
WDR3	1699.58	2709	690	0.255	-1.973	3.93E-79	1.39E-76
IRF8	3847.35	6369	1325	0.208	-2.264	9.33E-79	3.22E-76
NOP16	472.23	811	134	0.165	-2.596	3.41E-74	1.05E-71
SERPINB2	371.12	681	61	0.091	-3.454	1.56E-73	4.63E-71
MYB	2935.62	4893	978	0.2	-2.322	1.46E-72	3.79E-70
FGL2	263.66	487	40	0.083	-3.586	5.52E-70	1.29E-67
EEF2K	654.19	1070	238	0.223	-2.165	2.60E-69	5.98E-67
CXorf21	1560.12	2574	546	0.213	-2.234	2.45E-68	5.48E-66
URB2	488.79	791	186	0.235	-2.087	3.45E-61	6.68E-59
ERLIN1	693.63	1102	285	0.259	-1.949	1.71E-60	3.22E-58
NAA15	2179.33	3343	1015	0.304	-1.718	2.23E-58	3.85E-56
WDR43	1257.6	1988	527	0.266	-1.912	1.02E-53	1.55E-51
NAV3	356.75	641	73	0.113	-3.139	1.35E-53	2.03E-51
POLR1B	702.6	1124	281	0.251	-1.997	1.38E-53	2.05E-51
TLR2	1211.42	1855	568	0.306	-1.707	1.52E-52	2.11E-50
LYST	9757.05	13683	5831	0.426	-1.23	1.22E-51	1.63E-49
SFMBT2	798.08	1249	347	0.279	-1.842	1.24E-51	1.64E-49
LTV1	1604.01	2382	826	0.347	-1.527	4.24E-50	5.31E-48
AKAP1	879.48	1416	343	0.243	-2.044	5.44E-50	6.75E-48
DDX21	2083.45	3310	858	0.259	-1.947	5.58E-50	6.86E-48
BRIX1	1003.9	1485	523	0.352	-1.505	1.12E-49	1.36E-47
ZFP36L2	5701.72	9089	2314	0.255	-1.973	6.71E-49	8.04E-47
FAM105A	1665.66	2643	688	0.261	-1.94	3.14E-48	3.64E-46
CD93	3250.64	4887	1614	0.33	-1.598	4.31E-48	4.96E-46
MAK16	1413.48	2075	752	0.363	-1.463	1.12E-47	1.26E-45
MRT04	906.28	1371	441	0.322	-1.635	1.09E-46	1.20E-44
FUT4	2003.6	2922	1085	0.372	-1.428	4.04E-46	4.41E-44
PRICKLE1	743.35	1145	341	0.298	-1.746	4.95E-46	5.36E-44
DKC1	1698.85	2491	907	0.365	-1.456	1.04E-45	1.09E-43
HK2	476.68	799	154	0.193	-2.374	6.05E-45	6.22E-43
GNL3	2189.61	3187	1192	0.374	-1.418	1.52E-44	1.53E-42
MPEG1	262.28	430	94	0.22	-2.187	3.69E-44	3.69E-42
P2RY2	917.98	1440	396	0.276	-1.859	4.35E-44	4.32E-42

Gene	Base Mean	Mean DMSO	Mean WFA	Fold Change	log2 Fold Change	pvalue	padj
PUS7	449.02	705	193	0.274	-1.869	6.90E-44	6.81E-42
SLC25A19	349.8	563	136	0.242	-2.044	1.23E-42	1.19E-40
NIFK	1241.53	1871	612	0.327	-1.612	1.27E-42	1.21E-40
KIAA0020	1392.17	2083	701	0.337	-1.571	4.17E-42	3.90E-40
CD3EAP	255.93	427	85	0.2	-2.323	4.23E-42	3.94E-40
ITGA4	1902.05	2820	984	0.349	-1.517	6.86E-42	6.34E-40
NOP56	1333.93	1919	749	0.39	-1.358	1.94E-41	1.77E-39
TXNIP	5035.52	7231	2840	0.393	-1.348	2.26E-40	2.00E-38
MARS2	230.64	388	73	0.189	-2.404	3.60E-39	3.04E-37
CXCR4	665.77	978	354	0.362	-1.468	4.43E-38	3.63E-36
BCL2	1673.57	2349	998	0.425	-1.233	4.68E-38	3.82E-36
PPRC1	330.63	518	143	0.277	-1.853	8.33E-38	6.68E-36
DCANP1	318.08	513	123	0.24	-2.059	9.77E-38	7.79E-36
UNG	697.86	1077	319	0.297	-1.753	5.01E-37	3.89E-35
KIT	127.61	230	26	0.113	-3.141	5.99E-37	4.60E-35
LMNB1	3463.6	4894	2033	0.416	-1.267	6.93E-37	5.26E-35
MYBBP1A	329.25	526	133	0.252	-1.986	2.50E-36	1.86E-34
MEF2D	3041.92	4201	1882	0.448	-1.159	3.35E-36	2.48E-34
PLXDC2	608.06	900	316	0.352	-1.507	5.84E-36	4.28E-34
PAQR8	1429.7	2154	705	0.328	-1.609	6.04E-36	4.41E-34
PIK3CB	2304.56	3357	1252	0.373	-1.422	2.28E-35	1.61E-33
METTL1	178.34	303	54	0.178	-2.491	2.76E-35	1.93E-33
HEATR1	2465.46	3443	1487	0.432	-1.21	2.94E-35	2.04E-33
SNHG16	869.87	1265	475	0.376	-1.412	5.67E-35	3.88E-33
AEN	282.64	446	119	0.268	-1.898	7.45E-35	5.08E-33
GTPBP4	813.72	1214	414	0.342	-1.55	8.41E-35	5.70E-33
BYSL	323.23	516	130	0.253	-1.983	1.15E-34	7.71E-33
PHACTR3	1021.62	1552	491	0.317	-1.658	1.22E-34	8.11E-33
ATP8B4	2387.45	3418	1357	0.397	-1.332	4.71E-34	3.06E-32
NPTX1	241.23	414	68	0.164	-2.604	3.06E-33	1.96E-31
MEIOB	431.08	681	181	0.266	-1.912	4.17E-33	2.65E-31
DIEXF	471.03	696	246	0.353	-1.501	4.92E-33	3.08E-31
POLR1A	719.2	1099	339	0.309	-1.694	9.16E-33	5.58E-31
TNFRSF21	551	871	231	0.266	-1.912	9.85E-33	5.98E-31
PES1	1083.17	1529	637	0.417	-1.261	1.03E-32	6.25E-31
XPO5	1718.37	2431	1006	0.414	-1.272	1.07E-32	6.44E-31
RCL1	417.8	648	188	0.291	-1.781	3.40E-32	2.01E-30
TRIM13	621.72	894	349	0.391	-1.353	7.50E-32	4.32E-30
ZNF146	3085.76	4224	1948	0.461	-1.116	2.57E-31	1.44E-29
CUL1	1757.43	2379	1136	0.477	-1.067	3.49E-31	1.94E-29

Gene	Base Mean	Mean DMSO	Mean WFA	Fold Change	log2 FoldChange	pvalue	padj
CTPS1	6616.39	8911	4322	0.485	-1.043	3.74E-31	2.07E-29
CAD	845.97	1232	460	0.373	-1.422	3.96E-31	2.19E-29
GPATCH4	1369.63	1978	761	0.385	-1.378	4.22E-31	2.32E-29
CECR6	314.16	512	116	0.228	-2.132	4.94E-31	2.69E-29
SAMSN1	266.55	423	110	0.26	-1.941	6.56E-31	3.57E-29
CCDC86	326.44	505	148	0.294	-1.766	1.40E-30	7.47E-29
SLC8A1	1327.1	1947	707	0.364	-1.46	1.93E-30	1.03E-28
NIP7	887.59	1258	517	0.412	-1.281	2.95E-30	1.55E-28
AGPAT5	1842.85	2624	1062	0.405	-1.304	3.77E-30	1.98E-28
NOM1	977.61	1387	568	0.41	-1.286	4.03E-30	2.10E-28
SAMHD1	5589.38	7676	3503	0.456	-1.131	4.99E-30	2.58E-28
NOC3L	486.97	709	265	0.373	-1.421	9.60E-30	4.96E-28
URB1	561.69	870	254	0.292	-1.776	1.05E-29	5.38E-28
TRMT10C	647.35	913	382	0.418	-1.257	1.51E-29	7.68E-28
HEATR3	426.65	626	227	0.363	-1.462	2.60E-29	1.31E-27
NOL11	1505.83	2043	968	0.474	-1.077	3.06E-29	1.54E-27
DDX10	667.02	984	351	0.357	-1.486	3.15E-29	1.58E-27
UBIAD1	323.77	495	153	0.309	-1.693	1.17E-28	5.73E-27
ABCE1	2564.22	3684	1444	0.392	-1.35	1.60E-28	7.79E-27
GEMIN5	678.52	987	370	0.376	-1.411	1.71E-28	8.30E-27
FASTKD2	690.41	992	388	0.392	-1.352	2.39E-28	1.16E-26
NOP2	352.37	531	174	0.327	-1.611	4.43E-28	2.12E-26
POLR1C	421.28	623	219	0.352	-1.506	4.52E-28	2.16E-26
EIF3B	3183.78	4253	2114	0.497	-1.009	8.08E-28	3.83E-26
GRAMD4	984.23	1400	568	0.406	-1.3	9.50E-28	4.49E-26
SLC25A30	244.56	373	117	0.313	-1.678	1.05E-27	4.91E-26
SUPT16H	4664.41	6284	3045	0.485	-1.045	1.13E-27	5.28E-26
UTP20	773.91	1132	415	0.367	-1.445	1.50E-27	6.97E-26
MS4A4A	283.01	442	124	0.282	-1.825	1.66E-27	7.68E-26
ZNF202	393.32	587	200	0.341	-1.551	1.99E-27	9.13E-26
TAF4B	214.03	343	85	0.248	-2.01	2.06E-27	9.44E-26
IRX3	430.23	624	236	0.378	-1.405	3.08E-27	1.40E-25
PPAT	415.33	600	231	0.385	-1.375	3.29E-27	1.49E-25
RRM2	1769.72	2642	897	0.339	-1.559	3.34E-27	1.51E-25
TSR1	730.61	1019	442	0.434	-1.204	4.34E-27	1.96E-25
SYNCRIP	8978.57	11973	5984	0.5	-1	6.84E-27	3.07E-25
RUNX1	2563.53	3552	1575	0.444	-1.173	8.54E-27	3.81E-25
KIAA0922	637.16	899	375	0.418	-1.259	1.32E-26	5.86E-25
PNO1	517.24	734	300	0.41	-1.287	1.38E-26	6.09E-25
ING5	235.02	355	115	0.322	-1.635	1.46E-26	6.45E-25
MCM3	4894.13	6825	2963	0.434	-1.203	1.53E-26	6.75E-25

Gene	Base Mean	Mean DMSO	Mean WFA	Fold Change	log2 FoldChange	pvalue	padj
SLC25A40	555.04	829	281	0.34	-1.556	1.58E-26	6.91E-25
FRMD3	186.34	299	73	0.244	-2.035	1.88E-26	8.22E-25
TARBP1	1098.43	1523	674	0.443	-1.176	2.65E-26	1.15E-24
AHRR	592.77	913	273	0.299	-1.741	4.39E-26	1.90E-24
NOLC1	1509.83	2138	882	0.413	-1.276	4.77E-26	2.05E-24
KNOP1	390.44	564	217	0.385	-1.378	9.46E-26	4.00E-24
RASSF2	674.01	924	424	0.459	-1.122	9.85E-26	4.16E-24
NOP14	1667.32	2239	1096	0.489	-1.031	1.14E-25	4.78E-24
ZEB2	4108.77	5695	2523	0.443	-1.174	1.21E-25	5.05E-24
C10orf2	125.04	206	44	0.215	-2.219	1.23E-25	5.10E-24
RRP15	900.6	1301	500	0.385	-1.377	1.44E-25	5.94E-24
TMEM229B	132.76	218	48	0.219	-2.19	1.73E-25	7.10E-24
RPF2	1260.86	1691	831	0.492	-1.024	2.95E-25	1.19E-23
MDN1	2236.3	3093	1380	0.446	-1.165	3.22E-25	1.30E-23
FAM78A	934.88	1253	617	0.492	-1.023	3.33E-25	1.33E-23
LYAR	755.8	1054	458	0.435	-1.201	3.61E-25	1.44E-23
TRPM2	882.54	1299	466	0.359	-1.478	5.96E-25	2.36E-23
CBFA2T3	241.72	372	111	0.298	-1.746	7.29E-25	2.87E-23
MFS2A	1966.66	2876	1058	0.368	-1.442	1.02E-24	3.99E-23
CD1D	480.24	707	253	0.358	-1.481	1.12E-24	4.36E-23
DHODH	140.82	228	54	0.236	-2.083	1.38E-24	5.33E-23
WDR74	356.27	520	193	0.371	-1.431	2.40E-24	9.23E-23
DDX42	2146.62	2893	1400	0.484	-1.047	2.54E-24	9.72E-23
WDR75	1029.97	1394	665	0.478	-1.066	2.67E-24	1.02E-22
MSH6	1905.43	2650	1161	0.438	-1.19	3.19E-24	1.21E-22
GPR18	105.72	176	35	0.201	-2.313	3.71E-24	1.40E-22
CA2	21507.8 1	31446	11569	0.368	-1.442	3.72E-24	1.40E-22
FXN	184.17	287	81	0.283	-1.82	4.13E-24	1.54E-22
APEX1	3087.46	4303	1872	0.435	-1.2	4.43E-24	1.64E-22
KIAA0930	6329.83	8824	3835	0.435	-1.202	5.41E-24	2.00E-22
MRPL15	1141.99	1535	749	0.488	-1.036	5.80E-24	2.13E-22
ASNSD1	842.86	1166	519	0.446	-1.166	7.73E-24	2.82E-22
DARS2	1075.28	1466	685	0.467	-1.098	8.02E-24	2.91E-22
SLC25A15	471.87	660	284	0.43	-1.217	8.44E-24	3.06E-22
SNRPD1	1308.06	1786	830	0.465	-1.105	1.11E-23	3.96E-22
IGSF6	368.31	555	182	0.328	-1.608	1.16E-23	4.12E-22
PBK	748.65	1055	442	0.419	-1.254	1.65E-23	5.80E-22
UTP18	930.99	1259	603	0.479	-1.061	1.97E-23	6.86E-22
LDLRAD4	195.54	299	92	0.307	-1.704	2.34E-23	8.14E-22
TSEN2	183.17	285	81	0.287	-1.803	2.42E-23	8.39E-22

Gene	Base Mean	Mean DMSO	Mean WFA	Fold Change	log2 FoldChange	pvalue	padj
NCAPH	758.01	1038	478	0.461	-1.118	2.95E-23	1.02E-21
GART	848.18	1135	561	0.495	-1.015	3.28E-23	1.13E-21
TRMT5	545.9	758	334	0.441	-1.18	3.97E-23	1.34E-21
ZNF850	391.48	560	223	0.399	-1.326	4.39E-23	1.48E-21
NXT1	192.92	294	92	0.311	-1.683	4.50E-23	1.52E-21
MRPL3	2518.01	3395	1641	0.484	-1.048	5.37E-23	1.79E-21
DPH2	424.98	620	230	0.373	-1.424	5.58E-23	1.86E-21
SLC46A1	189.28	300	79	0.264	-1.922	9.53E-23	3.15E-21
PREX1	1881.74	2641	1122	0.425	-1.235	1.27E-22	4.17E-21
TGM5	135.82	219	53	0.242	-2.047	1.60E-22	5.22E-21
IKZF1	1954.59	2640	1270	0.481	-1.055	1.92E-22	6.25E-21
TDRD7	1039.89	1445	635	0.44	-1.185	2.02E-22	6.54E-21
MGAT4A	1436.83	1989	885	0.445	-1.167	2.07E-22	6.70E-21
TFAP4	120.83	203	39	0.196	-2.352	2.08E-22	6.72E-21
FUBP1	1507.2	2166	848	0.392	-1.352	2.27E-22	7.26E-21
CEBPZ	1860.02	2495	1225	0.491	-1.026	2.62E-22	8.37E-21
UMPS	815.56	1094	537	0.49	-1.028	3.08E-22	9.77E-21
IL1RN	395.32	578	213	0.369	-1.437	3.47E-22	1.09E-20
VASH1	996.94	1378	615	0.447	-1.162	4.00E-22	1.25E-20
RXFP1	745.78	1029	463	0.451	-1.15	4.46E-22	1.39E-20
EHD4	555.98	799	313	0.391	-1.354	4.92E-22	1.53E-20
SEH1L	1105.5	1544	667	0.433	-1.209	5.12E-22	1.59E-20
SLC2A1	1407.96	1898	918	0.483	-1.049	5.86E-22	1.80E-20
NEK6	1531.59	2093	970	0.464	-1.108	7.30E-22	2.24E-20
CDC42EP3	1197.99	1622	774	0.478	-1.066	1.16E-21	3.49E-20
TIFAB	122.14	203	42	0.207	-2.273	1.66E-21	4.98E-20
PNPT1	1192.15	1605	780	0.486	-1.04	1.98E-21	5.89E-20
KPNA2	3098.42	4156	2041	0.491	-1.026	2.42E-21	7.16E-20
WDR12	771.18	1029	513	0.499	-1.003	2.70E-21	7.96E-20
PATZ1	606.37	853	360	0.423	-1.242	2.76E-21	8.13E-20
UTP14A	650.08	886	414	0.468	-1.095	2.88E-21	8.47E-20
CIRH1A	226.19	334	119	0.356	-1.491	3.06E-21	8.97E-20
CCNE1	277.97	400	156	0.39	-1.359	3.43E-21	1.00E-19
PPARGC1B	228.58	346	111	0.321	-1.64	3.56E-21	1.03E-19
WDR36	1071.59	1506	638	0.424	-1.238	3.61E-21	1.05E-19
TNFRSF1B	625.24	854	397	0.465	-1.105	3.64E-21	1.05E-19
PDCD11	842.67	1152	534	0.464	-1.108	3.96E-21	1.14E-19
SACS	937.34	1335	540	0.404	-1.307	5.59E-21	1.59E-19
TMEM170B	1349.02	1849	850	0.46	-1.12	6.07E-21	1.72E-19
COA7	663.89	902	426	0.472	-1.083	6.70E-21	1.89E-19
ADRBK2	399.48	564	235	0.417	-1.262	7.10E-21	2.00E-19

Gene	Base Mean	Mean DMSO	Mean WFA	Fold Change	log2 FoldChange	pvalue	padj
ENC1	263.67	384	144	0.376	-1.411	8.02E-21	2.24E-19
TIMM9	417.32	592	243	0.41	-1.285	1.03E-20	2.86E-19
AIMP2	463.76	646	282	0.437	-1.195	1.34E-20	3.70E-19
TOE1	349.15	495	203	0.41	-1.286	1.41E-20	3.87E-19
TFB2M	498.86	708	290	0.411	-1.283	2.36E-20	6.42E-19
UTP15	445.81	646	246	0.382	-1.388	3.15E-20	8.52E-19
SNHG3	167.49	258	78	0.3	-1.736	3.62E-20	9.76E-19
LOC90784	196.71	298	95	0.32	-1.646	3.95E-20	1.06E-18
GEMIN4	241.25	349	133	0.381	-1.391	4.20E-20	1.13E-18
USP31	546.26	741	352	0.476	-1.072	4.56E-20	1.22E-18
RRP9	238.79	347	131	0.378	-1.404	4.82E-20	1.28E-18
LAIR1	115.94	184	48	0.264	-1.92	4.84E-20	1.29E-18
EXOSC2	644.97	886	404	0.456	-1.133	5.00E-20	1.32E-18
RRP12	371.3	532	211	0.397	-1.332	7.68E-20	2.01E-18
NOB1	664.15	918	410	0.447	-1.162	9.31E-20	2.42E-18
WDR77	975.21	1305	645	0.495	-1.016	1.11E-19	2.87E-18
ZNF551	307.9	436	180	0.411	-1.282	1.38E-19	3.56E-18
TMCC1-AS1	173.88	265	82	0.312	-1.68	1.42E-19	3.66E-18
PRKX	407.77	572	244	0.426	-1.23	1.54E-19	3.97E-18
PIK3CG	1188.3	1596	781	0.49	-1.03	1.69E-19	4.34E-18
PAK1IP1	271.91	387	157	0.406	-1.301	1.77E-19	4.54E-18
FAM208B	679.58	927	433	0.468	-1.096	2.05E-19	5.25E-18
ELAC2	425.54	582	269	0.461	-1.117	2.33E-19	5.93E-18
ASUN	1184.2	1597	772	0.484	-1.048	2.59E-19	6.59E-18
PTK2B	2112.2	2898	1326	0.458	-1.127	3.04E-19	7.69E-18
ANKLE1	87.74	145	31	0.215	-2.217	3.67E-19	9.21E-18
ANAPC1	944.32	1262	627	0.497	-1.01	4.27E-19	1.07E-17
GCNT1	650.75	918	384	0.419	-1.256	4.92E-19	1.22E-17
NUFIP1	233.94	341	128	0.374	-1.42	5.48E-19	1.36E-17
PDE7B	177.37	265	90	0.34	-1.556	6.84E-19	1.69E-17
CLTCL1	688.51	972	405	0.417	-1.262	7.17E-19	1.76E-17
SLC7A2	124.73	201	48	0.24	-2.061	7.60E-19	1.87E-17
MAD2L1	1017.38	1369	666	0.487	-1.038	7.75E-19	1.90E-17
RGS16	100.43	166	35	0.212	-2.239	1.03E-18	2.49E-17
HMBS	329.05	461	197	0.428	-1.225	1.03E-18	2.49E-17
NACC2	635.71	863	408	0.473	-1.08	1.03E-18	2.49E-17
SLC25A32	739.45	1006	472	0.47	-1.089	1.16E-18	2.79E-17
IMP3	504.15	706	302	0.428	-1.226	1.49E-18	3.58E-17
RASSF5	757.64	1014	501	0.494	-1.016	1.97E-18	4.70E-17
MARVELD1	598.1	806	390	0.485	-1.044	2.11E-18	5.01E-17
PUS1	290.41	421	160	0.38	-1.397	2.18E-18	5.16E-17

Gene	Base Mean	Mean DMSO	Mean WFA	Fold Change	log2 FoldChange	pvalue	padj
RHOA	892.53	1203	582	0.484	-1.046	2.39E-18	5.65E-17
CMPK2	232.67	350	115	0.33	-1.598	2.67E-18	6.30E-17
UCK2	812.23	1108	517	0.467	-1.098	2.83E-18	6.66E-17
RAB3D	597.33	822	372	0.453	-1.142	3.73E-18	8.68E-17
SASH1	1751.98	2400	1104	0.46	-1.121	4.59E-18	1.06E-16
CSPG4	211.6	327	97	0.296	-1.756	4.68E-18	1.08E-16
WT1	161.06	245	78	0.319	-1.648	5.12E-18	1.17E-16
RIOK1	340.97	484	198	0.409	-1.288	6.02E-18	1.37E-16
FAM216A	275.57	403	148	0.369	-1.438	6.88E-18	1.56E-16
DIMT1	420.65	577	264	0.458	-1.126	9.08E-18	2.04E-16
CX3CR1	797.6	1102	493	0.448	-1.16	9.89E-18	2.21E-16
FBXO5	945.99	1278	614	0.48	-1.058	1.06E-17	2.35E-16
CCNE2	964.95	1318	612	0.464	-1.106	1.50E-17	3.28E-16
PMM2	472.72	648	297	0.459	-1.124	1.82E-17	3.96E-16
CD244	540.79	726	356	0.49	-1.028	1.86E-17	4.04E-16
DCAF4	157.23	241	73	0.302	-1.727	2.10E-17	4.52E-16
OAF	553.88	753	354	0.47	-1.089	2.31E-17	4.95E-16
SNHG15	173.13	258	88	0.34	-1.555	2.52E-17	5.39E-16
LINC00925	103.24	169	37	0.222	-2.17	2.79E-17	5.95E-16
C1orf162	391.07	531	252	0.475	-1.074	2.85E-17	6.07E-16
CCDC64	222.42	326	119	0.363	-1.46	4.32E-17	9.12E-16
DSCC1	397.42	561	234	0.416	-1.264	5.21E-17	1.10E-15
VAV2	377.99	545	211	0.388	-1.367	5.94E-17	1.24E-15
EHD1	331.7	466	198	0.425	-1.233	6.91E-17	1.44E-15
TARP	137.02	214	60	0.283	-1.824	8.17E-17	1.70E-15
MTM1	560.92	752	369	0.492	-1.024	8.19E-17	1.70E-15
CD36	780.51	1078	483	0.448	-1.157	8.65E-17	1.79E-15
NFE2L3	82.43	134	31	0.233	-2.099	1.11E-16	2.28E-15
ZMYND19	426.57	574	279	0.486	-1.042	1.16E-16	2.38E-15
TBRG4	451.49	632	271	0.429	-1.219	1.27E-16	2.59E-15
PSMD5	344.97	477	213	0.446	-1.166	1.32E-16	2.70E-15
MS4A7	2586.15	3627	1545	0.426	-1.23	1.66E-16	3.35E-15
ATP8B1	214.44	310	119	0.384	-1.381	1.81E-16	3.65E-15
NFE2	122.86	189	57	0.302	-1.729	2.09E-16	4.19E-15
FAM135B	50.16	89	11	0.128	-2.967	2.70E-16	5.40E-15
GPR183	146.02	223	70	0.314	-1.673	6.02E-16	1.17E-14
MAGEF1	158.27	237	80	0.338	-1.563	7.50E-16	1.44E-14
PMS1	393.4	534	252	0.473	-1.081	7.61E-16	1.46E-14
TTC27	440.33	588	293	0.499	-1.004	8.04E-16	1.54E-14
NTSR1	155.74	243	68	0.282	-1.827	8.57E-16	1.64E-14
PFAS	282.57	390	175	0.449	-1.154	8.72E-16	1.67E-14

Gene	Base Mean	Mean DMSO	Mean WFA	Fold Change	log2 FoldChange	pvalue	padj
TMPO-AS1	485.48	655	316	0.482	-1.053	1.02E-15	1.93E-14
DHRS9	1765.24	2475	1056	0.427	-1.229	1.03E-15	1.94E-14
GAS7	717.89	977	459	0.47	-1.089	1.09E-15	2.05E-14
LANCL2	282.23	387	177	0.458	-1.128	1.18E-15	2.23E-14
KCNA3	85.09	141	29	0.207	-2.274	1.26E-15	2.36E-14
HAL	197.06	289	105	0.361	-1.468	1.41E-15	2.62E-14
OSBPL5	208.98	318	100	0.313	-1.674	1.59E-15	2.96E-14
DDHD2	756.66	1012	501	0.496	-1.011	1.60E-15	2.97E-14
TRMT6	280.06	393	167	0.426	-1.231	2.04E-15	3.77E-14
MRPL12	603.31	815	392	0.481	-1.056	2.33E-15	4.28E-14
KIF20A	610.22	832	388	0.467	-1.1	3.45E-15	6.25E-14
PGGT1B	389.36	532	247	0.465	-1.105	3.59E-15	6.49E-14
FUT7	112.63	171	55	0.32	-1.642	3.80E-15	6.85E-14
NOCT	264.49	369	160	0.433	-1.209	5.11E-15	9.08E-14
USP36	571.35	771	371	0.482	-1.052	5.37E-15	9.53E-14
DHX37	434.07	599	270	0.45	-1.151	5.77E-15	1.02E-13
LIMA1	625.29	858	392	0.458	-1.126	6.05E-15	1.06E-13
RBFA	212.43	300	125	0.417	-1.263	6.77E-15	1.19E-13
BMP8B	1663.58	2274	1053	0.464	-1.109	9.20E-15	1.59E-13
STEAP3	303.24	434	173	0.399	-1.326	1.12E-14	1.93E-13
EEF2KMT	145.39	212	79	0.376	-1.413	1.20E-14	2.05E-13
POLR3E	436.78	599	275	0.46	-1.122	1.22E-14	2.08E-13
HNF4G	214.81	303	126	0.419	-1.257	1.33E-14	2.27E-13
BAHCC1	673.72	898	449	0.499	-1.002	1.45E-14	2.46E-13
SAAL1	338.17	453	224	0.495	-1.015	1.57E-14	2.66E-13
POLR3H	453.64	614	294	0.478	-1.064	1.65E-14	2.78E-13
NRP1	431.12	582	280	0.48	-1.058	1.66E-14	2.80E-13
FAM117B	337.63	456	219	0.481	-1.057	1.66E-14	2.80E-13
RRP1	377.05	515	239	0.465	-1.105	1.72E-14	2.89E-13
PRIM1	618.02	824	412	0.5	-1.001	2.16E-14	3.59E-13
RASGRP2	582.06	807	357	0.443	-1.175	2.36E-14	3.92E-13
AIM1	683.1	936	430	0.46	-1.121	3.51E-14	5.73E-13
CCL2	54.77	95	15	0.156	-2.681	3.97E-14	6.48E-13
TIMM8A	165.43	236	95	0.404	-1.307	4.23E-14	6.87E-13
DLEU1	138.74	204	74	0.364	-1.458	4.97E-14	8.02E-13
LPXN	262.5	366	159	0.436	-1.196	5.81E-14	9.32E-13
TRNT1	296.2	400	193	0.483	-1.05	5.84E-14	9.35E-13
LOC100506585	84.81	136	33	0.246	-2.026	8.26E-14	1.31E-12
IMP4	369.45	501	238	0.475	-1.075	8.74E-14	1.38E-12
MRPL17	444.02	598	290	0.486	-1.04	9.94E-14	1.55E-12

Gene	Base Mean	Mean DMSO	Mean WFA	Fold Change	log2 FoldChange	pvalue	padj
ALKBH8	205.46	288	123	0.428	-1.224	1.04E-13	1.61E-12
ANKRD44	273.08	375	171	0.458	-1.128	1.22E-13	1.88E-12
NUP35	236.33	328	145	0.441	-1.18	1.26E-13	1.94E-12
PM20D2	596.67	799	394	0.494	-1.016	1.31E-13	2.02E-12
ZNF614	352.73	474	231	0.488	-1.034	1.52E-13	2.33E-12
TGIF2	307.5	417	198	0.476	-1.07	1.54E-13	2.36E-12
CARNMT1	257.34	356	159	0.446	-1.165	1.68E-13	2.57E-12
MMACHC	228.09	313	144	0.459	-1.122	1.73E-13	2.62E-12
CYP1B1	706.83	1277	137	0.107	-3.22	2.12E-13	3.20E-12
CHCHD4	271.66	369	174	0.472	-1.084	2.25E-13	3.38E-12
NT5DC3	282.27	390	175	0.448	-1.159	2.29E-13	3.44E-12
POLR3B	271.08	373	169	0.453	-1.144	2.44E-13	3.66E-12
GRWD1	386.73	524	250	0.477	-1.069	2.47E-13	3.69E-12
CD300A	110.96	167	55	0.332	-1.589	2.87E-13	4.26E-12
DDX31	223.52	314	133	0.424	-1.239	3.06E-13	4.53E-12
TMA16	553.28	738	368	0.499	-1.002	3.18E-13	4.70E-12
CCDC26	124.66	185	64	0.348	-1.521	3.42E-13	5.03E-12
APBB1IP	902.42	1249	556	0.446	-1.165	3.52E-13	5.17E-12
HPDL	36.26	65	8	0.122	-3.036	3.85E-13	5.63E-12
DCTPP1	276.25	387	165	0.426	-1.23	3.87E-13	5.64E-12
RALGAPA2	395.28	538	252	0.469	-1.094	4.23E-13	6.15E-12
ADGRG5	133.3	209	58	0.276	-1.859	5.25E-13	7.58E-12
DNA2	258.07	349	168	0.48	-1.058	6.41E-13	9.18E-12
ZNF485	60.23	98	22	0.231	-2.113	6.60E-13	9.43E-12
ESPL1	231.38	325	137	0.421	-1.25	7.68E-13	1.09E-11
TEX15	178.54	259	98	0.381	-1.394	9.70E-13	1.37E-11
IQGAP2	385.84	514	257	0.499	-1.001	1.03E-12	1.44E-11
TNFAIP3	299.56	410	189	0.462	-1.115	1.25E-12	1.75E-11
TCF4	268.21	361	176	0.488	-1.034	1.37E-12	1.91E-11
MYCL	357.88	495	221	0.446	-1.165	1.56E-12	2.16E-11
MPP6	177.95	248	108	0.437	-1.195	1.64E-12	2.27E-11
FERMT1	74.29	116	32	0.278	-1.847	1.65E-12	2.28E-11
PTX3	68.22	108	28	0.261	-1.936	1.66E-12	2.29E-11
AMER1	168.29	237	99	0.418	-1.257	1.69E-12	2.33E-11
PLD1	242.15	329	155	0.471	-1.087	2.04E-12	2.78E-11
PALD1	321.53	435	208	0.478	-1.066	2.79E-12	3.76E-11
AFMID	191.28	266	117	0.439	-1.187	2.87E-12	3.86E-11
ZNRF3	181.8	260	104	0.402	-1.315	3.28E-12	4.37E-11
NHSL2	114.37	170	59	0.346	-1.533	3.35E-12	4.46E-11
LINC01184	123.31	179	68	0.377	-1.408	4.57E-12	5.97E-11

Gene	Base Mean	Mean DMSO	Mean WFA	Fold Change	log2 FoldChange	pvalue	padj
LOC101927070	31.26	56	7	0.116	-3.105	4.80E-12	6.25E-11
CCR2	2974.91	4992	958	0.192	-2.381	4.94E-12	6.41E-11
NEURL1B	106.37	156	56	0.361	-1.472	5.92E-12	7.66E-11
XAF1	352.36	478	227	0.474	-1.078	7.35E-12	9.41E-11
NARS2	228.24	307	150	0.488	-1.034	7.50E-12	9.58E-11
SLA	546.41	742	351	0.473	-1.081	8.28E-12	1.05E-10
NANP	204.67	289	121	0.421	-1.25	9.12E-12	1.15E-10
IPO11	313.32	428	199	0.465	-1.104	1.03E-11	1.28E-10
DZANK1	136.75	200	74	0.37	-1.434	1.16E-11	1.45E-10
FAM124B	57.79	93	22	0.239	-2.067	1.18E-11	1.47E-10
KLF13	130.8	190	72	0.38	-1.398	1.27E-11	1.57E-10
NCALD	166.65	238	95	0.4	-1.321	1.35E-11	1.66E-10
PDSS1	163.59	228	99	0.436	-1.199	1.45E-11	1.78E-10
SETMAR	196.14	269	123	0.459	-1.124	1.78E-11	2.16E-10
SLC16A9	70.08	109	31	0.289	-1.791	2.05E-11	2.47E-10
SCAMP5	325.01	444	206	0.465	-1.105	3.80E-11	4.44E-10
RPP40	79.73	121	39	0.321	-1.639	3.84E-11	4.48E-10
MT1X	60.74	96	25	0.263	-1.929	4.36E-11	5.04E-10
ACOX3	207.4	279	135	0.485	-1.045	4.47E-11	5.17E-10
CDCA7	886.61	1184	590	0.499	-1.003	4.78E-11	5.51E-10
CTU2	148.21	215	81	0.378	-1.402	6.17E-11	7.06E-10
HRH2	130.9	186	76	0.407	-1.297	6.29E-11	7.19E-10
DTX4	97.58	145	50	0.347	-1.526	7.79E-11	8.81E-10
GEMIN6	200.61	269	132	0.489	-1.031	8.61E-11	9.70E-10
ZNF367	618.05	825	411	0.499	-1.004	1.08E-10	1.21E-09
KCTD15	98.88	145	53	0.364	-1.46	1.08E-10	1.21E-09
ZNF239	60.55	94	27	0.293	-1.769	1.50E-10	1.64E-09
TNS1	167.74	238	97	0.407	-1.296	1.69E-10	1.84E-09
SLC19A1	194.25	265	124	0.469	-1.092	1.80E-10	1.95E-09
DLEU7	62.12	99	25	0.258	-1.952	1.88E-10	2.03E-09
GDAP1	161	223	99	0.445	-1.168	2.66E-10	2.82E-09
CARD9	481.21	647	316	0.489	-1.032	2.82E-10	2.98E-09
PLXNC1	380.51	511	250	0.489	-1.031	3.01E-10	3.16E-09
ANTXR1	430.43	584	277	0.476	-1.072	3.04E-10	3.19E-09
ZNF593	108.79	156	62	0.396	-1.336	3.61E-10	3.74E-09
TBC1D9	156.26	215	98	0.455	-1.137	3.93E-10	4.06E-09
KIAA1462	187.51	254	121	0.474	-1.076	4.15E-10	4.27E-09
MRPS17	189.43	254	125	0.49	-1.029	4.23E-10	4.34E-09
PLD6	135.84	191	81	0.425	-1.236	5.11E-10	5.20E-09
CACNA2D3	307.07	519	95	0.182	-2.456	5.17E-10	5.25E-09

Gene	Base Mean	Mean DMSO	Mean WFA	Fold Change	log2 FoldChange	pvalue	padj
RFTN1	166.99	230	104	0.452	-1.144	5.24E-10	5.31E-09
DEPTOR	141.92	197	86	0.439	-1.189	5.46E-10	5.51E-09
PTRH2	287.57	384	191	0.497	-1.007	6.58E-10	6.57E-09
NLE1	146.3	210	83	0.395	-1.342	6.75E-10	6.72E-09
PSTPIP2	237.02	326	148	0.456	-1.133	6.88E-10	6.83E-09
TMTC2	184.22	258	111	0.428	-1.223	7.50E-10	7.43E-09
DCAF12L1	188.02	260	116	0.447	-1.162	7.94E-10	7.85E-09
SNHG17	133.83	187	80	0.43	-1.216	9.20E-10	9.05E-09
MYBPH	91.11	134	49	0.364	-1.458	1.06E-09	1.04E-08
COL15A1	117.03	167	67	0.405	-1.306	1.38E-09	1.34E-08
RPUSD2	154.69	212	98	0.461	-1.118	1.50E-09	1.44E-08
MT1E	141.91	197	86	0.436	-1.197	1.54E-09	1.47E-08
FPR2	22.39	41	4	0.083	-3.585	1.69E-09	1.61E-08
LACC1	391.06	522	260	0.498	-1.007	2.31E-09	2.16E-08
THG1L	176.53	236	117	0.495	-1.014	2.36E-09	2.20E-08
WDR4	124.8	173	77	0.441	-1.181	2.54E-09	2.35E-08
XYLB	177.21	245	110	0.448	-1.159	2.74E-09	2.53E-08
FRMD4A	111.08	156	66	0.427	-1.227	3.15E-09	2.88E-08
SLC25A22	177.18	240	114	0.476	-1.072	3.22E-09	2.94E-08
NUDT16L1	180.68	243	118	0.488	-1.034	3.51E-09	3.19E-08
TESPA1	43.43	69	18	0.259	-1.949	3.74E-09	3.38E-08
POLR3G	79.14	116	42	0.367	-1.447	4.14E-09	3.71E-08
RPL36A	85.23	127	43	0.342	-1.547	4.17E-09	3.73E-08
HNRNPA1L2	84.61	123	46	0.373	-1.423	4.44E-09	3.95E-08
OAS3	140.69	193	88	0.456	-1.133	4.91E-09	4.33E-08
PDPN	158.28	213	103	0.482	-1.052	5.33E-09	4.68E-08
GPR82	43.79	72	15	0.211	-2.242	5.38E-09	4.71E-08
THBS4	82.08	118	46	0.385	-1.376	6.55E-09	5.64E-08
NCF1	64.06	96	32	0.328	-1.61	7.65E-09	6.52E-08
WWC1	112.33	159	66	0.416	-1.264	8.08E-09	6.87E-08
SETD6	125.21	173	78	0.453	-1.142	8.22E-09	6.98E-08
RCSD1	1486.84	2206	768	0.348	-1.521	9.83E-09	8.25E-08
ALKBH2	66.11	99	33	0.339	-1.559	1.39E-08	1.14E-07
POU4F2	206.53	294	120	0.408	-1.294	1.56E-08	1.28E-07
PADI2	136.09	184	88	0.478	-1.064	1.79E-08	1.45E-07
FAM120C	217.16	291	144	0.496	-1.013	1.81E-08	1.47E-07
SMYD5	240.11	320	160	0.5	-1	1.89E-08	1.53E-07
AMIGO2	117.33	161	74	0.456	-1.132	2.28E-08	1.83E-07
LINC00504	135.18	183	88	0.48	-1.058	2.34E-08	1.87E-07
CDK20	76.88	111	43	0.391	-1.356	2.36E-08	1.88E-07
TNFSF13B	92.35	131	54	0.411	-1.283	2.43E-08	1.93E-07

Gene	Base Mean	Mean DMSO	Mean WFA	Fold Change	log2 FoldChange	pvalue	padj
PRAM1	221.32	306	137	0.45	-1.152	2.80E-08	2.22E-07
PLA2G7	136.1	194	78	0.402	-1.316	3.03E-08	2.39E-07
F3	106.93	149	64	0.431	-1.214	3.19E-08	2.51E-07
TP73	138.51	185	92	0.495	-1.013	3.25E-08	2.56E-07
NHS	58.58	88	29	0.328	-1.607	4.00E-08	3.10E-07
NCBP2-AS2	163.56	219	108	0.493	-1.02	4.79E-08	3.68E-07
ZNF556	74.9	110	40	0.367	-1.448	5.30E-08	4.04E-07
CBX2	102.71	142	64	0.45	-1.152	6.78E-08	5.10E-07
SCIMP	42.6	66	19	0.29	-1.785	7.95E-08	5.93E-07
SMIM10	105.68	147	65	0.444	-1.172	8.30E-08	6.16E-07
DLX1	95.94	133	59	0.448	-1.159	9.19E-08	6.78E-07
TLR8	29.23	48	10	0.206	-2.276	1.02E-07	7.49E-07
PSMG4	51.35	77	26	0.34	-1.556	1.05E-07	7.70E-07
GPR65	100.28	141	60	0.428	-1.225	1.29E-07	9.29E-07
SIGLEC6	95.35	139	52	0.371	-1.429	1.44E-07	1.04E-06
NLRC3	74.47	108	41	0.383	-1.385	1.58E-07	1.13E-06
PCED1B	43.57	67	21	0.304	-1.716	1.63E-07	1.16E-06
METTL25	111.44	151	73	0.483	-1.049	1.74E-07	1.23E-06
C20orf197	58.07	88	28	0.316	-1.66	1.87E-07	1.32E-06
TGFBR3	147.86	201	95	0.471	-1.086	1.94E-07	1.36E-06
SGIP1	176.36	236	116	0.492	-1.023	1.94E-07	1.36E-06
LOC100996455	23.38	40	7	0.171	-2.55	1.97E-07	1.38E-06
LGALS12	27.58	47	9	0.182	-2.456	2.04E-07	1.42E-06
GBP4	70.05	101	39	0.382	-1.387	2.11E-07	1.47E-06
MTUS1	104.65	147	62	0.422	-1.245	2.15E-07	1.49E-06
KIAA1211L	37.48	59	16	0.281	-1.832	2.19E-07	1.52E-06
A4GALT	127.16	172	83	0.481	-1.056	2.22E-07	1.54E-06
P2RX7	94.41	131	58	0.444	-1.17	2.23E-07	1.55E-06
FAM86EP	47.05	71	23	0.325	-1.622	2.35E-07	1.62E-06
SNORD76	25.62	42	9	0.211	-2.247	2.57E-07	1.76E-06
E2F5	46.75	72	22	0.305	-1.714	2.94E-07	1.99E-06
TBC1D4	107.71	150	65	0.436	-1.197	3.10E-07	2.09E-06
PDE4B	44.38	67	22	0.322	-1.633	4.49E-07	2.96E-06
SGK494	87.96	125	51	0.413	-1.275	4.61E-07	3.03E-06
SNORD22	42.58	65	20	0.31	-1.69	5.39E-07	3.51E-06
LINC00926	100.52	146	55	0.38	-1.396	5.78E-07	3.75E-06
RIBC2	109.75	153	66	0.433	-1.208	5.86E-07	3.79E-06
DTWD2	139.08	186	92	0.498	-1.005	8.22E-07	5.21E-06
KCND2	30.98	49	13	0.26	-1.941	1.03E-06	6.43E-06
GRIN3A	27.89	45	11	0.245	-2.03	1.03E-06	6.47E-06

Gene	Base Mean	Mean DMSO	Mean WFA	Fold Change	log2 FoldChange	pvalue	padj
NRARP	41.08	62	21	0.336	-1.576	1.34E-06	8.23E-06
WNT7B	18.31	32	5	0.15	-2.733	1.39E-06	8.54E-06
SNORD79	24.6	40	9	0.221	-2.176	1.82E-06	1.09E-05
C12orf45	89.3	120	58	0.479	-1.061	2.07E-06	1.23E-05
ANKRD55	26.35	43	10	0.232	-2.109	2.08E-06	1.23E-05
FAM86C1	80.97	111	50	0.452	-1.145	2.19E-06	1.29E-05
NR1D1	29.28	46	13	0.278	-1.845	3.13E-06	1.80E-05
SARS2	113.62	152	75	0.498	-1.006	3.21E-06	1.84E-05
LOC10192774 6	18.72	32	6	0.172	-2.536	3.39E-06	1.94E-05
PIPOX	54.69	80	30	0.377	-1.407	3.77E-06	2.14E-05
SNORD47	42.32	63	22	0.346	-1.533	3.89E-06	2.20E-05
LINC00977	66.35	95	37	0.393	-1.347	3.95E-06	2.23E-05
CDK5R1	124.54	167	82	0.49	-1.03	5.22E-06	2.90E-05
GAPT	580.92	928	234	0.252	-1.988	5.34E-06	2.96E-05
ZNF57	76.77	104	49	0.474	-1.077	5.84E-06	3.21E-05

Appendix 2. 500 most down-regulated genes in THP1 Cells following treatment with Withaferin A.

Gene	Base Mean	DMSO	WFA	Fold Change	log2 Fold Change	pvalue	padj
HSPA6	2826.83	15	5639	390.672	8.61	5.40E-71	1.33E-68
THEGL	16.86	0	34	190.862	7.576	1.78E-09	1.69E-08
ALOXE3	15.24	0	30	172.626	7.432	4.32E-09	3.85E-08
RFPL2	22.15	0	44	128.121	7.001	1.37E-08	1.13E-07
LPPR5	105.64	2	209	109.824	6.779	1.84E-27	8.48E-26
CYP39A1	52.95	1	105	82.397	6.365	1.55E-16	3.14E-15
LOC344887	204.04	5	403	79.348	6.31	1.43E-58	2.50E-56
MPDZ	12.15	0	24	70.02	6.13	1.57E-06	9.51E-06
CHST1	10.6	0	21	60.676	5.923	6.35E-06	3.47E-05
PGF	89.43	3	176	50.104	5.647	6.28E-32	3.65E-30
TUBBP5	16.21	1	32	50.066	5.646	3.27E-07	2.20E-06
C9orf172	14.58	1	29	44.631	5.48	1.13E-06	7.01E-06
TREML3P	86.59	4	169	44.219	5.467	1.12E-31	6.41E-30
C2orf91	40.91	2	80	44.098	5.463	2.04E-06	1.21E-05
CREG2	11.86	1	23	36.287	5.181	4.93E-06	2.75E-05
OSGIN1	628.25	38	1218	31.936	4.997	3.02E-160	4.38E-157
EDNRB	451.47	29	874	29.919	4.903	3.93E-111	4.07E-108
CLU	914.12	63	1765	27.85	4.8	4.47E-175	8.12E-172
TRIM16L	154.95	11	299	26.889	4.749	2.76E-56	4.51E-54
P4HA2	1156.62	89	2224	24.756	4.63	4.70E-228	1.71E-224
HEPACAM2	11.59	1	22	23.312	4.543	2.67E-06	1.55E-05
HTRA3	84.65	7	162	23.306	4.543	3.27E-34	2.16E-32
SERHL	15.34	1	29	22.994	4.523	1.14E-07	8.30E-07
DCSTAMP	14.8	1	28	22.213	4.473	1.14E-07	8.34E-07
COL1A1	63.42	6	121	22.206	4.473	2.55E-25	1.04E-23
HSPA1B	247.91	22	474	21.723	4.441	5.83E-73	1.60E-70
CACNA1G	10.29	1	20	20.366	4.348	1.29E-05	6.68E-05
BAG3	2257.29	222	4293	19.328	4.273	2.15E-257	1.04E-253
ARHGAP5	45.45	4	87	19.326	4.272	2.85E-19	7.22E-18
ACTRT3	150.98	15	287	18.392	4.201	1.26E-16	2.57E-15
LINC01269	15.28	2	29	18.325	4.196	6.92E-08	5.19E-07
SPTA1	88.45	10	168	18.039	4.173	4.46E-34	2.93E-32
DFNB31	118.89	12	225	17.747	4.15	8.00E-38	6.45E-36
HUNK	62.88	7	119	17.725	4.148	1.57E-25	6.44E-24
CSRP2	89.5	10	170	17.276	4.111	4.28E-33	2.72E-31
LUCAT1	63.26	7	119	16.178	4.016	5.53E-24	2.04E-22
MMP16	29.32	3	55	15.947	3.995	1.55E-12	2.15E-11

Gene	Base Mean	DMSO	WFA	Fold Change	log2 Fold Change	pvalue	padj
KLHL25	64.28	8	121	15.817	3.983	3.29E-25	1.32E-23
LINC00942	41.1	5	77	15.149	3.921	2.86E-18	6.73E-17
TRPA1	42.51	5	80	14.704	3.878	1.21E-18	2.91E-17
SERPINH1	8736.52	1124	16349	14.536	3.862	1.32E-221	3.82E-218
ULBP2	265.26	35	496	14.218	3.83	9.44E-16	1.79E-14
OLFM2	11.81	2	22	13.923	3.799	4.69E-06	2.63E-05
CPAMD8	24.44	3	45	13.008	3.701	2.58E-11	3.07E-10
LOC653513	12.8	2	24	12.357	3.627	1.44E-06	8.82E-06
ALDH1A2	12.75	2	24	12.263	3.616	1.75E-06	1.05E-05
DNAJB4	883.62	143	1624	11.326	3.502	7.62E-137	9.22E-134
DNAJB1	12060.7	1986	22136	11.146	3.478	3.75E-41	3.40E-39
FAM227A	60.33	10	110	10.846	3.439	1.16E-23	4.12E-22
EGF	93.12	16	170	10.713	3.421	5.38E-32	3.15E-30
GCLM	5152.25	885	9419	10.634	3.411	1.25E-197	2.60E-194
SERHL2	36.5	6	67	10.527	3.396	8.30E-14	1.31E-12
ULBP1	474.08	83	865	10.386	3.377	3.88E-65	8.04E-63
FAM167A	15.08	3	28	10.265	3.36	0.013221	0.033974
MSC	506.54	90	923	10.178	3.347	1.22E-105	9.32E-103
TREM1	314.69	57	573	10.129	3.34	1.28E-15	2.39E-14
ARG2	125.88	23	229	9.851	3.3	1.05E-42	1.02E-40
ASAP3	10.23	2	19	9.706	3.279	5.71E-05	0.00026
TMEM132A	23.65	4	43	9.642	3.269	6.25E-10	6.26E-09
SV2C	20.25	4	37	9.591	3.262	8.75E-09	7.39E-08
CHRNA5	520.58	99	942	9.489	3.246	4.28E-104	2.96E-101
ADM	22.09	4	40	9.461	3.242	6.44E-08	4.87E-07
B4GALNT1	124.24	24	224	9.288	3.215	2.44E-32	1.45E-30
C9orf173-AS1	11.53	2	21	9.193	3.201	2.13E-05	0.000106
LAMA5	148.11	29	267	9.149	3.194	3.94E-35	2.71E-33
SLC48A1	877.46	176	1579	8.962	3.164	5.83E-117	6.51E-114
SRRM3	32.88	7	59	8.847	3.145	3.90E-13	5.68E-12
FABP3	23.63	5	42	8.408	3.072	3.04E-09	2.79E-08
ZFAND2A	616.7	131	1102	8.393	3.069	6.85E-88	3.10E-85
TTC39A	14.15	3	25	8.018	3.003	4.81E-06	2.69E-05
CAP2	153.03	34	272	7.927	2.987	6.08E-46	6.44E-44
SRXN1	1570.77	353	2788	7.89	2.98	1.77E-205	4.29E-202

Gene	Base Mean	DMSO	WFA	Fold Change	log2 Fold Change	pvalue	padj
DUSP4	497.94	113	883	7.804	2.964	2.70E-75	8.70E-73
DNAJB2	410.46	95	726	7.64	2.933	3.50E-75	1.10E-72
SWT1	135.62	31	239	7.613	2.929	3.10E-34	2.06E-32
THBS1	129.85	30	230	7.535	2.914	5.35E-29	2.66E-27
TRIM16	259.37	61	458	7.514	2.91	4.51E-64	9.23E-62
HSPH1	29647.48	6970	52325	7.505	2.908	1.29E-174	2.08E-171
KLF2	62.17	14	110	7.484	2.904	1.06E-17	2.35E-16
EMP1	206.89	49	365	7.441	2.896	2.05E-07	1.43E-06
B4GALNT3	133.71	31	236	7.432	2.894	1.84E-37	1.45E-35
GEMIN8P4	82.61	19	146	7.325	2.873	1.55E-23	5.46E-22
ABCB1	113.83	28	200	7.191	2.846	4.46E-26	1.92E-24
RAET1K	15.74	4	28	7.185	2.845	3.71E-06	2.11E-05
HSPB1	5363.03	1323	9403	7.105	2.829	6.77E-29	3.35E-27
WBP5	750.5	186	1315	7.032	2.814	8.58E-98	5.42E-95
ABHD4	276.73	69	485	7.022	2.812	6.53E-43	6.36E-41
NES	25.52	6	45	6.975	2.802	1.13E-08	9.41E-08
RASGRP1	16.52	4	29	6.943	2.796	1.17E-06	7.25E-06
FKBP4	2932.73	737	5128	6.947	2.796	1.25E-108	1.01E-105
ARC	23.8	6	42	6.871	2.781	2.68E-08	2.12E-07
CSF1	38.98	10	68	6.845	2.775	1.95E-12	2.66E-11
EFCAB7	374.35	96	653	6.825	2.771	1.39E-70	3.31E-68
STC2	38.79	10	67	6.684	2.741	5.74E-09	5.00E-08
ADM2	194.19	51	338	6.676	2.739	9.10E-11	1.02E-09
KIAA0895	42.6	11	74	6.663	2.736	2.32E-13	3.48E-12
DEDD2	609.37	160	1059	6.611	2.725	1.78E-56	2.94E-54
ANK1	21.68	6	37	6.527	2.706	4.96E-08	3.80E-07
MSX1	42.47	12	74	6.391	2.676	2.70E-13	4.02E-12
CCDC85A	64.25	17	111	6.389	2.676	2.28E-17	4.89E-16
SPHK1	83.29	23	144	6.37	2.671	9.26E-20	2.42E-18
LINC01127	25.93	7	45	6.359	2.669	4.91E-09	4.33E-08
DPEP1	19.77	5	34	6.331	2.662	5.79E-07	3.75E-06
KIAA1683	16.4	5	28	6.285	2.652	5.03E-06	2.80E-05
NCKAP1	106.51	29	184	6.284	2.652	1.50E-20	4.12E-19
PODNL1	32.64	9	56	6.26	2.646	5.61E-09	4.90E-08
BEND4	400.38	111	690	6.206	2.634	5.29E-74	1.60E-71
LRRC8E	24.3	7	42	6.177	2.627	8.92E-08	6.59E-07
DMRT1	11.43	3	20	6.16	2.623	0.000149	0.000627
ENGASE	799.5	223	1375	6.16	2.623	1.89E-75	6.22E-73
NECAB2	94.6	26	163	6.11	2.611	1.66E-23	5.82E-22

Gene	Base Mean	DMSO	WFA	Fold Change	log2 Fold Change	pvalue	padj
IL7R	163.86	46	281	6.073	2.602	2.44E-39	2.08E-37
ELOVL4	90.93	26	157	6.066	2.601	2.06E-20	5.61E-19
ENO2	63.55	18	109	6.063	2.6	5.93E-14	9.48E-13
MAP1A	131.92	38	226	6.043	2.595	3.74E-24	1.40E-22
GABARAPL1	145.62	42	250	6.019	2.59	7.36E-36	5.28E-34
ACER2	141.06	40	242	6.007	2.587	5.67E-33	3.51E-31
EFEMP1	25.38	7	43	5.974	2.579	1.18E-08	9.79E-08
HSP90AA1	135961.8	39836	232087	5.826	2.542	5.60E-111	5.42E-108
ADGRF3	28.18	8	48	5.75	2.524	6.42E-09	5.53E-08
ME1	1323.13	392	2255	5.753	2.524	7.82E-105	5.67E-102
PDLIM4	152.57	45	260	5.716	2.515	6.54E-32	3.78E-30
GGTA1P	31.67	10	54	5.645	2.497	5.39E-10	5.45E-09
SLC35E4	20.89	6	36	5.609	2.488	8.71E-07	5.50E-06
HSPA7	43.53	13	74	5.594	2.484	0.005502	0.015713
PPP1R26-AS1	35.52	11	60	5.571	2.478	2.17E-10	2.33E-09
HAPLN4	13.48	4	23	5.439	2.443	8.26E-05	0.000365
BMP4	91.63	29	155	5.377	2.427	5.42E-20	1.43E-18
SLC12A7	34.29	11	58	5.358	2.422	4.81E-10	4.91E-09
RIT1	2159.09	679	3639	5.36	2.422	3.54E-95	1.97E-92
AVPI1	21.1	7	35	5.348	2.419	6.66E-07	4.27E-06
C1QL4	12.79	4	22	5.343	2.418	0.00016	0.000665
SERPINE1	24.24	8	41	5.325	2.413	3.77E-07	2.51E-06
CRYZ	364.46	115	614	5.294	2.404	2.45E-49	2.97E-47
HSPA4L	2285.33	727	3844	5.283	2.401	4.33E-73	1.21E-70
HIBCH	930.82	300	1562	5.207	2.38	2.24E-79	8.55E-77
KIAA1522	176.15	57	296	5.187	2.375	1.64E-32	9.83E-31
JPH4	13.75	4	23	5.166	2.369	6.30E-05	0.000285
TCP11L2	24.48	8	41	5.152	2.365	1.02E-07	7.49E-07
P4HA1	1526.07	498	2554	5.133	2.36	5.78E-95	3.10E-92
GNAL	122.33	40	205	5.114	2.354	5.93E-28	2.82E-26
CACFD1	108.97	35	183	5.109	2.353	1.61E-22	5.26E-21
CEP295NL	10.71	3	18	5.104	2.352	0.000646	0.002333
SLC7A11	1603.43	526	2681	5.102	2.351	3.53E-09	3.20E-08
RGS2	255.79	84	427	5.089	2.347	3.46E-40	2.99E-38
PANX2	30.72	10	51	5.08	2.345	4.08E-08	3.16E-07
SORBS1	49.97	16	84	5.07	2.342	4.09E-13	5.96E-12
ESRP1	64.24	21	107	5.055	2.338	7.77E-12	9.90E-11
SIX4	28.79	10	48	5.053	2.337	1.31E-08	1.08E-07
TUBB3	25.86	8	43	5.044	2.335	8.60E-08	6.37E-07

Gene	Base Mean	DMSO	WFA	Fold Change	log2 Fold Change	pvalue	padj
KLHDC8B	91.38	30	153	5.039	2.333	4.93E-20	1.31E-18
PHOSPHO1	13.58	4	23	5.034	2.332	9.68E-05	0.000421
CHORDC1	3068.73	1017	5120	5.029	2.33	5.36E-69	1.21E-66
EVA1B	13.22	4	22	4.99	2.319	0.000259	0.001025
MAP2	19.94	7	33	4.984	2.317	2.98E-06	1.72E-05
PIR	111.76	37	186	4.97	2.313	9.37E-18	2.10E-16
INHBE	17.39	6	29	4.949	2.307	9.03E-05	0.000395
HSD17B7	311.73	105	519	4.937	2.304	8.06E-51	1.04E-48
CHAC1	52.98	18	88	4.922	2.299	1.15E-09	1.12E-08
RAB30	67.41	23	112	4.919	2.298	6.31E-16	1.22E-14
DUSP16	118.22	40	197	4.916	2.298	2.68E-17	5.73E-16
KIAA0513	212.21	71	353	4.912	2.296	1.44E-36	1.07E-34
SQSTM1	4196.64	1419	6974	4.911	2.296	2.81E-79	1.05E-76
IL18BP	379.52	128	631	4.896	2.292	1.22E-53	1.85E-51
MFAP3L	30.73	11	51	4.86	2.281	1.04E-08	8.74E-08
GDF15	17.75	6	30	4.855	2.28	2.21E-05	0.00011
MCOLN3	1208.6	414	2004	4.852	2.279	6.06E-67	1.29E-64
LINC01085	21.33	7	35	4.843	2.276	2.57E-06	1.50E-05
WBP2	1761.17	605	2917	4.814	2.267	6.14E-89	2.97E-86
TMEM56	67.29	23	111	4.798	2.262	9.42E-14	1.48E-12
CYP27A1	137.07	47	227	4.791	2.26	2.14E-25	8.72E-24
NEAT1	6923.95	2393	11455	4.787	2.259	4.75E-21	1.36E-19
KCNQ1OT1	274.06	95	453	4.785	2.259	1.08E-30	5.80E-29
HIST1H2AC	20.33	7	33	4.765	2.253	3.04E-06	1.75E-05
DNAJB6	2684.54	931	4438	4.762	2.252	4.32E-102	2.85E-99
MORC4	456.24	158	754	4.758	2.25	2.07E-52	2.84E-50
MIAT	16.65	6	28	4.737	2.244	5.34E-05	0.000245
BTN2A3P	47.71	17	79	4.731	2.242	2.17E-11	2.60E-10
IER5	1071.26	374	1768	4.724	2.24	8.65E-48	9.81E-46
RP9P	197.52	69	326	4.714	2.237	8.24E-33	5.05E-31
DNAJB5	88.33	31	146	4.698	2.232	1.14E-17	2.53E-16
TIGD4	10	3	17	4.693	2.23	0.001131	0.00386
SLC41A2	60.31	22	99	4.646	2.216	2.67E-13	3.98E-12
GPR155	118.91	42	196	4.632	2.212	4.28E-20	1.15E-18
CYTIP	125.9	45	207	4.611	2.205	1.49E-25	6.13E-24
MLLT11	34.84	12	57	4.595	2.2	2.23E-09	2.09E-08
BTBD19	33.04	12	54	4.56	2.189	3.36E-07	2.25E-06
CNTN1	130.22	47	213	4.556	2.188	9.84E-25	3.85E-23
TMEM255A	98.66	36	162	4.535	2.181	1.04E-16	2.14E-15

Gene	Base Mean	DMSO	WFA	Fold Change	log2 Fold Change	pvalue	padj
DACT1	21.93	8	36	4.52	2.176	2.39E-06	1.40E-05
ULBP3	49.52	18	81	4.519	2.176	1.43E-10	1.57E-09
PXDC1	58.89	21	96	4.514	2.174	6.19E-14	9.88E-13
DNAJA1	17120.6	6209	28032	4.514	2.174	1.69E-110	1.53E-107
MXD1	650.89	239	1063	4.452	2.155	1.13E-44	1.15E-42
TRAM2	2437.12	897	3977	4.432	2.148	4.13E-67	8.94E-65
BTN2A2	165.1	61	270	4.418	2.143	1.58E-29	8.02E-28
FOXO4	147.19	54	240	4.404	2.139	9.68E-28	4.56E-26
METRNL	13.12	5	21	4.396	2.136	0.000534	0.001971
IL2RB	35.81	14	58	4.346	2.12	1.51E-08	1.24E-07
UNKL	430.23	161	699	4.338	2.117	1.20E-46	1.32E-44
LINC00877	25.83	10	42	4.332	2.115	3.02E-06	1.74E-05
TNFRSF12A	37.71	14	61	4.326	2.113	7.50E-09	6.41E-08
TP53INP1	175.3	66	285	4.325	2.113	8.10E-25	3.19E-23
TMEM243	325.49	122	529	4.31	2.108	6.21E-40	5.33E-38
SNAI2	11.95	5	19	4.285	2.099	0.000736	0.002626
NR4A2	43.79	17	71	4.268	2.094	1.60E-09	1.52E-08
RGMB	14.29	5	23	4.263	2.092	0.000401	0.001521
SOCS3	73.5	28	119	4.247	2.086	3.01E-14	4.94E-13
TSC22D3	435.95	166	706	4.239	2.084	4.40E-41	3.94E-39
RHBDD2	496.41	190	803	4.22	2.077	1.70E-52	2.35E-50
KLHL6	1210.89	464	1958	4.22	2.077	8.41E-86	3.59E-83
HAVCR2	84.86	32	137	4.204	2.072	1.00E-13	1.56E-12
MAP1B	567.17	218	916	4.197	2.069	2.68E-07	1.83E-06
NRCAM	36.77	15	59	4.184	2.065	2.08E-08	1.67E-07
NPY1R	13.11	5	21	4.166	2.059	0.000449	0.001683
FGD6	46.37	18	75	4.145	2.051	1.92E-09	1.81E-08
SLAMF7	83.87	33	135	4.125	2.044	1.47E-11	1.80E-10
TMEM221	13.81	5	22	4.12	2.043	0.000343	0.001321
STX1B	10.75	4	17	4.118	2.042	0.002852	0.008866
EPHA2	11.94	5	19	4.119	2.042	0.001287	0.00434
SLC26A11	14.95	6	24	4.103	2.037	0.000629	0.002278
CCDC92	13.18	5	21	4.098	2.035	0.000557	0.002045
USP9Y	103.53	41	166	4.061	2.022	2.28E-13	3.42E-12
RBM11	17.56	7	28	4.052	2.019	7.71E-05	0.000343
FTH1	11910.54	4717	19104	4.05	2.018	1.72E-15	3.19E-14
MSC-AS1	510.15	202	818	4.048	2.017	4.67E-55	7.36E-53
SLC12A8	54.67	22	88	4.013	2.005	5.26E-11	6.06E-10
PLEKHH2	48.6	19	78	4.009	2.003	3.50E-09	3.18E-08

Gene	Base Mean	DMSO	WFA	Fold Change	log2 Fold Change	pvalue	padj
TGFA	69.22	28	111	4.005	2.002	2.85E-14	4.70E-13
DOK2	2489.37	994	3985	4.006	2.002	2.24E-63	4.52E-61
MMP19	53.61	22	86	3.999	2	6.61E-09	5.69E-08
PLEKHA7	39.4	16	63	3.986	1.995	1.23E-08	1.02E-07
C6orf223	66.22	26	106	3.985	1.995	4.70E-11	5.43E-10
EPHX1	1135.22	455	1816	3.986	1.995	4.06E-73	1.16E-70
FCMR	13.63	5	22	3.973	1.99	0.001354	0.004547
CDKN1A	615.65	249	983	3.951	1.982	8.25E-11	9.31E-10
MARK1	23.41	9	38	3.948	1.981	1.51E-05	7.70E-05
CCNO	20.33	8	32	3.943	1.979	2.25E-05	0.000112
PPP1R15A	1113.55	451	1776	3.942	1.979	7.02E-10	6.97E-09
IL12RB2	2882.76	1168	4597	3.935	1.976	4.99E-89	2.50E-86
ZNF774	30.31	12	48	3.927	1.973	3.73E-07	2.48E-06
LBX2-AS1	202.84	82	323	3.926	1.973	1.06E-30	5.75E-29
LOC101929709	45.94	19	73	3.924	1.972	1.99E-09	1.87E-08
PRKACB	2740.5	1114	4367	3.92	1.971	1.29E-54	2.01E-52
TMEM47	50.82	21	81	3.91	1.967	1.05E-08	8.81E-08
ID3	141.32	58	225	3.902	1.964	2.87E-13	4.26E-12
GPR89B	88.32	36	141	3.875	1.954	5.93E-16	1.15E-14
KLHL24	566.33	233	900	3.866	1.951	4.18E-52	5.62E-50
SAMD4A	39.5	16	63	3.857	1.947	1.35E-07	9.74E-07
LOC100129940	22.35	9	35	3.853	1.946	1.59E-05	8.11E-05
LOC103021296	14.56	6	23	3.833	1.938	0.000597	0.002177
PPME1	1475.76	615	2336	3.791	1.923	2.35E-58	4.00E-56
ABCC3	120.83	50	191	3.79	1.922	5.23E-16	1.03E-14
TSHZ1	689.98	288	1092	3.783	1.919	4.75E-59	8.51E-57
IER5L	148.89	62	236	3.779	1.918	2.35E-18	5.56E-17
C14orf37	10.81	5	17	3.775	1.917	0.003472	0.010528
LOC729603	91.63	38	145	3.776	1.917	2.11E-11	2.54E-10
TMEM51-AS1	18.14	8	29	3.773	1.916	0.000223	0.000899
EPB41L1	113.18	48	179	3.765	1.913	4.29E-15	7.70E-14
HSPD1	33742.63	14159	53326	3.766	1.913	2.17E-94	1.12E-91
DUSP1	56.53	24	89	3.755	1.909	9.64E-08	7.08E-07
IL20RB	42.07	18	66	3.753	1.908	5.70E-06	3.13E-05
GDPD1	99.08	42	157	3.751	1.907	4.75E-16	9.33E-15
AIFM2	118.04	50	186	3.743	1.904	8.92E-14	1.40E-12

Gene	Base Mean	DMSO	WFA	Fold Change	log2 Fold Change	pvalue	padj
SESN2	306.87	130	484	3.732	1.9	3.71E-22	1.17E-20
MRPL18	4506.61	1906	7108	3.728	1.899	5.14E-80	2.02E-77
SORCS1	14.41	6	23	3.719	1.895	0.002332	0.007384
HSPE1	1554.5	658	2451	3.72	1.895	1.12E-72	2.95E-70
MKNK2	2340.21	993	3687	3.711	1.892	3.77E-71	9.42E-69
LINC-PINT	28.51	12	45	3.708	1.891	2.72E-06	1.58E-05
FAM83G	71.04	30	112	3.71	1.891	3.32E-10	3.47E-09
SERTAD1	132.19	56	208	3.707	1.89	1.91E-21	5.69E-20
ABHD3	1077.24	458	1697	3.701	1.888	1.62E-71	4.12E-69
RHOB	186.17	79	293	3.698	1.887	3.90E-24	1.46E-22
MAPRE3	46.47	20	73	3.691	1.884	7.12E-09	6.10E-08
SLC25A34	21.44	9	34	3.682	1.88	9.06E-05	0.000397
ADGRG6	206.2	88	324	3.677	1.878	1.64E-28	7.97E-27
ABLIM3	21.48	9	34	3.668	1.875	4.94E-05	0.000228
CYP2R1	146.82	63	231	3.663	1.873	5.97E-19	1.48E-17
AHSA1	5076.83	2179	7974	3.657	1.871	2.92E-79	1.06E-76
IGF2BP1	10.5	4	17	3.652	1.869	0.004156	0.012325
BST2	1502	645	2359	3.653	1.869	2.21E-53	3.20E-51
PGR	233.48	100	367	3.642	1.865	4.33E-24	1.61E-22
NUPR1	316.85	136	497	3.626	1.859	1.84E-22	5.98E-21
MTHFS	17.43	8	27	3.614	1.854	0.000251	0.000998
BCAR1	83.24	36	131	3.605	1.85	1.89E-14	3.17E-13
GPX8	129.53	56	203	3.603	1.849	2.21E-19	5.65E-18
SPR	615.95	268	964	3.587	1.843	3.88E-51	5.08E-49
TSPYL4	905.73	395	1416	3.582	1.841	3.49E-56	5.62E-54
TRIM2	95.87	42	150	3.575	1.838	7.44E-15	1.30E-13
FOSB	26.42	11	41	3.57	1.836	3.32E-05	0.000159
RANGAP1	2560.53	1121	4000	3.568	1.835	1.15E-70	2.78E-68
TESK1	353.14	155	552	3.555	1.83	1.20E-35	8.53E-34
TNFSF14	1390.95	612	2170	3.546	1.826	7.34E-67	1.54E-64
SLC5A3	2565.55	1131	4000	3.536	1.822	3.42E-73	9.93E-71
PARD6G-AS1	21.46	9	33	3.523	1.817	5.55E-05	0.000254
PRNP	1316.6	582	2051	3.523	1.817	1.75E-60	3.26E-58
UST	134.9	60	210	3.518	1.815	1.34E-15	2.51E-14
NQO1	1212.34	537	1888	3.511	1.812	1.99E-30	1.05E-28
TBXA2R	16.49	7	26	3.498	1.807	0.000381	0.001452
OLMALINC	68.71	31	107	3.477	1.798	7.41E-10	7.33E-09
C9orf41-AS1	10.74	5	17	3.464	1.793	0.004333	0.01278
HGD	12.77	6	20	3.466	1.793	0.001853	0.006027
MAFF	34.2	15	53	3.463	1.792	1.47E-06	8.96E-06

Gene	Base Mean	DMSO	WFA	Fold Change	log2 Fold Change	pvalue	padj
CDKL3	129.22	58	201	3.461	1.791	3.99E-16	7.86E-15
NOV	16.12	7	25	3.459	1.79	0.001226	0.004154
ZNF366	392.93	176	610	3.459	1.79	7.85E-39	6.51E-37
C15orf65	19.23	9	30	3.447	1.785	0.000186	0.000763
C6orf165	23.69	10	37	3.441	1.783	9.38E-05	0.000409
GPR180	753.53	339	1168	3.442	1.783	8.12E-54	1.25E-51
TMEM79	190.21	85	295	3.439	1.782	2.96E-17	6.28E-16
GLYCTK	40.96	18	64	3.43	1.778	2.33E-07	1.61E-06
MOK	70.24	32	109	3.429	1.778	9.90E-11	1.11E-09
PGD	5125.17	2314	7937	3.429	1.778	2.84E-59	5.14E-57
STIP1	9504.56	4295	14715	3.425	1.776	1.24E-75	4.18E-73
HPCAL4	25.68	12	40	3.421	1.775	0.000741	0.002641
MAP3K9	14.85	7	23	3.419	1.774	0.001064	0.003658
SMAD1	21.75	10	34	3.419	1.773	7.24E-05	0.000324
MOCS2	1044.8	473	1616	3.413	1.771	3.91E-56	6.23E-54
TXNRD1	6777.89	3072	10483	3.412	1.771	9.63E-96	5.59E-93
PCSK4	12.68	6	20	3.41	1.77	0.006005	0.016964
ADAT3	20.87	9	32	3.403	1.767	0.000191	0.000782
HDAC11	44.28	20	69	3.404	1.767	1.32E-07	9.50E-07
KCTD11	73.28	33	113	3.395	1.764	1.69E-11	2.06E-10
ATF3	106.98	48	165	3.396	1.764	3.99E-15	7.16E-14
ATP9A	258.13	117	399	3.394	1.763	2.12E-22	6.82E-21
TNFRSF10C	16.03	7	25	3.391	1.762	0.00102	0.003516
BAZ2A	3302.41	1506	5099	3.387	1.76	9.91E-53	1.41E-50
CLIP2	551.92	252	852	3.38	1.757	5.37E-36	3.95E-34
PHLDB1	386.59	177	597	3.376	1.755	1.35E-36	1.02E-34
BANP	313.15	143	483	3.366	1.751	7.37E-27	3.30E-25
PTPRR	13.8	6	21	3.356	1.747	0.001848	0.006012
SLC2A3	165.72	76	255	3.355	1.746	3.23E-21	9.45E-20
LDLR	708.37	325	1091	3.352	1.745	6.35E-37	4.85E-35
SNAP23	2663	1224	4102	3.35	1.744	3.17E-63	6.31E-61
GFPT2	10.5	5	16	3.344	1.742	0.008687	0.023509
PLOD1	1550.4	714	2387	3.341	1.74	3.20E-58	5.40E-56
PLCD3	68.5	31	106	3.337	1.739	4.20E-09	3.76E-08
CACYBP	5997.8	2765	9230	3.337	1.739	1.47E-56	2.45E-54
PLEKHF1	50.49	23	78	3.335	1.738	3.36E-08	2.64E-07
SDC1	38.99	18	60	3.333	1.737	3.20E-07	2.16E-06
ZC3HAV1	5362.12	2475	8249	3.332	1.737	1.19E-67	2.61E-65
ENPP5	30.21	14	46	3.328	1.735	6.55E-06	3.57E-05
CYR61	24.37	11	37	3.326	1.734	6.73E-05	0.000303

Gene	Base Mean	DMSO	WFA	Fold Change	log2 Fold Change	pvalue	padj
BCL6	304.42	140	468	3.326	1.734	2.40E-32	1.43E-30
EFCAB13	78.03	36	120	3.309	1.727	2.88E-12	3.86E-11
SUGT1	1634.37	759	2510	3.307	1.725	6.87E-59	1.21E-56
ARHGAP21	542.07	252	832	3.303	1.724	4.49E-37	3.50E-35
HSD17B14	16.42	8	25	3.302	1.723	0.001013	0.003495
EPB41L5	96.17	44	148	3.299	1.722	2.41E-11	2.88E-10
CDR2L	81.81	38	126	3.3	1.722	1.41E-11	1.74E-10
HSP90AB1	72418.82	33733	111105	3.294	1.72	8.42E-73	2.26E-70
SLC6A9	27.9	13	43	3.288	1.717	0.000222	0.000896
SAMD14	13.37	6	21	3.283	1.715	0.002724	0.0085
ARHGEP37	12.35	6	19	3.278	1.713	0.003514	0.010642
C11orf84	499.07	233	766	3.279	1.713	4.51E-34	2.95E-32
ANXA1	7927.99	3709	12147	3.275	1.711	5.42E-47	6.05E-45
RNF122	133.1	62	204	3.268	1.709	1.32E-17	2.90E-16
LOC100499489	12.38	6	19	3.267	1.708	0.006068	0.017111
USP53	373.97	175	573	3.268	1.708	7.99E-21	2.24E-19
KIAA0355	26.59	12	41	3.265	1.707	0.000106	0.000457
GNA15	403.19	189	617	3.26	1.705	5.20E-29	2.59E-27
BCO2	21.28	10	33	3.258	1.704	0.000276	0.001083
SLC35G2	16.41	8	25	3.25	1.7	0.00112	0.003826
LAMB2P1	23.11	11	36	3.245	1.698	0.000176	0.000731
LSMEM1	18.78	9	29	3.24	1.696	0.000371	0.001418
EFNA4	62.7	30	96	3.221	1.687	1.04E-09	1.02E-08
ZNF425	97.49	46	149	3.217	1.685	4.08E-14	6.63E-13
AHSA2	762.55	363	1162	3.21	1.683	4.23E-31	2.32E-29
HERC4	1113.04	529	1697	3.209	1.682	1.56E-61	3.06E-59
GBP3	411.8	196	628	3.203	1.68	5.22E-34	3.38E-32
TESK2	143.77	68	219	3.193	1.675	2.69E-17	5.73E-16
NFAT5	1200.13	574	1827	3.188	1.672	2.27E-48	2.68E-46
ARHGAP31-AS1	10.12	5	15	3.182	1.67	0.010803	0.028425
RCAN2	20.77	10	32	3.179	1.668	0.00027	0.001063
TFE3	836.61	401	1273	3.175	1.667	2.55E-48	2.98E-46
FAM214A	390.32	187	594	3.173	1.666	4.28E-30	2.23E-28
ARAP3	108.74	52	166	3.17	1.664	7.05E-15	1.23E-13
TTC9	69.72	33	106	3.165	1.662	2.43E-10	2.60E-09
ANKMY2	874.76	420	1330	3.161	1.66	5.68E-53	8.17E-51
FAM46C	42.58	20	65	3.146	1.653	5.88E-07	3.80E-06
SYTL2	30.8	15	47	3.144	1.652	3.94E-05	0.000185

Gene	Base Mean	DMSO	WFA	Fold Change	log2 Fold Change	pvalue	padj
POPDC3	40.86	20	62	3.143	1.652	3.02E-07	2.05E-06
C7orf60	352.03	170	534	3.141	1.651	1.04E-34	6.98E-33
CAMSAP3	84.84	41	129	3.137	1.65	3.97E-12	5.22E-11
CDC42EP2	13.08	6	20	3.132	1.647	0.004032	0.012031
SLC7A5	3343.15	1619	5068	3.13	1.646	3.03E-35	2.09E-33
DDIT3	777.96	377	1179	3.124	1.643	5.74E-23	1.91E-21
CASP7	425.85	206	645	3.122	1.642	5.71E-38	4.63E-36
SYT11	110.67	54	168	3.11	1.637	3.65E-10	3.78E-09
FAM214B	346.87	169	525	3.107	1.636	3.13E-23	1.08E-21
CPEB4	625.58	304	947	3.109	1.636	7.98E-36	5.70E-34
OXTR	24.69	12	37	3.102	1.633	8.07E-05	0.000358
FBXO32	113.17	55	172	3.102	1.633	1.84E-12	2.52E-11
CREBRF	509.63	248	771	3.1	1.632	1.08E-35	7.68E-34
GEM	49.79	24	75	3.097	1.631	2.34E-07	1.62E-06
TULP3	189.14	92	286	3.094	1.63	9.21E-22	2.80E-20
PALLD	60.96	30	92	3.093	1.629	2.48E-08	1.97E-07
KITLG	492.35	240	744	3.089	1.627	2.70E-25	1.09E-23
TFPI	16.28	8	25	3.085	1.625	0.001356	0.004554
LOC729950	12.39	6	19	3.082	1.624	0.00575	0.016344
LARP6	56.61	28	86	3.081	1.624	5.11E-08	3.90E-07
TACC2	100.45	49	152	3.083	1.624	3.43E-13	5.05E-12
MLKL	985.19	483	1487	3.079	1.622	4.12E-52	5.59E-50
RTN4RL2	14.81	7	23	3.076	1.621	0.002981	0.009218
PAQR6	35.26	17	53	3.074	1.62	8.06E-06	4.33E-05
KIAA1549	205.73	101	310	3.066	1.616	7.41E-21	2.08E-19
TCF7L1	56.13	28	85	3.064	1.615	1.82E-08	1.47E-07
FERMT2	102.8	51	155	3.058	1.612	5.43E-08	4.13E-07
FAM109A	84	41	127	3.058	1.612	9.42E-12	1.18E-10
PHF1	16.62	8	25	3.047	1.608	0.001484	0.004939
LURAP1L	19.09	9	29	3.04	1.604	0.000776	0.002751
BAALC	21.57	11	32	3.037	1.603	0.000371	0.001418
MBOAT2	720.88	357	1085	3.038	1.603	9.65E-30	4.97E-28
LINC00963	342.78	170	516	3.033	1.601	4.38E-33	2.76E-31
C6orf1	242.26	120	364	3.026	1.598	3.28E-18	7.67E-17
MDGA1	26.09	13	39	3.025	1.597	0.000423	0.001597
SLC6A6	910.96	454	1368	3.012	1.591	5.81E-33	3.59E-31
HSPA4	10545.05	5258	15832	3.011	1.59	2.66E-88	1.24E-85
TSPAN13	63.05	31	95	3.002	1.586	2.38E-09	2.22E-08
FOXL2NB	46.07	23	69	2.982	1.576	3.16E-06	1.81E-05

Gene	Base Mean	DMSO	WFA	Fold Change	log2 Fold Change	pvalue	padj
KPNA5	130.48	66	196	2.981	1.576	2.19E-12	2.97E-11
OSER1	873.18	439	1308	2.978	1.575	3.92E-39	3.29E-37
CEP126	53.22	27	80	2.974	1.573	0.014021	0.035776
PPP2R5B	100.11	50	150	2.976	1.573	1.09E-12	1.53E-11
COL24A1	141.17	71	211	2.972	1.572	3.53E-16	6.99E-15
ZNF540	10.83	5	16	2.969	1.57	0.014831	0.03748
DAPK1	821.98	414	1230	2.966	1.569	5.43E-46	5.84E-44
IFFO2	363.06	183	543	2.964	1.567	8.65E-24	3.12E-22
SPATA41	19.38	10	29	2.951	1.561	0.000668	0.002402
PTRF	32.32	16	48	2.951	1.561	2.93E-05	0.000142
SEMA6C	35.07	18	52	2.948	1.56	3.58E-05	0.00017
TNFRSF10D	206.49	105	308	2.946	1.559	5.70E-16	1.11E-14
JAG1	107.95	55	161	2.944	1.558	8.99E-14	1.41E-12
C4orf19	29.81	15	45	2.94	1.556	3.95E-05	0.000186
ZSWIM4	68.84	35	103	2.935	1.553	1.50E-07	1.07E-06
TSKU	22.47	11	33	2.93	1.551	0.000307	0.001191
MUM1	1286.37	654	1919	2.93	1.551	2.75E-40	2.41E-38
SMIM10L2A	13.63	7	21	2.927	1.549	0.004802	0.013951
HSD17B7P2	27.65	14	41	2.923	1.547	0.000114	0.000489
HRAT5	11.08	6	17	2.912	1.542	0.011911	0.030997
MAGIX	21.64	11	32	2.909	1.541	0.001203	0.004088
MVD	234.37	120	349	2.91	1.541	5.06E-21	1.44E-19
PIH1D2	16.5	9	25	2.906	1.539	0.006231	0.017522
GSR	3472.35	1778	5167	2.905	1.539	1.77E-59	3.26E-57
RAB3B	101.94	52	152	2.9	1.536	1.35E-10	1.49E-09
SERAC1	241.88	124	360	2.897	1.535	3.49E-20	9.44E-19
GLDC	33.43	17	50	2.895	1.534	3.99E-05	0.000187
MCU	703.13	361	1046	2.897	1.534	1.51E-33	9.74E-32
HSPA8	82022.97	42097	121950	2.897	1.534	1.27E-45	1.32E-43
ROCK1P1	14.34	7	21	2.893	1.533	0.004642	0.013576
LRIG1	1170.85	601	1740	2.894	1.533	7.09E-42	6.52E-40
ALPK3	788	405	1171	2.892	1.532	1.53E-31	8.69E-30
PLCD4	11.01	6	17	2.888	1.53	0.013766	0.0352
POU6F1	27.15	14	40	2.886	1.529	0.000154	0.000644
MAPK8IP1	14.41	7	21	2.881	1.526	0.010038	0.026682
PPP1R36	11.86	6	18	2.874	1.523	0.012001	0.031203
TLX3	15.75	8	23	2.874	1.523	0.005448	0.01557
FTL	62958.67	32526	93392	2.871	1.522	1.65E-45	1.71E-43
SYNM	632.9	327	938	2.869	1.52	5.29E-37	4.09E-35

Gene	Base Mean	DMSO	WFA	Fold Change	log2 Fold Change	pvalue	padj
TMEM37	65.53	34	97	2.865	1.519	5.87E-08	4.45E-07
MCC	41.17	21	61	2.864	1.518	2.30E-05	0.000114
CELF6	16.11	8	24	2.862	1.517	0.005357	0.015369
VWA5A	126.61	65	188	2.861	1.517	5.59E-13	8.07E-12
PHTF1	1490.61	772	2209	2.861	1.516	9.02E-44	8.84E-42
CERS6-AS1	24.94	13	37	2.857	1.515	0.000561	0.00206
SPATS2L	1869.97	969	2771	2.857	1.515	1.29E-37	1.03E-35
ANO8	37.24	19	55	2.855	1.514	1.36E-05	6.99E-05
ATP2C1	2963.03	1538	4388	2.854	1.513	3.82E-50	4.82E-48
ZNF580	108.92	57	162	2.853	1.512	1.21E-12	1.70E-11
PLCD1	52.99	28	79	2.848	1.51	1.28E-07	9.24E-07
S100P	72.85	38	108	2.849	1.51	4.45E-08	3.43E-07
SH3PXD2B	245.96	128	364	2.848	1.51	6.39E-15	1.12E-13
LOC10013087 2	17.78	9	26	2.844	1.508	0.002702	0.008439
WWTR1	108.58	57	161	2.825	1.498	1.66E-11	2.03E-10
NUDC	3728.27	1949	5508	2.825	1.498	1.33E-50	1.69E-48
GKAP1	143.45	75	212	2.823	1.497	4.35E-15	7.80E-14
PPID	1965.37	1030	2901	2.814	1.493	1.16E-52	1.63E-50
ERRFI1	86.29	46	127	2.809	1.49	3.89E-10	4.02E-09
NAPSA	11.56	6	17	2.804	1.488	0.015742	0.039461
NUAK2	17.64	9	26	2.8	1.486	0.002286	0.007259
TSPYL2	164.48	87	243	2.8	1.486	6.84E-13	9.76E-12
SMAD9	13.33	7	20	2.799	1.485	0.007744	0.021203
MATN2	333.75	176	492	2.8	1.485	7.69E-24	2.81E-22
LOC10106009 1	15.23	8	23	2.789	1.48	0.004768	0.013868
MAST3	545.71	288	804	2.789	1.48	2.22E-23	7.71E-22
MRPS6	1061.75	560	1564	2.789	1.48	1.34E-38	1.10E-36
ARVCF	16	8	24	2.78	1.475	0.004573	0.013402
PRSS23	49.02	26	72	2.767	1.468	4.06E-06	2.29E-05
RASGEF1B	13.18	7	19	2.764	1.467	0.009171	0.024666
CREM	106.22	56	156	2.765	1.467	3.81E-10	3.94E-09
RPL21P44	10.8	6	16	2.76	1.464	0.015234	0.038345
MAFB	426.86	227	627	2.759	1.464	8.95E-24	3.22E-22
MAGI3	578.31	308	849	2.756	1.463	5.16E-26	2.21E-24
SPSB1	131.04	69	193	2.754	1.462	2.89E-13	4.29E-12
NUCB1	2364.56	1259	3470	2.754	1.462	4.61E-48	5.26E-46
AHCYL2	457.55	244	672	2.754	1.461	9.20E-24	3.31E-22
UBE2H	1453.81	775	2133	2.754	1.461	7.97E-41	7.09E-39
BBC3	35.2	19	52	2.75	1.46	3.31E-05	0.000159

Gene	Base Mean	DMSO	WFA	Fold Change	log2 Fold Change	pvalue	padj
DDIT4	149.1	79	219	2.749	1.459	1.57E-10	1.72E-09

Appendix 3. 500 most up-regulated genes in THP1 Cells following treatment with Withaferin A